Feedback Ramp Metering in Intelligent Transportation Systems

Feedback Ramp Metering in Intelligent Transportation Systems

Dr. Pushkin Kachroo
Virginia Polytechnic Institute and State University
Blacksburg, Virginia

and

Dr. Kaan Ozbay
Rutgers University
Piscataway, New Jersey

Springer Science+Business Media, LLC

Library of Congress Cataloging-in-Publication Data

Kachroo, Pushkin.
Feedback ramp metering in intelligent transportation systems/Pushkin Kachroo, Kaan Ozbay.
p. cm.
Includes bibliographical references and index.
ISBN 978-1-4613-4737-8 ISBN 978-1-4419-8961-1 (eBook)
DOI 10.1007/978-1-4419-8961-1
1. Electronic traffic controls. 2. Adaptive control systems. 3. Roads—Interchanges and intersections. 4. Intelligent Vehicle Highway Systems. I. Özbay, Kaan, 1964– II. Title.

TE228.K35 2003
625.7'94—dc22

2003061056

ISBN 978-1-4613-4737-8

Originally published by Kluwer Academic / Plenum Publishers, New York in 2003
Softcover reprint of the hardcover 1st edition 2003

http://www.wkap.nl/

10 9 8 7 6 5 4 3 2 1

A C.I.P. record for this book is available from the Library of Congress

List of Figures

List of Tables

Contents

Acknowledgments

Dedicated to my brother, Raju Bhaiya.

Pushkin Kachroo

I would like to thank my graduate students Harsh Doshi and Ilgin Yasar for helping me in editing certain chapters and for running various simulation scenarios.

Kaan Ozbay

Chapter 1

INTRODUCTION

This chapter introduces the ramp-metering problem. It discusses the congestion problem on highways and how ramp metering is used to alleviate this problem. It also gives an overview of feedback control theory as we use it in this book. This is intended for those readers who do not have a background in that area.

1. INTRODUCTION

Increasing dependence on car-based travel has led to the daily occurrence of recurrent and non recurrent freeway congestions not only in the United States but also around the world. Congestion on freeways forms when the demand exceeds capacity.

Recurrent congestion reduces substantially the available infrastructure capacity at rush hour, i.e., at the time this capacity is most urgently needed, causing delays, increased environmental pollution, and reduced traffic safety. Similar effects are observed in the frequent case of nonrecurrent congestions caused by traffic incidents such as crashes, disabled vehicles, adverse weather conditions, work zones, special events and other temporary disruptions to the highway transportation system, etc. (Figure 1-1).

P. Kachroo et al., *Feedback Ramp Metering in Intelligent Transportation Systems*

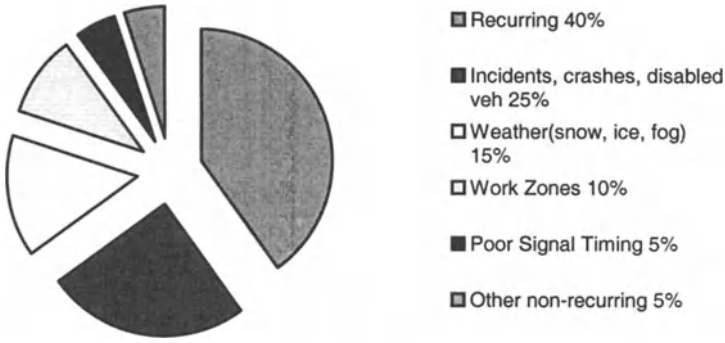

Figure 1-1: How Is the Congestion Pie Sliced? [2]

Congestion, both recurrent and nonrecurrent, is characterized by some annoying features, such as slow travel speeds, erratic speeds (stop-and-go movement), increased and inconsistent travel times, increased accident potential, inefficient operation, and other undesirable conditions that cause user dissatisfaction. The following illustrates the severity of congestion in the United States [2]. Congestion results in 5.7 billion person-hours of delay annually in the United States. Between 1980 and 1999, route miles of newly constructed highways increased 1.5 percent while vehicle miles of travel grew by 76 percent. Over 42,500 miles of highways in the 50 states and the District of Columbia were congested in 2000 (as defined by vehicle/service ratios of 0.8 or higher). Over 6,000 of these miles were in rural areas. Texas Transportation Institute (TTI) estimates that within major U.S. urban areas, over 32% of our daily travel occurs within congested conditions and the trend continues to climb. In small urban areas alone (<500,000 population), congested travel increased 300% between 1982 and 1997. This congestion adds up to 4.5 billion hours of delay in 68 urban areas according to a recent TTI report published in 1999. Annual delay per person was estimated as 36 hours per year. The delay is estimated as 41 hours per person per year in cities over 3 million population. In one of the metropolitan areas most seriously affected by this congestion problem, Los Angeles, the delay was found to be 56 hours per person per year. Between 1982 and 1999 annual delay per person in the 68 metropolitan areas increased at a compound rate of 7 percent (from 11 to 36 hours). The individual cost of congestion exceeded $900 per driver in 1997, resulting in over $72 billion in lost wages and wasted fuel.

The congestion problem can be addressed employing different measures ranging from building new roads to a number of congestion management strategies such as ride sharing programs. It has been recently realized that mere infrastructure expansion cannot provide a complete solution to these problems due to economic and environmental reasons or, in metropolitan areas, simply due to lack of space [2].

2. INTELLIGENT APPROACH TO CONGESTION PROBLEM: RAMP METERING

Since new construction is often not feasible or insufficient to significantly reduce congestion, the transition from inefficient to optimal traffic conditions can be achieved if the conventional use of the freeway infrastructure is improved by suitable control actions such as ramp metering, real-time speed control, and others.

Ramp metering is one of the most widely used control measures that are historically employed in freeway networks. Ramp metering is a direct and efficient way to control and upgrade freeway traffic by regulating the number of vehicles entering the freeway. The rate of metering is calculated depending on the specific strategy deployed.

Ramp metering aims to maintain uninterrupted, non congested flow on the freeway, thereby providing increase in mainline throughput due to avoidance or reduction of congestion duration. In many cases, ramp metering also enables a smoother ramp merging operation, which helps to maintain safe operation, by breaking up the platoons from entrance ramps to reduce the chance of traffic breakdown by the ramp traffic [3].

It is well known, from previous theoretical investigations and field operational tests, that ramp metering has various positive effects, if appropriately applied, such as [10]:

- Maintain freeway operations at noncongested condition
- Maximize mainline throughput
- Increase travel speed (upstream and/or downstream, depending on the strategy)
- Reduce travel time
- Reduce auto emissions and accidents due to a smoother mainline flow

There exist various kinds of ramp metering algorithms, some of which have been tested and implemented in the USA and Europe, while others at the empirical stage waiting to undergo the same procedures.

Overall, there are two types of ramp metering control systems:

Local Ramp Metering: A local ramp control system considers an isolated section of the network consisting of a freeway section with one on-ramp, and the controller responds only to the changes in the local conditions.

Systemwide Ramp Metering: Systemwide ramp metering is the application of metering to a series of entrance ramps.

Another ramp metering strategy that combines local and systemwide ramp metering is known as Hierarchical Ramp Metering. A systemwide model at the upper level defines the overall desired network states, while a local model at the lower level performs to adjust the metering rate to achieve system states close to the system target.

Based on traffic responsiveness, ramp metering can be divided into three categories:

Operator Controlled Metering: The freeway section (consisting of on-ramps) to be metered is controlled by an operator with the help of cameras and/or other methods.

Pretimed Ramp Metering: Pretimed metering is the simplest form of on-ramp metering. Ramp metering rates are constant and determined based on off-line demand for particular time-of-day historical traffic observation data, without the use of real-time measurements of sensors. It can be effective in eliminating recurrent congestion, if severe incidents or sudden changes in demand that cannot be captured by the historical measurements do not occur. However, since traffic demand is not constant, it varies during day, and on different days. Moreover, incidents may perturb traffic conditions in a nonpredictable way. All these unexpected fluctuations in demand can render pretimed ramp metering strategies ineffective. These pretimed ramp metering strategies may thus lead either to overload of the mainstream flow (congestion) or to underutilization of the freeway by achieving the opposite of it is trying to avoid, congested traffic conditions on the freeways.

Traffic Responsive Metering: In contrast, traffic responsive metering rates are determined based on information about the state of the traffic flow on the mainline and/or on the ramp traffic conditions. Based on the prevailing traffic conditions captured by real-time traffic data, such as occupancy, flow rate on the freeway and/or ramp, the metering rates are varied over time to effectively respond to traffic fluctuations.

2.1 Local Ramp Metering Control Strategies

Some local ramp metering control strategies are briefly discussed in the following sections.

2.1.1 Demand Capacity Control

In demand capacity control [1], metering rate is determined based on the comparison of upstream volume and downstream capacity. Mean upstream volume is compared either with a preset value of downstream capacity, or with a real-time value computed each time step using real-time sensor data. The difference between the upstream volume and the downstream capacity determines the metered ramp flow for the next control interval (e.g., 1 min). However, if the upstream volume becomes greater than the downstream capacity, minimum metering rate for the ramp is used.

2.1.2 Upstream Occupancy Control

This strategy uses real-time occupancy upstream of the on-ramp to determine the ramp metering rate of the next control interval. First, the upstream occupancy is measured during the current control time step. Then, a metering rate is selected among the predetermined metering rates based on the occupancy measurements taken during the current time step. Predetermined metering rate for a particular occupancy value is chosen using a plot of historical volume occupancy data collected at each measurement location. One example of such plots is given in Figure 1-2. If the measured occupancy exceeds or is equal to preset capacity occupancy, a minimum metering rate is selected.

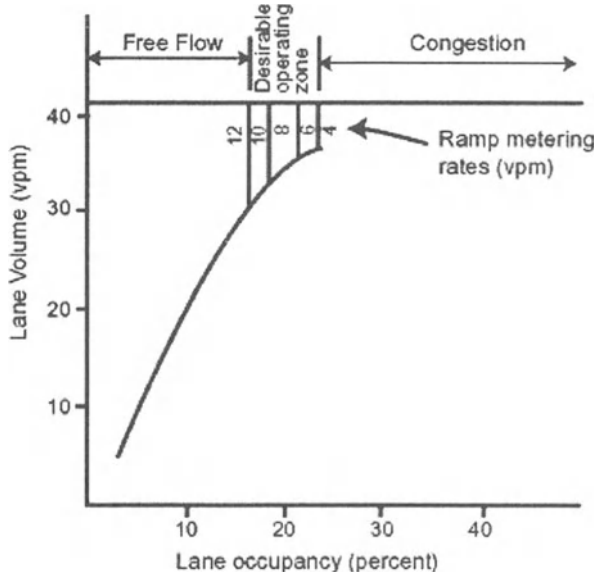

Figure 1-2: Typical Volume Occupancy Plot Used in the Calculation of Entrance Ramp Metering Rates, Chicago, IL [3]

2.1.3 Gap-Acceptance Control

Gap acceptance control uses occupancy measurements taken upstream of the ramp in order to determine the signal time in the next time period. When an available gap in the merging lane on the freeway, where vehicles on the ramp have sufficient time to merge into, is detected, the ramp signal turns green in response. This is intended to maximize the number of entrance ramp vehicles merging safely without causing disruption of the freeway traffic. However, this control faces some difficulties due to no lane change assumption, such as unreliability of acceleration behavior of vehicles, and lane changing, which closes the gaps measured by the detectors.

2.1.4 Closed-Loop Local Control Strategies

Ramp control systems can also be categorized as open loop and closed loop. In an open-loop ramp control system (demand capacity control, upstream occupancy control, gap acceptance control, etc.), the control input (e.g., ramp metering rate) is independent of the system output, the existing traffic conditions (e.g., volume, occupancy, gap, etc.). On the other hand, in closed-loop control, the system output is fed back, and the input is modified by an appropriate regulator to keep the output near its set value despite the

influences of time-variant disturbances (e.g., flow on the upstream of the ramp).

One of the most widely used algorithms in this category is ALINEA [10]. ALINEA is a linearized local-feedback control algorithm that adjusts the metering rate to keep the occupancy downstream of the on-ramp at a prespecified level, called the occupancy set point.

ALINEA uses feedback regulation to maintain a desired level of occupancy, or the target occupancy, which is usually chosen to be the critical occupancy, and apply the kinematic wave theory with locally calibrated fundamental diagrams as the underlying traffic model.

ALINEA (Figure1-3) closed-loop ramp metering strategy, suggested by Papageorgiou*et al. (1991)*, to be applied at the time instants $kT, k = 0,1,2,...$, for any sample time interval T (e.g., $T = 60\,\text{sec}$) is

$$r(k) = r(k-1) + K_R[\hat{o} - o_{out}(k)] \tag{1}$$

where $K_R > 0$ is a regulator parameter and $\hat{o}$ is a set (desired) value for the downstream occupancy (typically, but not necessarily, $\hat{o} = o_{cr}$ may be set, in which case the downstream freeway flow becomes close to q_{cap}, see Figure 1-3.

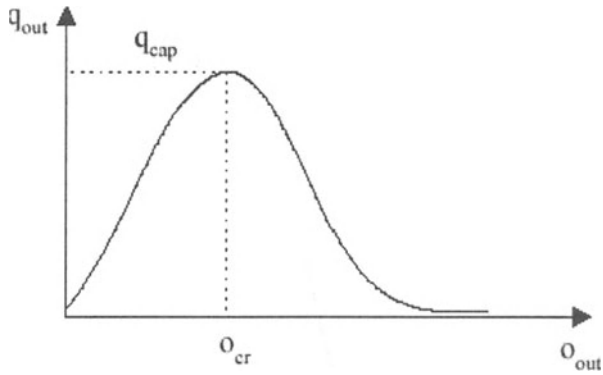

Figure 1-3: The Fundamental Diagram (May, Adolf)

The set value $\hat{o}$, may be changed any time, and thus ALINEA may be embedded into a hierarchical control system with set values of the individual ramps being specified in real time by a superior coordination level or by an operator.

A preliminary version of ALINEA and some popular previous control strategies have been implemented and tested on an on-ramp of the Boulevard Peripherique in Paris during an experimentation period of 6 months. Results of this study and other field results from current operational sites, such as Brancion, Chatillion, and Italie of the Boulevard Peripherique in Paris, showed a clear success of ALINEA in preventing congestion and increasing traffic throughput.

Artificial intelligence based closed-loop local control strategies have also received increasing attention recently. Fuzzy logic based ramp control proposed by Meldrum and Taylor [6] uses linguistic variables similar to human reasoning, and rules, which incorporate operator expertise. It is a nonlinear algorithm, which allows it to successfully handle a wide variety of situations, including incidents without modifying control parameters, and a robust control. The parallel nature of the FLC's rule base simultaneously balances multiple objectives. It is observed to produce systemwide benefits when implemented as the default metering algorithm on all 126 on-ramps in the greater Seattle area. It turned out that 80% of the 126 ramp meters performed best using the systemwide defaults. However, in order to handle special cases, such as inadequate ramp storage, secondary queues, etc. tuning was necessary.

Artificial neural networks were used to design nonlinear traffic-responsive ramp controls (Zhang et al. 1996, and Zhang et al. 1997). Neural network-based ramp control is shown to be able to directly handle nonlinear systems without resorting to linearization. It also can be tuned on-line, which makes them adaptive to a changing environment. Neural control algorithm uses feedback regulation concept similar to ALINEA to maintain a desired level of occupancy, or the target occupancy.

New Control is a new nonlinear control design proposed by Kachroo and Ozbay and discussed in later chapters of this book for an isolated ramp metering problem. This control law guarantees that $\lim_{k\to\infty}(\rho-\rho_{cr})^2 \to 0$, which is the objective of the controller. In fact, it guarantees that the rate of convergence of $o-o_{cr}$ is geometric at a rate dictated by the control gain K.

2.2 Systemwide Ramp Control Strategies

In many cases, in order to produce desired performance improvements, such as reduction of the volume to bring mainline volume below capacity, metering of a single on-ramp might not be sufficient. This is because of a number of possible factors, such as minimum metering volume constraints, lack of vehicle storage space, or too large a capacity deficiency. Therefore,

systemwide ramp metering strategies provide increased levels of control by distributing the metering task over a number of upstream ramps.

Some systemwide ramp metering controls are briefly introduced in this section.

Systemwide Pretimed Metering: This is the application of pretimed metering to a series of on-ramps. The metering rate for each ramp is determined in accordance with its local demand capacity constraint, and demand capacity constraints at the other ramps.

One example [9] of systemwide pretimed metering is optimal ramp metering algorithm that uses a fixed time of day input volumes. The objective is to maximize the number of vehicles served when the demand is very high. This problem can be represented as a linear programming problem that produces optimal input volumes in steady state. Computation time and storage needed to solve this linear programming problem increase with the number of unknowns and constraints and for larger networks with complex situations on-line solution generation might not be feasible.

Systemwide Traffic Actuated Metering: Dynamic optimal ramp control [8] is one example of systemwide traffic actuated metering. This type of control strategy overcomes the shortcomings of the pretimed version, in which mainline flow is assumed to be in the steady-state condition. A dynamic ramp control problem optimizes the performance index or control objective subject to the constraints of dynamic traffic flow model, and ramp queue and capacity constraints.

Systemwide versions of some of the feedback controllers are also available, such as METALINE, fuzzy logic algorithm for systemwide control, and so on. METALINE [10] is an extension of the control algorithm ALINEA. It was implemented on certain freeways in France, the United States, and the Netherlands. Similarly, there is also a systemwide version of fuzzy logic algorithm. Often only a few rules are needed for local control strategies, whereas for systemwide control, the rule base can be quite complex, which might require a great amount of effort to calibrate the parameters (tuning the rules and membership functions) [10].

3. RAMP METERING IMPLEMENTATIONS IN THE USA

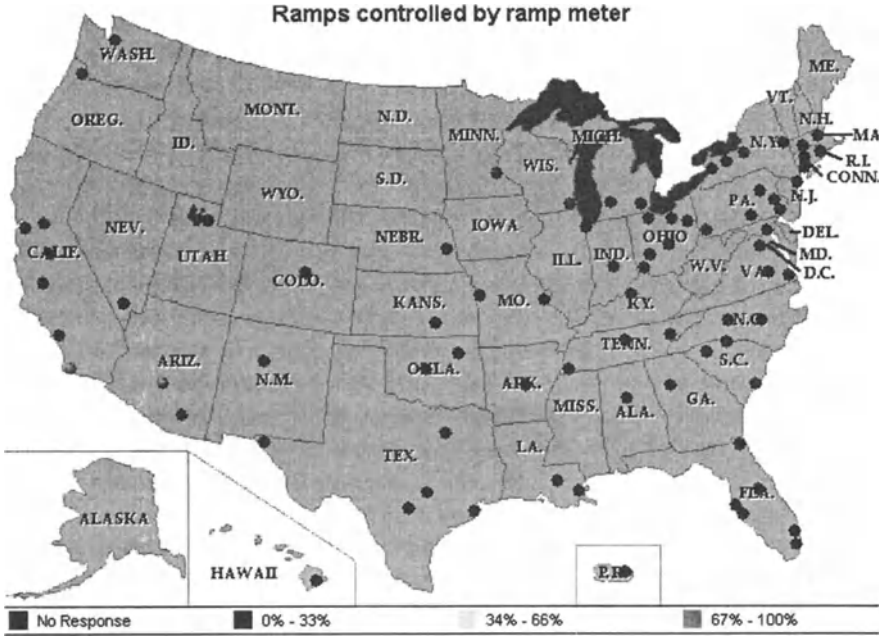

Figure 1-4: The Number of Ramps Controlled by Ramp Meter in the USA Is1981, 8% of the Whole Nation [4].

According to the ITS Deployment Tracking 2000 Survey Results, 24 agencies report having ramp metering technology.

Table 1-1: Ramp Metering Use in USA [4]

Metropolitan Area	Agency	Number
Minneapolis, St. Paul, MN	Minnesota Department of Transportation	427
San Diego, CA	Caltrans District 11	252
San Francisco, Oakland, San Jose, CA	Caltrans District 4	190
Los Angeles, Anaheim, Riverside, CA	Caltrans District 8	152
Phoenix, AZ	Arizona Department of Transportation	122
Chicago, IL; Gary, IN; Lake County, IL	Illinois Department of Transportation	113
Milwaukee, Racine, WI	Wisconsin Department of	113

	Transportation	
Portland, OR; Vancouver, WA	Oregon Department of Transportation	100
Seattle, Tacoma, WA	Washington State Department of Transportation Northwest Region	99
Houston, Galveston, Brazoria, TX	Texas Department of Transportation Houston District	97
New York, NY; Northern New Jersey, NJ; Southwestern Connecticut, CT	New York State DOT Long Island Region 10	81
Sacramento, CA	Caltrans District 3	75
Detroit, Ann Arbor, MI	Michigan Department of Transportation	60
Fresno, CA	Caltrans District 6	29
Los Angeles, Anaheim, Riverside, CA	Caltrans District 7	20
Allentown, Bethlehem, Easton, PA	Pennsylvania Department of Transportation Allentown	14
Salt Lake City, Ogden, UT	Utah Department of Transportation Region 2	9
Columbus, OH	Columbus City	8
Philadelphia, PA; Wilmington, DE; Trenton, NJ	Pennsylvania Department of Transportation District 6-0	6
Dallas, Fort Worth, TX	Texas Department of Transportation Fort Worth District	5
Atlanta, GA	Georgia Department of Transportation	5
El Paso, TX	Texas Department of TransportationEl Paso District	2
Salt Lake City, Ogden, UT	Utah Department of TransportationRegion 1	1
New York, NY; Northern New Jersey, NJ; Southwestern Connecticut, CT	Port Authority of New York and New Jersey	1
Total		1,981

Nine agencies report having traffic responsive ramp meters:

Table 1-2: Traffic Responsive Ramp Metering Use in USA [4]

Metropolitan Area	Agency	Number
Minneapolis, St. Paul, MN	Minnesota Department of Transportation	416
Los Angeles, Anaheim, Riverside, CA	Caltrans District 12	370
Los Angeles, Anaheim, Riverside, CA	Caltrans District 8	139
Milwaukee, Racine, WI	Wisconsin Department of Transportation	113
San Francisco, Oakland, San Jose, CA	Caltrans District 4	109

Sacramento, CA	Caltrans District 3	75
Fresno, CA	Caltrans District 6	29
Washington, DC	Virginia Department of Transportation	26
El Paso, TX	Texas Department of TransportationEl Paso District	2
Total		1,279

Eleven agencies report having pretimed ramp metering:

Table 1-3: Pretimed Ramp Metering Use in USA [4]

Metropolitan Area	Agency	Number
Portland, OR; Vancouver, WA	Oregon Department of Transportation	95
San Francisco, Oakland, San Jose, CA	Caltrans District 4	81
New York, NY; Northern New Jersey, NJ; Southwestern Connecticut, CT	New York State DOT Long Island Region 10	81
Los Angeles, Anaheim, Riverside, CA	Caltrans District 8	14
Minneapolis, St. Paul, MN	Minnesota Department of Transportation	11
Salt Lake City, Ogden, UT	Utah Department of Transportation Region 2	9
Philadelphia, PA; Wilmington, DE; Trenton, NJ	Pennsylvania Department of Transportation District 6-0	6
Atlanta, GA	Georgia Department of Transportation	5
El Paso, TX	Texas Department of Transportation El Paso District	2
New York, NY; Northern New Jersey, NJ; Southwestern Connecticut, CT	Port Authority of New York and New Jersey	1
Salt Lake City, Ogden, UT	Utah Department of Transportation Region 1	1
Total		306

Moreover, there are 962 centrally controlled ramp meters, and 370 corridor coordinated ramp meters in Los Angeles, Anaheim and Riverside, CA, which is the only location for such technology [4].

4. BENEFITS OF RAMP METERING

Ramp metering is implemented across the United States and Europe. There are no uniform or standard evaluation criteria and the measures of effectiveness (MOE) vary with the system objectives. In the following

section, some potential benefits of ramp metering are given with a couple of implementation examples.

Ramp metering provides efficient use of capacity. If there is excess capacity on surface streets, it may be worthwhile to divert traffic from congested freeways to surface streets, and discourage trip paths with high societal costs. In Detroit, Michigan, metering was initiated in 1982 with six ramps on eastbound I-94, with many more ramps added later. In Detroit [5], ramp metering increased speeds by about 8%, even though volumes on the mainline increased from 5600 vph to 6400 vph. Ramp metering can also result in temporal diversion, where drivers shift ramp arrival time. Empirical results show these shifts can result in up to 15% reductions compared with premetering volumes. This is mainly due to spreading out flow peaks over a longer period thus resulting in better freeway capacity utilization.

It is clear that if properly implemented, ramp metering can significantly increase peak speeds and reduce travel times on the freeway. However, in spite of the increase of ramp delays as a result of metering, systemwide delay reductions can still be significant, thereby providing overall improvements in the system. In Houston, Texas [5], ramp meters along the I-10 Katy Freeway were installed in late 1996, and evaluated in early 1997. The total daily estimated travel time savings were estimated as 2,875 vehicle-hours for an average value of time of $12.88 per vehicle-hour. These time savings were calculated to result in benefits of $37,030 per day. Similarly, in Long Island, New York, 60 ramp meters were installed on the eastbound Long Island Expressway as part of the Information for Motorists project (INFORMS). The evaluation was performed between 1987 and 1990. After the installation of the ramp metering system mainline travel times decreased from 26 to 22 minutes, and the average motorist using a metered ramp saved 13% in travel time. Average speeds increased from 29 to 35 mph. For the AM peak the number of detectors showing a speed less than 30 mph decreased by 50%. The average queue lengths at ramp meters ranged from 1.2 to 3.4 vehicles, representing 0.1% of vehicle-hours traveled.

Ramp metering can also improve safety by breaking up the platoons of entering vehicles from on-ramps, by leading to the reduction of sideswipe and rear-end type accidents at the merge areas. Likewise, since metering prevents bottlenecks, safer traffic conditions are expected due to the reduced variance in speed distributions. In Seattle, Washington, beginning in 1981, as part of the FLOW program, WDOT implemented metering on I-5 north of the Seattle CBD [5]. A six-year evaluation consisted of seventeen southbound ramps during the AM peak and five northbound during the PM peak along a 6.9-mile test corridor. Among other observed benefits, the accident rate dropped about 39%. In Minneapolis, meters were installed in the 1970s as part of the Twin Cities Metropolitan Area Freeway

Management System [5]. The first installation, along a section of I-35 E, included several meters initially operated on a fixed time metering scheme, but later upgraded to isolated traffic responsive operation. After 14 years of operation, in addition to other benefits, the average number of peak period accidents decreased by 24% and the peak period accident rate decreased by 38%.

Smoother traffic flow resulting in less speed variation on a metered freeway can lead to substantial reduction in emissions and fuel savings. In Portland, Oregon, meters were installed along I-5, a major north south link and important commuter route, in 1981. Sixteen meters in fixed cycle operation were evaluated. It was estimated that fuel consumption, including that caused by ramp delay, was reduced by 540 gallons per weekday.

5. PROBLEM DESCRIPTION

Ramp metering can help in providing a smooth flow of traffic on urban freeways. It can also help in alleviating congestion on the freeways. The design of ramp metering entails measuring some traffic variables on the freeway and adjusting the ramp metering rate to provide smooth flow. This structure of performing measurements using sensors and in real time adjusting the ramp metering rates renders the problem that of a closed-loop feedback control problem. The overall structure of a feedback control problem is shown in Figure 1-5.

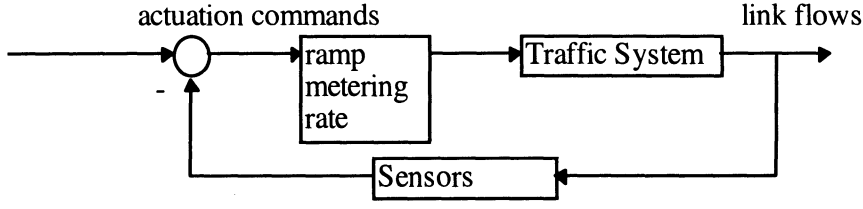

Figure 1-5: Block Diagram for DTR Feedback Control

Ramp metering attempts to keep mainline volumes below capacity by controlling the number of vehicles entering the freeway. Under ideal conditions, the wait on the entrance ramp would be compensated for by increased speeds once on the freeway. Ramp meters can increase freeway speeds while providing increased safety in merging and reducing rear-end

collisions on the ramps themselves. The topology of a ramp metering system is shown in Figure 1-6.

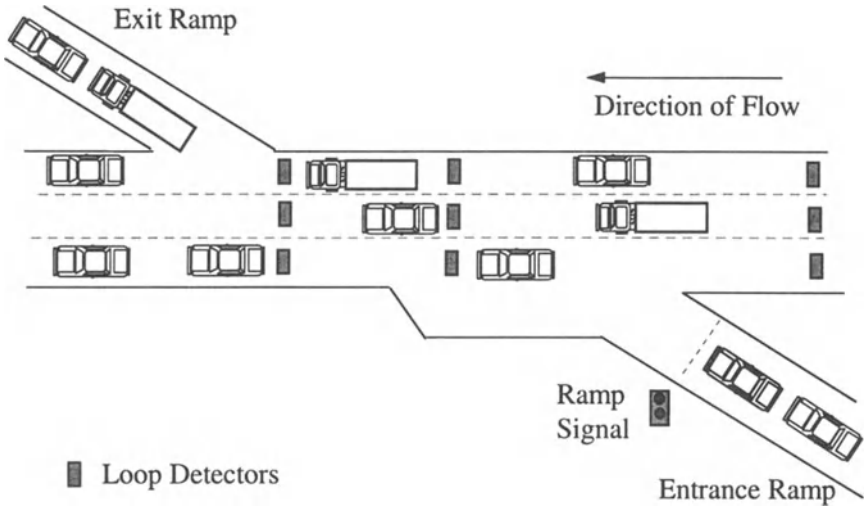

Figure 1-6: Ramp Metering Topology

Figure 1-6 shows the topology for an isolated ramp-metering problem. In general, ramp metering can be in multiple locations on a freeway connected to an arterial and a general freeway network. A network system is shown in Figure 1-7, where a freeway sections with multiple ramps is connected with an arterial street. Hence, this is a multiple input control problem, which will have travel time considerations on alternate routes, which vehicles not taking one upstream ramp might encounter in choosing the downstream ramp. The network problems are not studied explicitly in this paper but the modeling, analysis, and design in this paper can provide a starting point for developing feedback control strategy for network-level systems. At present, only off-line techniques are used for network-level problems. For instance, for a problem such as the one shown in Figure 1-7, the ramp flows are distributed in upstream ramps based on the knowledge of traffic demand and capacity in the various sections. This is done off-line, and then the calculated ramp rates are implemented. A very powerful method would be for the system to calculate these based on real-time information in a feedback setting. Isolated ramp control in general can also be used as a part of a system-level network control in which the isolated ramp plays a role in part of an overall scheme for control and coordination in a hierarchical methodology. Hierarchical

technique coordinates between various local controllers to achieve some overall global performance.

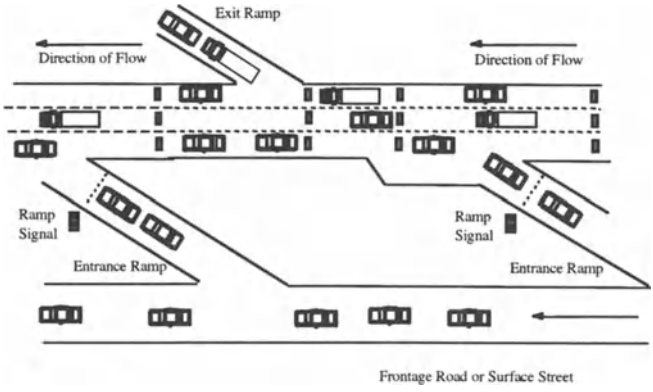

Figure 1-7: Coordinated Ramp Metering

6. PRELIMINARY CONSIDERATIONS FOR USING FEEDBACK CONTROL FOR RAMP METERING

Feedback control for ramp metering can be an effective solution for alleviating traffic congestion. However, the success of such a system depends on the effective modeling of the system as well as the design of the appropriate control law. The designer of the controller needs to address issues such as controllability and observability of the traffic system, actuation and sensing, robustness, and stability of the closed-loop system shown in Figure 1-5.

Actuation and sensing: The actuation of this system is achieved by the light signal which indicates whether the vehicles can go into the freeway or not. State variables such as the traffic density, average traffic speed, etc. can be sensed using various types as traffic sensors such as inductive loops, traffic cameras, transponders, etc.

Controllability and Observability: The designer should analyze the system before designing the controller to determine if the system is controllable and observable. Controllability implies that a suitable control law can be devised in order obtain a desired response from the system. Observability implies that the system state variables can be observed from the sensed output.

Robustness and stability: The effectiveness of the control design can be measured in terms of its robustness, stability, and transient characteristics. A robust controller will perform well even in the presence of uncertainties in the nominal model of the system. Models representing traffic systems cannot represent the system fully, and therefore there are uncertainties in the system, which have to be dealt with. A control law should provide stability to the system and desirable transient response.

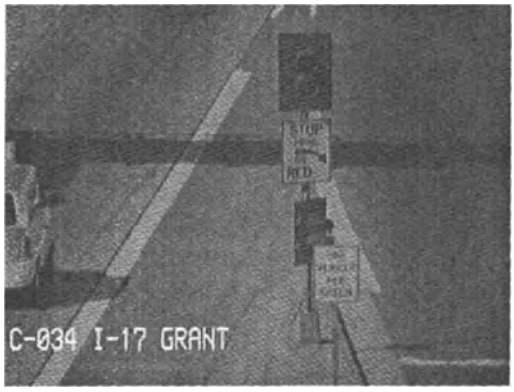

Figure 1-8: Ramp Signal

Figure 1-9: Inductive Loops [36], [37]

7. EFFECT OF RAMP METERING

To understand the need for ramp metering, we will present here some simulation runs. Let us consider a highway section connected to an input actuated ramp. In this section we present a macroscopic simulation for the

system. In macroscopic simulation we use a fluid flow model for the traffic that is characterized by traffic density on the mainline and queue length for the input ramp. We will not go into the details of mathematical modeling or numerical simulation technique in this chapter. Those will be covered in detail in subsequent chapters. The present section will use the results of the simulation to show the importance of ramp metering. The simulation is run using Matlab. Files oramp.m, orampdynamics.m, u.m, fcoord.m, and rcoord.m are used in the simulations in this section. File oramp.m is the file that is executed in Matlab. It uses the other files for the simulation. The files are listed below.

```
% Ramp Metering Code
clear;
clf;
clc;
global rhom rhoc vf gain l

% Input Parameters
l=1;  The length of the freeway section

rhom = 60;                    % Jam density
rhoc = rhom/2;                % Critical density
vf = 15;                      % Freeflow velocity
t0 = 0.0;                     % Initial time
tf = 15;                      % Final time
h = 0.01;                     % Time step
m = (tf-t0)/h;                % No. of steps
x0=[35 5];                    % Initial state values (traffic
density and queue length)
T=zeros(m,1);            % m rows (mx1)
X=zeros(m,length(x0));  % m rows, length state columns
T(1)=t0;
f(1)=fcoord(t0);
r(1)=rcoord(t0);
uvar(1)=u(t0,x0);
X(1,:)=x0;
%There are m-1 steps and m points maximum
for I=1:m-1;
   tI=T(I);
   clc;
   tI
  xI=X(I,:);
  k1=h*feval('orampdynamics',tI,xI)';   % Runga Kutta Algo.
  k2=h*feval('orampdynamics',tI+h/2,xI+k1/2)';
  k3=h*feval('orampdynamics',tI+h/2,xI+k2/2)';
```

```
k4=h*feval('orampdynamics',tI+h,xI+k3)';
```

```
X(I+1,:)=xI+(k1+2*k2+2*k3+k4)/6;
T(I+1)=t0 + h*I;
f(I+1)=fcoord(T(I+1));
fa(I)=f(I);
r(I+1)=rcoord(T(I+1));
uvar(I+1)=u(T(I+1),X(I+1,:));
ua(I)=uvar(I);

  if (X(I+1,2)<0),     % Projection Dynamic Constraints
      X(I+1,2)=0;
  end
  if (X(I+1,1)<0),
     X(I+1,1)=0;
  end
 if (X(I+1,1)>=rhom),
     X(I+1,1)=rhom;
  end


 if (X(I,1)/rhom)>0.9,      % Actual Variables Calculation
    qout = vf*X(I,1)*0.1;
  else
    qout = vf*X(I,1)*(1-X(I,1)/rhom);
  end

 Res = qout + (X(I+1,1)-X(I,1))/h;

 if (X(I+1,2)<0)&(X(I+1,1)>=rhom),

     ua(I) = rcoord(T(I));
     fa(I) = Res - ua(I);
  end

  if (X(I+1,2)>0)&(X(I+1,1)>=rhom),
     ua(I) = uvar(I);
     fa(I) =  Res - ua(I);
  end

 if (X(I+1,2)<0)&(X(I+1,1)<rhom)&(X(I+1,1)>0),
     ua(I) = rcoord(T(I));
```

```
    end
```

```
 end

 ua(m)=uvar(m);
 fa(m)=f(m);

subplot(221);
plot(T,X(:,1));
title('Traffic Density');
xlabel('Time');
subplot(222);
plot(T,X(:,2));
title('Queue Length');
xlabel('Time');
subplot(223);
plot(T,f,'-',T,r,'-.');
title('Mainline Inflow & Ramp Inflow');
xlabel('Time');
subplot(224);
plot(T,uvar);
title('Control Variable');
xlabel('Time');

pause;
subplot(221);
plot(T,ua,'-',T,uvar,'-.');
title('Actual and Demanded Applied Control');
xlabel('Time');
subplot(222);
plot(T,fa,'-',T,f,'-.');
title('Actual and Demanded Inflow');
xlabel('Time');
subplot(223);
plot(T,uvar-ua);
title('Control Difference');
xlabel('Time');
```

```
subplot(224);
plot(T,f-fa);
title('Inflow Difference');
xlabel('Time');
```

Code Listing 1: oramp.m Matlab file

```
function dy = orampdynamics(t,y)
dy = zeros(2,1);          % a column vector
global rhom vf l
%closed loop dynamics
if (y(1)/rhom)>0.9,
   qout = vf*y(1)*0.1;
else
   qout = vf*y(1)*(1-y(1)/rhom);
end

dy(1) = (-qout+fcoord(t)+u(t,y))/l;
dy(2) = rcoord(t)-u(t,y);
```

Code Listing 2: orampdynamics.m Matlab file

```
function u = u(t,x)

global rhom vf rhoc gain l
v1=vf*(1-(x(1)/rhom));
qout1=v1*x(1);

%u = rcoord(t);
u=0;
```

Code Listing 3: u.m Matlab file

```
function fcoord = fcoord(t)
fcoord = 73*(1.5+sin(1.0*t));          % mainline inflow
```

Code Listing 4: fcoord.m Matlab file

```
function rcoord = rcoord(t)
```

```
rcoord = 25*(1.5+sin(0.5*t));          % ramp inflow
```

Code Listing 5: rcoord.m Matlab file

The simulations presented here are based on the scenario of an isolated ramp metering problem shown in Figure 1-5.

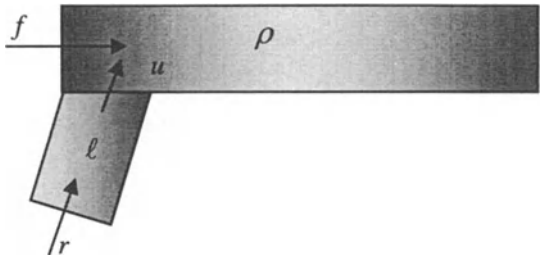

Figure 1-10: Isolated Ramp Metering Simulation

The main highway section has an inflow and a flow rate given by f. The inflow controlled from the ramp is given by u. The ramp has a queue of length ℓ, and has an inflow to it given by r. The traffic density on the main highway section is shown as the variable ρ. If the traffic density reaches the "jam density" (taken to be 60 in these simulations) then there is a traffic jam. In the simulation presented below, we let the ramp controller not allow any vehicles to enter the highway. The results are shown.

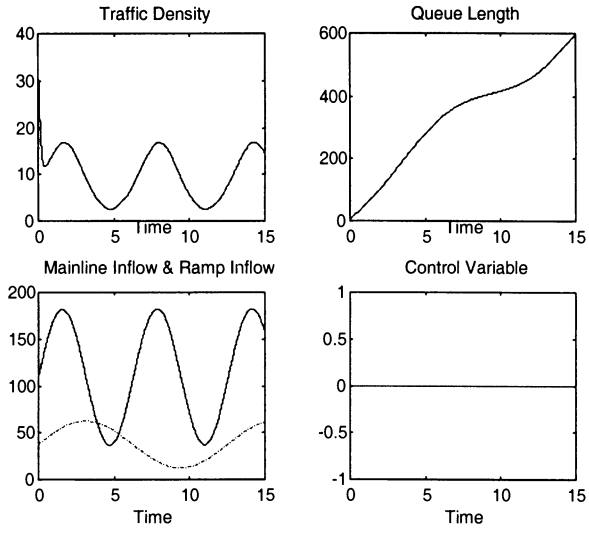

Figure 1-11: Simulation Results for No Ramp Input

This simulation shows that when the ramp controller does not allow any vehicles to enter the highway from the ramp, the highway density value remains much below the jam density. However, the queue length on the ramp keeps increasing. The simulation results when the ramp controller allows all the cars at the ramp to enter the highway are shown below. In simulating this scenario, we replace the line u = 0 in the file u.m with u = rcoord(t).

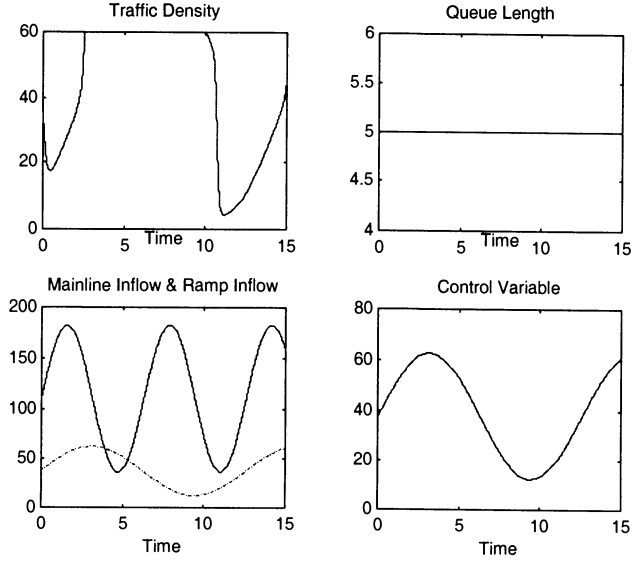

Figure 1-12: Simulation Results for Open Always Ramp

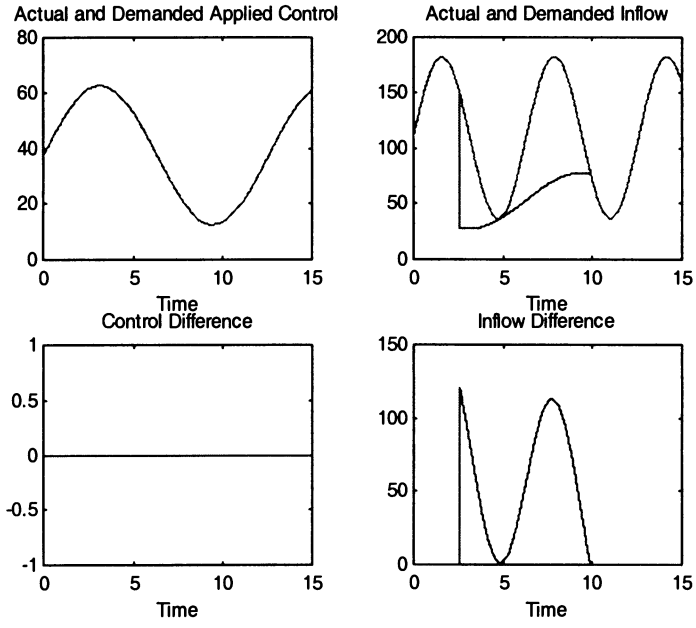

Figure 1-13: Actual versus Demanded Values of Variables for the Open Always Ramp

We see in Figure1-13 that although the queue length here remains fixed, the mainline traffic density reaches the jam density and that causes congestion on the highway. There are some constrains on the variables in the simulation. For instance, the traffic density has to be positive and cannot exceed the jam density. Similarly, the queue length also has to be positive. Therefore, sometimes the demanded flows into the ramp and the mainline are not always satisfied. For instance, when in a section the traffic density has reached the jam density and very little flow is coming out of the section, if we allow a large amount of input flow to enter the section, the traffic density value would rise to above the jam density. This would not be possible physically, since jam density implies that there is no more space for vehicles in the section. Therefore, the section only can accommodate that much inflow that does not make the density value go above the jam density. This effect essentially causes shock waves. This can be seen in real traffic conditions where downstream incidents affect the behavior at upstream. These results are shown in Figure 1-14. We cover these constraint requirements using "projection dynamics." The details of dynamics, numerical simulations, and projections will be covered in detail in later

chapters. In this section, we have just seen that in one extreme when the ramp is off, we get very large queues, and when it is on all the way, it can create congestion. Therefore, our aim should be to design a ramp flow rate that is a function of the current state of the system, so that we obtain optimal performance. This book will systematically present the models, control designs, and results of the applications of feedback control to the ramp control problem.

8. FEEDBACK CONTROL

To understand feedback control, let us discuss the signal timing control problem. A pretimed signal-timing plan has no feedback since there is no use of the real-time traffic variables. Time of day signal timing plans also do not fall into the category of real-time feedback control even if the decisions for which traffic plans to use might be dependent on the average traffic conditions. Although in this case there is a feedback loop, the loop is not closed at each sample interval when data are available. A real-time signal timing control would be the case when traffic data from sensors such as cameras or loop detectors at every sample time (or some time interval comparable to that) are input to a processor, which then makes immediate decisions about affecting the traffic intersection control signals. This is very similar to the case when a police officer directs traffic at an intersection with his hands after looking at the queues at each time and deciding which stream of traffic to block and which stream to let go. The police officer's eyes do the work of traffic sensors, his or her brain does the job of the processor, and his or her hands do the job of signal lights.

The topic of control systems deals with dynamic systems that can be controlled by some variables to produce a desired system behavior. There are two types of control systems: open loop and closed loop. Open-loop systems are generally used for planning kinds of problems, where one needs to determine the control values for some time interval. On the other hand, closed-loop systems (also called feedback control systems) are control systems where the control variable is a function of the output of the system. For instance, we might be driving a car with the aim of maintaining a constant speed and staying in the middle of a lane. These are the two objectives of the controller. The control actuators are the steering angle and the throttle pedal. The driver (controller) of the case reads the speed of the car and if it is different than the desired speed, the driver presses or releases the pedal. Similarly, his steering angle also changes depending on how close he is to the center of the lane. Hence, this is a closed-loop system where at

each time, the control variables are the pedal angle and lateral deviation. This book is concerned with the design of feedback control laws for ramp metering systems.

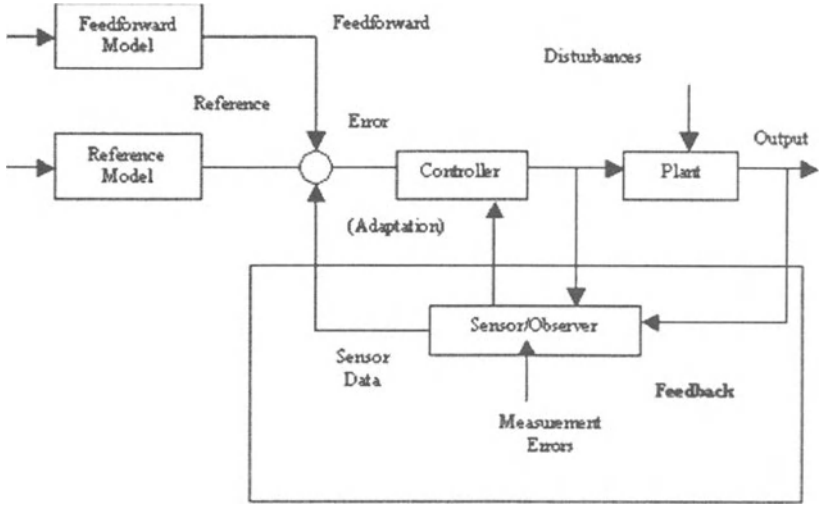

Figure 1-14: Feedback Control Block Structure

Figure 1-14 shows a generic control block diagram. The model of the system to be controlled (the traffic system in this case) is represented by the "Plant" block. The plant can be modeled as linear time invariant (LTI) differential equations, linear time varying (LTV) differential equations, or nonlinear differential equations. More generally, the plant could also be represented by partial differential equations. If we remove the "feedback" connection shown, then the system will become open-loop control. The controller acts on the error signal, which is generally the difference between the desired state and what is obtained from the sensor data. There are also some controllers that are adaptive. The adaptation mechanism allows for real-time tuning of some controller parameters based on the input and the output of the system. In essence, the controller calculates how the input is affecting the output of the system in the feedback control loop, and then changes the control parameters in realtime to further improve the performance of the system.

8.1 Control Design Steps

The first step in control design is to come up with a mathematical model of the system to be controlled. These models are usually represented in terms of differential equations where the state variables represent various physical entities of the system. For instance, in vehicle control, the speed of the car is a state variable. The model thus obtained can be analyzed and a control law designed. The model of a system is obtained either from basic principles or by data fitting. Conducting experiments on the system, collecting the data, and then performing some data fitting obtain the parameters of the model. Detailed knowledge of the system to be controlled is the most important aspect to a successful control. Design should be given the most importance. Once the control law is designed, it can be tested in simulations with the mathematical models and then on the actual system. With the advent of microprocessors and sensor technology, most of the control implementation is based on their usage. Microprocessors are used to read the sensor values and control the actuators. The control algorithms are written in assembly language or a higher-level language like C.

Control systems are generally designed using either ordinary differential equations or difference equations. The following section gives a brief introduction to both.

8.2 Ordinary Differential Equations

The relation between a variable and its derivatives with respect to an independent variable is called an ordinary differential equation (ODE). In control theory problems, the independent variable is time t. An example of an ODE is

$$\ddot{y} + 2t\dot{y} - 3\ddot{y}^2 = 0 \tag{2}$$

The highest degree of the dependent variable x defines the degree of the system. Equation (2) has the degree 3. It is a nonlinear ODE because of the presence of the term $\ddot{y}^2$, and it is time varying (inhomogeneous) due to the presence of the time variable t in the second term. This ODE can be represented in a vector differential equation form

$$\dot{x} = f(t, x(t)) \tag{3}$$

where x is the state variable vector, $x = [x_1, ..., x_n] = [y, \dot{y}, ..., y^{n-1}]^T$, and n is the system order, which is 3 for this case. We can rewrite (2) now as

$$\begin{aligned} \dot{x}_1 &= x_2 \\ \dot{x}_2 &= x_3 \\ \dot{x}_3 &= 3x_3^2 - 2tx_2 \end{aligned} \tag{4}$$

which is of the form (3) with $f(t,x(t)) = [x_2, x_3, 3x_3^2 - 2tx_2]^T$. In general, if $f(t,x(t))$ is linear in x, it is called a linear system; otherwise, it is nonlinear. Moreover, if it is independent of t, it is called time invariant; otherwise, it is called time varying. The initial values problem for an ODE is the problem of finding the value of $x(t)$ for all future time, when system (3) is given with the value of x at initial time.

8.3 Difference Equations

The general form of a vector difference equation is similar to (3) and is given by

$$x(k+1) = f(k,x(k)) \tag{5}$$

where k is the sample time instant. Instead of derivatives in continuous times, we have time incremented terms such as $x(k+1), x(k+2)$, etc. Difference equations are classified the same way, as are ODE. For difference equations, we are also interested in initial value problems.

8.4 Feedback Control Example

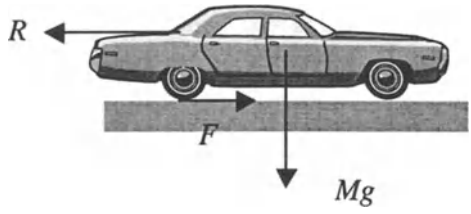

Figure 1-15: Feedback Control Example

Mathematically, feedback control laws are designed so that the control variable is a function of the sensed variables, and the error variable goes to zero in time. Let us consider a simple model for the longitudinal cruise control for a car as shown in Figure 1-15.

The tractive force driving the car is given by F, which is the control variable (and can be controlled by the throttle angle in the engine intake manifold). R represents all the resistance to the car longitudinal motion and includes the air drag and other resistances like rolling and grade resistances. R in general is dependent on the car speed. M is the mass of the vehicle and g is the acceleration due to gravity. If we denote x as the velocity of the car (state variable for the system) and x_d the desired speeds, then we can write the differential equation for the system as

$$\dot{x}(t) = -\frac{R(x,t)}{M} + \frac{F(t)}{M} \tag{6}$$

Our aim is to design a control law that will take the error variable defined as $e(t) = x(t) - x_d(t)$ to zero. Since the desired cruise speed is constant, we have

$$x_d(t) = 0 \tag{7}$$

Subtracting (6) from (7) yields

$$\dot{e}(t) = -\frac{R(x,t)}{M} + \frac{F(t)}{M} \tag{8}$$

Now, if we take the control law as

$$F(t) = M[\frac{R(x,t)}{M} - ke(t)] \tag{9}$$

then by substituting this equation in (8) we obtain the closed-loop dynamics of the system as

$$\dot{e}(t) = -ke(t) \tag{10}$$

The solution of this differential equation is easily obtained by integration and is given by

$$e(t) = e(0)e^{-kt} \tag{11}$$

This shows that $e(t)$ will go exponentially to zero if we choose k to be a positive constant in the control law (9). This plot of $e(t)$ is shown in Figure

1-16, where t is the x-axis, and $e(t)$ is on the y-axis starting from an initial value of 0, and with a value of 1 for k.

This example was easy, but in general, there are many complications in designing control systems. For example, usually the problem will have a higher order than this system. The number of control variables can also be more than one. There can be uncertainties in the system, implying that the controller does not have exact knowledge of the parameters such as M and R.

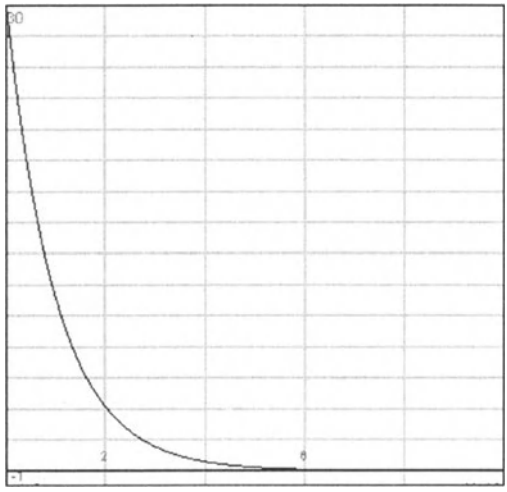

Figure 1-16: Plot of $e(t)$

9. SUMMARY

In this chapter, we studied:

- what ramp metering is
- how ramp metering is useful for traffic congestion control
- what researchers have done in this area
- various types of ramp metering problems
- what feedback control is and how it can be useful in ramp metering,
- some supporting simulation results
- brief introduction of ordinary differential equations and difference equation

10. QUESTIONS

1. What is ramp metering and why is it important?
2. Give two objectives that a ramp metering control law should satisfy
3. What is the difference between open-loop and closed-loop traffic control?
4. What is feedback control, and how can it be applied to ramp metering?
5. What kinds of sensors are used for traffic surveillance, and what traffic variables do they sense?
6. What are some mechanisms to control traffic behavior?
7. Explain why one of the objectives of ramp metering control is to keep the freeway density below critical level. (Hint: Use fundamental diagram)
8. What are the types of ramp metering problems and the ways to provide ramp control?
9. Choose one ramp metering strategy. Define the performance measures that are used to evaluate the ramp control.
10. Name possible drawbacks of ramp metering. How can those drawbacks be dealt with? Give (at least) one suggestion.
11. For a closed-loop ramp metering control, define state variables, input and output variables. Show the system in simple block diagram form.

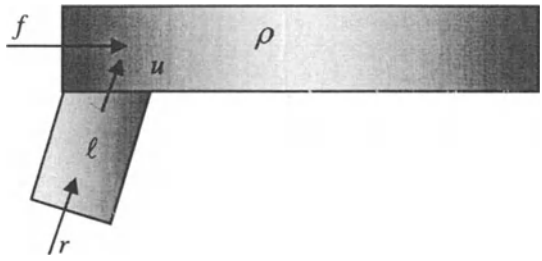

11. PROBLEMS

1. Take the file named u2.m and change the name to u.m and run the program. Compare the results (plots) with Figure 1-11 and explain the differences. And give the advantages of ramp metering control from the results.
2. Using the parameters given in the diagram write down the projection dynamic constraints for a ramp metering problem. (Hint: 1) Use 1 min time steps, and take the length of the freeway section as 1 unit) 2) Study the simulation code in section 6.

12. REFERENCES

1. Effect of Responsive Limitations on Traffic-Responsive Ramp Metering (Banks, 1990)
2. http://www.fhwa.dot.gov/congestion/index.htm
3. Traffic Control Systems Handbook, U.S. department of Transportation, Federal Highway Administration, Report No.: FHWA-SA-95-032,1996
4. http://itsdeployment2.ed.ornl.gov/its2000/definitions.asp ITS Deployment Tracking, 2000 Survey Results
5. http://www.path.berkeley.edu/~leap/TTM/Traffic_Control/ramp_metering.htm
6. FHWA Traffic Control handbook, June 1996.
7. Papageorgiou, M.,"Traffic Control," In Handbook of Transportation Science, R.W. Hall, editor, Kluwer Academic 1999, 233-267.
8. Zhang, H. M., and Ritchie, S. G., Freeway ramp metering using artificial neural networks, Transportation Research C, 5,1997, 273-286.
9. H. Zhang, S. G. Ritchie, W. W. Recker, Some General Results on the Optimal Ramp Control Problem.
10. Van Aerde, M., "Evaluation of Ramp Metering System Design," Working Paper, Department of Civil Engineering, Queen's University, Kingston, Canada, 1997.
11. Taylor, C, and Meldrum, D, "Evaluation of a Fuzzy Logic Ramp Metering Algorithm: A Comparative Study Between Three Ramp Metering Algorithms Used in the Greater Seattle Area", WA-RD Technical Report to be published, National Technical Information Service.
12. Kosko, B., Neural Networks and Fuzzy Systems: Dynamical Systems Approach to Machine Intelligence, Prentice-Hall, 1993.
13. "Results of the On-Line Implementation and Testing of a Fuzzy Logic Ramp Metering Algorithm", Cynthia Taylor, Deirdre Meldrum, and Les Jacobson, TRB Paper #00-1624, A3A09.
14. Papageorgiou, M.,"Traffic Control," In Handbook of Transportation Science, R.W. Hall, editor, Kluwer Academic 1999, 233-267.
15. Zhang, H. M., Ritchie, S.G. and Recker, W. W., Some general results on the optimal ramp control problem, Transportation Research - C, 4, 2, 1996,. 51-69.
16. Wattleworth, J. A., "System Demand Capacity Analysis on the Inbound Gulf Freeway," Texas Transportation Institute Report. 24-8, 1964.
17. Drew, D. R., "Gap Acceptance Characteristics for Ramp Freeway Surveillance and Control," Texas Transportation Institute Report. 24-12, 1965.
18. Pinnell, C.,Drew, D. R., McCasland, W. R., and Wattleworth, J. A., "Inbound Gulf Freeway Ramp Control Study I," Texas Transportation Institute Report. 24-10, 1965.
19. Pinnell, C.,Drew, D. R., McCasland, W. R., and Wattleworth, J. A., "Inbound Gulf Freeway Ramp Control Study II," Texas Transportation Institute Report. 24-10, 1965.
20. ITE Traffic Control Systems Handbook, Institute of Transportation Engineers, 1996, 4-14 4-40.
21. Yuan, L. S., and Kreer, J. B., "Adjustment of Freeway Ramp Metering Rates to Balance Entrance Ramp Queues," Transportation Research, .5,1971, 127-133.
22. Wattleworth, J. A., and Berry, D. S., "Peak Period Control of a Freeway System-Some Theoretical Investigations," Highway Research Record, 89, 1-25.
23. May, A. D., "Optimization Techniques Applied to Improving Freeway Operations," Transportation Research Record, 495, 75-91.

24. Hellinga, B., and Van Aerde, M, "Examining the Potential of Using Ramp Metering as a Component of an ATMS ," Transportation Research Record, 1494, pp. 75-83, 1995.
25. Papageorgiou, M., Habib, H. S., and Blosseville, J. M., "ALINEA: A Local Feedback Control Law for On-ramp Metering," Transportation Research Record 1320, 1991, 58-64.
26. Chen, L. L., May, A. D., and Auslander, D. M., "Freeway Ramp Control using Fuzzy Set Theory for Inexact Reasoning," Transportation Research A, . 24 , 1990, .15-25.
27. Goldstein, N. B., and Kumar, K. S. P., "A Decentralized Control Strategy for Freeway Regulation," Transportation Research-B, 161982, 279-290.
28. Zhang, H., and Ritchie, S. G., and Lo, Z., "A Local Neural Network Controller for Freeway Ramp Metering,"IFAC Transportation Systems, Tianjin, 1994, 655-658.
29. Masher, D. P., Ross, D. W., Wong, P. J., Tuan, P. L., Zeidler, H. M., and Petracek, S., "Guidelines for Design and Operation of Ramp Control Systems," Stanford Research Institute, Menid Park, CA, 1975.
30. Hadj-Salem, H, Davee, M. M., Blosseville, J. M., and Papageorgiou, M., "ALINEA: Un Outil de Regulation d'Acces Isole sur Autoroute," Rapport INRETS 80, Arcueil, 1988.
31. Pera, R. La, and Nenzi, R., "TANA An Operating Surveillance System for Highway Traffic Control," Proc., Institute of Electrical and Electronics Engineers, 61, 1973, 542-556.
32. Helleland, N., Joeppen, W., and Reichelt, P., "Die Rampendosierung an der A5 Bonn/Siegburg der BAB 3 in Richtung Koln," Strassenverkehrstechnik, . 22,.1978, 44-51.
33. NN: Ramp Metering in Auckland, Traffic Engineering and Control, 24, 1983, 552-553.
34. Owens, D., and Schofield, M. J., "Access Contr on the M6 Motorway: Evaluation of Britain's First Ramp Metering Scheme," Traffic Engineering and Control, 29, 1988, 616-623.
35. Buijn, H., Middelham, F., "Ramp Metering Control in the Netherlands," Proc., 3rd IEE International Conference on Road Traffic Control, United Kingdom, 1990, 199-203.
36. http://www.azfms.com/About/ramp.html
37. http://www.azfms.com/About/loop.html

Chapter 2

DISTRIBUTED RAMP MODEL

This chapter introduces the conservation-based Partial Differential Equation (PDE) model for the highway ramp system. Various static and dynamic equations are used to describe the relationship between traffic velocity and traffic density. A numerical model for simulation is presented for the PDE and some basic simulation results are shown.

1. CONSERVATION EQUATION

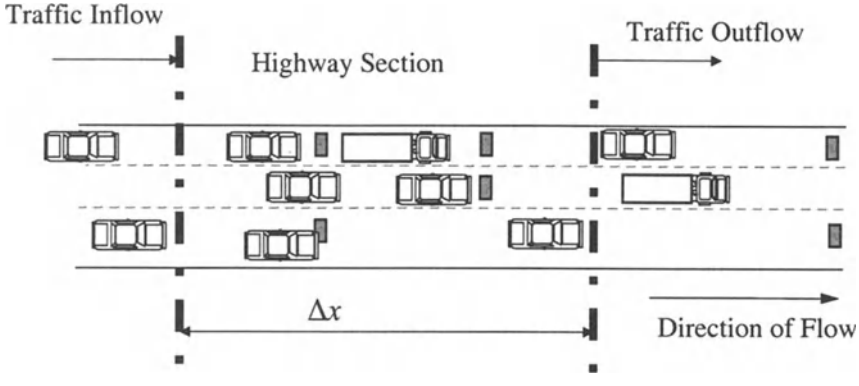

Figure 2-1: Highway Section to Illustrate Conservation Equation

The conservation equation lays the foundation for any mathematical model used for traffic systems. Essentially, it implies that vehicles cannot be created or destroyed in any section of the system. This is true everywhere

P. Kachroo et al., *Feedback Ramp Metering in Intelligent Transportation Systems*

except at the source nodes where the traffic is generated and the sink nodes where the traffic ends. Let us study the highway section as shown in Figure 2-1. In this figure, we see a highway section of length Δx. There is some traffic inflow into the section from the left that brings in vehicles into the section, and traffic flow out of the section that takes out vehicles from the right. Let us consider an amount of infinitesimal time Δt and consider the conservation law during that time. Let the total number of vehicles in the section at time t be given by $N(t)$. At time, $t+\Delta t$ the number of vehicles is given by $N(t+\Delta t)$. Therefore, the change in the number of vehicles in time Δt is given by

$$\text{Change in the number of vehicles in the section} = N(t+\Delta t) - N(t) \quad (1)$$

Let the flow of traffic be given as a function $q(t,x)$. This function indicates the number of vehicles flowing in the direction of traffic flow in a given unit time. The number of vehicles that enter the section in a given infinitesimal time Δt is $q(t,x)\,\Delta t$. Similarly, the number of vehicles leaving the same section at the right-hand side (in Figure 2-1) is given by $q(t,x+\Delta x)\,\Delta t$. Therefore, we have the following relationship.

$$\text{Change in the number of vehicles in the section} = [q(t,x) - q(t,x+\Delta x)]\Delta t \quad (2)$$

We see that we can equate the right-hand sides of equations (1) and (2) to obtain

$$N(t+\Delta t) - N(t) = [q(t,x) - q(t,x+\Delta x)]\Delta t \quad (3)$$

Now we will consider a fluid model representation of the same highway. This is called a hydrodynamic model where we consider the traffic to be a continuum rather than discrete vehicles. This model is shown in Figure 2-2. In this model we use $\rho(t,x)$ to indicate the traffic density as a function of time t and position x on the highway. If the section length Δx is infinitesimal, then we will have:

$$N(t) = \rho(t,x)\Delta x \quad (4)$$

Using (4) in (3) gives us the following equation:

$$[\rho(t+\Delta t,x) - \rho(t,x)]\Delta x = [q(t,x) - q(t,x+\Delta x)]\Delta t \quad (5)$$

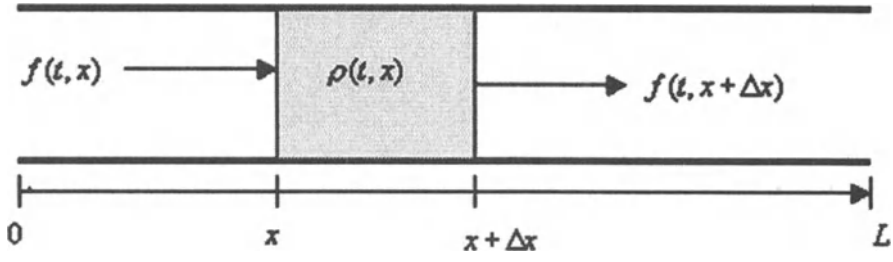

Figure 2-2: Traffic Continuum Model

Rearranging equation (5) yields

$$[\rho(t+\Delta t,x)-\rho(t,x)]/\Delta t=[q(t,x)-q(t,x+\Delta x)]/\Delta x \tag{6}$$

Taking the appropriate limits on both sides, and moving the right-hand side expression to the left gives

$$Lt_{\Delta t,\Delta x\to 0}\left[\frac{[\rho(t+\Delta t,x)-\rho(t,x)]}{\Delta t}+\frac{[q(t,x+\Delta x)-q(t,x)]}{\Delta x}\right]=0 \tag{7}$$

Equation (7) can be written in the following conservation equation form:

$$\frac{\partial\rho(t,x)}{\partial t}+\frac{\partial q(t,x)}{\partial x}=0 \tag{8}$$

Another way of deriving the conservation equation is as follows. The change in number of vehicles in the section of length Δx is given by

$$\frac{d}{dt}\int_{x}^{x+\Delta x}\rho(\ell,t)d\ell \tag{9}$$

The change in the number of cars in this section is also equal to the number of cars going out of this section subtracted from the number of vehicles coming in, as shown below:

$$\frac{d}{dt}\int_{x}^{x+\Delta x}\rho(\ell,t)d\ell=q(x,t)-q(x+\Delta x) \tag{10}$$

Now, we can use the fundamental theorem of calculus to rewrite equation (10) as

$$\int_{x}^{x+\Delta x} \frac{\partial \rho(\ell,t)}{\partial t} d\ell = -\int_{x}^{x+\Delta x} \frac{\partial q(\ell,t)}{\partial \ell} d\ell \tag{11}$$

Note that instead of the interval x and $x+\Delta x$ we could have used any interval from a to b, and the same analysis would work. Consequently, we obtain (8) from (11).

Conservation equations have been studied extensively and we refer to Refs. 1,2 and 3 as they relate to traffic flow.

2. DENSITY-FLOW RELATIONSHIP

Many models have been proposed to represent the relationship between traffic density and traffic flow. The following is a brief description of some of these models.

2.1 Greenshield's Model

In Greenshield's model, the speed density relationship is a linear relationship given by [4]

$$v = v_f\left(1 - \frac{\rho}{\rho_{\max}}\right) \tag{12}$$

Traffic flow, traffic speed, and traffic density have a fundamental relationship that is true in any model. These variables are related as

$$q = v\rho \tag{13}$$

Therefore, for Greenshield's model

$$q = \rho v_f\left(1 - \frac{\rho}{\rho_{\max}}\right) \tag{14}$$

The relationships between the three variables are shown in Figure 2-3. In the first plot in the figure, we see that the slope of the flow density

relationship is equal to the free flow speed. This can be shown by differentiating (14) to obtain

$$\frac{dq}{d\rho} = v_f - 2v_f \frac{\rho}{\rho_{\max}} \tag{15}$$

The value of this slope at $\rho = 0$ is v_f. We can obtain the maximum flow $\rho_{\max}$ by equating (15) to 0. That gives us the value of the density ρ_c at maximum flow as

$$\rho_c = \frac{\rho_{\max}}{2} \tag{16}$$

We also obtain

$$q_{\max} = \frac{v_f \rho_{\max}}{4} \tag{17}$$

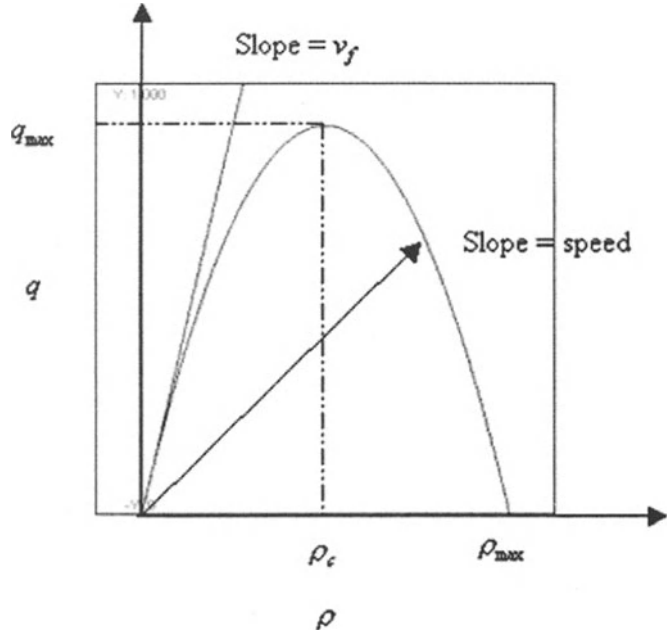

Figure 2-3: Traffic Flow vs. Density

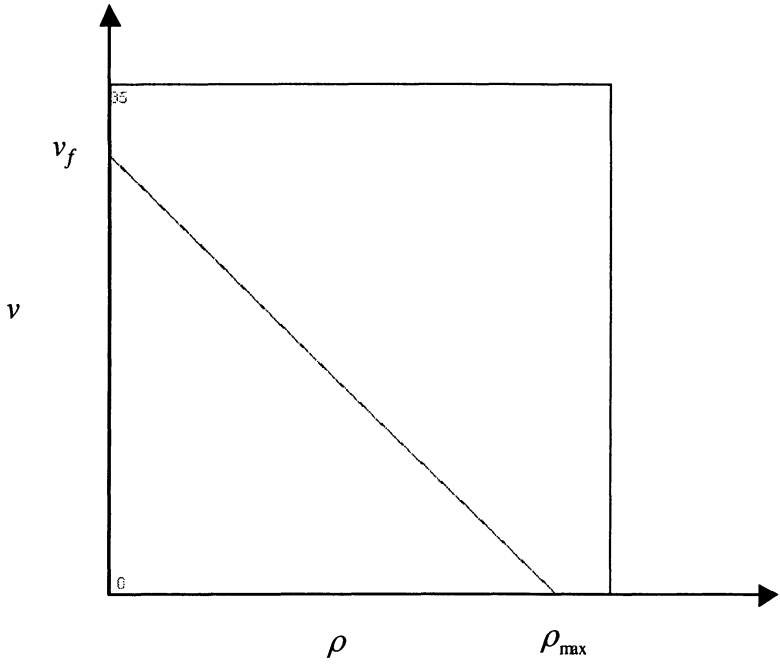

Figure 2-4: Traffic Speed vs. density

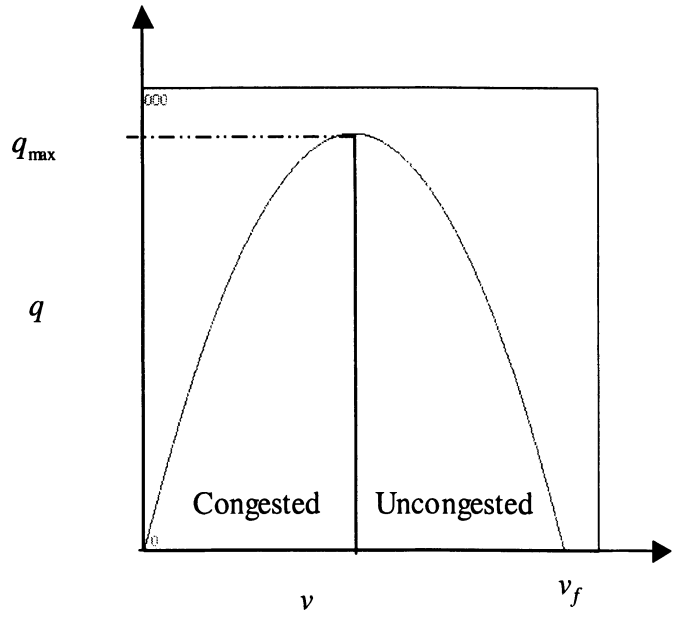

Figure 2-5: Traffic Flow vs. Speed

2.2 Greenberg's Model

In the Greenberg model [5], the speed density relationship is given by

$$v = v_0 \ln(\frac{\rho}{\rho_{max}}) \tag{18}$$

2.3 Underwood's Model

In the Underwood model [6], the speed density relationship is given by

$$v = v_f e^{-\rho/\rho_0} \tag{19}$$

2.4 Northwestern University Model

In the Northwestern University model [7], the speed density relationship is given by

$$v = v_f e^{-\frac{1}{2}(\rho/\rho_0)^2} \tag{20}$$

2.5 Drew's Model

In the Drew model [8], the speed density relationship is given by

$$v = v_f \left[1 - \left(\frac{\rho}{\rho_{\max}} \right)^{n+\frac{1}{2}} \right] \tag{21}$$

Drew's model is a generalization of earlier models, where taking the value of n = 1 gives a linear model, n = 0 gives a parabolic model, and n = -1 gives an exponential model.

2.6 Pipes Munjal Model

In the Pipes Munjal model [9], the speed density relationship is given by

$$v = v_f \left[1 - \left(\frac{\rho}{\rho_{\max}} \right)^{n} \right] \tag{22}$$

The Pipes Munjal model, like Drew's model, also is a generalization where by taking different values of *n*, we obtain different models.

2.7 Multi-regime Models

In multiregime models [10], different regions of traffic are modeled by different equations. For example, congested regions and uncongested regions might use different models.

2.8 Diffusion Models

In order to account for the fact that drivers look ahead and modify their speeds accordingly [11], (12) can be replaced by

$$v_e = v_f[1-\frac{\rho}{\rho_{\max}}] - D[\frac{\partial \rho}{\partial x}]/\rho \tag{23}$$

Using (23) and (13) we can write

$$q(t,x) = v_f \rho(t,x)\left(1-\frac{\rho(t,x)}{\rho_{\max}}\right) - D\left(\frac{\partial \rho(t,x)}{\partial x}\right) \tag{24}$$

Here D is a diffusion coefficient given by

$$D = \tau v^2{}_r \tag{25}$$

In (25), v_r is a random velocity, and τ is a parameter. Diffusion is a useful concept mentioned by many researchers as an extension to the existing traffic flow models to improve their realism [11, 12, 13]. Diffusion term represents "the diffusion effect" due to the fact that each driver's gaze is concentrated on the road in front of him, so that he adjusts his speed according to the concentration ahead. This adjustment creates a dependence of flow on concentration gradient that leads to an effective diffusion. This models the gradual rather than instantaneous reduction of speed by the drivers in response to the shock waves. Combining (8) and (24) gives

$$\left[\frac{\partial}{\partial t}\rho(x,t) + v_f \frac{\partial}{\partial x}\rho(x,t)\right] - 2\frac{\rho}{\rho_{\max}} v_f \frac{\partial}{\partial x}\rho(x,t) - D\frac{\partial^2}{\partial x^2}\rho(x,t) = 0 \tag{26}$$

If we introduce a moving reference frame

$$\xi(x,t) = -x + v_f t \tag{27}$$

and non dimensionalize $\rho(x,t)$ by $\rho_{\max}/2$, and t by t_0, equation (26) is transformed to

3. MICROSCOPIC TRAFFIC CHARACTERISTICS

Macroscopic traffic dynamics represent traffic in terms of traffic density, flow, and speed. We can also view traffic in terms of its microscopic characteristics, i.e., studying individual vehicle behavior, fortunately there is a link between the two as presented below.

Microscopic traffic characteristics are described in terms of the car-following models [20-22]. The car-following model is developed based on Figure 2-4. The vertical double line is a reference from where the x-axis distance for cars is calculated. We show the situation where car n+1 is following car n. L is the distance between the two cars at rest and is a constant. The variable h is the headway distance between the cars. The car-following model is based on assumptions of how human drivers vary h as a function of other variables.

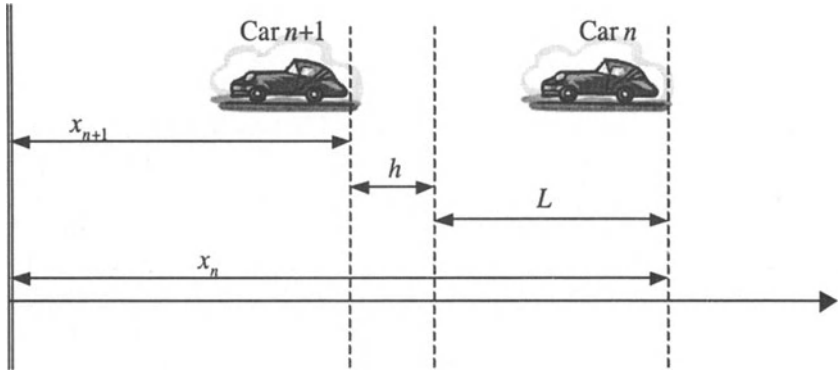

Figure 2-6: Car-Following Model

For example, if we make h a linear function of the speed of the follower, we obtain

$$x_n - x_{n+1} = k\dot{x}_{n+1} + L \tag{32}$$

Here k and L also are constants. By differentiating (32) we get

$$\ddot{x}_{n+1} = \frac{1}{k}\left[\dot{x}_n - \dot{x}_{n+1}\right] \tag{33}$$

Figure 2-6: Car-Following Model

For example, if we make h a linear function of the speed of the follower, we obtain

$$x_n - x_{n+1} = k\dot{x}_{n+1} + L \tag{32}$$

Here k and L also are constants. By differentiating (32) we get

$$\ddot{x}_{n+1} = \frac{1}{k}\left[\dot{x}_n - \dot{x}_{n+1}\right] \tag{33}$$

This model is enhanced by introducing a driver delay τ to the stimulus provided by the leader car. We also replace (1/k) by another variable λ called the sensitivity. Using this, (33) takes the form

$$\ddot{x}_{n+1}(t+\tau) = \lambda\left[\dot{x}_n(t) - \dot{x}_{n+1}(t)\right] \tag{34}$$

where

$$\lambda = \lambda_0 \frac{\left[\dot{x}_{n+1}(t+\tau)\right]^m}{\left[x_n(t) - x_{n+1}(t)\right]^L} \tag{35}$$

Here, m, and L are integer values and λ_0 is a constant. It is very remarkable that we can obtain the macroscopic models by choosing different values for m and L and then integrate Equation (34). For Greenshield's model m=0, and L=2 and for Greenberg model, m=0 and L=1. For example, let us take m=0 and L=2 in (35). We get

$$\ddot{x}_{n+1}(t+\tau) = \lambda_0 \frac{\left[\dot{x}_n(t) - \dot{x}_{n+1}(t)\right]}{\left[x_n(t) - x_{n+1}(t)\right]^2} \tag{36}$$

Integrating the above, we obtain

$$\dot{x}_{n+1}(t+\tau) = -\frac{\lambda_0}{x_n(t) - x_{n+1}(t)} + C \tag{37}$$

where C is a constant of integration. We use the relationship between average space headway and traffic density as

$$x_n - x_{n+1} = \frac{1}{\rho} \tag{38}$$

and also consider steady-state conditions so that

$$\dot{x}_{n+1}(t+\tau) = \dot{x}_n(t) = v \tag{39}$$

Using (38) and (39), we obtain

$$v = -\lambda_0 \rho + C \tag{40}$$

By using the boundary conditions such that $v = v_f$ at $\rho = 0$ and $v = 0$ at $\rho = \rho_{\max}$, we obtain

$$v = v_f\left(1 - \frac{\rho}{\rho_{\max}}\right) \tag{41}$$

which is the same as the Greenshield formula. Similarly, there is a correspondence between various microscopic and macroscopic formulas.

TRAFFIC MODEL

We will use the following notation from [23]:

$$u_t = \frac{\partial u}{\partial t},\ u_x = \frac{\partial u}{\partial x}, \text{ and } u_{xx} = \frac{\partial^2 u}{\partial x^2} \tag{42}$$

The traffic problem in the PDE (partial differential equations) setting is given by

$$\frac{\partial}{\partial t}\mathrm{P}(x,t) = -\frac{\partial}{\partial x} q(x,t),\ -\infty < x < \infty,\ 0 < t < \infty \tag{43}$$

with the initial condition

$$\rho(x,0) = \phi(x),\ 0 < t < \infty \tag{44}$$

We can write

$$\frac{\partial q}{\partial x} = \frac{\partial q}{\partial \rho}\frac{\partial \rho}{\partial x} \tag{45}$$

or

$$\frac{\partial q}{\partial x} = c(\rho)\frac{\partial \rho}{\partial x} \tag{46}$$

where

$$c(\rho) = \frac{\partial q}{\partial \rho} \tag{47}$$

Substituting this in (43) and using the notation (42) we get the representation of the traffic dynamics as

$$\text{PDE: } \rho_t + c(\rho)\rho_x = 0,\ -\infty < x < \infty,\ 0 < t < \infty \tag{48}$$

$$\text{IC: } \rho(x,0) = \phi(x),\ -\infty < x < \infty \tag{49}$$

Here, IC stands for initial condition. In this model [(48) and (49)] we are using an infinite length highway. If we want to model a finite length model with length L, we would use the following model:

$$\text{PDE: } \rho_t + c(\rho)\rho_x = 0,\ 0 \le x \le L,\ 0 < t < \infty \tag{50}$$

$$\text{IC: } \rho(x,0) = \phi(x),\ 0 \le x \le L \tag{51}$$

$$\text{BC: } \rho(0,t) = \psi(t),\ 0 < t < \infty \tag{52}$$

Here, BC stands for boundary condition, which dictates how the traffic is entering the highway section.

4. CLASSIFICATION OF PDE

In this section we will classify the traffic problem. In order to do that, we first present the basic information on PDEs [23 - 25].

Variables: In (48 and 49), ρ is the *dependent variable*, which depends on the two *independent variables* x and t. We can have systems of PDEs which contain more than one dependent variable. We will encounter problems like this in traffic routing.

Order of PDE: Order of a PDE is the order of the highest partial derivative. In (48), the order of the PDE is 1.

Linearity: PDEs are linear if the dependent variable with all its derivatives appears linearly in the equation. For example, a second-order linear PDE in two independent variables x and y is

$$Au_{xx} + Bu_{xy} + Cu_{yy} + Du_x + Eu_y = G \tag{53}$$

Where A, B, C, D, E, F, and G are either constants or functions of the independent variables x and y (but not u or any or its derivatives). If $G(x,y)$ is identically zero, then (53) is called *homogeneous*, otherwise it is *nonhomogeneous*. If a PDE is not *linear,* then it is *nonlinear.* If any of A ,B, C, D, E, F, and G is a function of u or any of its derivatives, then this equation is called *quasilinear.* If only G is a function of u, and if A, B, C, D, E, F are independent of u, then this will be called an *almost-linear* PDE. If only linear second-order PDEs like (53) are of the following three kinds.

Parabolic: If a PDE like (53) satisfies $B^2 - 4\,AC = 0$, then it is parabolic. Heat flow and diffusion equations are of this type, e.g., $u_t = u_{xx}$.

*Hyperbolic:*If a PDE like (53) satisfies $B^2 - 4\,AC > 0$, then it is hyperbolic. Vibrating systems and wave motion equations are of this type, e.g., $u_{tt} = u_{xx}$.

Elliptic: If a PDE like (53) satisfies $B^2 - 4\,AC < 0$, then it is elliptic. Laplace's equations is an example of this kind, e.g., $u_{xx} + u_{yy} = 0$.

The traffic problem (50) is a nonlinear first-order PDE with two independent variables and one dependent variable. It is also classified as a quasilinear PDE since the nonlinear element $c(\rho)$ enters linearly in the equation.

Boundary Conditions: These are three types of boundary conditions. In one condition (*Dirichlet boundary condition* or the boundary condition of the first kind), the value of the dependent variable is specified, in the second

kind (*Neumann boundary condition* or the boundary condition of the second kind), the gradient of the dependent variable is specified, and in the third kind (*Robin boundary condition* or the boundary condition of the third kind), a sum of the first two is specified. For example

$$u(0,t) = g_1(t); \quad u(L,t) = g_2(t) \tag{54}$$

is a Dirichlet boundary condition.

$$u_x(0,t) = g_1(t); \quad u_x(L,t) = g_2(t) \tag{55}$$

is a Neumann boundary condition.

$$u(0,t) + u_x(0,t) = g(t) \tag{56}$$

is a Robin boundary condition.

5. EXISTENCE OF SOLUTION

After the physical system like the traffic problem is modeled, the well-posedness of the model is to be addressed. A problem is well posed if

1. A solution of the problem exists
2. The solution is unique
3. The solution depends continuously on the data of the problem

The existence of a solution for the traffic problem can be studied by analyzing the following PDE:

$$P(t,x,\rho)\rho_t + Q(t,x,\rho)\rho_x = R(t,x,\rho) \tag{57}$$

where P, Q, and R are functions defined and C^1 in some domain belonging to R^3. C^1 functions are those functions that are continuous with continuous partial derivatives up to order 1. The solution of this problem is a function exists $\rho(t,x)$ is defined and C^1 in some domain belonging to R^2, so that when it is substituted in (57), it gives identity for all (t,x) in the domain.
Let us consider the characteristic equation for

$$u(t,x,\rho) = 0 \tag{58}$$

We parametrize the curve generated by the solutions as

$$t = t(\tau),\ x = x(\tau),\ \rho = \rho(\tau) \tag{59}$$

Since u is a constant, we obtain

$$\frac{\partial}{\partial t}u(t(\tau),x(\tau),\rho(\tau)) = \frac{\partial u}{\partial t}\frac{\partial t}{\partial \tau} + \frac{\partial u}{\partial x}\frac{\partial x}{\partial \tau} + \frac{\partial u}{\partial \rho}\frac{\partial \rho}{\partial \tau} \tag{60}$$

$$= \frac{\partial u}{\partial t}P + \frac{\partial u}{\partial x}Q + \frac{\partial u}{\partial \rho}R = 0$$

where

$$P = \frac{\partial t}{\partial \tau},\ Q = \frac{\partial x}{\partial \tau},\ R = \frac{\partial \rho}{\partial \tau} \tag{61}$$

We can solve the problem by using (61) as

$$\frac{dt}{P} = \frac{dx}{Q} = \frac{d\rho}{R} \tag{62}$$

Applying the implicit function theorem[1] on (60) gives

---

[1] **Implicit Function Theorem:** Let F be a variable of three variables of class C^1 in an open set O given by

$$F(x,y,z) = C$$

Then z can be solved in terms of x and y for (x,y,z) near the point (x_0,y_0,z_0) if $F_z(x_0, y_0, z_0) \neq 0$. Moreover,

$$\frac{\partial z}{\partial x} = -\frac{F_x}{F_z}, \frac{\partial z}{\partial y} = -\frac{F_y}{F_z}$$

$$\rho_t = -\frac{u_t}{u_p}, \qquad \rho_x = -\frac{u_x}{u_p} \tag{63}$$

Therefore,

$$P\rho_t + Q\rho_x = -\frac{Pu_t + Qu_x}{u_p} = \frac{Ru_z}{u_z} = R \tag{64}$$

which shows that the characteristic equation method does solve (57).

5.1 Traffic Problem

Let us analyze the following traffic problem for the existence of a solution from (48-49).

$$\rho_t + c(\rho)\rho_x = 0 \tag{65}$$

IC: $\rho(x,0) = \phi(x)$, $0 \le x \le L$ (66)

To find the solution, we use (62) to obtain

$$\frac{\partial t}{1} = \frac{\partial x}{c(\rho)} = \frac{\partial \rho}{0} \tag{67}$$

Solving these ODE's (ordinary differential equations), we get two independent solutions as

$$u_1 = \rho, \quad u_2 = x - c(\rho)t, \tag{68}$$

If u_1 and u_2 are two independent solutions of the PDE, then $F(u_1,u_2)$, which is an arbitrary C^1 function of u_1 and u_2 and provides the following general integral of the PDE.

$$F(u_1(t,x,\rho), u_2(t,x,\rho)) = 0 \tag{69}$$

We can take a specific form of (69) as

$$u_2(t,x,\rho) = G(u_2(t,x,\rho)) \tag{70}$$

So, using (69) and (70) with (68) we get the following as the general integral of (65).

$$\rho = G(x - c(p)t) \tag{71}$$

For this solution to satisfy the initial condition (66), we obtain

$$\rho = \phi(x - c(p)t) \tag{72}$$

Equation (72) can be rewritten as

$$\rho - \phi(x - c(p)t) = 0 \tag{73}$$

From the implicit function theorem, the solution for ρ in terms of t, x is implied by (73) if the following condition is satisfied:

$$1 + c'(p)t\phi'(x - c(p)t) \neq 0 \tag{74}$$

Here the prime implies that the differentiation is to be performed with respect to the variable in the parentheses. Now at initial condition, t=o. hence, at t=0, the left hand side of (74) > 0. This implies that the solution will exist as long as left hand side of (74) > 0, and as soon as it becomes equal to zero, the solution ceases to exist. When this condition is not satisfied the derivatives of the traffic density becomes infinite creating a discontinuity in the solution, which is called a traffic shock. This condition is restated as

$$1 + c'(p)t\phi'(x - c(p)t) > 0 \tag{75}$$

If we use Greenshield's formula (14), and using (47), we get

$$c(p) = \frac{\partial q}{\partial p} = v_f - 2\frac{v_f}{p_{\max}}p \tag{76}$$

Differentiating (76) yields

$$c'(p) = \frac{\partial c(p)}{\partial p} = -2\frac{v_f}{p_{\max}} \tag{77}$$

Substituting (77) in (75) gives

$$1 - 2\frac{v_f}{p_{\max}} t\phi'(x - c(p)t) > 0 \tag{78}$$

Notice that if $\phi'(x) \leq 0$ for all x, then (78) is always satisfied, and no shocks or discontinuities will be created for any $t \geq 0$. However, if $\phi'(x) > 0$ for any distance, a shock will be developed after some time. The next section illustrates how to analyze the traffic PDEs for solutions and shock waves.

6. METHOD OF CHARACTERISITICS TO SOLVE FIRST ORDER PDES

We can use the method of characteristics to solve a first-order PDE of the form

$$a(x,t)ux + b(x,t)ut + c(x,t)u + 0 \tag{79}$$

Notice that if we make a function of a variable s, then

$$\frac{du}{ds} = u_x \frac{d_x}{d_s} + u_t \frac{d_t}{d_s} \tag{80}$$

If we compare (79) and (80) we can choose

$$\frac{dx}{ds} = a(x,t), \qquad \frac{dt}{d_s} = b(x,t) \tag{81}$$

Thus the PDE (79) is transformed into the ODE (82).

$$\frac{du}{ds} + c(x,t)u = 0 \tag{82}$$

This can be solved with the initial condition given in terms of another variable m. the variable m changes along the initial curve, such as the curve $t = 0$, and the variable s will change along the characteristics curve. We will notice below that for the traffic problem s will be the same as t, and the variable m is the initial density on the highway, which is propagated over the characteristic curves.

Comparing (79) to (65), we notice that u in (79) is the same as ρ and $b(x,t) = 1$. Since $b(x,t) = 1$, we get from (81) that $s = t$, and therefore, we get again from (81)

$$\frac{dx}{dt} = c(\rho) \tag{83}$$

Along the characteristic, ρ remains constant and is equal to ρ_0. This method lets us follow a traffic density given at initial time. We follow the density in time and space. We can rewrite (83) as

$$\frac{dx}{dt} = c(\rho_0) \tag{84}$$

Integrating this equation, we get

$$x(t) = c(\rho_0)t + x(O) \tag{85}$$

which is a straight line with the slope $c(\rho_0)$. We can also derive these characterisitics in the following way. We want to track a constant traffic density, which is given by

$$\rho(x(t),t) = \rho\ (x_0, O) = \rho_0 \tag{86}$$

Here the *x(t)* and *t* are the variables which show how the constant density is moving in the *x t* plane. Therefore ρ is constant along a curve in the *x t* plane and this curve is called the characteristic curve. We can differentiate (86) to obtain

$$\frac{dp(x(t),t)}{dt} = \frac{\partial p(x(t),t)}{dt} + \frac{\partial p(x(t),t)}{dx}\frac{\partial x(t)}{dt} = 0 \tag{87}$$

Substituting (65) in (87) we again get (84).

The slope of the curve (75), given by $c(p) = \frac{\partial q}{\partial p}$, is called the *local wave velocity* for ρ_0. It shows how disturbances travel in the traffic. Notice that the disturbances can travel forward or backward in *x*. Obviously the local wave velocity is not the same as the average traffic velocity *v* which only moves forward.

Example 1: Let us consider the traffic system given by

$$\rho_t + c(\rho)\rho_x = 0 \tag{88}$$

where, using Greenshield's model, we have

$$c(p) = \frac{\partial q}{\partial p} = v_f - 2\frac{v_f}{p_{\max}} p \tag{89}$$

Let the initial condition given by (Figure 2-7)

$$p(x,0) = \begin{cases} 1 & x \le 0 \\ 1-x & 0 < x < 1 \\ 0 & 1 \le x \end{cases} \qquad -\infty < x < \infty \tag{90}$$

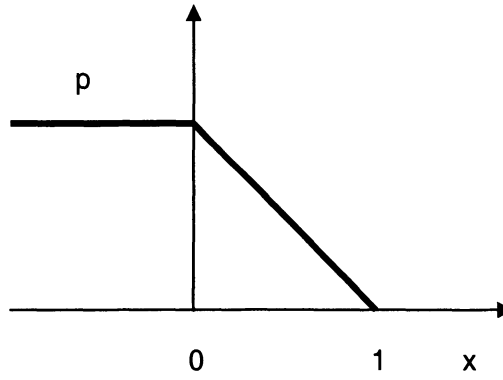

Figure 2-7: Initial Traffic Density

The slope of the characteristic curve is given by

$$c(\rho_0) = v_f - 2\frac{v_f}{\rho_m}\rho_0 \tag{91}$$

Therefore, for $\rho_0 = 0$, the slope is given by v_f. Note that for $\rho_0 < \rho_m / 2$, the slope is positive and for $\rho_0 > \rho_m / 2$, it is negative (showing back propagation of the wave). The propagation of the traffic densities for this problem is shown in Figure 2-8.

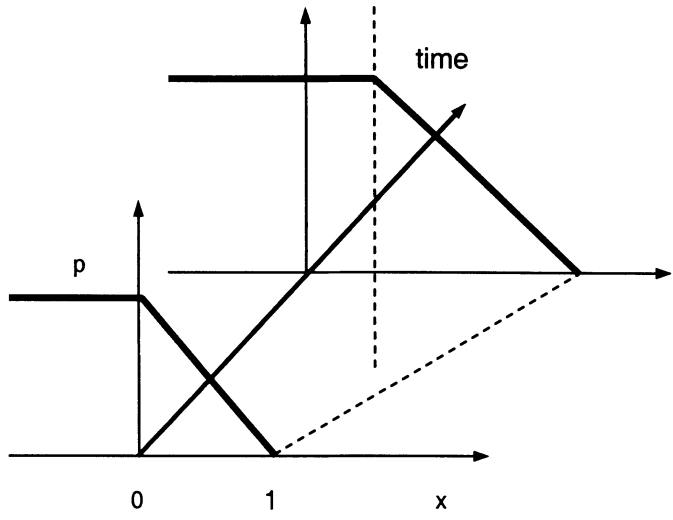

Figure 2-8: Traffic Density vs. Time

The characteristics of the same problem in the t x plane are shown in Figure 2-9.

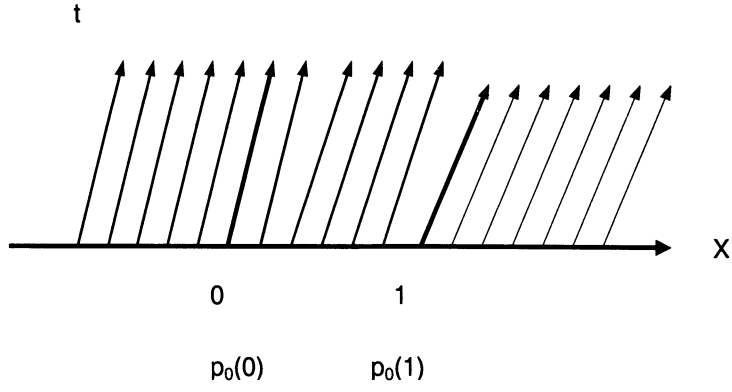

Figure 2-9: Traffic Density Characteristics

Example 2 (shock formation): Let us consider the traffic system given by

$$\rho_t + c(\rho)\rho_x = 0 \tag{92}$$

where, using Greenshield's model, we have

$$c(p) = \frac{\partial q}{\partial p} = v_f - 2\frac{v_f}{p_{\max}} p \tag{93}$$

Let the initial condition be given by (Figure 2-10)

$$p(x,0) = \begin{cases} 1 & x \le 0 \\ 1-x & 0 < x < 1 \\ 0 & 1 \le x \end{cases} \qquad -\infty < x < \infty \tag{94}$$

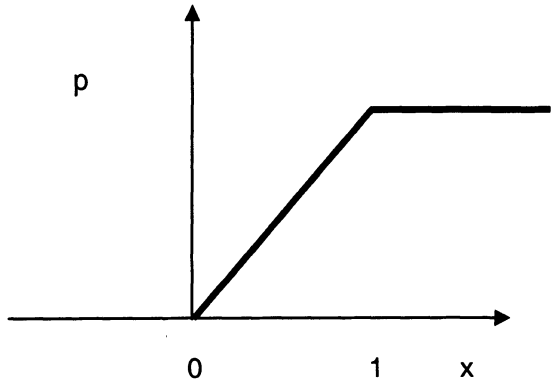

Figure 2-10: Initial Traffic Density

The slope of the characteristic curve is given by

$$c(\rho_0) = v_f - 2\frac{v_f}{\rho_m}\rho_0 \tag{95}$$

The propagation of the traffic densities for this problem is shown in Figure 2-11.

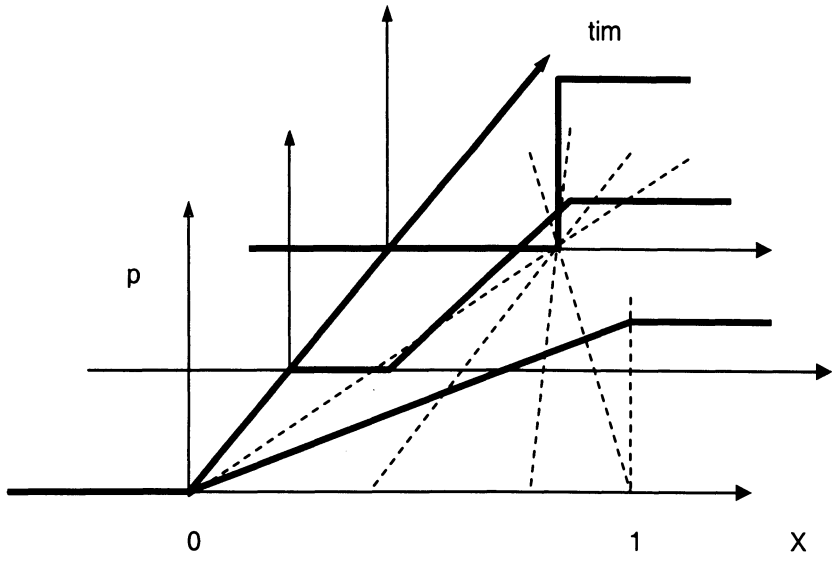

Figure 2-11: Traffic Density vs. Time

The characteristics of the same problem in the t x plane are shown in Figure 2-12.

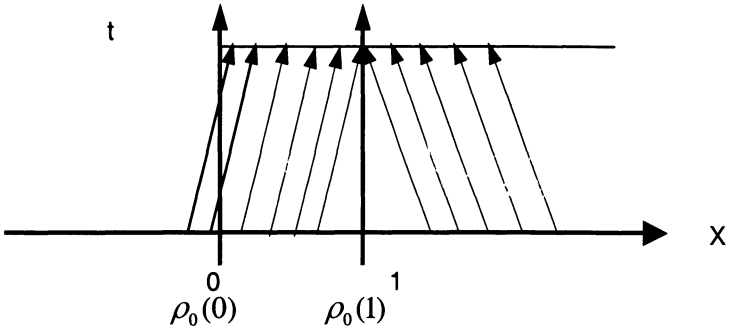

Figure 2-12: Traffic Density Characteristics

This example shows that a discontinuity (shock) is created sometime after we started with a continuous density profile with positive gradient. We can see that after the shock is formed we have multiple values of density at each x and t (above the horizontal line in Figure 2-12). The question which needs to be answered is how does the shock propagate after it is formed. This is addressed in the next section.

7. TRAFFIC SHOCK WAVE PROPAGATION

We will develop the shock propagation equation in two ways. The first way presents the development in an intuitive way and the second uses the conservation equation in the integral form to derive the equation.

Shock waves show how discontinuities in the traffic are propagated. To understand this, let us consider the highway section shown in Figure 2-13. In this figure, the highway is divided into two separate homogenous sections, one with density ρ_1 and the other with density ρ_2. The line separating the two regions is traveling with the velocity v. To derive the expression for v, we use the fact that the flow going into the line should be equal to the flow coming out from the line.

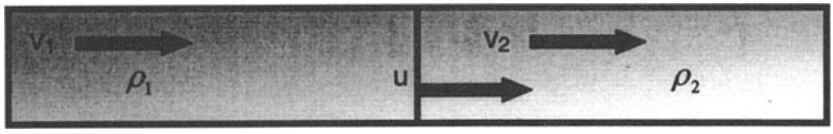

Figure 2-13: Traffic Shock Wave

The speed of vehicles on the left of the line relative to the line is $v_1 - u$ and for the vehicles on the right is given by $v_2 - u$. Hence, we obtain

$$\rho_1(v_1 - u) = \rho_2(v_2 - u) \tag{96}$$

Using the fact that $\rho_1 v_1 = q_1$ and $\rho_2 v_2 = q_2$, we obtain

$$u = \frac{q_2 - q_1}{\rho_2 - \rho_1} \tag{97}$$

Notice that if we consider a continuous change in flow and density, then we can use

$$q_1 = q \ , \ q_2 = q + \Delta q \ , \ p_1 = p \ , \ p_2 = p + \Delta p \ , where \Delta \to 0 \tag{98}$$

Using (98) in (97) gives

$$u = \frac{\partial q}{\partial \rho} \tag{99}$$

Hence, the slope of the flow density curve gives the shock wave speed. For the uncongested region, the slope is positive (the shock wave travels forward), and in the congested region, the slope is negative giving a backward traveling shock wave. This is shown in Figure 2-14.

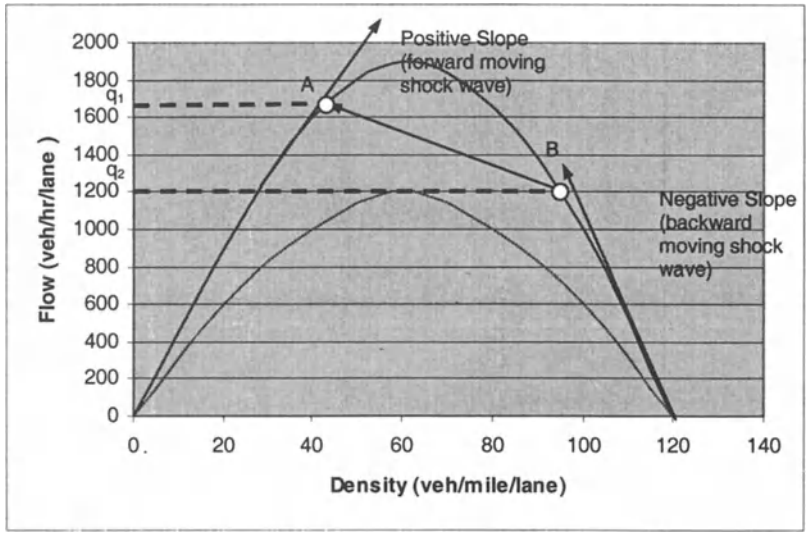

Figure 2-14: Shock Wave Analysis on Flow Density Curves

This figure shows two curves: the curve with the higher value of maximum flow is for section 1 of Figure 2-13 and the other curve is for section 2, indicating a sudden drop in the capacity. Since at the bottleneck, q_1 is greater than the maximum flow possible in section 2, we achieve q_2, the maximum value in the section. The slope from point B to point A shows a negative value, giving a backward traveling shockwave. Note that we can use various models for speed density relationships to determine the shock wave speeds.

Now we will present the alternate method to derive (97). We study the traffic propagation along a characteristic defined by a curve $x = s(t)$ in the $t\,x$ plane. Figure 2-15 shows that the shock is created at time t and then propagates along the dark arrow. To find out at what speed the shock wave travels after it is created, we will consider the shock path curve (which in Figure 2-13 is a straight line but in general can be a curve) as shown in

Figure 2-16. We can apply the conservation equation in the integral form knowing that there is a discontinuity at $x = s(t)$ at time t.

$$\frac{d}{dt}\int_{a}^{s(t)}\rho(x,t)dx+\frac{d}{dt}\int_{s(t)}^{b}\rho(x,t)dx = q(a,t)-q(b,t) \qquad (100)$$

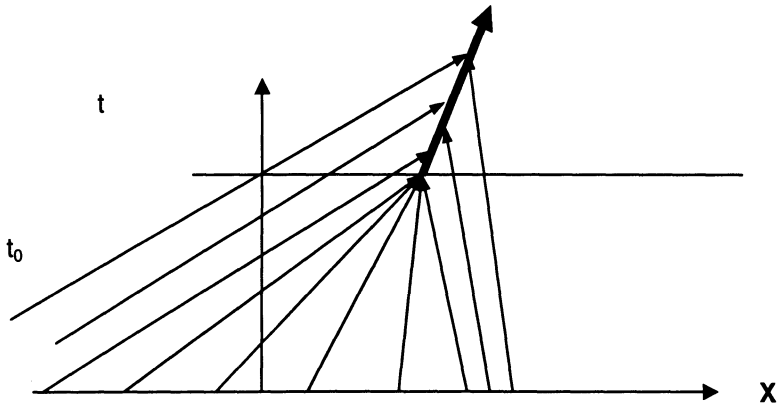

Figure 2-15: Shock Wave Propagation

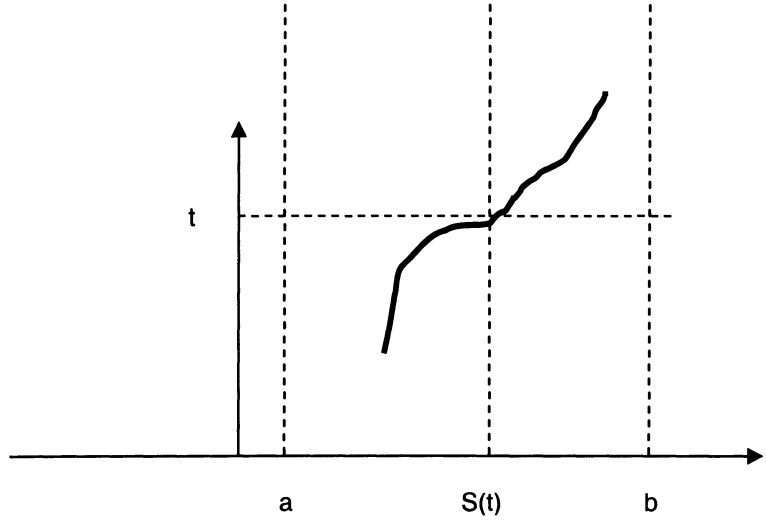

Figure 2-16: Shock Path

We apply Leibniz' rule to (100) since the limits of integration involve variable t, to obtain

$$\int_a^{s(t)} \rho_t(x,t)dx + \int_{s(t)}^{b} \rho_t(x,t)dx + \rho(s^+,t)\frac{ds}{st} - \rho(s^-,t)\frac{ds}{st} \qquad (101)$$

$$= q(a,t) - q(b,t)$$

Here *s(t)* is called the shock path, *ds/dt* is called the shock speed, and the magnitude of the jump in the traffic density is called the shock strength. Notice that ρ_t is continuous from *a* to *s(t)* to *b*. Hence, if we take the limits

$$a \rightarrow s(t)^- \text{ and } b \rightarrow s(t)^+,$$

$$\text{we get} \quad \frac{ds}{st} = \frac{q(s^+,t) - q(s^-,t)}{p(s^+,t) - p(s^-,t)} \qquad (102)$$

which is the same result as (97).

8. TRAFFIC MEASUREMENTS

Traffic variables such as traffic flow, traffic density, and traffic speed are needed to use traffic control measures. There are many traffic sensors, loop detectors being traditionally the most commonly used. Loop detectors provide measurements on the spot for a fixed point or section of the road. Some new detectors like the video cameras provide more distributed information. The understanding of the following terms is necessary to be able to design and implement effective controllers.

8.1 Time Mean Speed

Time mean speed is the arithmetic mean of the speed of vehicles passing over a point (which could be measured by a loop detector, or some other traffic sensor). The time mean speed is defined as

$$\bar{u}_{time} = \frac{1}{n}\sum_{i=1}^{n} u_i \qquad (103)$$

where

n = number of vehicles passing the detector or a point on the road

ui = speed of the i^{th} vehicle

8.2 Space Mean Speed

Space mean speed is calculated by dividing the total distance traveled by some number of vehicles divided by the total time required by all those vehicles to travel the same distance. This measurement can be done by having two loop detectors kept at a fixed distance apart and making measurements on those. The space mean speed is given by

$$\bar{u}_{space} = \frac{nL}{\sum_{i=1}^{n} t_i} = \frac{n}{\sum_{i=1}^{n} (1/u_i)} \tag{104}$$

Where

L = length of the section of the road

t_i = time taken by the i^{th} vehicle to traverse the distance L

Space mean speed is used more in traffic engineering and can be derived from time mean speeds (requiring only one detector) using a statistical relationship between the two as [23]

$$\bar{u}_{space} = \bar{u}_{time} - \frac{\sigma^2_{time}}{\bar{u}_{time}} \tag{105}$$

where σ_{time}^2 is the variance about the time mean speed.

8.3 Time Headway

Time headway is given by the difference between the times two consecutive vehicles (leading and following vehicle) pass the same point (e.g., loop detector) on the road.

8.4 Space Headway

Space headway is the distance between the front of one vehicle and the front of the following vehicle.

8.5 Flow measurements:

Traffic flow is measured by counting the number of vehicles N passing a detector in some fixed amount of time T. The flow is given by $q = N/T$. we can also calculate flow for each vehicle by measuring time headway between the vehicle and its follower and taking its reciprocal. If h_i denotes the time headway for the i^{th} vehicle and q_i the instantaneous flow for i^{th} vehicle, then

$$q_i = 1/h_i \tag{106}$$

For average flow we have

$$q = \frac{N}{T} = \frac{N}{\sum_{i=1}^{N} h_i} = \frac{1}{\frac{1}{N}\sum_{i=1}^{N} h_i} = \frac{1}{\bar{h}} \tag{107}$$

This equation shows that the average flow is the harmonic mean of the individual flows.

8.6 Traffic Density Measurements

Traditionally, traffic density is not measured directly but calculated from

$$\rho = \frac{q}{u_{space}} \tag{108}$$

Traffic density can also be calculated using occupancy, which is described next.

8.7 Occupancy

With ITS distributed sensors such as cameras, many traffic variables such as traffic density, traffic mean speed, or traffic flow in theory can be obtained. However, it is difficult for loop detectors or spot detectors to do the same. They use an indirect method of calculating traffic density by measuring occupancy. Occupancy is defined as the percent of time a detector is sensing a vehicle presence to the total time in some chosen time interval. There is a relationship between occupancy and density. Traffic density is

linearly proportional to occupancy. For instance, if we use number of vehicles per mile as the unit for traffic density then, we have

$$p = \gamma \frac{5280}{L_{eff}} \tag{109}$$

Where γ is the occupancy, L_{eff} is the effective vehicle length in feet.

8.8 Distributed Measurements

Camera sensors give us distributed information which can be used to measure the traffic variables. The density is simply the number of vehicles divided by the length of some section in which the vehicles are counted. We can also calculate density for each vehicle as the reciprocal of the distance of the vehicle from the vehicle ahead. Speed can be calculated by capturing positions of vehicles in different time frames. Flow can be calculated by just multiplying traffic speed and density.

8.9 Moving Observer Method

This method utilizes a moving vehicle taking measurements of variables such as the number of vehicles passing it, and the number of vehicles it passes. This method is not amenable for real-time traffic control in an automated fashion.

9. SUMMARY

This chapter presented the traffic theory in a concise fashion, which should build the foundation of the reader for designing and analyzing traffic controllers for traffic assignment and routing.

10. EXERCISES

Questions

1: What is the conservation law for highways? Describe in words.
2: Explain the diffusion term (in equation 5) in a few sentences describing how a human driver's behavior relates to it?

3. What is the difference between time mean speed and space mean speed? What kind of errors can you expect if you use one instead of the other?
4. What is the difference between time headway and space headway. Derive relationship between the two.
5. How can a computer be used to automatically calculate the traffic variables from distributed measurements?
6. Prove the implicit function theorem.
7. State Leibniz's rule.
8. Why is the moving observer method not useful for real-time traffic control?
9. What is the advantage of diffusion models over the other density flow models?
10. Why do we use PDE to represent the traffic problem? (or why do we use PDE to model the traffic?)
11. For a finite model with length L (equations 50- 52), prove that ρ (the density of the highway section of length L) is a dependent variable, which depends on the independent variables x and t.
12. Why is the density not measured directly? And how can the density be calculated indirectly?

Problems

1. Write down traffic flow q in terms of traffic density by utilizing equation (2) and (3). Find out the value of the traffic density at which the traffic flow is maximum.

2. If we write the Greenshield's model as

$$v_i = v_f(1-\eta_i), \quad \text{where } \eta_i = \frac{\rho_i}{\rho_{mzx}}$$

then using (13) in (97), show that $u = v_f[1-(\eta_1+\eta_2)]$; note that this formula can be used to study the following three cases:

a. **Density Nearly Equal:**

When $\eta_1 \approx \eta_2$, then $u = v_f[1 - 2\eta_1]$

b.**Stopping Waves:**

When a traffic light at an intersection turns red, then η_2= 1, which gives $u = -v_f \eta_1$.

c.**Starting Waves**

When a traffic light at an intersection turns green from red, then η_1 = 1, which gives $u = -v_f \eta_2$. Since $\eta_2 = 1 - (\frac{v_2}{v_f})$, we get $u = -v_f + v_2$.

Note that velocity v_2 is usually small and can be neglected.

3. On one section of the I-81 corridor in Virginia, there is only one lane available to the traffic which is flowing at a rate of 1200 vehicles/hour at a density of 30 vehicles/mile. A truck enters the highway and travels at a slower speed creating a local traffic density behind the truck of 60 vehicles/mile and a flow of 900 vehicles/hour. Calculate the rate of increase of the queue length behind the truck?

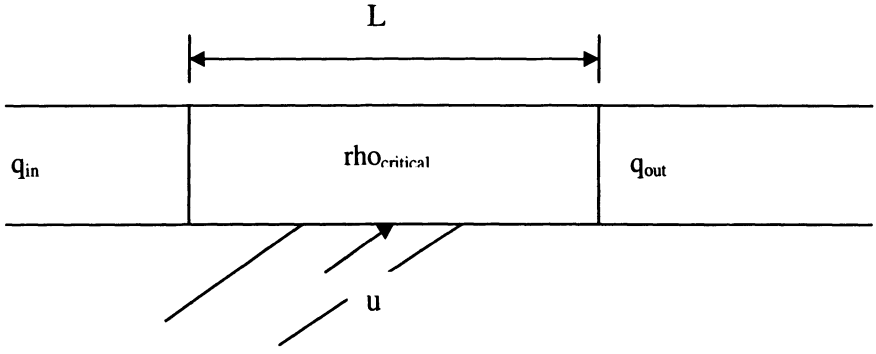

Given: $q_{in}(n)$ = 10 veh/min, $q_{out}(n)$ = 8 veh/min, $u(n)$ = 2 veh/min, $q_{in}(n+1)$ = 9 veh/min, $rho_{critical}$= 32 veh/mile, V_f= 1 veh/min

Find: The maximum number of vehicles that can be released from the ramp at time step *(n+1), (u(n+1))*.

Answer:

a) For the n-th time step,

Number of veh in the section= $q_{in}(n) + u(n) - q_{out}(n) = 10 + 2 - 8 = 4$ veh/min

b) Use Greenshields model to find the section's capacity(q_{max})

$rho_{critical} = rho_{max}/2$ .....(eqn (16))

$rho_{max} = 2 * rho_{critical}l = 2*32 = 64$veh/mile

$q_{max} = (v_f * rho_{max})/4 = 1*64/4 = 16$ veh/min

c) At time step n+1

$q_{in}(n+1) + u(n+1)$ + the number of vehicles in the section remained from the nth time step <= q_{max}

gives

$9 + u(n+1) + 4 <= 16 \Rightarrow u(n+1) <= 3$. Therefore, max $u(n+1) = 3$ veh/min

11. REFERENCES

1.Zachmanoglou, E. C., and Thoe, D. W., Introduction to Partial Differential Equations with Applications, Dover, 1986.

2. Farlow, S. J., Partial Differential Equations for Scientists and Engineers, Dover, 1993.

3. Gustafson, K. E., Introduction to Partial Differential Equations and Hilbert Space Methods, Dover, 1999.

4. Greenshield, B. D., "A Study in Highway Capacity, Highway Research Board," Proceedings, 14, 1935, 458.

5. Greenberg, H., "An Analysis of Traffic Flow," Operations Research, 7., 1959, 78-85.

6. Underwood, R. T., "Speed, Volume, and Density Relationships, Quality and Theory of Traffic Flow," Yale Bureau of Highway Traffic, New Haven, , 1961, 141-188.

7. Drake, J.S., Schofer, J. L., and May, A. D., Jr., "A Statistical Analysis of Speed Density Hypothesis," Third Symposium on the Theory of Traffic Flow Proceedings, North-Holland Elsevier , 1967.

8. Drew, D. R., Traffic Flow Theory and Control, McGraw-Hill, 1968, Chapter 12.

9. Pipes, L. A., "Car-Following Models and the Fundamental Diagram of Road Traffic," Transportation Research, 1, ,1967, pages 21-29.

10. May, A. d., Traffic Flow Fundamentals, Prentice-Hall, 1990.

11. Musha, T., and Higuchi, H., "Traffic Current Fluctuation and the Burgers' Equation," Japanese Journal of Applied Physics, 17, 1978, 811-816.

12. Burns, J. A. And Kang, S., "A Control Problem for Burgers' Equation with Bounded Input/Output", Nonlinear Dynamics 2, 1991, 235-262.
13. Cole, J. D., "On a Quasi-Linear Parabolic Equation Occurring in Aerodynamics", Quart. Appl. Math. IX, 1951, 225-236.
14. Glimm, J. and Lax, P., *Decay of Solutions of Systems of Nonlinear Hyperbolic Conservation Laws*, Amer. Math. Soc. Memoir 101, 1970.
15. Hopf, E., "The Partial Differential Equation $u_t + uu_x = \mu u_{xx}$," Common. Pure Appl. Math 3, 1950, 201-230.
16. Lax, P.D., *Hyperbolic Systems of Conservation Laws and the Mathematical Theory of Shock Waves*, CBMS-NSF Regional Conference Series in Applied Mathematics 11, SIAM, 1973.
17. Maslov, V. P., "On a New Principle of Superposition for Optimization Problems", *Uspekhi Matematicheskikh. Nauk* 42, 1987, 39-48.
18. Maslov, V. P., "A New Approach to Generalized Solutions of Nonlinear Systems", *Soviet Math. Dokl.* 35, 1987,29-33.
19. Curtain, R. F., "Stability of Semi Linear Evolution Equations in Hilbert space", J. Math. Pures Appl. 63, 1984, 121-128.
20. Papageorgiou, "Applications of Automatic Control Concepts to Traffic Flow Modeling and Control", Springer-Verlag, 1983.
21. Garber, N. J., and Hoel, L. A., Traffic and Highway Engineering, Pws Publishing Company, 1997.
22. Gazis, D.C., Herman, R., Potts, R., "Car-Following Theory of Steady-State Traffic Flow," Operations Research, 7,1959, 499-595.
23. Farlow, Stanley J., Partial Differential Equations for Scientists and Engineers, Dover, 1992.
24. Zachmanoglou, E. C., and Thoe, D. W., Introduction to Partial Differential Equations with Applications, Dover, 1986.
25. Logan, J. D., An Introduction to Nonlinear Partial Differential Equations, John Wiley, 1994.

Chapter 3

DISTRIBUTED MODELING AND PROBLEM FORMULATION

This chapter presents the modeling for the ramp metering problem in the distributed setting. It gives a detailed description of the dynamics and presents its limitations. The chapter also presents the control problem formulations in the distributed setting. The concept of projection dynamics is used to tackle the problems associated with the model.

1. SYSTEM

The first step in the design of feedback controllers for ramp metering is to model the system dynamics appropriately. A macroscopic model of the traffic can effectively be used in this context. From the macroscopic perspective, the traffic flow is considered analogous to a fluid flow, which is a distributed parameter system represented by partial differential equations. Mass conservation model of a highway, characterized by $x \in [0, L]$, which is the position on the highway, is given by.

$$\frac{\partial \rho(t,x)}{\partial t} + \frac{\partial q(t,x)}{\partial x} = 0 \tag{1}$$

where $\rho(t,x)$ is the density of the traffic as a function of x and time t, and $q(t,x)$ is the flow at given x and t. The flow $q(t,x)$ is a function of $\rho(t,x)$ and the velocity $v(x,t)$:.

P. Kachroo et al., *Feedback Ramp Metering in Intelligent Transportation Systems*

$$q(t,x) = \rho(t,x)v(t,x) \tag{2}$$

This model of a highway section is shown in Figure 3-1.

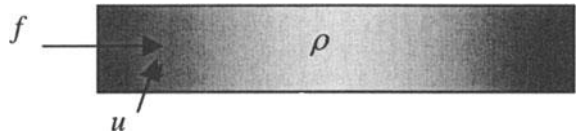

Figure 3-1: Segment of Highway Model

There are various static and dynamic models which have been used to represent the underlying relationship between $v(x,t)$ and $\rho(t,x)$ as shown in Chapter 2. One of the most simple models is that proposed by Greenshield [1], which hypothesizes a linear relationship between the two variables.

$$v = v_f(1 - \frac{\rho}{\rho_{\max}}) \tag{3}$$

where v_f is the free flow speed and $\rho_{\max}$ is the jam density.

Now, we can also add the dynamics of the ramp itself. This will allow us to design control laws that also take into account the ramp queues. Let us consider the mainline highway section as well as a connected ramp as shown in Figure 3-2.

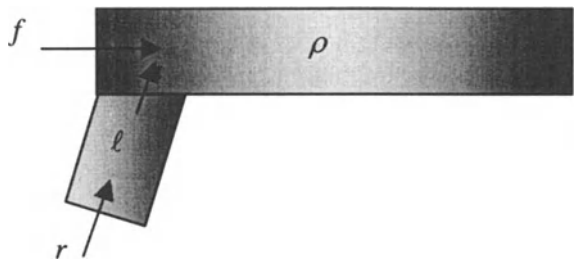

Figure 3-2: Isolated Ramp Model

Now, we can use the conservation equation on the ramp also. Since ramp lengths are small compared to the mainline, we choose a discretized dynamic

model for the ramp. Let $\ell(t)$ be the queue length in the ramp, $u(t)$ be the flow rate entering the highway mainline from the ramp, and $r(t)$ be the inflow entering the ramp. In time Δt, the "amount" of vehicles that have entered the ramp is given by $\ell(t+\Delta t)-\ell(t)$. Due to the conservation law, this should be equal to this change caused by the inflow and outflow during the same time given by $[r(t)-u(t)]\Delta t$. Equating the two, we get the following equation:

$$\ell(t+\Delta t)-\ell(t)=[r(t)-u(t)]\Delta t \tag{4}$$

After taking limits, we obtain (5) and that leads to (6):

$$Lt_{\Delta t\to 0}\frac{\ell(t+\Delta t)-\ell(t)}{\Delta t}=Lt_{\Delta t\to 0}[r(t)-u(t)] \tag{5}$$

$$\dot{\ell}=r(t)-u(t) \tag{6}$$

Here $\dot{\ell}$ indicates differentiation with respect to time. The control variable enters the PDE via the boundary condition. Hence, this problem is called boundary injection control. The overall dynamics of the system now can be written as

$$\text{Dynamics: } \begin{cases} \dfrac{\partial \rho(t,x)}{\partial t}+\dfrac{\partial[\rho(t,x)v_f(1-\dfrac{\rho(t,x)}{\rho_{\max}})]}{\partial x}=0 \\ \dot{\ell}=r(t)-u(t) \end{cases} \tag{7}$$

$$\text{Boundary Condition: } \rho(t,0)v_f(1-\frac{\rho(t,0)}{\rho_{\max}})=f(t)+u(t) \tag{8}$$

$$\text{Initial Condition: } \rho(0,x)=\psi(x) \tag{9}$$

The initial condition is given in terms of a function that signifies a known function. That means that the initial condition on the mainline is given. In the modeling shown here, we have chosen Greenshield's model for the speed flow relationship. In general, we could have chosen any of the models that

are shown in Chapter 2 for that. For instance, if we use Greenberg's formula [2], then (7) and (8) becomes

$$\text{Dynamics: } \begin{cases} \dfrac{\partial \rho(t,x)}{\partial t} + \dfrac{\partial[\rho(t,x) v_f \ln(\dfrac{\rho(t,x)}{\rho_{\max}})]}{\partial x} = 0 \\ \dot{\ell} = r(t) - u(t) \end{cases} \tag{10}$$

$$\text{Boundary Condition: } \rho(t,0) v_f \ln(\frac{\rho(t,0)}{\rho_{\max}}) = f(t) + u(t) \tag{11}$$

$$\text{Initial Condition: } \rho(0,x) = \psi(x) \tag{12}$$

If we use a diffusion model [3-5], we obtain

$$\text{Dynamics: } \begin{cases} \left[\dfrac{\partial}{\partial t}\rho(x,t) + v_f \dfrac{\partial}{\partial x}\rho(x,t)\right] - 2\dfrac{\rho}{\rho_{\max}} v_f \dfrac{\partial}{\partial x}\rho(x,t) - D\dfrac{\partial^2}{\partial x^2}\rho(x,t) = 0 \\ \dot{\ell} = r(t) - u(t) \end{cases} \tag{13}$$

$$\text{Boundary Condition: } \rho(t,0) v_f (1 - \frac{\rho(t,0)}{\rho_{\max}}) - D\left.\frac{\partial \rho}{\partial x}\right|_{(t,0)} = f(t) + u(t) \tag{14}$$

$$\text{Initial Condition: } \rho(0,x) = \psi(x) \tag{15}$$

2. CONTROL OBJECTIVE

We can design control objectives for any of the models we can create (as shown above). We will work on the following one using equations (7), (8), and (9). These are repeated here for convenience.

$$\text{Dynamics: } \begin{cases} \dfrac{\partial \rho(t,x)}{\partial t} + \dfrac{\partial[\rho(t,x)v_f(1-\dfrac{\rho(t,x)}{\rho_{\max}})]}{\partial x} = 0 \\ \dot{\ell} = r(t) - u(t) \end{cases} \tag{16}$$

$$\text{Boundary Condition: } \rho(t,0)v_f(1-\frac{\rho(t,0)}{\rho_{\max}}) = f(t) + u(t) \tag{17}$$

$$\text{Initial Condition: } \rho(0,x) = \psi(x) \tag{18}$$

This model uses the Greenshield's formula (3) for speed flow relationship. We see in Figure 3-3 below that if we can maintain the traffic density at the critical value, we can obtain the highest traffic flow.

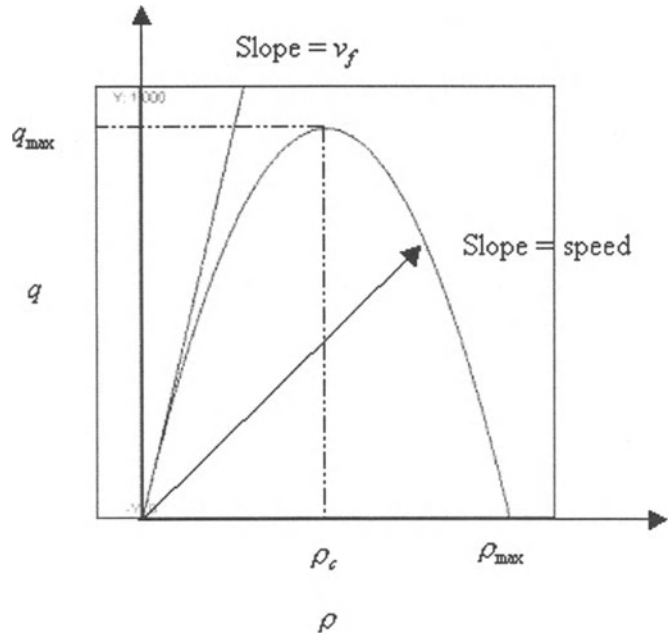

Figure 3-3: Greenshield Traffic Flow Density Relationship

Based on this figure, we would like to design the control law so that the inflow to the mainline from the ramp is such that the traffic density at the mainline is maintained at the critical density. Therefore, our aim would be to satisfy the following condition:

$$\forall x \in [0, L], Lt_{t\to\infty} \rho(t, x) = \rho_c \tag{19}$$

It is easier to check a scalar measure of this behavior than the condition (19). One appropriate scalar measure is used in (16) below to show a control design objective

$$Lt_{t\to\infty} \int_0^t (\rho(s, x) - \rho_c)^2 ds = 0 \tag{20}$$

There can be many control laws that satisfy (19) and (20). We might want to design possible control laws that minimize the control objective. The control law then can be designed as

$$u(\rho(t,.)) = \arg\min_{u(.,.)}\left(\int_0^\infty \int_0^L (\rho(s,x) - \rho_c)^2 \, dx ds\right) \tag{21}$$

This shows that the control law $u(.,.)$ at time t is a function of the traffic density at the entire highway mainline. This makes the control law a feedback mechanism, so that it can respond to changing traffic conditions.

In the control objectives presented in 19-21 we have only considered the mainline. We also need to control the effect on the ramp queue length. We do not want the ramp queue lengths to get large. Therefore, a good control objective would give weights to the mainline effect as well as ramp queues. Based on this, criteria (19), (20), and (21) become the following three criteria:

$$\begin{cases} \forall x \in [0, L], Lt_{t\to\infty} \rho(t,x) = \rho_c \\ \qquad Lt_{t\to\infty} \ell(t) = 0 \end{cases} \tag{22}$$

$$Lt_{t\to\infty}[w_1 \ell + \int_0^t w_2 (\rho(s,x) - \rho_c)^2 \, ds] = 0 \tag{23}$$

$$u(\rho(t,.)) = \arg\min_{u(.,.)}\left(\int_0^\infty [w_1 \ell + w_2 \int_0^L (\rho(s,x) - \rho_c)^2 \, dx] ds\right) \tag{24}$$

It is very important to keep in mind that we are interested essentially in feedback control laws. Therefore, our control variable, the inflow rate into the highway from the ramp, *u(t)*, should be a function of the state of the system (i.e., the traffic density and/or queue length on the ramp). Of course, we need sensors so that those variables are measured and then used by the processor in order to calculate the control rate, which then can be used to actuate the ramp lights.

3. LIMITATIONS OF THE MODELS

In any of the models we have chosen, it is imperative that they retain the essential dynamics of the system behavior. We have modeled two main elements of the physical system. One is the "conservation principle" and the other is the "traffic flow density" relationship. There are a few more intricacies we have to make sure are followed. These are discussed next.

3.1 Jam Density

We have seen from Greensheild's formula that when the traffic reaches the jam density, the traffic velocity becomes equal to zero. The jam density is a condition that corresponds to traffic when the vehicles are in the closest spacing possible. Thus, the density should not exceed the jam density at all times for all roads. Consider the following figure

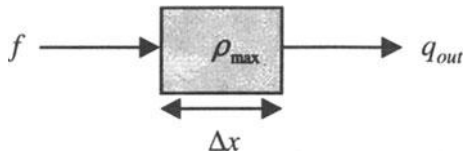

Figure 3-4: Jam Density Condition

In this figure we see a section that has reached jam density. Now in time Δt, the inflow into the section of length Δx will be $f\Delta t$. The outflow during the same time will be $q_{out}\Delta t$. The outflow using (2) and (3) is given by

$$q_{out} = v_f \rho(1 - \frac{\rho}{\rho_{max}}) \tag{25}$$

Now, since $\rho = \rho_{max}$, we get $q_{out} = 0$. This implies that if the inflow is positive, then the traffic density of this infinitesimal section will reach a value greater than ρ_{max}.

3.2 Maximum Queue Length

Analogous to the above condition of the mainline, we can have a similar condition at the ramp. As we have seen in (6), the ramp dynamics are given by

$$\dot{\ell} = r(t) - u(t) \tag{26}$$

Now, if at a certain time t, the length has reached the maximum value that is possible in a ramp, and then if $r(t)$ is greater than $u(t)$, then the ramp length will reach a value greater than the maximum allowed.

3.3 Negative Density

The mathematical model we choose for control design should also not allow negative traffic density. If the mainline does not have any exit ramps and if we do not allow negative in-flows, then this condition should not occur. We argue a proof of this as follows. The only way a negative density can be achieved on the mainline is when there is more outflow than inflow and the mainline density is already zero. Now, when the density is zero, then according to (2) and (3) combined, the outflow is also zero. If the outflow is zero, then since the inflow cannot be negative, the outflow cannot be greater than the inflow.

3.4 Negative Queue Length

Looking at dynamics (26), we see that we can also have negative queue lengths if length has reached the zero value in a ramp, and then if $r(t)$ is less than $u(t)$. This condition also does not have any physical significance, since length cannot be negative.

3.5 Traffic Jam Time

When the traffic density reaches the jam density, according to Greenshield's formula, there will be no outflow from the section. That means that once there is a traffic jam, the section will remain in a jam forever.

3.6 Projection Dynamics

The solution to the above-mentioned problems is in treating the dynamics problem in the framework of projection dynamics. Projection dynamics essentially refers to a mechanism to force the trajectories (or integral curves) of the system in a prespecified region. Let us say that we are given a region K as shown in Figure 3-5 . The system trajectories should remain inside this region at all times in order for the system to have a physical meaning for the problem. This is similar to our case, where, for instance, the traffic density needs to remain nonnegative at all times. Since the righthand side of the differential equations governing our system is smooth, the dynamics only on the boundary will dictate if the system trajectories will remain in the region K or go outside.

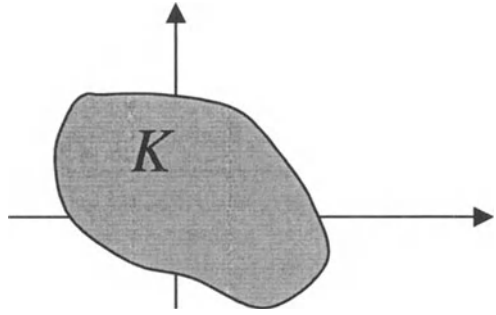

Figure 3-5: Physically Viable Region K

If the dynamics of the system are not the projection dynamics, then a trajectory starting inside the region K may go outside the region as shown by the solid line trajectory in Figure 3-6. These dynamics need to be modified at the boundary of the region so that the trajectory always stays inside. This can be accomplished by modifying the vector field at the boundary so that the trajectory, instead of moving outward, starts moving either transversally to the boundary or it moves inside (as shown by the dashed line in the figure).

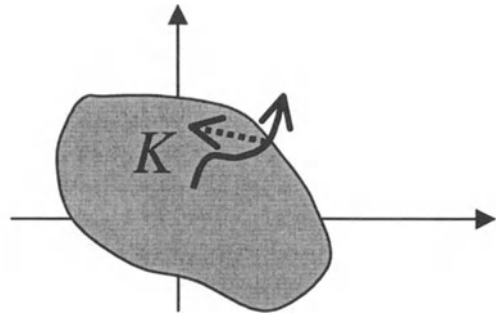

Figure 3-6: Physically Viable Region K and Some Trajectories

Now, we will apply this principle to our problem. Our region is shown in Figure 3-7.

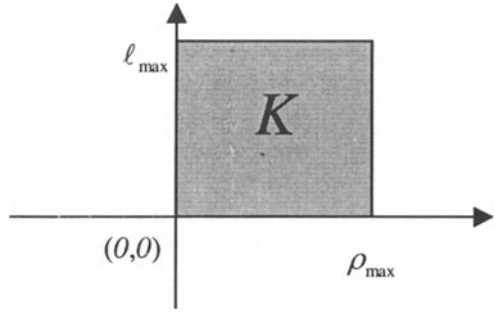

Figure 3-7: Physically Viable Region K for the Ramp Problem

A trajectory can go outside from the interior of K at eight different places. These are the four sides and the four corners of the rectangular viable region. These various ways are studied below.

3.6.1 Right Face

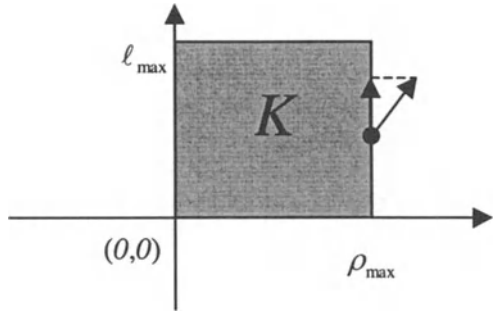

Figure 3-8: Right Face Dynamics

Right face dynamics are the ones described in Section 3.1. In this situation $\rho = \rho_{max}$, and therefore, we get $q_{out} = 0$. Therefore, if the inflow f is positive, then the traffic density immediately after will exceed the jam density value. The only way the physically viable dynamics can be satisfied is by forcing the inflow to be zero. This essentially cancels the component of the vector field normal to the surface K (as shown in Figure 3-8). Therefore, the resultant vector field (or the projection dynamics) is now given by the projection of the applied vector field onto the surface K.

Once the right face is reached, we would like the system to get out of the jam density region. The current model does not allow that. To understand this, let us look at the model. Let us take an infinitesimal section of the highway as shown in Figure 3-9.

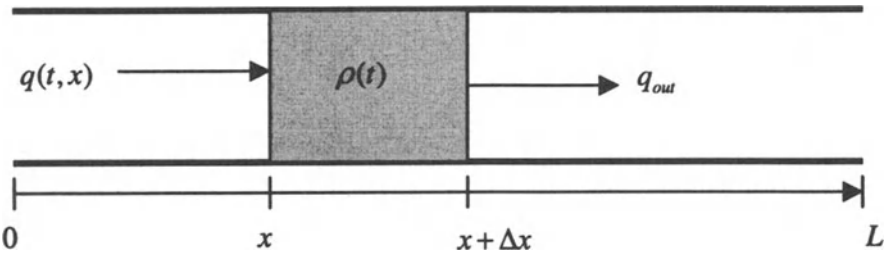

Figure 3-9: Infinitesimal Section

Now the dynamics for this section can be derived from equation (1) as

$$\dot{\rho}(t) = \frac{1}{\Delta x}[q(t,x) - q_{out}(t)] \tag{27}$$

Using (21) for the outflow, we can rewrite (23) as

$$\dot{\rho}(t) = \frac{1}{\Delta x}[q(t,x) - v_f \rho(t)(1 - \frac{\rho(t)}{\rho_{\max}})] \tag{28}$$

We know that the inflow cannot be negative. This is true because the outflow of one section is an inflow to the next section. Outflow because of its equation can only vary from zero to its maximum value (equations (2) and (3)), and hence cannot be negative. The inflow can also come from the term f that we always specify as nonnegative. In addition, at jam density, the outflow term is zero. Thus when the system reaches jam density, there is no way for the system to get out of it. Let us illustrate this more clearly through (28). We can rewrite (28) by expanding the lefthand side as

$$\frac{\rho(t+\Delta t) - \rho(t)}{\Delta t} = \frac{1}{\Delta x}[q(t,x) - v_f \rho(t)(1 - \frac{\rho(t)}{\rho_{\max}})] \tag{29}$$

Now we can collect terms to one side to get the traffic density as

$$\rho(t+\Delta t) = \rho(t) + \frac{\Delta t}{\Delta x}[q(t,x) - v_f \rho(t)(1 - \frac{\rho(t)}{\rho_{\max}})] \tag{30}$$

Let us say that at time T, the density of this section reaches the jam density. This means that the system is now operating on the right face. Then the density at an infinitesimal time after T will be given by

$$\rho(T+\Delta t) = \rho_{\max} + \frac{\Delta t}{\Delta x} q(T,x) \tag{31}$$

Since

$$q(T,x) \geq 0 \tag{32}$$

we get the following constraint:

$$\rho(T+\Delta t) \geq \rho_{\max} \tag{33}$$

Since we are at the right face, we add the projection dynamics to force (32) to become the following equality:

$$q(T,x)=0 \tag{34}$$

Using this projection constraint, we see that we will get

$$\rho(T+\Delta t)=\rho_{\max} \tag{35}$$

The analysis from (27) to (35) has shown why when the section reaches the jam density, the system is stuck at that density. This shows that the Greenshield model is not appropriate for the behavior after a traffic jam. We can add a diffusion term to the velocity equation so that the vehicles can diffuse out of the section after a traffic jam. As shown in the previous chapter the diffusion term addition will give us the following formula for the velocity:

$$v(T)=v_f\left(1-\frac{\rho(T)}{\rho_{\max}}\right)-D\left(\frac{\partial\rho}{\partial x}\right)/\rho(T) \tag{36}$$

Using this in (2) gives us the following formula for traffic flow:

$$q_{out}=v_f\rho(T)\left(1-\frac{\rho(T)}{\rho_{\max}}\right)-D\left(\frac{\partial\rho(t,x)}{\partial x}\right) \tag{37}$$

By addition of the diffusion term, we see that at time T when the traffic jam has happened, we will have

$$q_{out}=-D\left(\frac{\partial\rho(t,x)}{\partial x}\right) \tag{38}$$

When the gradient of the traffic density is negative, i.e. when the traffic density at the downstream is less than that at the section, then the outflow will be positive. Thus in that case the traffic density in the section would be reduced if the outflow were greater than the inflow. On the other hand, if the inflow were greater than the outflow, then the inflow would be forced to be equal to the outflow, so that the traffic would stay at the jam density. Hence, when the system trajectory reaches the right face, after some time

spent on the boundary, the trajectory might come back to the interior of the region as shown in Figure 3-10 .

Notice that based on (37), it is possible for the outflow to be negative. Therefore, we have to choose the parameter D in such a way that that condition never happens. We have to choose D based on the experimental data, and of course, in order for the outflow to be nonnegative, it should at the least satisfy the following constraint:

$$D \le v_f \rho(T)\left(1-\frac{\rho(T)}{\rho_{\max}}\right)/\left(\frac{\partial \rho(t,x)}{\partial x}\right) \tag{39}$$

Using this in (37) gives us the desired condition:

$$q_{out} \ge 0 \tag{40}$$

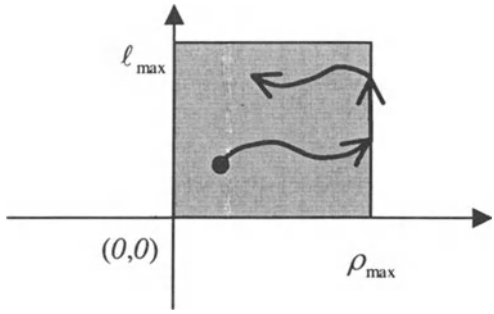

Figure 3-10: Right Face Viable Dynamics

Notice that there is a very important constraint on the outflow. That comes from the section right at the downstream of the section under consideration. The section at the downstream can put constraints on the outflow of the upstream section. If the downstream section has already reached its jam density, then the outflow from the section will be zero. This effect is valid for behavior everywhere.

3.6.2 Left Face

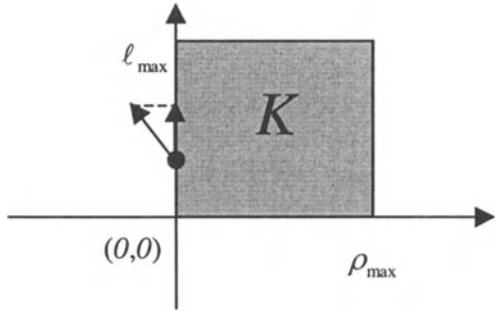

Figure 3-11: Left Face Dynamics

Left face dynamics are the ones described in Section 3.3 on negative density. When the system has reached the left face, then the traffic density is zero. The dynamics of the infinitesimal section whose density is zero is again given by

$$\dot{\rho}(t) = \frac{1}{\Delta x}[q(t,x) - v_f \rho(t)(1 - \frac{\rho(t)}{\rho_{max}})] \tag{41}$$

This equation is valid when there is no diffusion considered. Now, since the density is zero at time instant T, we will get

$$\dot{\rho}(t) = \frac{1}{\Delta x} q(T,x) \tag{42}$$

Discretizing in time, we get

$$\rho(T + \Delta t) = \rho(T) + \frac{\Delta t}{\Delta x} q(T,x) \tag{43}$$

which for the condition of zero density is the same as

$$\rho(T + \Delta t) = \frac{\Delta t}{\Delta x} q(T,x) \tag{44}$$

The q term can be the inflow into a section from the ramp or from another section. In any case, only when this term is negative does the traffic density of the section become negative. Therefore, putting a nonnegative constraint on the outflow is enough to guarantee the satisfaction of the viability at the left face.

If we use the diffusion term, then as shown before

$$q_{out} = v_f \rho(T)\left(1 - \frac{\rho(T)}{\rho_{\max}}\right) - D\left(\frac{\partial \rho(t,x)}{\partial x}\right) \tag{45}$$

The infinitesimal section dynamics become

$$\dot{\rho}(t) = \frac{1}{\Delta x}[q(t,x) - v_f \rho(t)(1 - \frac{\rho(t)}{\rho_{\max}}) + D\frac{\partial \rho(t,x)}{\partial x}] \tag{46}$$

After discretizing this equation we get

$$\rho(T + \Delta t) = \rho(T) + \frac{\Delta t}{\Delta x}[q(T,x) - v_f \rho(T)(1 - \frac{\rho(T)}{\rho_{\max}}) + D\frac{\partial \rho(t,x)}{\partial x}] \tag{47}$$

Noting that the traffic density is zero at the left face, we get

$$\rho(T + \Delta t) = \frac{\Delta t}{\Delta x}[q(T,x) + D\frac{\partial \rho(t,x)}{\partial x}] \tag{48}$$

Equation (48) puts the following constraint on the relationship between the inflow and the diffusion term for the traffic density to not violate the viability at the left face:

$$q(T,x) \geq -D\frac{\partial \rho(t,x)}{\partial x} \tag{49}$$

3.6.3 Top Face

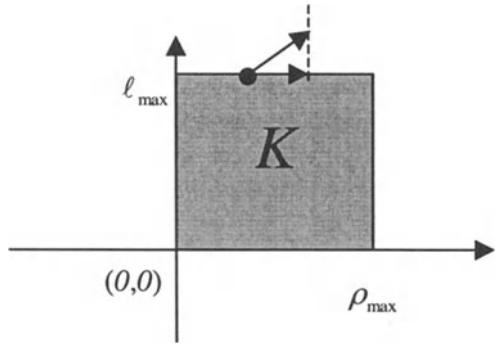

Figure 3-12: Top Face Dynamics

Top face dynamics are the ones described in Section 3.2. To understand these dynamics let us rewrite the queue dynamics below:

$$\dot{\ell} = r(t) - u(t) \tag{50}$$

At the top face boundary, the queue length has reached the maximum. For the system to be viable, there should be no increase of the queue length from the top face. Looking at (50) this is possible only if the following is satisfied at time T (the time the system is at the top face):

$$r(T) - u(T) \leq 0 \tag{51}$$

The actual traffic only allows nonnegative values for both $r(t)$ and $u(t)$, since the traffic is unidirectional on any road. Therefore, at the top face, we can constrain the control law design to satisfy

$$r(T) = u(T) \tag{52}$$

3.6.4 Bottom Face

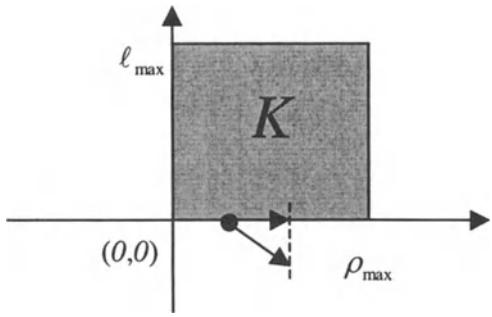

Figure 3-13: Bottom Face Dynamics

Bottom face dynamics are the ones described in Section 3.4. To understand these dynamics let us rewrite the queue dynamics:

$$\dot{\ell} = r(t) - u(t) \tag{53}$$

At the bottom face boundary, the queue length has reached the lowest value of zero. For the system to be viable, there should be no decrease of the queue length from the bottom face. Looking at (26) this is possible only if the following is satisfied at time T (the time the system is at the bottom face):

$$r(T) - u(T) \geq 0 \tag{54}$$

We can also study the four corner conditions and find out exactly what constraints should be satisfied for the system to be viable. For instance, at the right-top corner we have the jam density and the maximum queue length reached as shown in Figure 3-14.

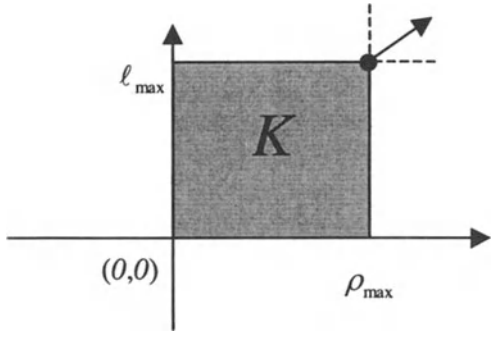

Figure 3-14: Top Right Dynamics

4. 4. SUMMARY

In this chapter, we studied:

- The distributed dynamics of the ramp metering system
- Various control objectives the control laws should be designed for
- Various limitations of the model presented
- Projection dynamics and how to apply the principles so that the system model behaves meaningfully.

5. QUESTIONS

1. What is boundary injection control?
2. What are the outcomes of choosing one speed flow relationship over others in the development of control? What are the criteria to be considered when selecting a speed flow model to be used in the control problem?
3. Explain why "maintaining the highway density at critical value" is chosen as a control objective.
4. Explain three criteria (22), (23), (24) in detail. Give a clear description of the use of the variables w_1 and w_2.
5. What are the projection dynamics for a ramp metering problem? What is the use of projection dynamics?
6. Why isn't Greenshield's model appropriate for the behavior after a traffic jam?

6. PROBLEM

1. In Section 3.6, face (top, bottom, right, left) conditions were studied. Now, for the corner conditions of the boundary surface, given in Section 3.6, find out what constraints should be satisfied for the system to be stable.

7. REFERENCES

1. Greenshield, B. D., "A Study in Highway Capacity, Highway Research Board," Proceedings, 14, 1935, 458.
2. Greenberg, H., "An Analysis of Traffic Flow," Operations Research, 7., 1959, 78-85.
3. Musha, T., and Higuchi, H., "Traffic Current Fluctuation and the Burgers' equation," Japanese Journal of Applied Physics, 17, 1978,, ,811-816.
4. Burns, J. A. and Kang, S., 'A Control Problem for Burgers' Equation with Bounded Input/Output", Nonlinear Dynamics 2, ,1991, 235-262.
5. Cole, J. D., 'On a Quasi-linear Parabolic Equation Occurring in Aerodynamics"', Quart. Appl. Math. IX, 1951, 225-236.

Chapter 4

SIMULATION SOFTWARE FOR DISTRIBUTED MODEL

This chapter presents the numerical software we have developed to perform simulations using the distributed model of the ramp system. The software is developed in Matlab. We present a simple algorithm first. Then we show the limitations of that algorithm. Those limitations are removed by adding the projection dynamics elements discussed in the last chapter.

1. BASIC MODEL

We present a basic distributed model developed in the last chapter for which we will develop a numerical method for solution. Then we will develop Matlab software for simulation. We will perform some simulations to assess the performance and make enhancements to remove the limitations of the model.

Using the same variables as used in the last chapter, we present the model developed in the last chapter as

$$\frac{\partial \rho(t,x)}{\partial t} + \frac{\partial q(t,x)}{\partial x} = 0 \tag{1}$$

$$q(t,x) = \rho(t,x)v(t,x) \tag{2}$$

P. Kachroo et al., *Feedback Ramp Metering in Intelligent Transportation Systems*

$$v = v_f(1 - \frac{\rho}{\rho_{\max}}) \tag{3}$$

$$\dot{\ell} = r(t) - u(t) \tag{4}$$

This model is for Figure 4-1

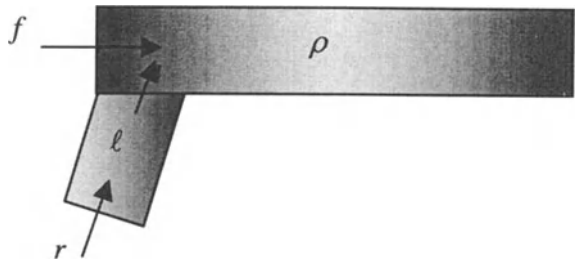

Figure 4-1: Isolated Ramp Model

Combining (1) to (4) and the initial condition, we get the combined model as

$$\text{Dynamics: } \begin{cases} \dfrac{\partial \rho(t,x)}{\partial t} + \dfrac{\partial[\rho(t,x)v_f(1 - \frac{\rho(t,x)}{\rho_{\max}})]}{\partial x} = 0 \\ \dot{\ell} = r(t) - u(t) \end{cases} \tag{5}$$

$$\text{Boundary Condition: } \rho(t,0)v_f(1 - \frac{\rho(t,0)}{\rho_{\max}}) = f(t) + u(t) \tag{6}$$

$$\text{Initial Condition: } \rho(0,x) = \psi(x) \tag{7}$$

2. NUMERICAL ALGORITHM

To develop a numerical algorithm to solve the system given by one partial differential equation and one ordinary differential equation (5) with the boundary condition (6), we will divide the highway mainline into multiple sections. This will effectively produce a space discretization of the mainline. This discretization is shown in Figure 4-2

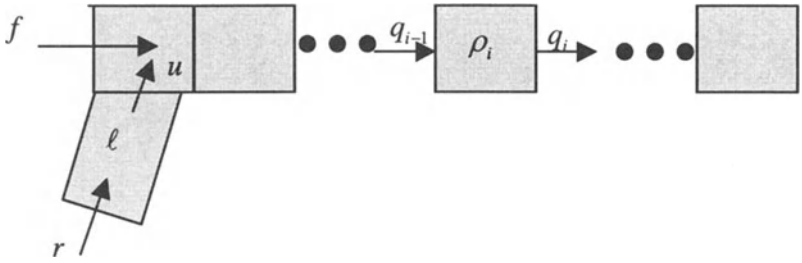

Figure 4-2: Space Discretization

The dynamics of the first section is given by

$$\dot{\rho}_1 = \frac{1}{L}[f - q_1 + u] \tag{8}$$

We have used L to indicate the fixed section length. Since

$$q_1 = v_f \rho_1 (1 - \frac{\rho_1}{\rho_{\max}}) \tag{9}$$

we can write the dynamics of the first section as

$$\dot{\rho}_1 = \frac{1}{L}[f - v_f \rho_1 (1 - \frac{\rho_1}{\rho_{\max}}) + u] \tag{10}$$

The dynamics of the i^{th} section is given by

$$\dot{\rho}_i = \frac{1}{L}[q_{i-1} - q_i] \tag{11}$$

Since

$$q_i = v_f \rho_i (1 - \frac{\rho_i}{\rho_{\max}}) \tag{12}$$

we can write the dynamics of the i^{th} section as

$$\dot{\rho}_i = \frac{1}{L}[v_f \rho_{i-1}(1 - \frac{\rho_{i-1}}{\rho_{\max}}) - v_f \rho_i (1 - \frac{\rho_i}{\rho_{\max}})] \tag{13}$$

We have essentially converted the PDE problem stated in (5), (6), and (7) into the following system of ODEs:

$$\text{Dynamics:} \quad \begin{cases} \dot{\rho}_1 = \frac{1}{L}[f - v_f \rho_1 (1 - \frac{\rho_1}{\rho_{\max}}) + u] \\ \dot{\rho}_i = \frac{1}{L}[v_f \rho_{i-1}(1 - \frac{\rho_{i-1}}{\rho_{\max}}) - v_f \rho_i (1 - \frac{\rho_i}{\rho_{\max}})], \quad 1 < i \le n \\ \dot{\ell} = r(t) - u(t) \end{cases} \tag{14}$$

$$\text{Initial Condition: } \rho_i(0) = \psi_i(x), \quad 1 < i \le n \tag{15}$$

We can numerically solve (14) and (15) using any of the numerical techniques available for solving ODEs (for example, Runga-Kutta algorithm). We will, however, discretize (14) in time using the Euler method, and obtain difference equations that can be easily solved on the computer.

Using the Euler approximation on (8) for the first section, we get

$$\frac{\rho_1(t+T) - \rho_1(T)}{T} = \frac{1}{L}[f - q_1 + u] \tag{16}$$

We use T as the sampling time, which we assume as a constant. Rearranging (16) gives

$$\rho_1(t+T) = \rho_1(T) + \frac{T}{L}[f - q_1 + u] \tag{17}$$

or

$$\rho_1(t+T) = \rho_1(t) + \frac{T}{L}[f - v_f \rho_1 (1 - \frac{\rho_1(t)}{\rho_{\max}}) + u] \tag{18}$$

The dynamics of the i^{th} section can be time discretized as

$$\frac{\rho_i(t+T) - \rho(t)}{T} = \frac{1}{L}[q_{i-1} - q_i] \tag{19}$$

We can write the time discretized dynamics of the i^{th} section as

$$\rho_i(t+T) = \rho_i(t) + \frac{T}{L}[v_f \rho_{i-1}(1 - \frac{\rho_{i-1}(t)}{\rho_{\max}}) - v_f \rho_i (1 - \frac{\rho_i(t)}{\rho_{\max}})] \tag{20}$$

The ramp queue length dynamics can also be discretized. Therefore, (4) would turn out to be

$$\ell(t+T) = \ell(t) + T[r(t) - u(t)] \tag{21}$$

Now the finite difference equation model for the system is the following:

Dynamics:

$$\begin{cases} \rho_1(t+T) = \rho_1(t) + \frac{T}{L}[f - v_f \rho_1 (1 - \frac{\rho_1(t)}{\rho_{\max}}) + u] \\ \rho_i(t+T) = \rho_i(t) + \frac{T}{L}[v_f \rho_{i-1}(1 - \frac{\rho_{i-1}(t)}{\rho_{\max}}) - v_f \rho_i (1 - \frac{\rho_i(t)}{\rho_{\max}})] \quad 1 < i \le n \\ \ell(t+T) = \ell(t) + T[r(t) - u(t)] \end{cases} \tag{22}$$

Initial Condition: $\rho_i(0) = \psi_i(x), \quad 1 < i \le n$ (23)

Now, we can easily write software code for the system (15) and (16) and perform simulations. This is done in the next section.

3. MATLAB SOFTWARE

The software is written in four files:

1. opdemixedramp.m
2. opdef.m
3. opder.m
4. opdeu.m

How these files use each other is shown in Figure 4-3. A directed arrow from file1 to file2 means that file1 is used in file2.

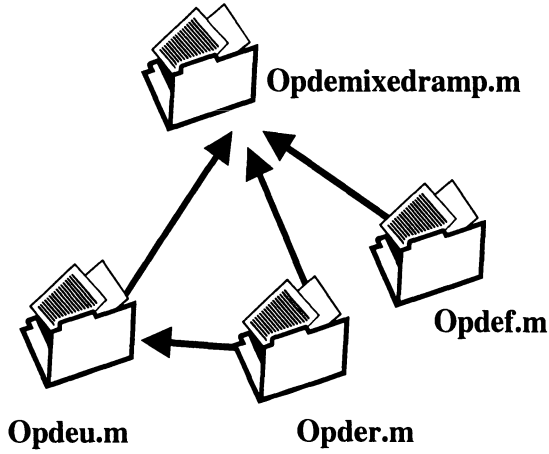

Figure 4-3: File Dependencies

The file odemixedramp.m is the main file and uses functions defined in the files opdeu.m, opder.m, and opdef.m. The function opdeu.m calculates the ramp outflow that goes into the main highway. The function opder.m is a function for providing the inflow to the ramp, and the function opdef.m provides the inflow to the main highway.

```
% Ramp Metering Code
clear;
clf;
clc;

% Input Parameters

Dx=1;   Length of the freeway section

rhom = 60;                          % Jam density
rhoc = rhom/2;                      % Critical density
```

```
vf = 15;                              % freeflow velocity

t0 = 0.0;
tf = 2;
h = 0.01;
m = (tf-t0)/h;
n = 10;                               % number of sections
rho=ones(m,n).*15;          % X array m rows, length state
columns
T=zeros(m,1);              % T array m rows (mx1)
L=[1:1:10]';
T(1)=t0;

l(1)=0;

uvar(1)=opdeu(1,rho(1,:),l(1));
rvar(1)=opder(1);
fvar(1)=opdef(1);

%There are m-1 steps and m points maximum
for i=1:m-1;
   clc
   T(i)
   T(i+1)=t0 + h*i;
   rho(i+1,1)=rho(i,1)+h*(opdef(i)+uvar(i)-vf*(1-
rho(i,1)/rhom)*rho(i,1))/Dx;
   l(i+1)=l(i)+h*(opder(i)-uvar(i));
   uvar(i+1)=opdeu(i+1,rho(i+1,:),l(i+1));
   rvar(i+1)=opder(i+1);
     fvar(i+1)=opdef(i+1);

   for j=2:n
     rho(i+1,j)=rho(i,j)+h*vf*(rho(i,j-1)*(1-rho(i,j-1)/rhom)-
rho(i,j)*(1-rho(i,j)/rhom))/Dx;
    end
end

subplot(221);
mesh(rho);
title('Traffic Density');

subplot(222);
plot(T,l);
title('Ramp Queues');
xlabel('Time');

subplot(223);
```

```
plot(T,uvar);
title('Control Rampflow');
xlabel('Time');

subplot(224);
plot(T,rvar);
title('Ramp Inflow');
xlabel('Time');


pause;
clf;
subplot(221);
plot(T,fvar);
title('Highway Inflow');
xlabel('Time');

subplot(222);
plot(L,rho(1,:));
title('Initial Traffic Density');
xlabel('Section');

subplot(223);
plot(L,rho(m,:));
title('Final Traffic Density');
xlabel('Section');

subplot(224);
plot(T,rho(:,n/2));
title('Traffic Density for Mid Section');
xlabel('Time');
```

Figure 4-4: File opdemixedramp.m

```
function opdeu = opdeu(t,x,l)
opdeu=opder(t);            % ramp outflow
```

Figure 4-5: File opdeu.m

```
function opder = opder(t)
opder = 10*(1.5+sin(0.025*t));      % ramp inflow
```

Figure 4-6: File opder.m

```
function opdef = opdef(t)
opdef = 30*(1.25+sin(0.025*t));          % mainline inflow
```

Figure 4-7: File opdef.m

4. SIMULATIONS

If we run the simulation as shown in the files of the previous section, the results we will get are plotted in Figure 4-8 and Figure 4-9.

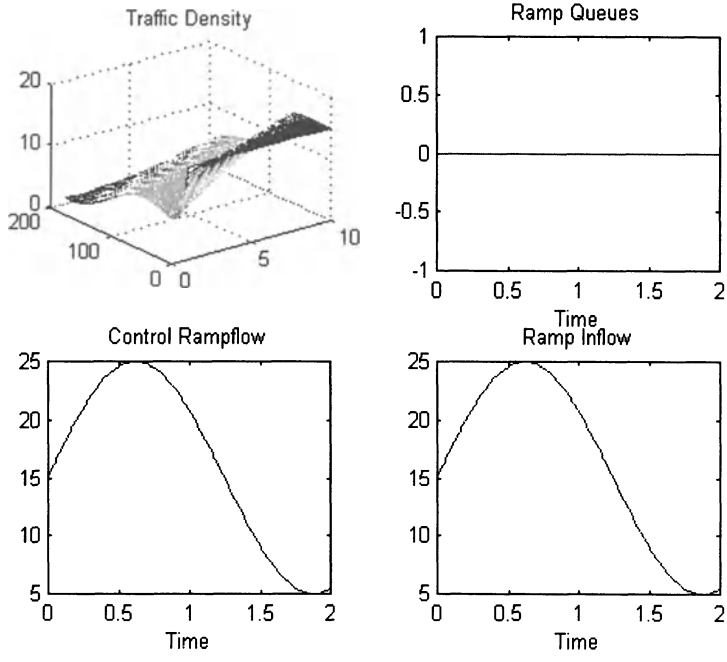

Figure 4-8: Matlab Plot 1

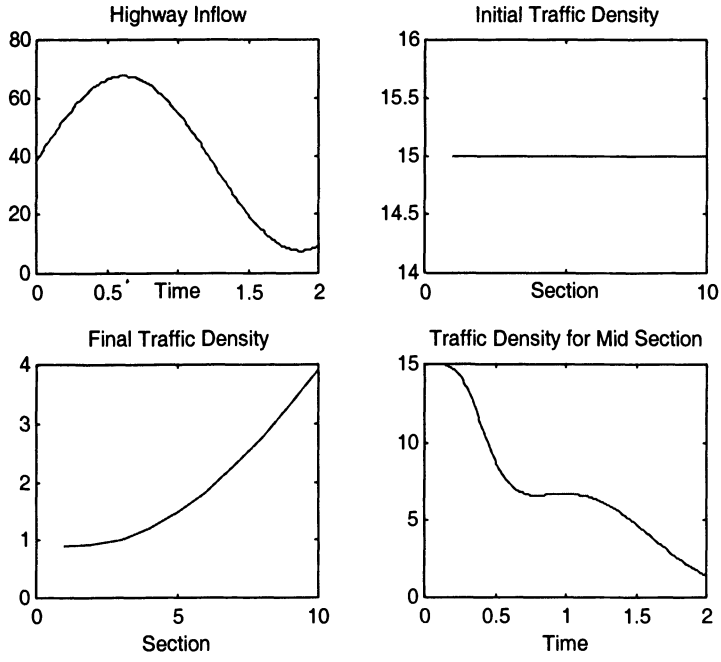

Figure 4-9: Matlab Plot 2

5. LIMITATIONS

In the last chapter, we studied the following limitations in the model that is shown in Section 4 of this chapter:

1. Attainment of queue lengths larger than the ramp capacity
2. Attainment of negative queue lengths
3. Attainment of negative traffic density on the mainline
4. Attainment of traffic density on the mainline higher than the maximum traffic density
5. Getting stuck at jam density on the mainline

Conditions 1 to 4 can be simply stated mathematically as

$$0 \leq \ell \leq \ell_{max}$$

$$0 \leq \rho \leq \rho_{max}$$

We now study all these cases here using the software and then we will make enhancements to the software so that it is able to give correct behavior of the system for these cases also.

5.1 Large Queue Length

To see this behavior we simulate the system making the ramp outflow into the mainline equal to zero. This way the ramp queue length keeps increasing. The only change we make is in the file opdeu.m. The new file is shown below.

```
function opdeu = opdeu(t,x,l)
opdeu = 0;                %ramp outflow
```

Figure 4-10: Modified Control File

The output of the system with this input is shown in the plot below.

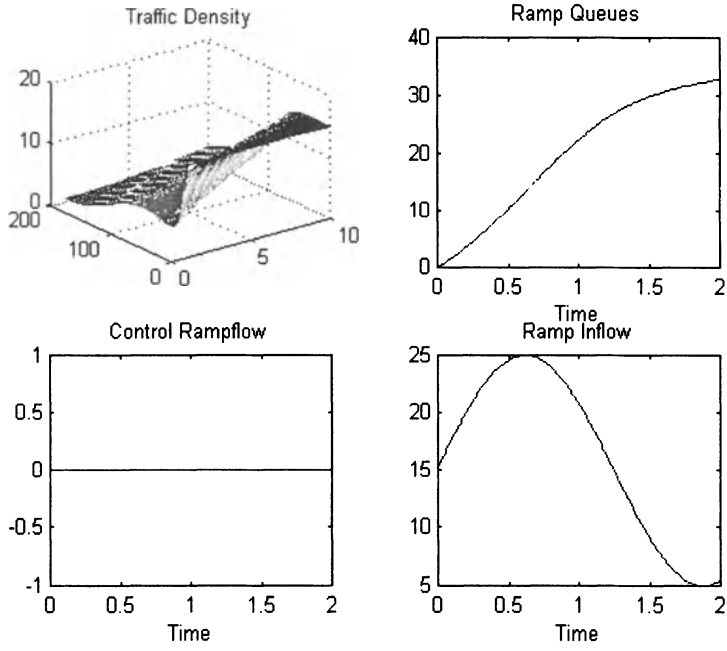

Figure 4-11: Plot for Large Queues

We see in this plot that the queue lengths, as expected, are increasing. Let us say that the capacity of the ramp is 30. Then not only the plot should saturate at 30, but we also should be able to plot the part of the ramp demand

that is being satisfied because some of it will be rejected corresponding to the saturated part.

The file opder.m is modified and the new version is shown below.

```
function opder = opder(t,l,lmax)
if l<lmax
   opder = 10*(1.5+sin(0.025*t));        % ramp inflow
else
   opder = 0;
end;
```

Figure 4-12: Modified Ramp Inflow File

Notice that the input arguments to the function opder have changed. Now we have three instead of one. The calling functions will also change accordingly. The modified part of the calling function opdemixedramp.m is shown below.

```
% Input Parameters

Dx=1;

rhom = 60;                          % Jam density
rhoc = rhom/2;                      % Critical density
vf = 15;                            % freeflow velocity
lmax = 30;

t0 = 0.0;
tf = 2;
h = 0.01;
m = (tf-t0)/h;
n = 10;                             % number of sections
rho=ones(m,n).*15;          % X array m rows, length state
columns
T=zeros(m,1);              % T array m rows (mx1)
L=[1:1:10]';
T(1)=t0;

l(1)=0;

uvar(1)=opdeu(1,rho(1,:),l(1),lmax);
rvar(1)=opder(1,l(1),lmax);
fvar(1)=opdef(1);



%There are m-1 steps and m points maximum
```

```
for i=1:m-1;
   clc
   T(i)
   T(i+1)=t0 + h*i;
   rho(i+1,1)=rho(i,1)+h*(opdef(i)+uvar(i)-vf*(1-
rho(i,1)/rhom)*rho(i,1))/Dx;
   l(i+1)=l(i)+h*(opder(i,l(i),lmax)-uvar(i));
   uvar(i+1)=opdeu(i+1,rho(i+1,:),l(i+1),lmax);
   rvar(i+1)=opder(i+1,l(i+1),lmax);
    fvar(i+1)=opdef(i+1);
```

Figure 4-13: Modified Ramp opdemixedramp.m File

The new plot based on these changes is shown below.

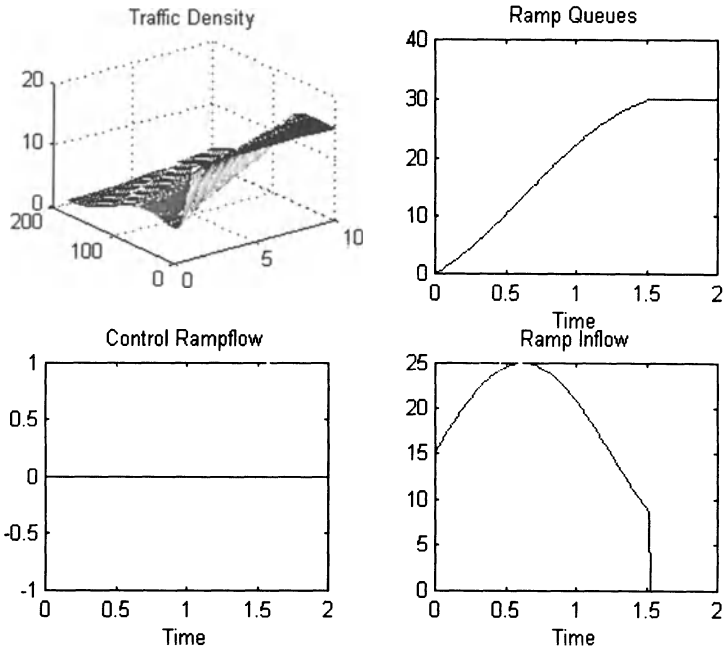

Figure 4-14: New Plot

5.2 Negative Queue Length

This situation can arise when the queue length is already zero, and then the inflow to the ramp is less than the outflow. Therefore, following projection dynamics argument, we have to modify the control law, such that the control variable does not exceed the ramp inflow when the queue length

is zero. To illustrate the effect of this change let us use the following control file.

```
function opdeu = opdeu(t,x,1,lmax,r)
opdeu = 10*(2.5+sin(0.025*t+3));          %ramp outflow
end
```

Figure 4-15: Control File for Negative Queue Length

The output of this control flow is given below.

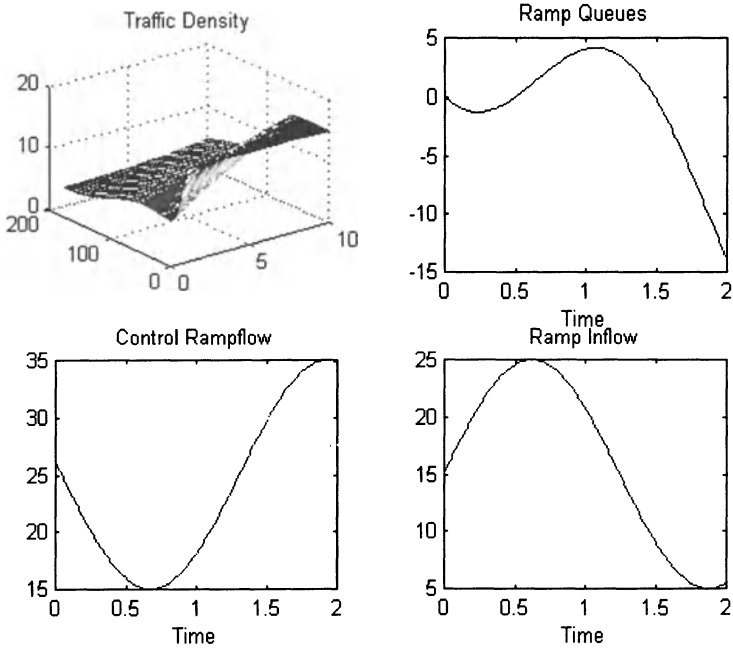

Figure 4-16: Output Showing Negative Queue Length

This output shows physically unrealizable negative queue lengths. In order to get rid of this spurious effect, we use the projection dynamics and modify the control file to get the file shown below.

```
function opdeu = opdeu(t,x,1,lmax,r)
opdeu = 10*(2.5+sin(0.025*t+3));          %ramp outflow
if 1<=0
   if r<opdeu
      opdeu = r;
   end
end
```

Figure 4-17: Control File for Negative Queue Length

The result based on this file is correct and is shown below.

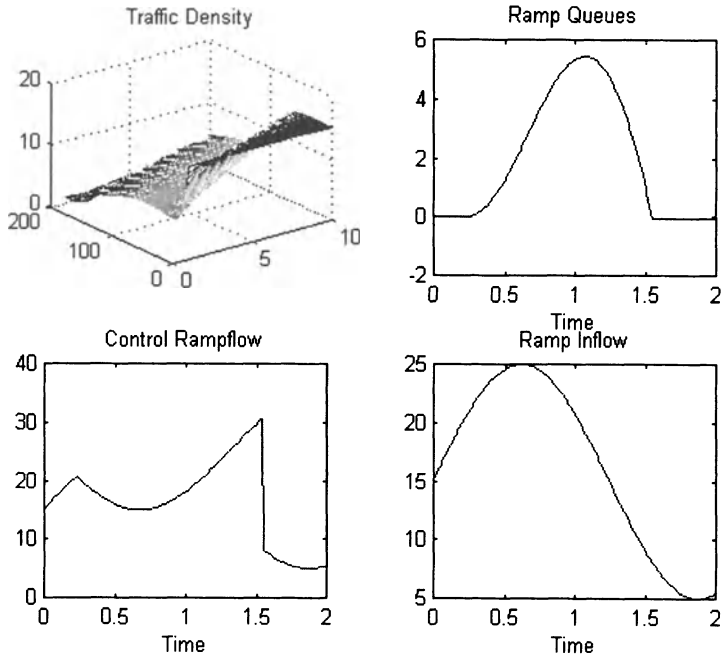

Figure 4-18: Output Using Projected Dynamics for Negative Queue Length

Notice that we have changed the input arguments for the control function in the opdeu.m file. This is because it needs the value of the ramp inflow variable for the projection dynamics. Correspondingly the modified part of the opdemixedramp.m file is shown below.

```
rvar(1)=opder(1,l(1),lmax);
uvar(1)=opdeu(1,rho(1,:),l(1),lmax,rvar(1));
fvar(1)=opdef(1);

%There are m-1 steps and m points maximum
for i=1:m-1;
   clc
   T(i)
   T(i+1)=t0 + h*i;
   rho(i+1,1)=rho(i,1)+h*(opdef(i)+uvar(i)-vf*(1-
rho(i,1)/rhom)*rho(i,1))/Dx;
   l(i+1)=l(i)+h*(opder(i,l(i),lmax)-uvar(i));
   rvar(i+1)=opder(i+1,l(i+1),lmax);
   uvar(i+1)=opdeu(i+1,rho(i+1,:),l(i+1),lmax,rvar(i+1));
```

```
    fvar(i+1)=opdef(i+1);


   for j=2:n
     rho(i+1,j)= rho(i,j)+h*vf*(rho(i,j-1)*(1-rho(i,j-
1)/rhom)-rho(i,j)*(1-rho(i,j)/rhom))/Dx;
    end
end
```

Figure 4-19: Modified Portion of opdemixedramp.m for Negative Queue Length

5.3 Negative Traffic Density on Mainline

As the model currently stands, since the ouflow from any section is zero when the traffic density is zero, therefore this condition cannot occur. However, when we add the diffusion term as explained in the previous chapter, we will have to be careful about not obtaining negative traffic densities.

5.4 Higher than Jam Density

Jam density (or maximum density) of a highway section corresponds to a situation when vehicles are in the closest packed configuration on the highway. Hence, the situation indicates traffic jam with the capacity of the section reached. Therefore, the traffic density on any section should never attain values that are higher than the jam density. Any software simulation package that gives higher than jam density values is giving spurious results. Let us study the condition under which density could reach higher than jam density values. Let us consider a section of the highway as shown in Figure 4-20.

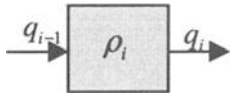

Figure 4-20: Highway Section

The section dynamics are given by

$$\dot{\rho}_i = \frac{1}{L}[q_{i-1} - q_i] \tag{24}$$

Since

$$q_i = v_f \rho_i (1 - \frac{\rho_i}{\rho_{\max}}) \tag{25}$$

we see that when

$$\rho_i = \rho_{\max} \quad \text{(traffic jam condition)} \tag{26}$$

then

$$q_i = 0 \tag{27}$$

The dynamics then give

$$\dot{\rho}_i = \frac{1}{L}[q_{i-1}] \tag{28}$$

This shows that if the inflow to the section (the same as the outflow from the previous section) is positive, the section will attain traffic density that is higher than jam density. Therefore, this puts the restriction on the previous section that its outflow will be zero if the traffic density of the section following it is equal to the traffic jam density. This implies that when the software simulation is carried out, the section densities have to be resolved starting from the last section to the first section in that order, i.e., by going in the reverse order.

Now, we will study the case of the first section, since its dynamics are different from those of the others due to the inclusion of the ramp flow term. The section dynamics are given by

$$\dot{\rho}_1 = \frac{1}{L}[f + u - q_1] \tag{29}$$

Since

$$q_1 = v_f \rho_1 (1 - \frac{\rho_1}{\rho_{\max}}) \tag{30}$$

we see that when

$$\rho_1 = \rho_{\max} \quad \text{(traffic jam condition)} \tag{31}$$

then

$$q_1 = 0 \tag{32}$$

The dynamics then give

$$\dot{\rho}_1 = \frac{1}{L}[f + u] \tag{33}$$

This shows that if the inflow to the section (the same as the sum of highway inflow and ramp inflow) is positive, the section will attain traffic density that is higher than jam density. Since the highway inflow and the ramp inflow are both nonnegative functions of time, any positive value of these two terms causes the traffic density of the first section to exceed jam density. Therefore, this puts the restriction on the two terms that when the traffic density of the first section is at the jam density value, the highway inflow and ramp inflow will be zero.

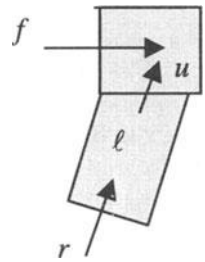

Figure 4-21: First Section

Notice that the phenomenon of performing simulations backward in space (x-axis) and the effect of downstream sections on upstream sections is typical of highway dynamics and is shown as the shock phenomenon.

Since the modifications caused by these developments to the simulation software files are extensive, we will present all four files completely here. These four files have the same names as the ones we have been using.

```
% Ramp Metering Code
clear;
clf;
clc;
```

```
% Input Parameters

Dx=1;

rhom = 60;                          % Jam density
rhoc = rhom/2;                      % Critical density
vf = 15;                            % freeflow velocity
lmax = 30;

t0 = 0.0;
tf = 2;
h = 0.01;
m = (tf-t0)/h;
n = 10;                             % number of sections
rho=ones(m,n).*15;          % X array m rows, length state
columns
T=zeros(m,1);              % T array m rows (mx1)
L=[1:1:10]';
T(1)=t0;

l(1)=0;

rvar(1)=opder(1,l(1),lmax);
uvar(1)=opdeu(1,rho(1,:),l(1),lmax,rvar(1),rhom);
fvar(1)=opdef(1);

%There are m-1 steps and m points maximum
for i=1:m-1;
   clc
   T(i)
   T(i+1)=t0 + h*i;

   flag=0;
   for j=n:-1:2
      qin=vf*(rho(i,j-1)*(1-rho(i,j-1)/rhom));
      if flag==0
         qout=vf*(rho(i,j)*(1-rho(i,j)/rhom));
      else
         qout=0;
      end
         rhoinc=h*(qin-qout)/Dx;
      if rho(i,j)>=rhom
         if (qin-qout)>=0
              rhoinc=rhom-rho(i,j);
         end
         flag=1;
      else
```

```
        flag=0;
    end
    rho(i+1,j)=rho(i,j)+rhoinc;
    end

  qin=opdef(i)+uvar(i);
  if flag==0
     qout=vf*(rho(i,1)*(1-rho(i,1)/rhom));
  else
     qout=0;
  end
  rhoinc=h*(qin-qout)/Dx;
  if rho(i,1)>=rhom
     if (qin-qout)>=0
        rhoinc=rhom-rho(i,1);
     end
  end
  rho(i+1,1)=rho(i,1)+rhoinc;
  l(i+1)=l(i)+h*(opder(i,l(i),lmax)-uvar(i));
  rvar(i+1)=opder(i+1,l(i+1),lmax);
  uvar(i+1)=opdeu(i+1,rho(i+1,:),l(i+1),lmax,rvar(i+1),rhom);
    fvar(i+1)=opdef(i+1);


end

subplot(221);
mesh(rho);
title('Traffic Density');

subplot(222);
plot(T,rvar,'-',T,fvar,'-.');
title('Ramp and Highway Inflow');
xlabel('Time');


subplot(223);
plot(L,rho(1,:),'-',L,rho(m,:),'-.');
title('Initial & Final Traffic Density');
xlabel('Section');


subplot(224);
plot(T,rho(:,1));
title('Traffic Density for the First Section');
xlabel('Time');
```

```
pause;
clf;
subplot(221);
plot(T,rho(:,n/2));
title('Traffic Density for the Mid Section');
xlabel('Time');

subplot(222);
plot(T,rho(:,n));
title('Traffic Density for the Last Section');
xlabel('Time');

subplot(223);
plot(T,l);
title('Ramp Queues');
xlabel('Time');

subplot(224);
plot(T,uvar);
title('Control Rampflow');
xlabel('Time');
```

Figure 4-22: opdemixedramp.m File for Jam Density Corrections

```
function opder = opder(t,l,lmax)
if l<lmax
   opder = 25*(1.5+sin(0.025*t));        % ramp inflow
else
   opder = 0;
end;
```

Figure 4-23: opder.m File for Jam Density Corrections

```
function opdef = opdef(t)
opdef = 100*(1.5+sin(0.025*t));          % mainline inflow
```

Figure 4-24: opdef.m File for Jam Density Corrections

```
function opdeu = opdeu(t,x,l,lmax,r,rmax)
opdeu=r;          % ramp outflow
% opdeu = 10*(2.5+sin(0.025*t+3));        %ramp outflow
if l<=0
   if r<opdeu
      opdeu = r;
   end
end
if x(1)>=rmax
   opdeu = 0;
end
```

Figure 4-25: opdeu.m File for Jam Density Corrections

After reviewing these files, one can easily see the changes in the software code for forcing the traffic densities to never exceed the jam density values. Figure 23 shows the file for ramp inflow. The file shows that when the ramp queue has reached its maximum value then the ramp inflow is forced to zero. The same is true for the ramp outflow file (Figure 4-25). This file shows the ramp outflow values become zero when the traffic density of the first section reaches the jam density value. Figure 4-24 does not show a similar condition because the main file (Figure 4-23) automatically takes care of that and also takes care of reverse iteration with reverse constraints on the section traffic densities. The simulation results are plotted next that show this expected correct behavior.

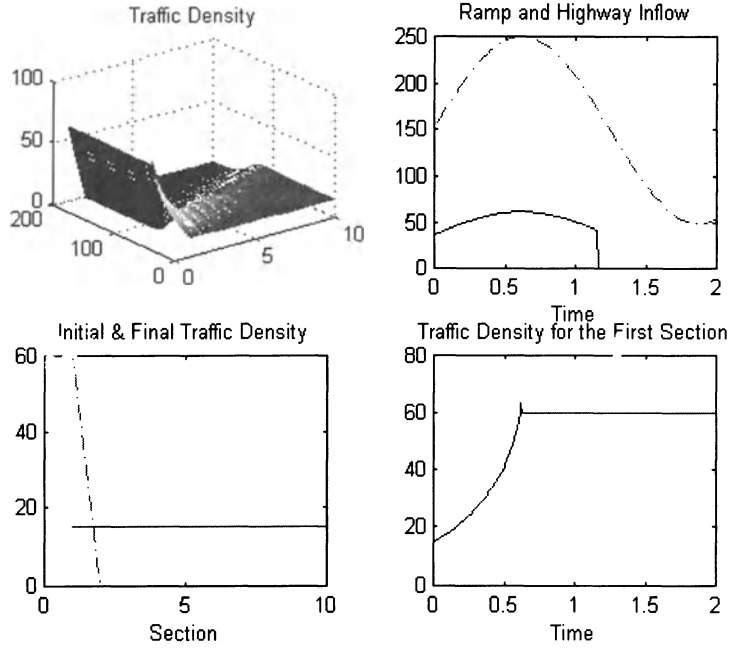

Figure 4-26: Plot-1 for Jam Density Corrections

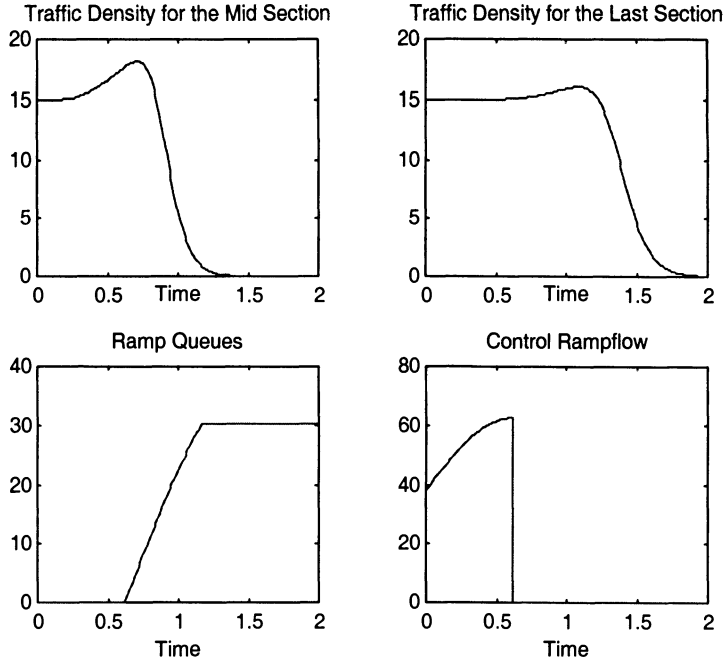

Figure 4-27: Plot-2 for Jam Density Corrections

These plots show that the first section reaches the jam density. After that there can be no inflow onto this section. However, all the other sections are meanwhile able to drain out all their traffic.

5.5 Traffic Diffusion

Traffic diffusion is needed so that once any section reaches the jam density, there is a way for the traffic to diffuse out of the section. Before we introduce this effect in the model and the simulation, let us look at a traffic situation in simulation, which we will compare with the model with diffusion terms later.

We use the following highway traffic inflow and ramp inflow files.

```
function opdef = opdef(t)
if t>75 & t<125
   opdef = 75*(1.5+sin(0.025*t));
else
   opdef = 20*(1.5+sin(0.025*t));
end
```

Figure 4-28: Traffic Inflow for Impulse Disturbance Case

```
function opder = opder(t,l,lmax)
if l<lmax
   opder = 5*(1.5+sin(0.025*t));          % ramp inflow
else
   opder = 0;
end;
```

Figure 4-29: Ramp Inflow for Impulse Disturbance Case

The simulation results using these inputs are plotted in the following figures. We see that the first section gets high traffic density but less than the jam density due to the extra disturbance introduced in the simulation. This high density of traffic flows out through the later sections.

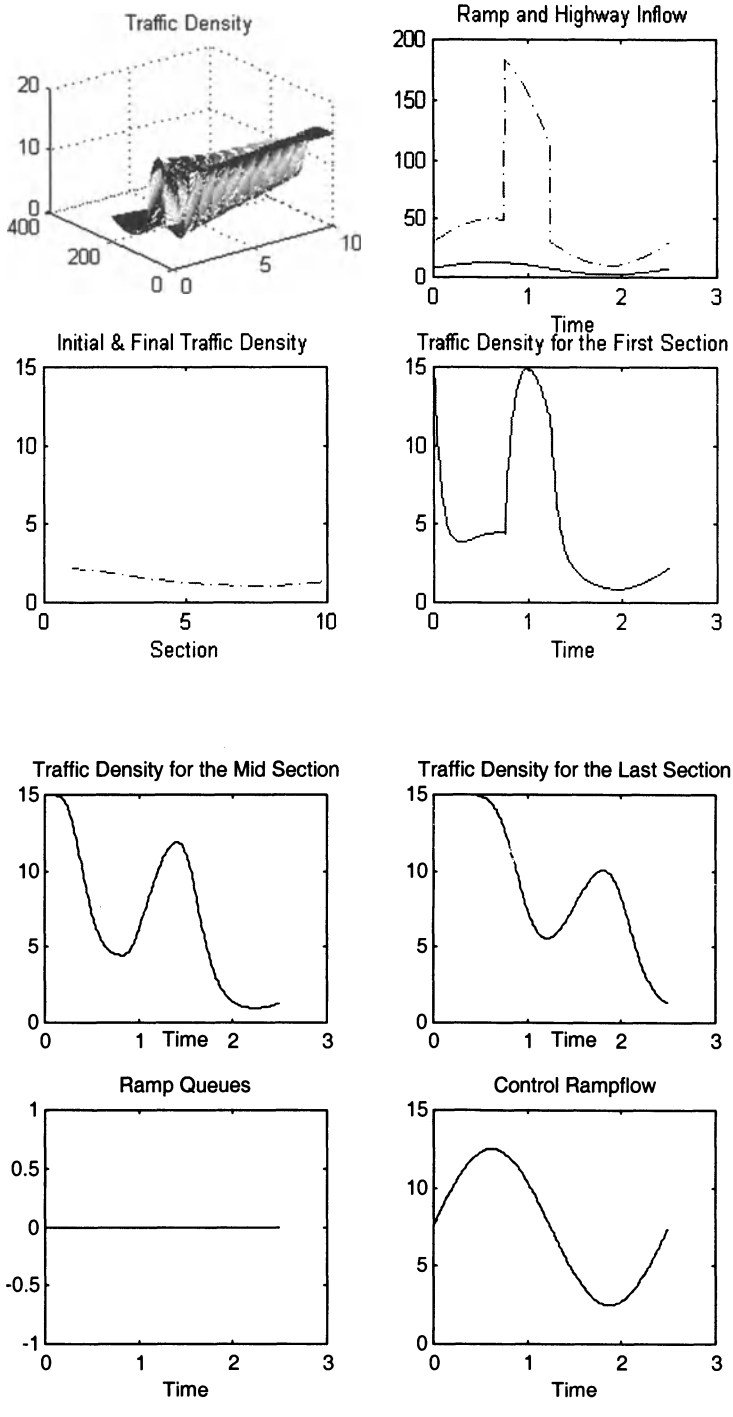

Figure 4-30: Plots for Impulse Disturbance Case

Now, if we increase the disturbance further as shown in the following file, then the first section reaches jam density. We will add the diffusion terms in the model to show how this traffic jam is diffused out using the diffusion model.

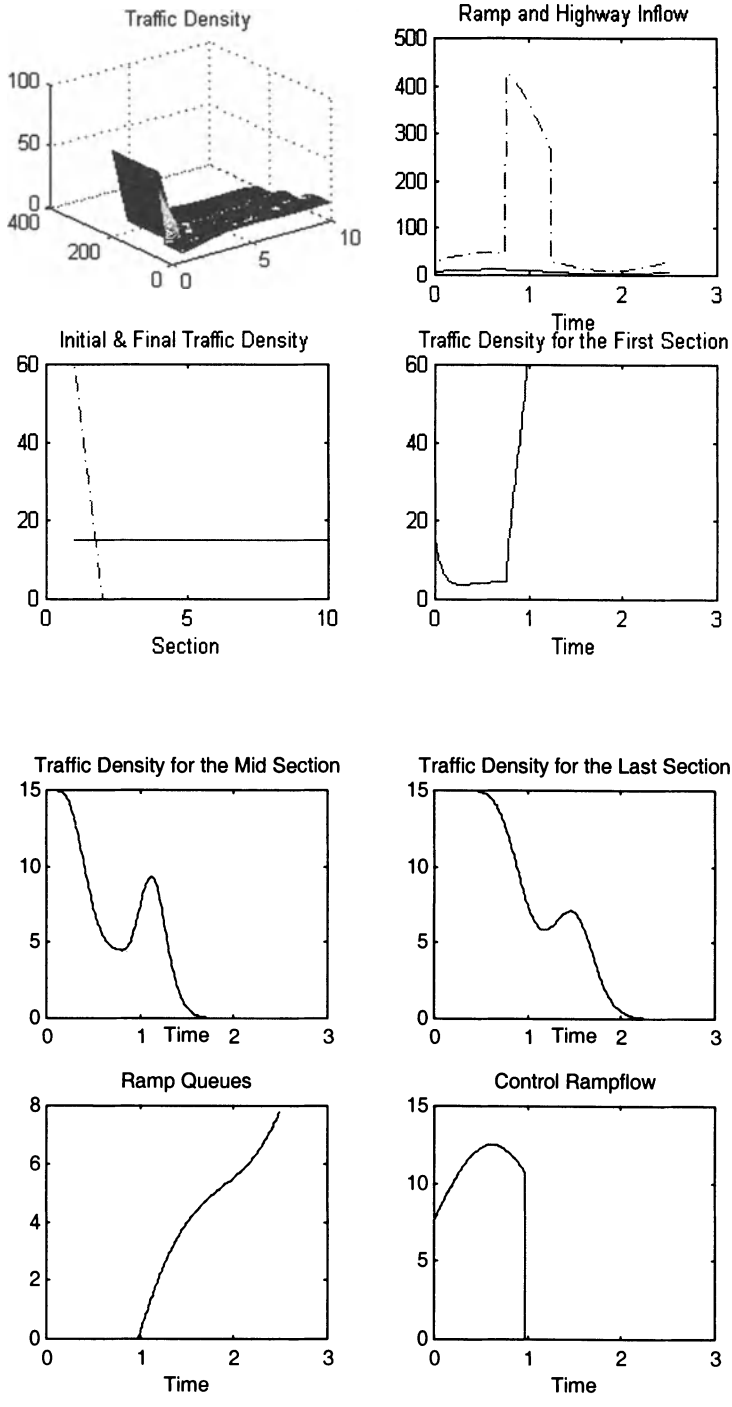

Figure 4-31: Plots for Impulse Disturbance Case with a Traffic Jam

The nonplotting part of the code in the file opdemixedramp.m with the diffusion terms included is given below.

```
% Ramp Metering Code
clear;
clf;
clc;

% Input Parameters

Dx=1;

rhom = 60;                          % Jam density
rhoc = rhom/2;                      % Critical density
vf = 15;                            % freeflow velocity
lmax = 30;
Diff=0.5;

t0 = 0.0;
tf = 2.5;
h = 0.01;
m = (tf-t0)/h;
n = 10;                             % number of sections
rho=ones(m,n).*15;          % X array m rows, length state
columns
T=zeros(m,1);              % T array m rows (mx1)
L=[1:1:10]';
T(1)=t0;

l(1)=0;

rvar(1)=opder(1,l(1),lmax);
uvar(1)=opdeu(1,rho(1,:),l(1),lmax,rvar(1),rhom);
fvar(1)=opdef(1);

rholast=0;

%There are m-1 steps and m points maximum
for i=1:m-1;
   clc
   T(i)
   T(i+1)=t0 + h*i;


   flag=0;
   qin=vf*(rho(i,n-1)*(1-rho(i,n-1)/rhom));
      if flag==0
         qout=vf*(rho(i,n)*(1-rho(i,n)/rhom))+Diff*(rho(i,n)-
```

```
rholast);
      else
         qout=0;
      end
         rhoinc=h*(qin-qout)/Dx;
      if rho(i,n)+rhoinc >=rhom
         rhoinc=rhom-rho(i,n);
         flag=1;
      else
         flag=0;
     end
     rho(i+1,n)=rho(i,n)+rhoinc;

   for j=n-1:-1:2
      qin=vf*(rho(i,j-1)*(1-rho(i,j-1)/rhom));
      if flag==0
         qout=vf*(rho(i,j)*(1-rho(i,j)/rhom))+Diff*(rho(i,j)-
rho(i,j+1));
      else
         qout=0;
      end
         rhoinc=h*(qin-qout)/Dx;
      if rho(i,j)+rhoinc >=rhom
         rhoinc=rhom-rho(i,j);
         flag=1;
      else
         flag=0;
     end
     rho(i+1,j)=rho(i,j)+rhoinc;
     end

   qin=opdef(i)+uvar(i);
   if flag==0
      qout=vf*(rho(i,1)*(1-rho(i,1)/rhom))+Diff*(rho(i,1)-
rho(i,2));
   else
      qout=0;
   end
   rhoinc=h*(qin-qout)/Dx;
   if rho(i,1)+rhoinc>=rhom
      rhoinc=rhom-rho(i,1);
   end
   rho(i+1,1)=rho(i,1)+rhoinc;
   l(i+1)=l(i)+h*(opder(i,l(i),lmax)-uvar(i));
   rvar(i+1)=opder(i+1,l(i+1),lmax);
   uvar(i+1)=opdeu(i+1,rho(i+1,:),l(i+1),lmax,rvar(i+1),rhom);
    fvar(i+1)=opdef(i+1);
```

```
end
```

Figure 4-32: Part of File opdemixedramp.m with Diffusion

You can easily see the diffusion terms that have been added to the outflow terms for all sections. The output plots using this file are given below. These show how the traffic is able to diffuse out even after a traffic jam has taken place.

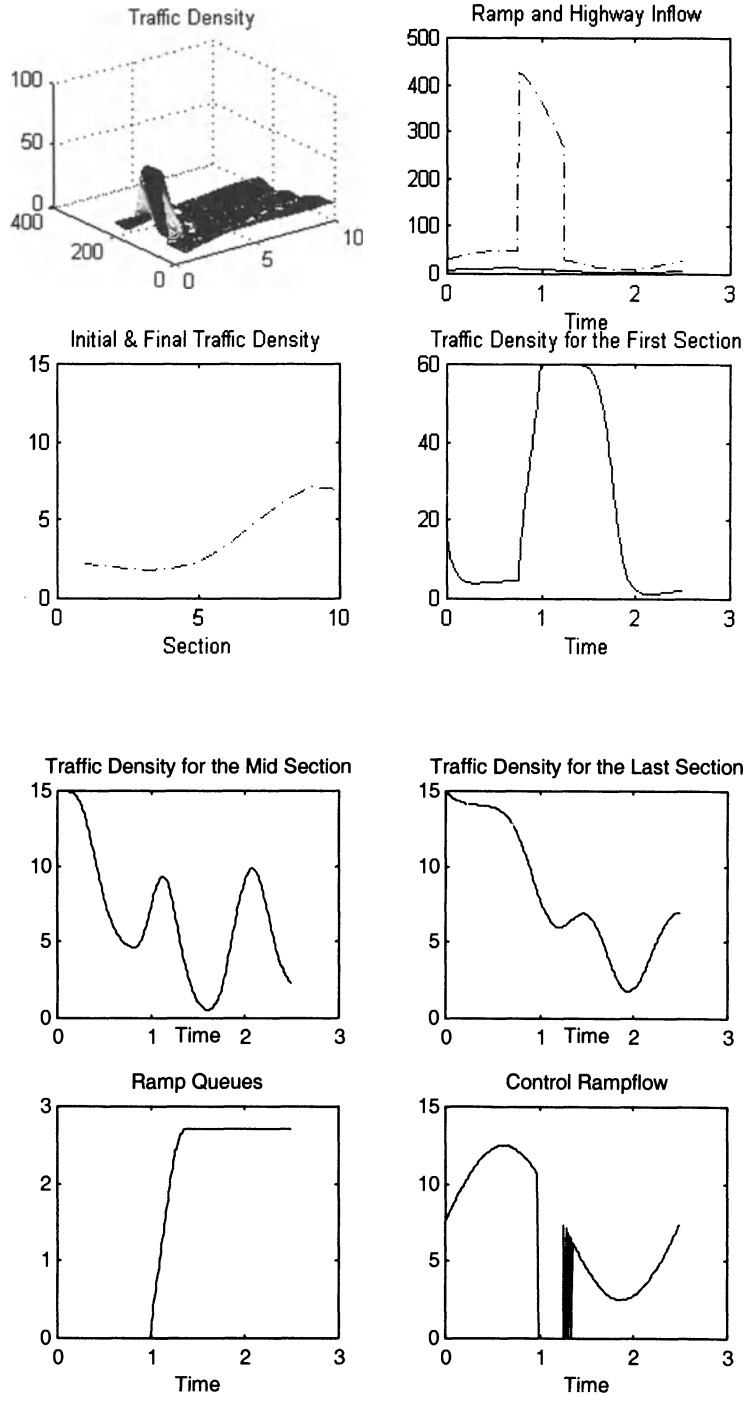

Figure 4-33: Traffic Plots with Diffusion

6. SUMMARY

In this chapter, we studied:

- How to discretize the distributed dynamics of the ramp metering system
- Software code and simulations for the model
- Various limitations of the model presented
- Projection dynamics and how to apply the principles so that the system model behaves meaningfully in the software setting.

7. QUESTIONS

1. Explain initial condition and dynamics equations of a ramp metering problem, presented by (14) and (15).
2. What are the limitations in the model given in this chapter? How were they handled? Explain briefly.
3. Study the code version given in section 4.1, and explain how "large queue length" was introduced to the system. How was the code changed in order to make the model physically realizable?
4. Explain how "Figure 4-13 plots" were obtained. What measurements and code changes have to be performed to prevent the unrealistic model results?
5. Explain why and when the traffic diffusion inclusion is needed in the model developed.
6. Explain the term "disturbance" (used on page 24) is, and how was the disturbance to the system handled in the model?

8. PROBLEMS

Write your own simple ramp metering Matlab code and test the limitations of the projection dynamics idea discussed in this chapter.Test the above Matlab code using different levels of ramp demands and determine the lower and upper bounds of demand that produce acceptable system performance.

9. REFERENCES

1. Hilderbrand, F. B., *Introduction to Numerical Analysis*, Dover, 1987.

2. Hamming, R., *Numerical Methods for Scientists and Engineers*, Dover, 1987.
3. Isaacson, E., and Keller, H. B., *Analysis of Numerical Methods*, Dover, 1994.

Chapter 5

FEEDBACK CONTROL DESIGN USING THE DISTRIBUTED MODEL

This chapter presents the feedback control design of an isolated ramp metering problem where we use the distributed model of the ramp system that has been developed till now. We show the stability properties of the closed-loop system that is obtained by the application of the feedback control law on the ramp system. We verify the effectiveness of the feedback control law by running some simulation experiments using the designed feedback control law on the isolated ramp system.

1. MODEL SUMMARY

The basic model used for the design of the feedback control law is presented below.

$$\text{Dynamics: } \begin{cases} \dfrac{\partial \rho(t,x)}{\partial t} + \dfrac{\partial[\rho(t,x)v_f(1-\dfrac{\rho(t,x)}{\rho_{\max}})]}{\partial x} = 0 \\ \dot{\ell} = r(t) - u(t) \end{cases} \tag{1}$$

$$\text{Boundary Condition: } \rho(t,0)v_f(1-\frac{\rho(t,0)}{\rho_{\max}}) = f(t) + u(t) \tag{2}$$

P. Kachroo et al., *Feedback Ramp Metering in Intelligent Transportation Systems*

Initial Condition: $\rho(0,x)=\psi(x)$ (3)

The summary of the diffusion model is

Dynamics:

$$\begin{cases}\left[\dfrac{\partial}{\partial t}\rho(x,t)+v_f\dfrac{\partial}{\partial x}\rho(x,t)\right]-2\dfrac{\rho}{\rho_{\max}}v_f\dfrac{\partial}{\partial x}\rho(x,t)-D\dfrac{\partial^2}{\partial x^2}\rho(x,t)=0 \\ \dot{\ell}=r(t)-u(t)\end{cases} \quad (4)$$

Boundary Condition: $\rho(t,0)v_f(1-\dfrac{\rho(t,0)}{\rho_{\max}})-D\dfrac{\partial\rho}{\partial x}\Big|_{(t,0)}=f(t)+u(t)$ (5)

Initial Condition: $\rho(0,x)=\psi(x)$ (6)

We will first design the feedback control law based on the basic model, and then in the next chapter, we will design a feedback control law based on the diffusion model. In practice, a substantial amount of work is done in collecting data in the field and then estimating which model is appropriate for the system. Therefore, if the data collected and analyzed indicates the basic model, we can use the feedback control law derived from the basic model. However, if the collected and analyzed field data indicates a diffusion model, then we use the feedback control law designed based on the diffusion model. The same argument is true for all the discretized models and control laws we will present in subsequent chapters.

2. CONTROL OBJECTIVE

Our aim is to design a feedback control law for the ramp-metering controller. That is, we need to control the inflow from the ramp into the highway and this rate should be a function of the current traffic conditions. Hence, we are aiming to design a real-time online traffic responsive control law. This scenario is shown in Figure 5-1.

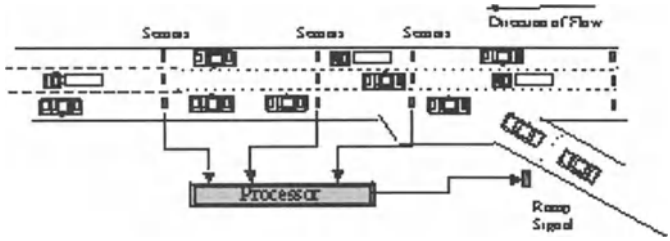

Figure 5-1: Sensors and Feedback Ramp Metering

The feedback control law (or algorithm) has to be designed to satisfy some system performance objective (as described in Chapter 3). Here we will design a control law whose aim is to keep the traffic density at a critical level for all the points on the highway. If we use the Greenshield formula, we can calculate the value of the critical density. Using the Greenshield formula, the traffic flow in terms of traffic density is given as

$$q(t,x) = v_f \rho(t,x)(1 - \frac{\rho(t,x)}{\rho_{\max}}) \tag{7}$$

We can calculate the density at which the flow is maximum (critical density) by solving

$$\rho_c(t,x) = \min_{\rho} \arg v_f \rho(t,x)(1 - \frac{\rho(t,x)}{\rho_{\max}}) \tag{8}$$

This is obtained by solving

$$\frac{\partial}{\partial \rho}[v_f \rho(t,x)(1 - \frac{\rho(t,x)}{\rho_{\max}})] = 0 \tag{9}$$

This is solved in the following steps:

$$\frac{\partial}{\partial \rho}[v_f (\rho(t,x) - \frac{\rho^2(t,x)}{\rho_{\max}})] = 0 \tag{10}$$

$$1 - 2\frac{\rho(t,x)}{\rho_{\max}} = 0 \tag{11}$$

Solving this gives the critical density as

$$\rho_c = \frac{\rho_{\max}}{2} \tag{12}$$

Using the aim of keeping the traffic density on the highway equal to the critical density at all points, we define an error function as

$$e(t) = \frac{1}{2}\int_0^L (\rho(t,x) - \rho_c)^2 dx \tag{13}$$

The function $e(.)$ is a mapping at each time t from the space of functions on $[0, L]$ to the space of nonnegative numbers. The values are always non-negative because it is an integral of the square of the differences. Its lowest value (value of zero) is obtained when the density at every point on the highway is equal to the critical density. Therefore, it would be desirable to design a feedback control law that attempts to satisfy the following objective:

$$\underset{t\to\infty}{Lt}\, e(t) = 0 \tag{14}$$

3. FEEDBACK CONTROL LAW FOR THE BASIC MODEL

In order to design a control law that attempts to achieve (14) we start by differentiating (13) by time to obtain

$$\frac{d}{dt}e(t) = \dot{e}(t) = \frac{d}{dt}\frac{1}{2}\int_0^L (\rho(t,x) - \rho_c)^2 dx \tag{15}$$

Simplifying this expression stepwise, we get the following equations:

$$\dot{e}(t) = \int_0^L (\rho(t,x) - \rho_c)\frac{d}{dt}(\rho(t,x) - \rho_c)dx \tag{16}$$

$$\dot{e}(t) = \int_0^L (\rho(t,x) - \rho_c) \frac{d}{dt}(\rho(t,x))dx \tag{17}$$

The total derivative of the density is given by

$$\frac{d}{dt}\rho(t,x) = \frac{\partial}{\partial t}\rho(t,x) + \frac{\partial}{\partial x}\rho(t,x)\dot{x} \tag{18}$$

Since there is no variation in x and we are looking for change in the density for a fixed x, we get

$$\frac{d}{dt}\rho(t,x) = \frac{\partial}{\partial t}\rho(t,x) \tag{19}$$

Now from the conservation equation from traffic we have

$$\frac{\partial}{\partial t}\rho(t,x) + \frac{\partial}{\partial x}q(t,x) = 0 \tag{20}$$

Using (19) and (20) in (17), we get

$$\dot{e}(t) = \int_0^L (\rho_c - \rho(t,x)) \frac{\partial}{\partial x}(q(t,x))dx \tag{21}$$

Simplifying this equation, we get

$$\dot{e}(t) = \int_0^L \rho_c \frac{\partial}{\partial x}(q(t,x))dx - \int_0^L \rho(t,x) \frac{\partial}{\partial x}(q(t,x))dx \tag{22}$$

Since the critical density is constant, we get

$$\dot{e}(t) = \rho_c \int_0^L \frac{\partial}{\partial x}(q(t,x))dx - \int_0^L \rho(t,x) \frac{\partial}{\partial x}(q(t,x))dx \tag{23}$$

Similar to the argument about the total derivative of density being equal to the partial derivative, we can use one for the case of traffic flow. Using that argument in (23), we get

$$\dot{e}(t) = \rho_c \int_0^L \frac{d}{dx}(q(t,x))dx - \int_0^L \rho(t,x)\frac{\partial}{\partial x}(q(t,x))dx \tag{24}$$

which gives

$$\dot{e}(t) = \rho_c \int_{q(t,0)}^{q(t,L)} dq(t,x) - \int_0^L \rho(t,x)\frac{\partial}{\partial x}(q(t,x))dx \tag{25}$$

Solving the first integral in (25) yields

$$\dot{e}(t) = \rho_c[q(t,L) - q(t,0)] - \int_0^L \rho(t,x)\frac{\partial}{\partial x}(q(t,x))dx \tag{26}$$

The flow at the left most boundary is produced by the highway and ramp inflows. Therefore, we have

$$q(t,0) = u + f(t) \tag{27}$$

Utilizing (27) in (26) introduces the control variable in the differential equation for the error variable. This is shown below.

$$\dot{e}(t) = \rho_c[q(t,L) - f(t) - u] - \int_0^L \rho(t,x)\frac{\partial}{\partial x}(q(t,x))dx \tag{28}$$

Our aim, as mentioned earlier, is to make the control variable u(.) a function of the traffic state variables in such a way that it can take the error variable to zero. In order to do that we present the feedback control law as

$$u = q(t,L) - f(t) + \frac{1}{\rho_c}[ke(t) - \int_0^L \rho(t,x)\frac{\partial}{\partial x}(q(t,x))dx] \tag{29}$$

In (29), the control gain k is chosen to be a positive constant. Let us study why this control law has the property of asymptotically taking the error variable to zero. To see this, plug in the expression for u in (29) into (28). Most of the terms cancel and we get a linear time-invariant first-order ordinary differential equation in the error variable. This technique is called feedback linearization [1,5], since we have effectively removed the nonlinearities from (28) by using the appropriate control law and have obtained a linear ordinary differential equation. The linear ordinary differential equation in the error variable we obtain is

$$\dot{e}(t) + ke(t) = 0 \tag{30}$$

We can solve (30) to confirm the asymptotic convergence. The steps in the solution are presented below.

$$\frac{de}{dt} = -ke \tag{31}$$

Moving terms changes (31) to

$$\frac{de}{e} = -kdt \tag{32}$$

Integrating both sides within the limits

$$\int_{e_0}^{e} \frac{dx}{x} = -\int_{0}^{t} kdt \tag{33}$$

and after taking exponentials of both sides of the resultant gives

$$\ln x\Big|_{e_0}^{e} = -kt \tag{34}$$

Taking exponentials of both sides and simplifying terms gives

$$e(t) = e_0 \exp(-kt) \tag{35}$$

This shows the exponential decaying of the error term and the satisfaction of (14).

3.1 Implementation of the Basic Feedback Control Law

Let us revisit the feedback control law we have designed. The control law derived above is re-presented below:

$$u = q(t,L) - f(t) + \frac{1}{\rho_c}[ke(t) - \int_{0}^{L} \rho(t,x)\frac{\partial}{\partial x}(q(t,x))dx] \tag{36}$$

Implementation of this law requires sensors to get various measurements from the highway. Using (7), this control law changes to

$$u = q(t,L) - f(t) + \frac{1}{\rho_c}[ke(t) - \int_0^L \rho(t,x)\frac{\partial}{\partial x}(v_f \rho(1 - \frac{\rho}{\rho_{\max}}))dx] \quad (37)$$

We will expand the term inside the integral as

$$\int_0^L \rho(t,x)\frac{\partial}{\partial x}(v_f \rho(1 - \frac{\rho}{\rho_{\max}}))dx = v_f \int_0^L (\rho(t,x)\frac{\partial \rho}{\partial x}(1 - 2\frac{\rho}{\rho_{\max}}))dx \quad (38)$$

Using (37) in (36) gives

$$u = q(t,L) - f(t) + \frac{1}{\rho_c}[ke(t) - v_f \int_0^L \rho(t,x)\frac{\partial \rho}{\partial x}(1 - 2\frac{\rho}{\rho_{\max}})dx] \quad (39)$$

We can expand (39) further using (13) to get

$$u = q(t,L) - f(t) + \frac{1}{\rho_c}[\frac{k}{2}\int_0^L (\rho(t,x) - \rho_c)^2 dx - v_f \int_0^L \rho(t,x)\frac{\partial \rho}{\partial x}(1 - 2\frac{\rho(t,x)}{\rho_{\max}})dx] \quad (40)$$

We can further expand the first term also so that the entire feedback control law that expresses the ramp inflow into the highway is a function of only traffic density along the highway mainline. This gives

$$\begin{aligned} u = {} & v_f \rho(t,L)(1 - \frac{\rho(t,L)}{\rho_{\max}}) - f(t) + \frac{1}{\rho_c}[\frac{k}{2}\int_0^L (\rho(t,x) - \rho_c)^2 dx \\ & - v_f \int_0^L \rho(t,x)\frac{\partial \rho}{\partial x}(1 - 2\frac{\rho(t,x)}{\rho_{\max}})dx] \end{aligned} \quad (41)$$

Looking at (41) tells us that we need the value of the traffic density at every point on the mainline as well as the value of the gradient of the traffic density at all points. To accomplish this we would need to deploy distributed sensors. For instance, a camera-based sensor could be used to provide the distributed information. On the other hand, point sensors like the loop detectors can also be used. They would give an approximate value for (41).

Let us divide the highway mainline into n sections, with section number $n+1$ being the one downstream of the last section. Then if we have one loop detector in each section, we can approximate the control law as

$$u = v_f \rho_n(t)(1 - \frac{\rho_n(t)}{\rho_{\max}}) - f(t)$$
$$+ \frac{1}{\rho_c}[-v_f \sum_{j=1}^{n}[\rho_j(t) \frac{(\rho_{j+1}(t) - \rho_j(t))}{\Delta x}(1 - 2\frac{\rho_j(t)}{\rho_{\max}}) + \frac{k}{2}(\rho_j(t) - \rho_c)^2] \quad (42)$$

3.2 Limitations on Achievable Performance

We see that if we apply the control law (42), we should achieve the performance shown by (35). However, we will see in simulations that the exact performance is not always obtained. The reason for that is as follows. If we were able to apply (42) always, then the performance (35) would be achieved, but when we use all the projection dynamics constraints, we are not able to get the desired u values but only those that are physically allowed by the system. The difference in the desired and the actual applied value produces a variation from the ideally desired (35) behavior. The difference is also produced by numerical discretization schemes we use and those produce disturbances.

3.3 Software Simulation for the Closed-Loop System

The software system for the closed loop is presented below in four files as before.

```
% Ramp Metering Code
clear;
clf;
clc;

global rhom rhoc vf lmax Dx k rholast n rmax

% Input Parameters

Dx=1;
k=5.5;

rhom = 60;                    % Jam density
rhoc = rhom/2;                % Critical density
vf = 15;                      % freeflow velocity
lmax = 200;
Diff=0.0;

t0 = 0.0;
tf = 5.0;
```

```
h = 0.01;
m = (tf-t0)/h;
n = 10;                              % number of sections
rho=ones(m,n).*5;                % X array m rows, length state
columns
T=zeros(m,1);                 % T array m rows (mx1)
L=[1:1:n]';
T(1)=t0;

l(1)=0;

rvar(1)=cpder(1,l(1));
uvar(1)=cpdeu(1,rho(1,:),l(1),rvar(1));
fvar(1)=cpdef(1);
evar(1)=0;
for j=1:n
   evar(1)=evar(1)+((rho(1,j)-rhoc)^2)/2;
end


rholast=0;

%There are m-1 steps and m points maximum
for i=1:m-1;
   clc
   T(i)
   T(i+1)=t0 + h*i;


   flag=0;
   qin=vf*(rho(i,n-1)*(1-rho(i,n-1)/rhom))+Diff*(rho(i,n-1)-
rho(i,n));
      if flag==0
         qout=vf*(rho(i,n)*(1-rho(i,n)/rhom))+Diff*(rho(i,n)-
rholast);
      else
         qout=0;
      end
         rhoinc=h*(qin-qout)/Dx;
      if rho(i,n)+rhoinc >=rhom
         rhoinc=rhom-rho(i,n);
         flag=1;
      else
         flag=0;
    end
    rho(i+1,n)=rho(i,n)+rhoinc;
```

```
   for j=n-1:-1:2
      qin=vf*(rho(i,j-1)*(1-rho(i,j-1)/rhom))+Diff*(rho(i,j-
1)-rho(i,j));
      if flag==0
         qout=vf*(rho(i,j)*(1-rho(i,j)/rhom))+Diff*(rho(i,j)-
rho(i,j+1));
      else
         qout=0;
      end
         rhoinc=h*(qin-qout)/Dx;
      if rho(i,j)+rhoinc >=rhom
         rhoinc=rhom-rho(i,j);
         flag=1;
      else
         flag=0;
     end
      rho(i+1,j)=rho(i,j)+rhoinc;

     end

   if flag==0
      qout=vf*(rho(i,1)*(1-rho(i,1)/rhom))+Diff*(rho(i,1)-
rho(i,2));
   else
      qout=0;
   end
   qin=cpdef(i)+uvar(i);
   rhoinc=h*(qin-qout)/Dx;
   if rho(i,1)+rhoinc>=rhom
      rhoinc=rhom-rho(i,1);
      fvar(i)=qout+Dx*rhoinc/h;;
   end
   rho(i+1,1)=rho(i,1)+rhoinc;
   l(i+1)=l(i)+h*(cpder(i,l(i))-uvar(i));
   rvar(i+1)=cpder(i+1,l(i+1));
   uvar(i+1)=cpdeu(i+1,rho(i+1,:),l(i+1),rvar(i+1));
   fvar(i+1)=cpdef(i+1);
   evar(i+1)=0;
         for j=1:n
         evar(i+1)=evar(i+1)+((rho(i+1,j)-rhoc)^2)/2;
         end

end

subplot(221);
mesh(rho);
title('Traffic Density');
```

```
subplot(222);
plot(T,rvar,'-',T,fvar,'-.');
title('Ramp and Highway Inflow');
xlabel('Time');


subplot(223);
plot(L,rho(1,:),'-',L,rho(m,:),'-.');
title('Initial & Final Traffic Density');
xlabel('Section');


subplot(224);
plot(T,rho(:,1));
title('Traffic Density for the First Section');
xlabel('Time');

pause;
clf;
subplot(221);
plot(T,rho(:,n/2));
title('Traffic Density for the Mid Section');
xlabel('Time');

subplot(222);
plot(T,evar);
title('Error Variable');
xlabel('Time');

subplot(223);
plot(T,l);
title('Ramp Queues');
xlabel('Time');

subplot(224);
plot(T,uvar);
title('Control Rampflow');
xlabel('Time');
```

Figure 5-2: File cpdemixedramp.m for Closed Loop Basic Isolated Ramp

```
function cpdef = cpdef(t)

if t>75 & t<150
    cpdef=185*(1.0+0.2*sin(0.025*t));
else
   cpdef = 175*(1.0+0.2*sin(0.025*t));
```

```
end
```

Figure 5-3: File cpdef.m for closed-Loop Basic Isolated Ramp

```
function cpder = cpder(t,l)
global lmax
if l<lmax
   cpder = 100*(1.0+0.2*sin(0.01*t));      % ramp inflow
else
   cpder = 0;
end;
```

Figure 5-4: File cpder.m for Closed Loop Basic Isolated Ramp

```
function cpdeu = cpdeu(t,x,l,r)

global rhom rhoc vf lmax Dx k rholast n rmax

e=0;
rdelqdx=0;
for j=1:n-1
   e=e+((x(j)-rhoc)^2)/2;
   qd=vf*x(j+1)*(1-(x(j+1)/rhoc));
   q=vf*x(j)*(1-(x(j)/rhoc));
   rdelqdx=rdelqdx+x(j)*(qd-q)/Dx;
end
qlast=vf*rholast*(1-(rhclast/rhoc));
q=vf*x(n)*(1-(x(n)/rhoc));
cpdeu=q-cpdef(t)-(-k*(e+(((x(n)-
rhoc)^2))/2)+rdelqdx+x(n)*(qlast-q))/rhoc;    % ramp outflow
if l<=0
   if r<cpdeu
      cpdeu = r;
   end
end
if x(1)>=rhom
   cpdeu = 0;
end
if cpdeu<0
   cpdeu=0;
end
```

Figure 5-5: File cpdeu.m for Closed Loop Basic Isolated Ramp

Notice that in this software, as compared to the ones used in the previous chapters, we have used global variables for the ease of programming. In this version, we also plot the actual traffic inflows to the highway as well as to the ramp as compared to the demanded ones.

The simulation results by running this file are shown below.

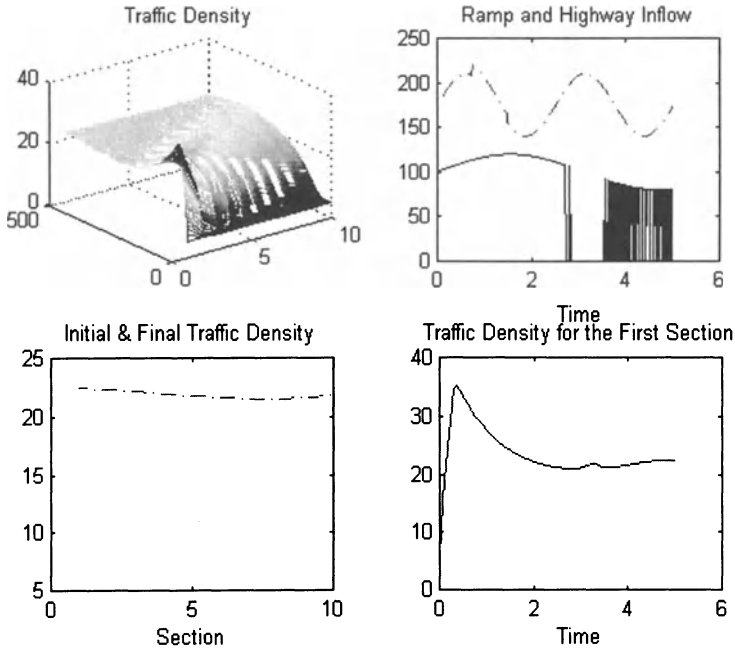

Figure 5-6: Plot-1 for Closed Loop Basic Isolated Ramp Simulation

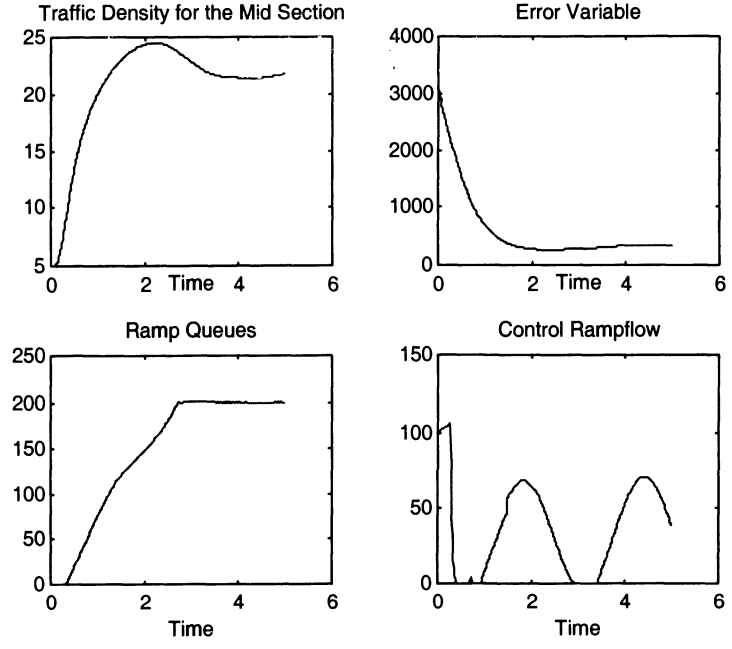

Figure 5-7: Plot-2 for Closed Loop Basic Isolated Ramp Simulation

We see in the simulations that the system reaches a steady state and achieves overall increased values of traffic density spread over the entire highway. We also observe a transient after which the steady state is reached.

We would like to reduce the steady state error. To achieve this, we can add an integral term in the control law. This is shown in the next section.

3.4 Integral Term in Control

We can replace the proportional feedback linearizing control (P-control) represented by (29) with a PI (Proportional-Integral) type of linearizing control:

$$u = q(t,L) - f(t) + \frac{1}{\rho_c}[k_1 e(t) + k_2 \int_0^t e(s)ds - \int_0^L \rho(t,x)\frac{\partial}{\partial x}(q(t,x))dx] \quad (43)$$

The implementable control with this term will change (41) to the following:

$$\begin{aligned} u = {} & v_f \rho(t,L)(1 - \frac{\rho(t,L)}{\rho_{\max}}) - f(t) + \frac{1}{\rho_c}[\frac{k_1}{2}\int_0^L (\rho(t,x) - \rho_c)^2 dx \\ & + \frac{k_2}{2}\int_0^t\int_0^L (\rho(t,s) - \rho_c)^2 dxds - v_f \int_0^L \rho(t,x)\frac{\partial \rho}{\partial x}(1 - 2\frac{\rho(t,x)}{\rho_{\max}})dx] \end{aligned} \quad (44)$$

The changes produced in simulation software are as follows. The control file is changed to:

```
function cpdeu = cpdeu(t,x,l,r)

global rhom rhoc vf lmax Dx k1 k2 rholast n rmax ie

e=0;
rdelqdx=0;
for j=1:n-1
   e=e+((x(j)-rhoc)^2)/2;
   qd=vf*x(j+1)*(1-(x(j+1)/rhoc));
   q=vf*x(j)*(1-(x(j)/rhoc));
   rdelqdx=rdelqdx+x(j)*(qd-q)/Dx;
end
ie=ie+e;
qlast=vf*rholast*(1-(rholast/rhoc));
q=vf*x(n)*(1-(x(n)/rhoc));
```

```
cpdeu=q-cpdef(t)-(-k1*(e+(((x(n)-rhoc)^2))/2)-
k2*ie+rdelqdx+x(n)*(qlast-q))/rhoc;    % ramp outflow
if l<=0
   if r<cpdeu
      cpdeu = r;
   end
end
if x(1)>=rhom
   cpdeu = 0;
end
if cpdeu<0
   cpdeu=0;
end
```

Figure 5-8: File cpdeu.m Where Integral Term is Used.

We notice that term ie is used for the integral term. It is passed as a global variable. The main program gets modified as well. The modified part of the main program is shown below.

```
global rhom rhoc vf lmax Dx k1 k2 rholast n rmax ie

% Input Parameters

Dx=1;
k1=5.5;
k2=0.03;

rhom = 60;                          % Jam density
rhoc = rhom/2;                      % Critical density
vf = 15;                            % freeflow velocity
lmax = 200;
Diff=0.0;

t0 = 0.0;
tf = 15.0;
h = 0.01;
m = (tf-t0)/h;
n = 10;                             % number of sections
rho=ones(m,n).*5;          % X array m rows, length state
columns
T=zeros(m,1);             % T array m rows (mx1)
L=[1:1:n]';
T(1)=t0;

l(1)=0;
ie=0;
```

Figure 5-9: Modified Part of File cpdemixedramp.m Where Integral Term is Used.

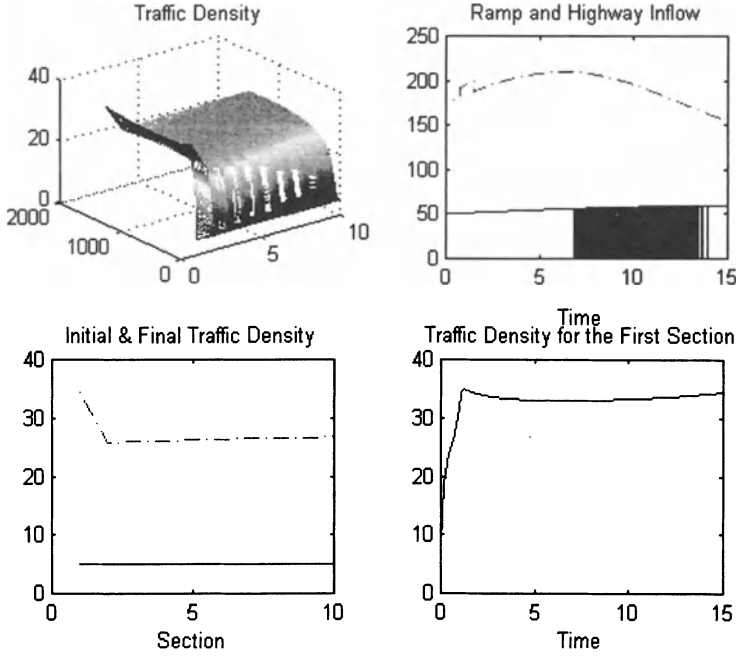

Figure 5-10: Plot-1 after Using Integral Term

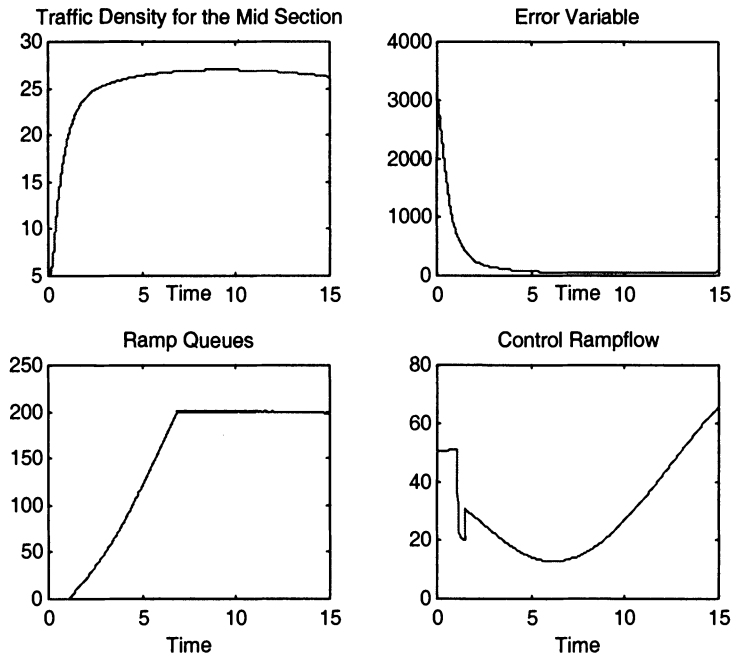

Figure 5-11: Plot-2 after Using Integral Term

3.5 Parametric Effect on Simulations

The feedback control gains have a profound effect on the performance of the feedback control law. If we set the value of k_2 to be 0.003 instead of 0.03 as in the previous section, the performance is degraded as shown below.

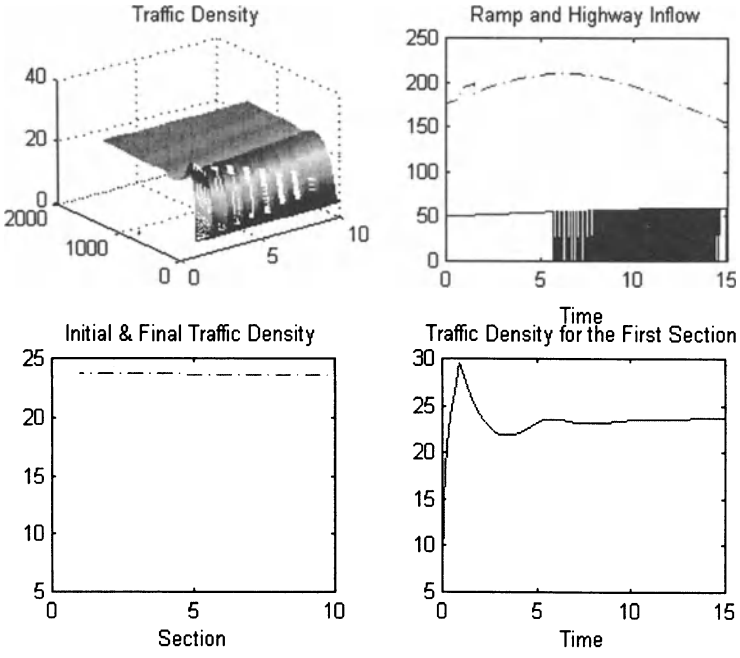

Figure 5-12: Plot-1 for Lowered Gain Basic Isolated Ramp Simulation

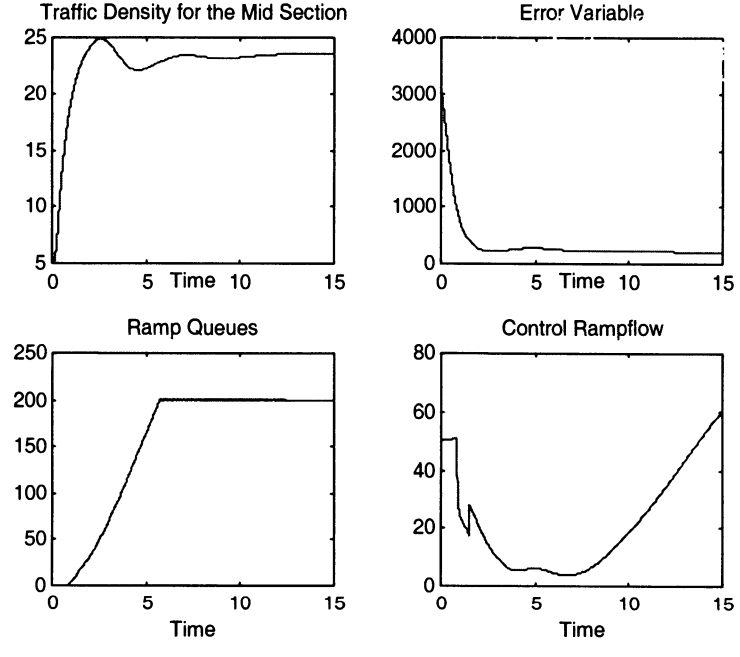

Figure 5-13: Plot-2 for Lowered Gain Basic Isolated Ramp Simulation

If we change the gain back to the original value and use only two sections as compared to ten, we get the following plots.

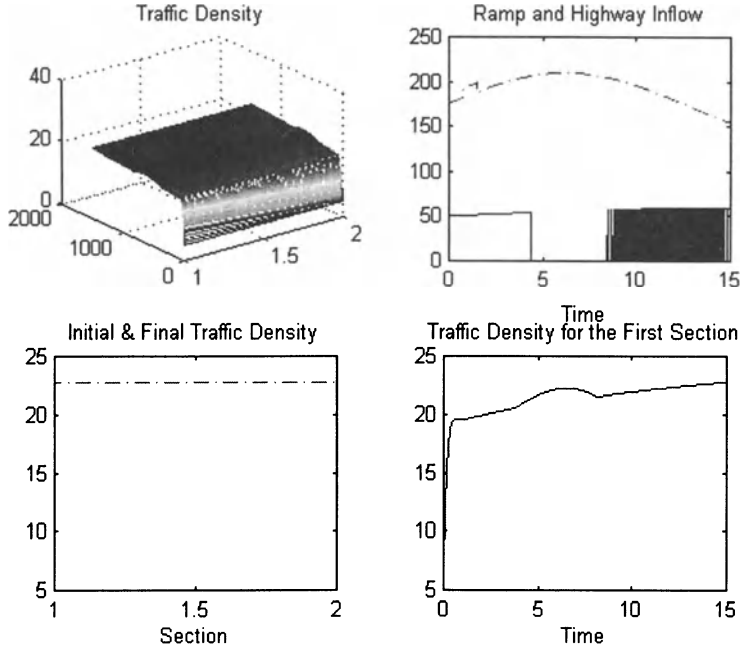

Figure 5-14: Plot-1 for Two-Section Basic Isolated Ramp Simulation

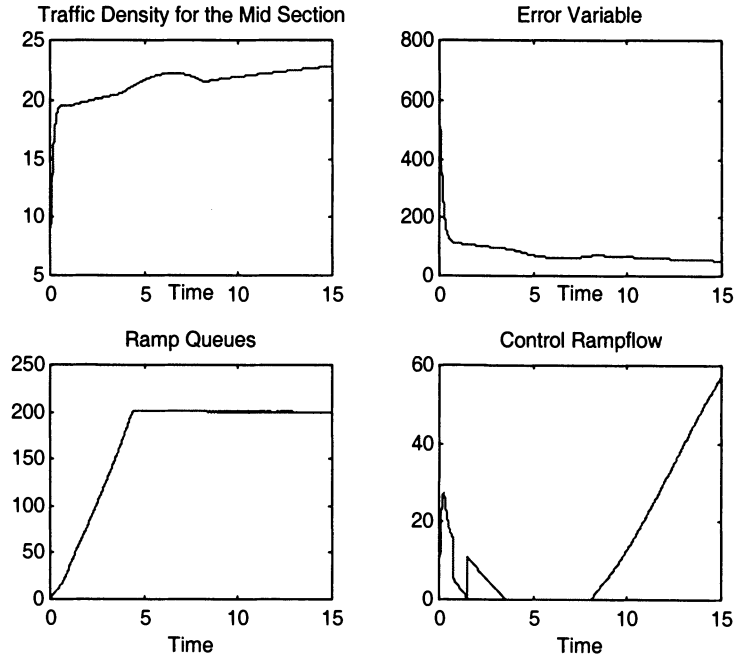

Figure 5-15: Plot-2 for Two-Section Basic Isolated Ramp Simulation

We see here that although the total error value is lower the traffic density values are not as high as we want them to be. The reason is that since there are only two sections, we are adding errors of only two sections, which makes the overall value zero. Choosing error per section would be a better variable to use for comparison.

We have used the model without diffusion to design the feedback control law and the model for the system in the simulation is the one without diffusion. We can see the effect of diffusion in the model by making the diffusion term *Diff* in the software equal to a nonzero term. If we change the value from 0 to 1.0 or some lower number like that, the effects are not large. However, if we change that value to 10.0, the results are more pronounced. We see that the downstream sections lose their traffic more rapidly as shown below.

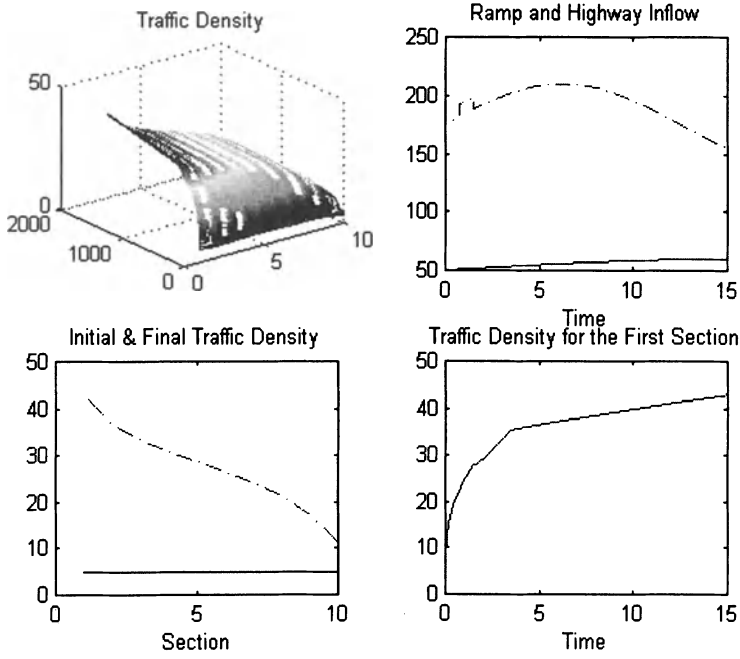

Figure 5-16: Plot-1 for Basic Isolated Ramp Simulation with Diffusion

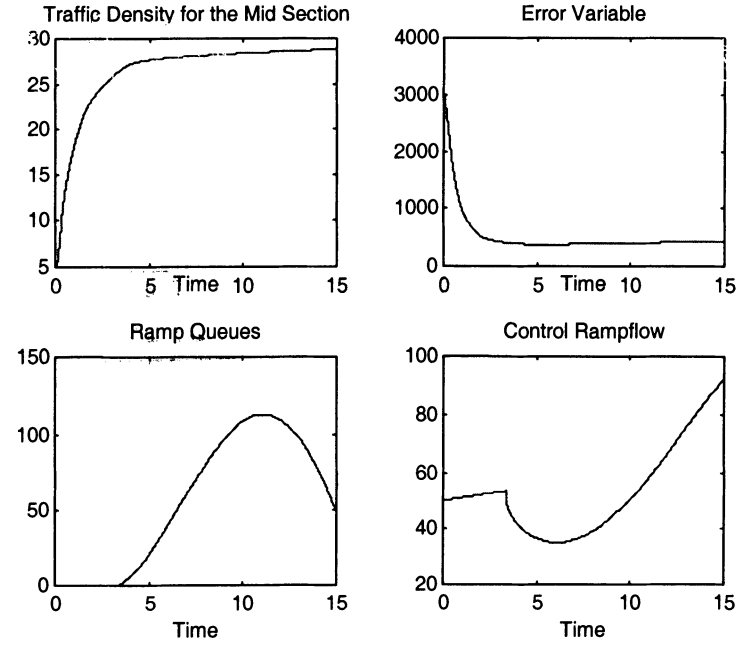

Figure 5-17: Plot-2 for Basic Isolated Ramp Simulation with Diffusion

4. SUMMARY

In this chapter, we studied:

- How to design feedback control laws for an isolated ramp metering problem using the distributed mathematical model for the ramp system.
- We performed simulations to see the effectiveness of the results.

5. QUESTIONS

1. What is feedback linearization? Why is it used?
2. Prove that equation (14) is an exponentially decaying function. Explain why such a function is used as an objective for the controller given in this chapter.
3. For any control law application, explain the terms "desired control values" and "physically allowed values." Do they having similar values? Why?
4. Study Figure 5-7. Explain subplot "Ramp Queue vs. Time" by taking the objective of the control law into consideration.
5. Explain why the feedback control gains have a profound effect on the performance of the feedback control law.
6. Study Figure 5-13. Explain why ramp conditions are improved by the addition of the diffusion term into the control law. If there are any, explain other improvements in the system with the addition of the diffusion term.

6. PROBLEMS

1. Use the MATLAB code given in the last section. Plot for diffusion term D=0, 0.5, and 10 in the same figure. And compare the results using the plot.
2. In the MATLAB code given in the last section, change the maximum ramp queue length to its half value, and compare the results with the previous results.

7. REFERENCES

1. Slotine, J. J. E., and Li, W., *Applied Nonlinear Control*, Prentice- Hall, 1990.
2. Khalil, H. K., *Nonlinear Systems*, Prentice-Hall, 2001.
3. Isidori, A. *Nonlinear Control Systems*, Springer-Verlag, 1995.
4. Nijmeijer, H., and Van der Schaft, A., *Nonlinear Dynamical Control Systems*, Springer Verlag, 1996.
5. Sastry, S., *Nonlinear Systems: Analysis, Stability and Control*, Springer-Verlag, 1999.

Chapter 6

FEEDBACK CONTROL DESIGN USING THE DISTRIBUTED MODEL WITH DIFFUSION

This chapter presents the feedback control design of an isolated ramp metering problem where we use the distributed model of the ramp system that also includes the diffusion term. Essentially, we are designing a feedback control law for the system whose model is the Burgers equation. We show the stability properties of the closed-loop system that is obtained by the application of the feedback control law on the ramp system. We verify the effectiveness of the feedback control law by running some simulation experiments using the designed feedback control law on the isolated ramp system.

1. MODEL SUMMARY OF THE DIFFUSION MODEL

The diffusion model used for the design of the feedback control law is presented below.

Dynamics:

$$\begin{cases} \left[\dfrac{\partial}{\partial t}\rho(x,t)+v_f\dfrac{\partial}{\partial x}\rho(x,t)\right]-2\dfrac{\rho}{\rho_{\max}}v_f\dfrac{\partial}{\partial x}\rho(x,t)-D\dfrac{\partial^2}{\partial x^2}\rho(x,t)=0 \\ \dot{\ell}=r(t)-u(t) \end{cases} \quad (1)$$

P. Kachroo et al., *Feedback Ramp Metering in Intelligent Transportation Systems*

Boundary Condition: $$\rho(t,0)v_f(1-\frac{\rho(t,0)}{\rho_{\max}})-D\frac{\partial\rho}{\partial x}\Big|_{(t,0)}=f(t)+u(t) \quad (2)$$

Initial Condition: $$\rho(0,x)=\psi(x) \quad (3)$$

We will use this model to design a feedback control law that provides desirable closed-loop dynamics.

2. CONTROL OBJECTIVE

Using the aim of keeping the traffic density on the highway equal to the critical density at all points, we use the same functional as in the previous chapter:

$$e(t)=\frac{1}{2}\int_0^L(\rho(t,x)-\rho_c)^2dx \quad (4)$$

Our aim for the control law design is to satisfy the following objective:

$$\lim_{t\to\infty} e(t)=0 \quad (5)$$

3. FEEDBACK CONTROL LAW FOR THE DIFFUSION MODEL

Following the feedback control design in the previous chapter, we get the following equation identical to equation (28) in the previous chapter:

$$\dot{e}(t)=\rho_c[\rho_c q(t,L)-f(t)-u]-\int_0^L\rho(t,x)\frac{\partial}{\partial x}(q(t,x))dx \quad (6)$$

In order to make the error go to zero asymptotically, we design the same feedback control law as in the previous chapter:

$$u = q(t,L) - f(t) + \frac{1}{\rho_c}[ke(t) - \int_0^L \rho(t,x)\frac{\partial}{\partial x}(q(t,x))dx] \tag{7}$$

Applying this control law into (6) gives the equation

$$\dot{e}(t) + ke(t) = 0 \tag{8}$$

which guarantees asymptotic convergence following

$$e(t) = e_0 \exp(-kt) \tag{9}$$

Therefore, even for the diffusion case the control law seems to be the same. The difference, however, comes from the expression for q. This is discussed in the following section.

3.1 Implementation of the Basic Feedback Control Law

Let us revisit the feedback control law we have designed. The control law derived above is re-presented below:

$$u = q(t,L) - f(t) + \frac{1}{\rho_c}[ke(t) - \int_0^L \rho(t,x)\frac{\partial}{\partial x}(q(t,x))dx] \tag{10}$$

Due to diffusion, the expression for the traffic flow is given by

$$q(t,x) = v_f \rho(t,x)(1 - \frac{\rho(t,x)}{\rho_{\max}}) - D\frac{\partial \rho(t,x)}{\partial x} \tag{11}$$

Implementation of this law requires sensors to get various measurements from the highway. Using (11), this control law changes to

$$\begin{aligned} u = {} & q(t,L) - f(t) + \frac{1}{\rho_c}[k\dot{e}(t) - \\ & \int_0^L \rho(t,x)\frac{\partial}{\partial x}(v_f \rho(1 - \frac{\rho}{\rho_{\max}}) - D\frac{\partial \rho(t,x)}{\partial x})dx] \end{aligned} \tag{12}$$

We will expand the term inside the integral as

$$\begin{aligned}&\int_0^L \rho(t,x)\frac{\partial}{\partial x}(v_f\rho(1-\frac{\rho}{\rho_{\max}})-D\frac{\partial\rho}{\partial x})dx\\&=\int_0^L (v_f\rho(t,x)\frac{\partial\rho}{\partial x}(1-2\frac{\rho}{\rho_{\max}})-D\rho(t,x)\frac{\partial^2\rho}{\partial x^2})dx\end{aligned} \tag{13}$$

Using (13) in the expression for u gives

$$\begin{aligned}&u=q(t,L)-f(t)+\frac{1}{\rho_c}[ke(t)\\&-\int_0^L (v_f\rho(t,x)\frac{\partial\rho}{\partial x}(1-2\frac{\rho}{\rho_{\max}})-D\rho(t,x)\frac{\partial^2\rho}{\partial x^2})dx]\end{aligned} \tag{14}$$

We can expand (14) further using (4) to get

$$\begin{aligned}&u=q(t,L)-f(t)+\frac{1}{\rho_c}[\frac{k}{2}\int_0^L(\rho(t,x)-\rho_c)^2dx\\&-\int_0^L (v_f\rho(t,x)\frac{\partial\rho}{\partial x}(1-2\frac{\rho}{\rho_{\max}})-D\rho(t,x)\frac{\partial^2\rho}{\partial x^2})dx]\end{aligned} \tag{15}$$

We can further expand the first term so that the entire feedback control law that expresses the ramp inflow into the highway is a function of only traffic density along the highway mainline:

$$\begin{aligned}&u=v_f\rho(t,L)(1-\frac{\rho(t,L)}{\rho_{\max}})-D\frac{\partial\rho(t,x)}{\partial x}\Big|_{x=L}+f(t)\\&+\frac{1}{\rho_c}[\frac{k}{2}\int_0^L(\rho(t,x)-\rho_c)^2dx\\&-\int_0^L (v_f\rho(t,x)\frac{\partial\rho}{\partial x}(1-2\frac{\rho(t,x)}{\rho_{\max}})-D\rho(t,x)\frac{\partial^2\rho}{\partial x^2})dx]\end{aligned} \tag{16}$$

Looking at (16) tells us that we need the value of the traffic density at every point on the mainline as well as the value of the gradient and of the second spatial derivative of the traffic density at all points. To accomplish

this we would need to deploy distributed sensors as before. Using point sensors would give an approximate value for the expression (17).

Let us divide the highway mainline into n sections, with section number n+1 being the one downstream of the last section, and n+2 being the one downstream to that. Then if we have one loop detector in each section, we can approximate the control law as

$$\begin{aligned} u = {} & v_f \rho_n(t)(1-\frac{\rho_n(t)}{\rho_{\max}}) - D\frac{(\rho_{n+1}(t)-\rho_n(t))}{\Delta x} + f(t) \\ & + \frac{1}{\rho_c}[\frac{k}{2}\sum_{j=1}^{n}(\rho_j(t)-\rho_c)^2 \\ & - \sum_{j=1}^{n}(v_f \rho_j(t)\frac{(\rho_{j+1}(t)-\rho_j(t))}{\Delta x}(1-2\frac{\rho_j(t)}{\rho_{\max}}) \\ & - D\rho_j(t)\frac{(\rho_{j+2}(t)-\rho_j(t))}{\Delta^2 x}) \end{aligned} \tag{17}$$

What we notice in this expression is that we need the traffic density of two sections beyond the last section (i.e., section n). This happened because of the particular approximation we chose for the gradient and the second derivative. If we change our choice of the discretization scheme, the dependence of the controller on various "outside" sections will change. We refer to "outside" sections as those sections that are either upstream of section 1 or downstream of section n. The next section discusses the various control implementations we can get by choosing different discretizing schemes.

3.2 Control Discretization

We can choose various schemes for discretizing the gradient and the second derivative term. The forward differencing scheme gives

$$\left.\frac{\partial \rho(t,x)}{\partial x}\right|_{\rho(t,x)=\rho_j(t)} = \frac{\partial \rho_j(t,x)}{\partial x} = \frac{\rho_{j+1}(t)-\rho_j(t)}{\Delta x} \tag{18}$$

Using this for the second derivative gives

$$\frac{\partial^2 \rho(t,x)}{\partial x^2} = \frac{1}{\Delta x}[\frac{\partial \rho_{j+1}(t)}{\partial x} - \frac{\partial \rho_j(t)}{\partial x}]$$
$$= \frac{1}{\Delta x}[\frac{\rho_{j+2}(t) - \rho_{j+1}(t)}{\Delta x} - \frac{\rho_{j+1}(t) - \rho_j(t)}{\Delta x}] = \frac{\rho_{j+2}(t) - \rho_j(t)}{\Delta^2 x} \quad (19)$$

When we apply (18) and (19) to (16) we get (17). The backward differencing scheme gives

$$\left.\frac{\partial \rho(t,x)}{\partial x}\right|_{\rho(t,x)=\rho_j(t)} = \frac{\partial \rho_j(t,x)}{\partial x} = \frac{\rho_j(t) - \rho_{j-1}(t)}{\Delta x} \quad (20)$$

Using this for the second derivative gives

$$\frac{\partial^2 \rho(t,x)}{\partial x^2} = \frac{1}{\Delta x}[\frac{\partial \rho_j(t)}{\partial x} - \frac{\partial \rho_{j-1}(t)}{\partial x}]$$
$$= \frac{1}{\Delta x}[\frac{\rho_j(t) - \rho_{j-1}(t)}{\Delta x} - \frac{\rho_{j-1}(t) - \rho_{j-2}(t)}{\Delta x}] = \frac{\rho_j(t) - \rho_{j-2}(t)}{\Delta^2 x} \quad (21)$$

When we apply (20) and (21) to (16) we get

$$u = v_f \rho_n(t)(1 - \frac{\rho_n(t)}{\rho_{\max}}) - D\frac{(\rho_n(t) - \rho_{n-1}(t))}{\Delta x} + f(t)$$
$$+ \frac{1}{\rho_c}[\frac{k}{2}\sum_{j=1}^{n}(\rho_j(t) - \rho_c)^2$$
$$- \sum_{j=1}^{n}(v_f \rho_j(t)\frac{(\rho_j(t) - \rho_{j-1}(t))}{\Delta x}(1 - 2\frac{\rho_j(t)}{\rho_{\max}})$$
$$- D\rho_j(t)\frac{(\rho_j(t) - \rho_{j-2}(t))}{\Delta^2 x}) \quad (22)$$

Using the backward scheme requires us to measure the traffic density of two sections that are upstream of the first section of the highway. The central differencing scheme gives

$$\left.\frac{\partial \rho(t,x)}{\partial x}\right|_{\rho(t,x)=\rho_j(t)} = \frac{\partial \rho_j(t,x)}{\partial x} = \frac{\rho_{j+1}(t) - \rho_{j-1}(t)}{\Delta x} \quad (23)$$

Using this for the second derivative gives

$$\begin{aligned}\frac{\partial^2\rho(t,x)}{\partial x^2} &= \frac{1}{\Delta x}[\frac{\partial\rho_{j+1}(t)}{\partial x} - \frac{\partial\rho_{j-1}(t)}{\partial x}] \\ &= \frac{1}{\Delta x}[\frac{\rho_{j+2}(t)-\rho_j(t)}{\Delta x} - \frac{\rho_j(t)-\rho_{j-2}(t)}{\Delta x}] = \frac{\rho_{j+2}(t)-\rho_{j-2}(t)}{\Delta^2 x}\end{aligned} \tag{24}$$

When we apply (23) and (24) to (16) we get

$$\begin{aligned}u &= v_f\rho_n(t)(1-\frac{\rho_n(t)}{\rho_{\max}}) - D\frac{(\rho_{n+1}(t)-\rho_{n-1}(t))}{\Delta x} + f(t) \\ &+ \frac{1}{\rho_c}[\frac{k}{2}\sum_{j=1}^{n}(\rho_j(t)-\rho_c)^2 \\ &- \sum_{j=1}^{n}(v_f\rho_j(t)\frac{(\rho_{j+1}(t)-\rho_{j-1}(t))}{\Delta x}(1-2\frac{\rho_j(t)}{\rho_{\max}}) \\ &- D\rho_j(t)\frac{(\rho_{j+2}(t)-\rho_{j-2}(t))}{\Delta^2 x})\end{aligned} \tag{25}$$

Using the central scheme requires us to measure traffic density of two sections that are upstream of the first section of the highway and two sections that are downstream of the last section.

If we use the forward differencing scheme on all the sections except the last section where we apply the backward differencing scheme, we will get:

$$\left.\frac{\partial\rho(t,x)}{\partial x}\right|_{\rho(t,x)=\rho_j(t)} = \frac{\partial\rho_j(t,x)}{\partial x} = \begin{cases}\dfrac{\rho_{j+1}(t)-\rho_j(t)}{\Delta x} & j=1,2,\ldots,n-1 \\ \dfrac{\rho_j(t)-\rho_{j-1}(t)}{\Delta x} & j=n\end{cases} \tag{26}$$

Using this for the second derivative gives

$$\frac{\partial^2 \rho(t,x)}{\partial x^2} = \frac{1}{\Delta x}[\frac{\partial \rho_{j+1}(t)}{\partial x} - \frac{\partial \rho_{j-1}(t)}{\partial x}]$$

$$= \begin{cases} \frac{1}{\Delta x}[\frac{\rho_{j+2}(t)-\rho_{j+1}(t)}{\Delta x} - \frac{\rho_{j+1}(t)-\rho_j(t)}{\Delta x}] & j=1,2,..,n-2 \\ \frac{1}{\Delta x}[\frac{\rho_j(t)-\rho_{j-1}(t)}{\Delta x} - \frac{\rho_j(t)-\rho_{j-1}(t)}{\Delta x}] & j=n-1,n \end{cases} \quad (27)$$

$$= \begin{cases} \frac{\rho_{j+2}(t)-\rho_j(t)}{\Delta^2 x} & j=1,2,...n-2 \\ 0 & j=n-1,n \end{cases}$$

When we apply (26) and (27) to (16) we get

$$u = v_f \rho_n(t)(1-\frac{\rho_n(t)}{\rho_{\max}}) - D\frac{(\rho_n(t)-\rho_{n-1}(t))}{\Delta x} + f(t)$$
$$+\frac{1}{\rho_c}[\frac{k}{2}\sum_{j=1}^{n}(\rho_j(t)-\rho_c)^2$$
$$-\sum_{j=1}^{n}(v_f \rho_j(t)\frac{(\rho_{j+1}(t)-\rho_j(t))}{\Delta x}(1-2\frac{\rho_j(t)}{\rho_{\max}}) \quad (28)$$
$$-\sum_{j=1}^{n-2} D\rho_j(t)\frac{(\rho_{j+2}(t)-\rho_j(t))}{\Delta^2 x}]$$

Now, this control law does not require any more measurements than available from the n sections of the highway.

3.3 Integral Term

With the integral term, the control law (10) becomes

$$u = q(t,L) - f(t) + \frac{1}{\rho_c}[ke(t) + \int_0^2 k_2 e(s)ds - \int_0^L \rho(t,x)\frac{\partial}{\partial x}(q(t,x))dx] \quad (29)$$

From the discretized version of this law using the method that utilizes only the measurements from the highway mainline sections, we get the following equation corresponding to (28):

$$
\begin{aligned}
u &= v_f \rho_n(t)(1-\frac{\rho_n(t)}{\rho_{\max}}) - D\frac{(\rho_n(t)-\rho_{n-1}(t))}{\Delta x} + f(t) \\
&+ \frac{1}{\rho_c}[\frac{k_1}{2}\sum_{j=1}^{n}(\rho_j(t)-\rho_c)^2 + \frac{1}{\rho_c}\int_0^t \frac{k_2}{2}\sum_{j=1}^{n}(\rho_j(s)-\rho_c)^2 ds \\
&- \sum_{j=1}^{n}(v_f \rho_j(t)\frac{(\rho_{j+1}(t)-\rho_j(t))}{\Delta x}(1-2\frac{\rho_j(t)}{\rho_{\max}}) \\
&- \sum_{j=1}^{n-2} D\rho_j(t)\frac{(\rho_{j+2}(t)-\rho_j(t))}{\Delta^2 x}]
\end{aligned}
\tag{30}
$$

The integral term can be discretized in time so that it becomes a summation in time. Doing that we will get

$$
\begin{aligned}
u(k) &= v_f \rho_n(t)(1-\frac{\rho_n(k)}{\rho_{\max}}) - D\frac{(\rho_n(k)-\rho_{n-1}(k))}{\Delta x} + f(k) \\
&+ \frac{1}{\rho_c}[\frac{k_1}{2}\sum_{j=1}^{n}(\rho_j(k)-\rho_c)^2 + \frac{1}{\rho_c}\frac{k_2}{2}\sum_{r=1}^{k}\sum_{j=1}^{n}(\rho_j(r)-\rho_c)^2 \\
&- \sum_{j=1}^{n}(v_f \rho_j(k)\frac{(\rho_{j+1}(k)-\rho_j(k))}{\Delta x}(1-2\frac{\rho_j(k)}{\rho_{\max}}) \\
&- \sum_{j=1}^{n-2} D\rho_j(t)\frac{(\rho_{j+2}(k)-\rho_j(k))}{\Delta^2 x}]
\end{aligned}
\tag{31}
$$

The next section presents the software and the simulation results using this controller.

3.4 Software Simulation for the Closed_Loop System

The software developed is presented in the five files below. We have kept the plotting code in a separate draw.m files.

```
% Ramp Metering Code
clear;
clf;
clc;

global rhom rhoc vf lmax Dx k1 k2 n rmax Diff ie

% Input Parameters
```

```
Dx=1;
k1=5.5;
k2=0.03;

rhom = 60;                          % Jam density
rhoc = rhom/2;                      % Critical density
vf = 15;                            % freeflow velocity
lmax = 200;
Diff=2.0;

t0 = 0.0;
tf = 40;
h = 0.01;
m = (tf-t0)/h;
n = 10;                             % number of sections
rho=ones(m,n).*25;          % X array m rows, length state
columns
T=zeros(m,1);              % T array m rows (mx1)
L=[1:1:n]';
T(1)=t0;
l(1)=0;
ie=0;

rvar(1)=opder(1,l(1));
uvar(1)=opdeu(1,rho(1,:),l(1),rvar(1));
fvar(1)=opdef(1);
evar(1)=0;
for j=1:n
   evar(1)=evar(1)+(rho(1,j)-rhoc)^2;
end

%There are m-1 steps and m points maximum
for i=1:m-1;
   clc
   T(i)
   T(i+1)=t0 + h*i;


   flag=0;
   qin=vf*(rho(i,n-1)*(1-rho(i,n-1)/rhom))+Diff*(rho(i,n-1)-
rho(i,n));
      if flag==0
         qout=vf*(rho(i,n)*(1-rho(i,n)/rhom))+Diff*(rho(i,n-
1)-rho(i,n));
      else
         qout=0;
      end
```

```
         rhoinc=h*(qin-qout)/Dx;
      if rho(i,n)+rhoinc >=rhom
         rhoinc=rhom-rho(i,n);
         flag=1;
      else
         flag=0;
     end
     rho(i+1,n)=rho(i,n)+rhoinc;

   for j=n-1:-1:2
      qin=vf*(rho(i,j-1)*(1-rho(i,j-1)/rhom))+Diff*(rho(i,j-
1)-rho(i,j));
      if flag==0
         qout=vf*(rho(i,j)*(1-rho(i,j)/rhom))+Diff*(rho(i,j)-
rho(i,j+1));
      else
         qout=0;
      end
         rhoinc=h*(qin-qout)/Dx;
      if rho(i,j)+rhoinc >=rhom
         rhoinc=rhom-rho(i,j);
         flag=1;
      else
         flag=0;
     end
     rho(i+1,j)=rho(i,j)+rhoinc;
     end

   if flag==0
      qout=vf*(rho(i,1)*(1-rho(i,1)/rhom))+Diff*(rho(i,1)-
rho(i,2));
   else
      qout=0;
   end
   qin=opdef(i)+uvar(i);
   rhoinc=h*(qin-qout)/Dx;
   if rho(i,1)+rhoinc>=rhom
      rhoinc=rhom-rho(i,1);
      fvar(i)=qout+Dx*rhoinc/h;;
   end
   rho(i+1,1)=rho(i,1)+rhoinc;
   l(i+1)=l(i)+h*(opder(i,l(i))-uvar(i));
   rvar(i+1)=opder(i+1,l(i+1));
   uvar(i+1)=opdeu(i+1,rho(i+1,:),l(i+1),rvar(i+1));
   fvar(i+1)=opdef(i+1);
   evar(i+1)=0;
```

```
        for j=1:n
        evar(i+1)=evar(i+1)+(rho(i+1,j)-rhoc)^2;
        end
end
```

Figure 6-1: File opdemixedramp.m with Diffusion

```
subplot(221);
mesh(rho);
title('Traffic Density');

subplot(222);
plot(T,rvar,'-',T,fvar,'-.');
title('Ramp and Highway Inflow');
xlabel('Time');


subplot(223);
plot(L,rho(1,:),'-',L,rho(m,:),'-.');
title('Initial & Final Traffic Density');
xlabel('Section');


subplot(224);
plot(T,rho(:,1));
title('Traffic Density for the First Section');
xlabel('Time');

pause;
clf;
subplot(221);
plot(T,rho(:,n/2));
title('Traffic Density for the Mid Section');
xlabel('Time');

subplot(222);
plot(T,evar);
title('Error Variable');
xlabel('Time');

subplot(223);
plot(T,l);
title('Ramp Queues');
xlabel('Time');

subplot(224);
plot(T,uvar);
title('Control Rampflow');
```

```
xlabel('Time');
```

Figure 6-2: draw.m

```
function opdeu = opdeu(t,x,l,r)

global rhom rhoc vf lmax Dx k1 k2 n rmax Diff ie

e=0;
rdelqdx=0;
e=e+((x(1)-rhoc)^2)/2;
qd=vf*x(2)*(1-(x(2)/rhoc))+Diff*(x(1)-x(2));
q=vf*x(1)*(1-(x(1)/rhoc))+Diff*(x(1)-x(2));
rdelqdx=rdelqdx+x(1)*(qd-q)/Dx;
for j=2:n-1
   e=e+((x(j)-rhoc)^2)/2;
   qd=vf*x(j+1)*(1-(x(j+1)/rhoc))+Diff*(x(j)-x(j+1));
   q=vf*x(j)*(1-(x(j)/rhoc))+Diff*(x(j-1)-x(j));
   rdelqdx=rdelqdx+x(j)*(qd-q)/Dx;
end
ie=ie+e;
qd=vf*x(n)*(1-(x(n)/rhoc))+Diff*(x(n-1)-x(n));
q=vf*x(n-1)*(1-(x(n-1)/rhoc))+Diff*(x(n-1)-x(n));
opdeu=q-opdef(t)-(-k1*(e+(((x(n)-rhoc)^2))/2)-
k2*ie+rdelqdx+x(n)*(qd-q))/rhoc;    % ramp outflow

if l<=0
   if r<opdeu
      opdeu = r;
   end
end
if x(1)>=rhom
   opdeu = 0;
end
if opdeu<0
   opdeu=0;
end
```

Figure 6-3: Control File for Diffusion (opdeu.m)

```
function opder = opder(t,l)
global lmax
if l<lmax
   opder = 50*(1.0+0.2*sin(0.001*t));      % ramp inflow
else
   opder = 0;
end;
```

Figure 6-4: Ramp Inflow File for Diffusion (opder.m)

```
function opdef = opdef(t)
if t>75 & t<150
   opdef = 185*(1.0+0.2*sin(0.0025*t));
else
   opdef = 175*(1.0+0.2*sin(0.0025*t));
end
```

Figure 6-5: Highway Inflow File for Diffusion (opdef.m)

The simulation results using these files are shown below.

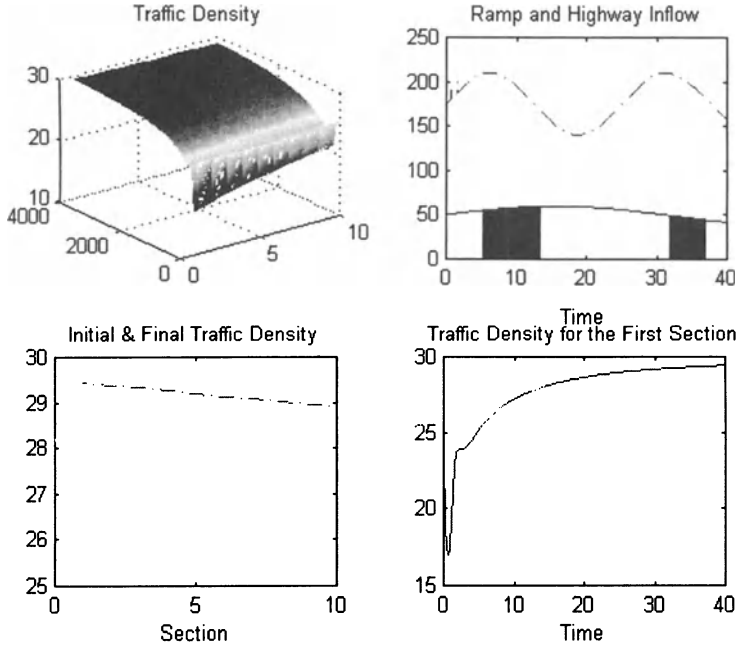

Figure 6-6: Plot-1 for Diffusion Control

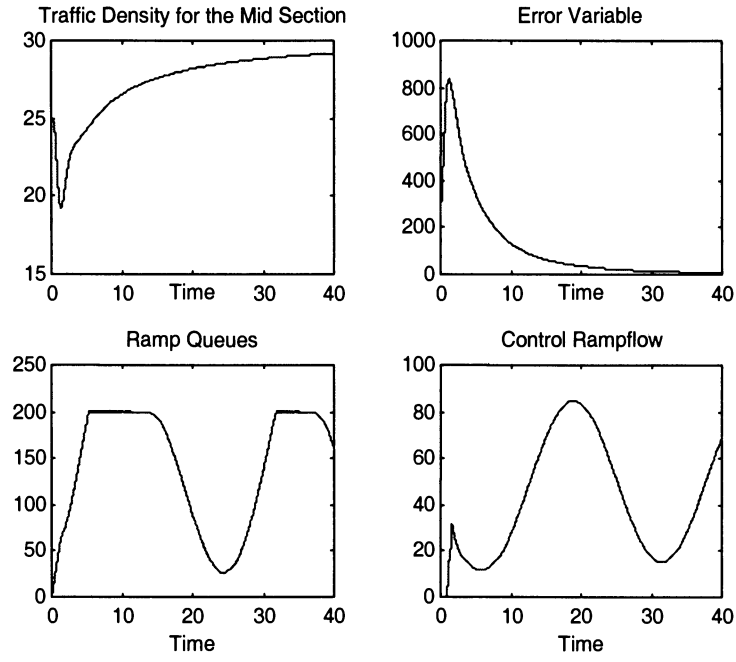

Figure 6-7: Plot-2 for Diffusion Control

4. SUMMARY

In this chapter, we studied:

- How to design feedback control laws for an isolated ramp metering problem using the distributed mathematical model for the ramp system where the model used the diffusion term in traffic velocity
- We performed simulations to see the effectiveness of the results.

5. QUESTIONS

1. What is the contribution of the diffusion term inclusion? Compare it with the case where no distribution term is included.
2. Which discretization techniques are used in the control law? Explain why multiple techniques are used to discretize the system.
3. Explain why the integral term is introduced in the control law.

6. PROBLEMS

1. Derive the control law without the integral term.
2. Write a MATLAB code (or modify the program code given in Section 3.4) that uses the control derived in Problem 1.
   a. Plot the figures (density (mesh), ramp queues, etc)
   b. Compare the plots with Figure 6-6 and Figure 6-7.

7. REFERENCES

1. Cheney, E. W., and Kincaid, D. R., *Numerical Mathematics and Computing*, Brooks/Cole, 1999.
2. Gerald, C. F., and Wheatley, P. O., *Applied Numerical Analysis*, Addison, Wesley, 1998.

Chapter 7

FEEDBACK CONTROL DESIGN FOR THE DISTRIBUTED MODEL FOR MIXED SENSITIVITY

This chapter presents the feedback control design of an isolated ramp metering problem where we use the distributed model of the ramp system with the control designed not only to keep the flow on the highway at a critical value but also to keep the queue length on the ramp small. We show the stability properties of the closed-loop system that is obtained by the application of the feedback control law on the ramp system. We verify the effectiveness of the feedback control law by running some simulation experiments using the designed feedback control law on the isolated ramp system.

1. SUMMARY OF THE BASIC MODEL

In this chapter, we will use the basic model to design the feedback control law that tries to not only keep the traffic density on the highway close to the critical value but also tries to keep the queue lengths lower. The model, for convenience, is presented below.

$$\text{Dynamics: } \begin{cases} \dfrac{\partial \rho(t,x)}{\partial t} + \dfrac{\partial[\rho(t,x) v_f (1 - \dfrac{\rho(t,x)}{\rho_{\max}})]}{\partial x} = 0 \\ \dot{\ell} = r(t) - u(t) \end{cases} \tag{1}$$

P. Kachroo et al., *Feedback Ramp Metering in Intelligent Transportation Systems*

$$\text{Boundary Condition: } \rho(t,0)v_f\left(1-\frac{\rho(t,0)}{\rho_{\max}}\right) = f(t)+u(t) \tag{2}$$

$$\text{Initial Condition: } \rho(0,x) = \psi(x) \tag{3}$$

We will use this model to design a feedback control law that provides desirable closed-loop dynamics.

2. CONTROL OBJECTIVE

Figure 7-1 shows the feedback control scenario in which the sensors used give measurements on the mainline highway as well as on the ramp queues.

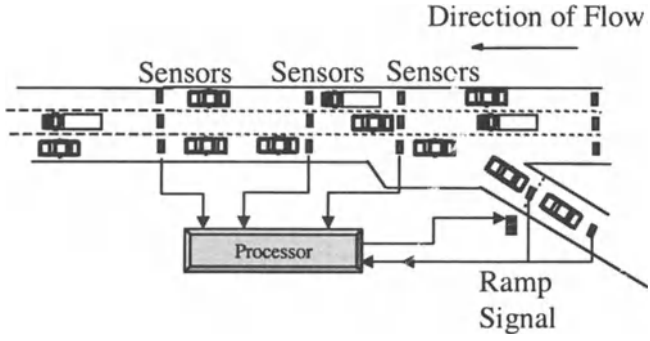

Figure 7-1: Sensors and Feedback Ramp Metering

The aim of the controller is to keep the traffic density at the critical value and, at the same time, keep the queue length small. Therefore, the error variable to accomplish both will be taken as

$$e(t) = \frac{w_1}{2}\int_0^L (\rho(t,x)-\rho_c)^2\,dx + w_2\ell \tag{4}$$

The error variable is a weighted average of the error used in the previous chapter and the queue length. Since the first term in (4) is a squared term

and the second term is the queue length, which is a nonnegative variable, the error term itself is always nonnegative. Our aim for the control law design is to satisfy the following objective:

$$\lim_{t\to\infty} e(t) = 0 \tag{5}$$

The methodology for the feedback control design will be the same that has been used in previous chapters, i.e. to use feedback linearization. With the integral term in the feedback linearization, the error dynamics in the closed loop will become

$$\dot{e}(t) + k_1 e(t) + k_2 \int_0^t e(s)ds = 0 \tag{6}$$

3. FEEDBACK CONTROL DESIGN

In order to design a control law that attempts to achieve (6) we start by differentiating (4) by time to get the following:

$$\frac{d}{dt}e(t) = \dot{e}(t) = \frac{d}{dt}[\frac{w_1}{2}\int_0^L (\rho(t,x) - \rho_c)^2 dx + w_2\ell] \tag{7}$$

Simplifying this expression stepwise, we get

$$\dot{e}(t) = w_1 \int_0^L (\rho(t,x) - \rho_c)\frac{d}{dt}(\rho(t,x) - \rho_c)dx + w_2\dot{\ell} \tag{8}$$

Using the conservation equation and dynamics (1) here gives us

$$\dot{e}(t) = w_1 \int_0^L (\rho_c - \rho(t,x))\frac{\partial}{\partial x}(q(t,x))dx + w_2(r(t) - u(t)) \tag{9}$$

Simplifying this equation, we get

$$\dot{e}(t) = w_1[\int_0^L \rho_c \frac{\partial}{\partial x}(q(t,x))dx - \int_0^L \rho(t,x)\frac{\partial}{\partial x}(q(t,x))dx] \\ + w_2(r(t) - u(t)) \tag{10}$$

Since the critical density is constant, we get

$$\dot{e}(t) = w_1[\rho_c \int_0^L \frac{\partial}{\partial x}(q(t,x))dx - \int_0^L \rho(t,x)\frac{\partial}{\partial x}(q(t,x))dx] \\ + w_2(r(t) - u(t)) \tag{11}$$

Equating the partial derivative to total derivative, we get

$$\dot{e}(t) = w_1[\rho_c \int_0^L \frac{d}{dx}(q(t,x))dx - \int_0^L \rho(t,x)\frac{\partial}{\partial x}(q(t,x))dx] \\ + w_2(r(t) - u(t)) \tag{12}$$

which gives

$$\dot{e}(t) = w_1[\rho_c \int_{q(t,0)}^{q(t,L)} dq(t,x) - \int_0^L \rho(t,x)\frac{\partial}{\partial x}(q(t,x))dx] \\ + w_2(r(t) - u(t)) \tag{13}$$

Solving the first integral in (13) yields

$$\dot{e}(t) = w_1[\rho_c[q(t,L) - q(t,0)] - \int_0^L \rho(t,x)\frac{\partial}{\partial x}(q(t,x))dx] \\ + w_2(r(t) - u(t)) \tag{14}$$

The flow at the left most boundary is produced by the highway and ramp inflows. Therefore, we have

$$q(t,0) = u + f(t) \tag{15}$$

Utilizing (15) in (14) introduces the control variable in the differential equation for the error variable. This is shown below:

$$\dot{e}(t) = w_1[\rho_c[q(t,L) - f(t) - u] - \int_0^L \rho(t,x)\frac{\partial}{\partial x}(q(t,x))dx] + w_2(r(t) - u(t)) \tag{16}$$

Combining the control terms together, we get

$$\dot{e}(t) = w_1[\rho_c[q(t,L) - f(t)] - \int_0^L \rho(t,x)\frac{\partial}{\partial x}(q(t,x))dx] + w_2 r(t) - [\rho_c w_1 + w_2]u(t) \tag{17}$$

This differential equation can be written cleanly in the following form:

$$\dot{e}(t) = F + Gu \tag{18}$$

where

$$F = w_1[\rho_c[q(t,L) - f(t)] - \int_0^L \rho(t,x)\frac{\partial}{\partial x}(q(t,x))dx] + w_2 r(t) \tag{19}$$

and

$$G = -[\rho_c w_1 + w_2] \tag{20}$$

Our aim, as mentioned earlier, is to make the control variable $u(\cdot)$ a function of the traffic state variables in such a way that it can take the error variable to zero. We want to design the control law to make the error dynamics follow (6). In order to do that we present the feedback control law as

$$u = G^{-1}[-F - k_1 e(t) - k_2 \int_0^t e(s)ds] \tag{21}$$

Using (21) in (18) gives (6), as desired.

4. SOFTWARE

The software for the simulation written in such a way that we can easily perform simulations using a controller without the mixed sensitivity design and also perform simulations using the controller presented above using the same files. The only difference is in the weights used. When the weight given to the ramp queues is zero, then the controller becomes the same as has been designed before this chapter. That controller does not take into account the ramp queues. With a nonzero weight on the ramp queue, the new controller tries to reduce the ramp queues as well. The error to compare the two controllers is the same and that is the weighted normed error that is used to design the controller of the previous section. The files are presented below. The draw.m file is the same as the one used in the previous chapter.

```
% Ramp Metering Code
clear;
clf;
clc;

global rhom rhoc vf lmax Dx k1 k2 n rmax Diff ie w1 w2

% Input Parameters
c=input('unmixed(1) or mixed-control(2)');

if c==1
   w1=1;
     w2=0;
else
     w1=0.05;
     w2=0.95;
end

we1=0.05;
we2=0.95;

Dx=1;
k1=5.5;
k2=0.03;

rhom = 60;                    % Jam density
rhoc = rhom/2;                % Critical density
vf = 15;                      % freeflow velocity
lmax = 200;
Diff=0.0;
```

```
t0 = 0.0;
tf = 20;
h = 0.01;
m = (tf-t0)/h;
n = 10;                          % number of sections
rho=ones(m,n).*25;          % X array m rows, length state
columns
T=zeros(m,1);             % T array m rows (mx1)
L=[1:1:n]';
T(1)=t0;
l(1)=0;
ie=0;

rvar(1)=opder(1,l(1));
uvar(1)=opdeu12(1,rho(1,:),l(1),rvar(1));
fvar(1)=opdef(1);
evar(1)=we2*l(1);
for j=1:n
   evar(1)=evar(1)+we1*((rho(1,j)-rhoc)^2)/2;
end

%There are m-1 steps and m points maximum
for i=1:m-1;
   clc
   T(i)
   T(i+1)=t0 + h*i;


   flag=0;
   qin=vf*(rho(i,n-1)*(1-rho(i,n-1)/rhom))+Diff*(rho(i,n-1)-
rho(i,n));
      if flag==0
         qout=vf*(rho(i,n)*(1-rho(i,n)/rhom))+Diff*(rho(i,n-
1)-rho(i,n));
      else
         qout=0;
      end
         rhoinc=h*(qin-qout)/Dx;
      if rho(i,n)+rhoinc >=rhom
         rhoinc=rhom-rho(i,n);
         flag=1;
      else
         flag=0;
```

```
    end
    rho(i+1,n)=rho(i,n)+rhoinc;

  for j=n-1:-1:2
    qin=vf*(rho(i,j-1)*(1-rho(i,j-1)/rhom))+Diff*(rho(i,j-
1)-rho(i,j));
     if flag==0
        qout=vf*(rho(i,j)*(1-rho(i,j)/rhom))+Diff*(rho(i,j)-
rho(i,j+1));
     else
        qout=0;
     end
        rhoinc=h*(qin-qout)/Dx;
     if rho(i,j)+rhoinc >=rhom
        rhoinc=rhom-rho(i,j);
        flag=1;
     else
        flag=0;
    end
    rho(i+1,j)=rho(i,j)+rhoinc;
    end

  if flag==0
     qout=vf*(rho(i,1)*(1-rho(i,1)/rhom))+Diff*(rho(i,1)-
rho(i,2));
  else
     qout=0;
  end
  qin=opdef(i)+uvar(i);
  rhoinc=h*(qin-qout)/Dx;
  if rho(i,1)+rhoinc>=rhom
     rhoinc=rhom-rho(i,1);
     fvar(i)=qout+Dx*rhoinc/h;;
  end
  rho(i+1,1)=rho(i,1)+rhoinc;
  l(i+1)=l(i)+h*(opder(i,l(i))-uvar(i));
  rvar(i+1)=opder(i+1,l(i+1));
  if c==3
    uvar(i+1)=opdeu3(i+1,rho(i+1,:),l(i+1),rvar(i+1));
    else
    uvar(i+1)=opdeu12(i+1,rho(i+1,:),l(i+1),rvar(i+1));
    end
  fvar(i+1)=opdef(i+1);

  evar(i+1)=we2*l(i+1);
```

```
    for j=1:n
    evar(i+1)=evar(i+1)+we1*((rho(i+1,j)-rhoc)^2)/2;
    end
end
```

Figure 7-2: File opdemixedramp.m to Run Mixed and Unmixed Ramp Control Problems.

```
function opdef = opdef(t)
if t>75 & t<150
   opdef = 185*(1.0+0.2*sin(0.0025*t));
else
   opdef = 175*(1.0+0.2*sin(0.0025*t));
end
```

Figure 7-3: File opdef.m to Run Mixed and Unmixed Ramp Control Problems

```
function opder = opder(t,1)
global lmax
if 1<lmax
   opder = 20*(1.0+0.2*sin(0.001*t));      % ramp inflow
else
   opder = 0;
end;
```

Figure 7-4: File opder.m to Run Mixed and Unmixed Ramp Control Problems

```
function opdeu12 = opdeu12(t,x,1,r)

global rhom rhoc vf lmax Dx k1 k2 n rmax Diff ie w1 w2

e=w2*1;;
rdelqdx=0;
e=e+w1*((x(1)-rhoc)^2)/2;
qd=vf*x(2)*(1-(x(2)/rhoc))+Diff*(x(1)-x(2));
q=vf*x(1)*(1-(x(1)/rhoc))+Diff*(x(1)-x(2));
rdelqdx=rdelqdx+x(1)*(qd-q)/Dx;
for j=2:n-1
   e=e+((x(j)-rhoc)^2)/2;
   qd=vf*x(j+1)*(1-(x(j+1)/rhoc))+Diff*(x(j)-x(j+1));
   q=vf*x(j)*(1-(x(j)/rhoc))+Diff*(x(j-1)-x(j));
   rdelqdx=rdelqdx+x(j)*(qd-q)/Dx;
end
ie=ie+e;
qd=vf*x(n)*(1-(x(n)/rhoc))+Diff*(x(n-1)-x(n));
```

```
q=vf*x(n-1)*(1-(x(n-1)/rhoc))+Diff*(x(n-1)-x(n));
G=-(rhoc*w1+w2);
F=w1*rhoc*(qd-opdef(t))-rdelqdx+x(n)*(qd-q)/Dx+w2*1;
opdeu12=(-F-k1*(e+(((x(n)-rhoc)^2))/2)-k2*ie)/G; % ramp
outflow

if 1<=0
   if r<opdeu12
      opdeu12 = r;
   end
end
if x(1)>=rhom
   opdeu12 = 0;
end
if opdeu12<0
   opdeu12=0;
end
```

Figure 7-5: File opdeu12.m to Run Mixed and Unmixed Ramp Control Problems.

When you execute the opdemixedramp.m file, the system prompt asks you to input the value of c. When you enter 1, the controller without mixed sensitivity is used, and when you input 2, the mixed sensitivity controller (21) is used.

5. SIMULATION RESULTS

Simulation results using the value of 1 for *c* are given below. These, therefore, are the results for a feedback controller that does not consider the ramp queues.

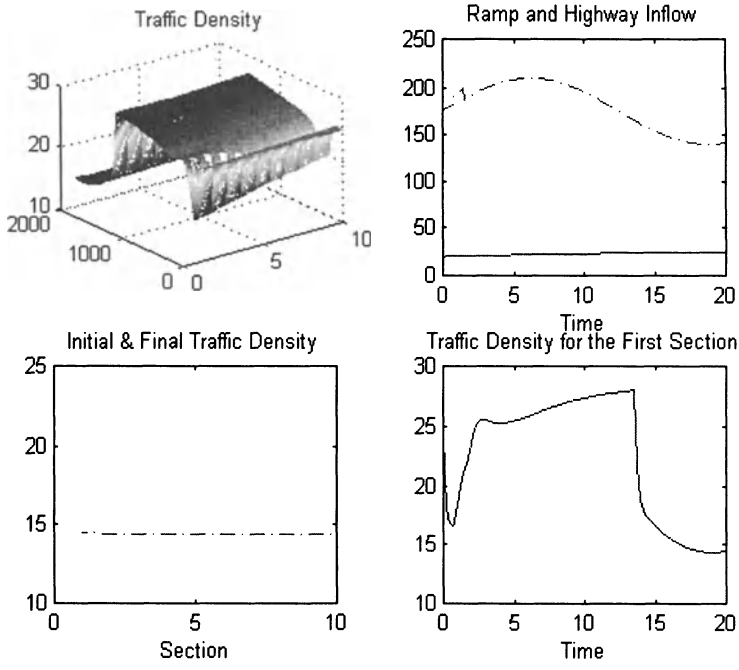

Figure 7-6: Plot-1 Using Unmixed Ramp Control

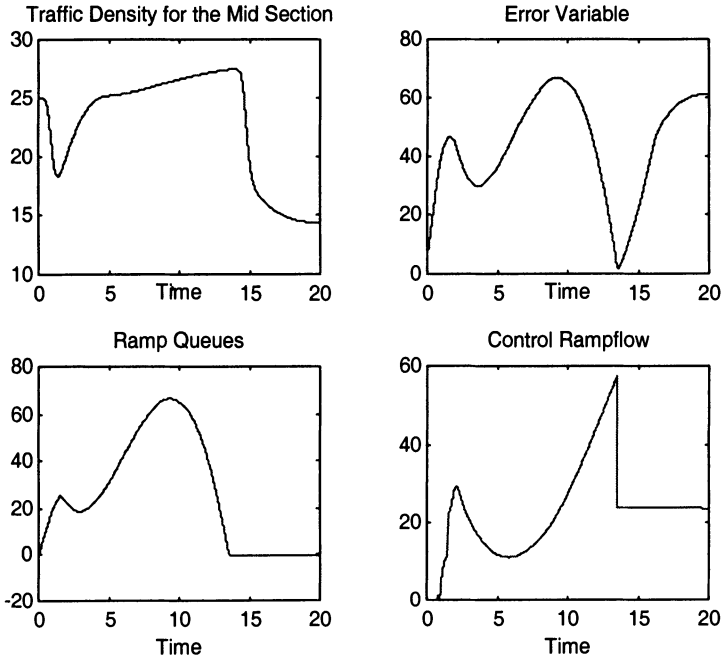

Figure 7-7: Plot-2 Using Unmixed Ramp Control

Simulation results using the value of 2 for c are given below. These, therefore, are the results for a feedback controller that does consider the ramp queues.

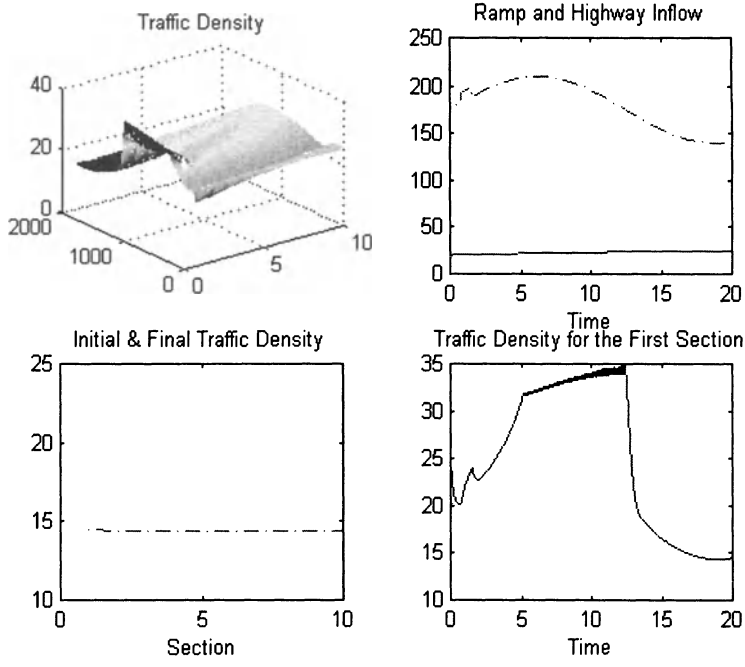

Figure 7-8: Plot-1 Using Mixed Ramp Control

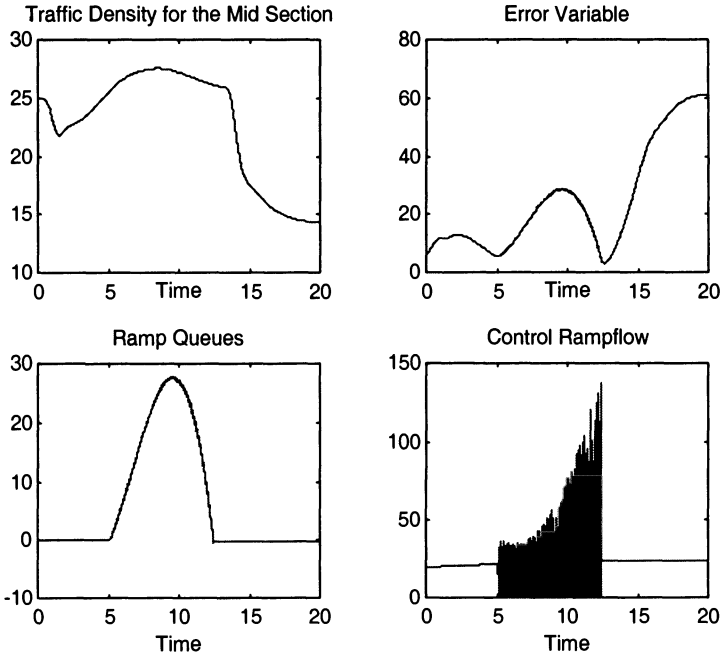

Figure 7-9: Plot-2 Using Mixed Ramp Control

By comparing the two sets of plots, we see clearly that the ramp queue lengths are reduced when we use the controller (21).

We can also perform simulations where the weight on the first term is 0.5 and the ramp queue term is 0.5, as compared to the plots above where the weights were 0.05 and 0.95, respectively.

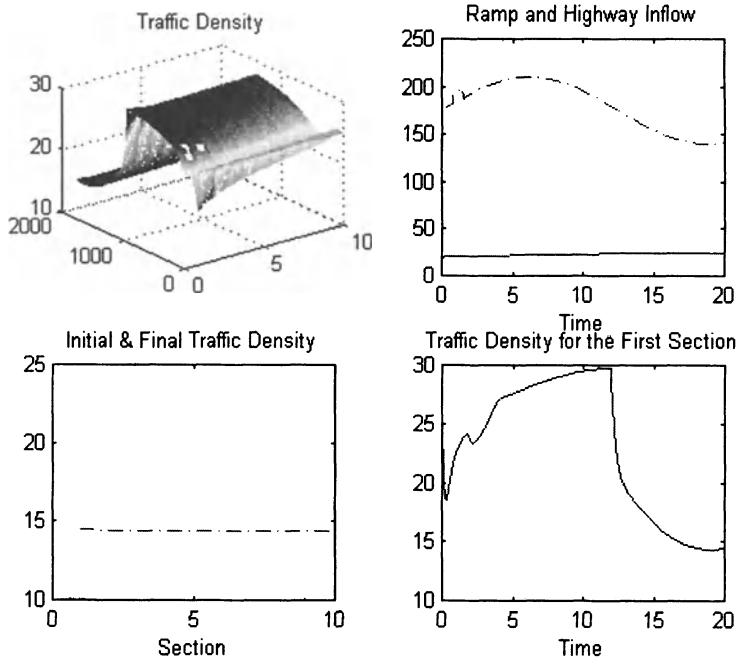

Figure 7-10: Plot-1 using Equal Weights Mixed Ramp Control.

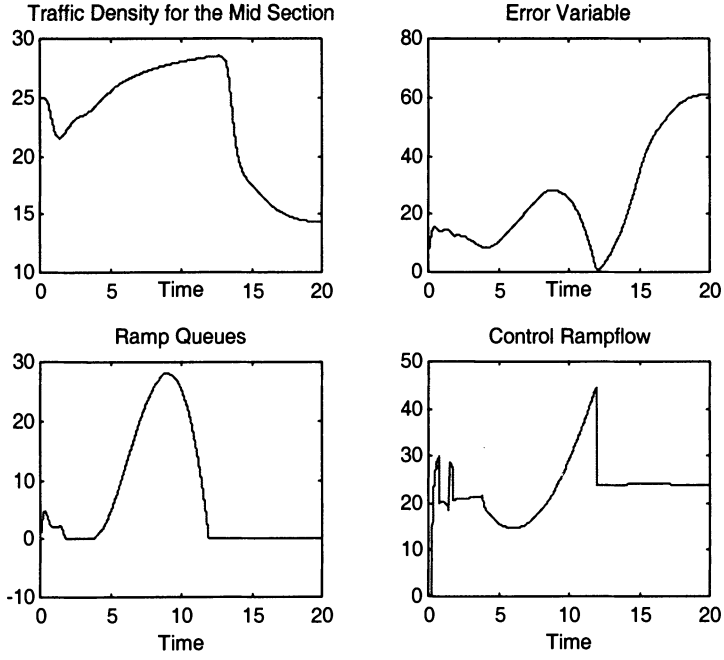

Figure 7-11: Plot-2 Using Equal Weights Mixed Ramp Control

6. SUMMARY

In this chapter, we studied:

- How to design feedback control laws for an isolated ramp metering problem using the distributed mathematical model for the ramp system where the control objective tries to minimize a weighted average of the norm of the difference of the highway traffic density from the critical value and the ramp queue length.
- We performed simulations to see the effectiveness of the results.

7. QUESTIONS

1. What is the objective of the mixed control? How does it achieve its aim?

2. Explain the importance of the weight factors w_1 and w_2 in the control law.
3. Explain the improvements in the system, when:
   a. w_1=1, w_2=0
   b. w_1=0.95, 0.05
   c. w_1=0.5, 0.5
   d. Which above case gives the optimum results in terms of providing freeway flow at critical density and reducing the ramp queues?

8. PROBLEMS

1. Using the mixed control given in this chapter, write your own simple MATLAB code. Test the Matlab code for different levels of freeway and ramp demands to determine the relationship between total demand and weight parameters. Plot the obtained values to show this relationship.
2. For total demand slightly above the maximum demand the system can handle based on your system characteristics, set the weight for the ramp to zero and run your Matlab simulation to observe the ramp queue. Then, incorporate a constraint that turns off the control when the queue is above the threshold value set for the maximum queue length for the ramp. Compare this solution with the solution that uses the optimal weight value in terms of total system delays.

9. REFERENCES

1. Hamming, R., *Numerical Methods for Scientists and Engineers*, Dover, 1987.
2. Isaacson, E., and Keller, H. B., *Analysis of Numerical Methods*, Dover, 1994.
3. Khalil, H. K., *Nonlinear Systems*, Prentice-Hall, 2001.
4. Isidori, A., *Nonlinear Control Systems*, Springer-Verlag, 1995.
5. Burns, J. A., and Kang S., 'A control problem for Burgers' Equation with Bounded Input/Output', Nonlinear Dynamics 2, 1991, 235-262.
6. Cole, J. D., "On a Quasi-linear Parabolic Equation Occurring in Aerodynamics", Quart. Appl. Math. IX, 1951, 225-236.

Chapter 8

FEEDBACK CONTROL DESIGN FOR COORDINATED RAMPS USING DISTRIBUTED MODELING

This chapter presents the feedback control design of a coordinated ramp metering problem where we use the distributed model of the ramp system. We show the stability properties of the closed-loop system that is obtained by the application of the feedback control laws on the ramp system. We verify the effectiveness of the feedback control law by running some simulation experiments using the designed feedback control law on the coordinated ramp system.

1. COORDINATED RAMP METERING

Coordinated ramp metering problem refers to a highway system that has ramps on it at various points. The question for design becomes how should the ramp metering be designed taking into account the interactions of the various ramps. The coordinated ramp problem is illustrated in Figure 8-1.

P. Kachroo et al., *Feedback Ramp Metering in Intelligent Transportation Systems*

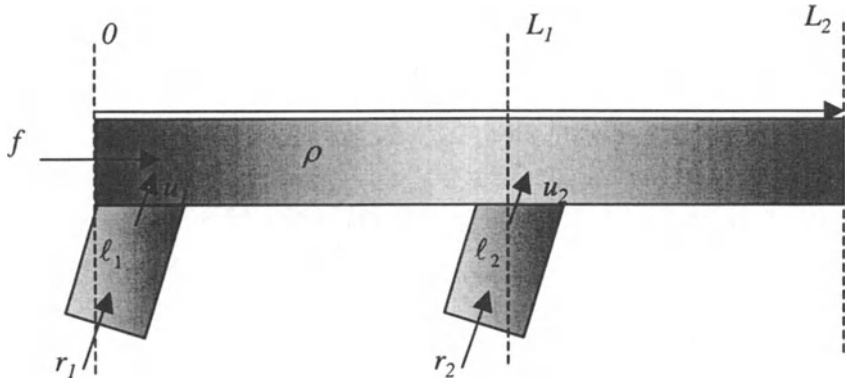

Figure 8-1: Coordinated Ramp Problem

We can express the coordinated ramp metering problem as the problem of controlling the traffic density on the entire mainline, or as a mixed sensitivity problem. We can use solutions that are decoupled or coupled. As decoupled solutions, we can totally ignore the ramp connections and treat each ramp as an isolated problem, and use the controllers that have been designed till now. We will study all these aspects in this chapter. We will start off with a new technique for isolated ramps that we have not studied before, and we will then use this technique as a motivational example to design a similar technique for the coordinated problem.

2. MOTIVATION EXAMPLE FOR ISOLATED RAMP PROBLEM

We present a new technique for isolated ramp control here, which will help us in designing effective and simple coordinated feedback ramp control laws.

2.1 Control Objective

The control objective for this new control law is to make the error term go to zero asymptotically. However, the design of the error variable will be different. The design is given as

$$e(t) = \int_0^L (\rho(t,x) - \rho_c)dx \tag{1}$$

We will again strive to achieve the closed-loop dynamics represented by

$$\dot{e}(t) + k_1 e(t) + k_2 \int_0^t e(s)ds = 0 \tag{2}$$

which will enable us to obtain

$$\lim_{t\to\infty} e(t) = 0 \tag{3}$$

We will show the feedback control law for the basic design as well as the diffusion-based model. In both models, the conservation equation is

$$\frac{\partial \rho(t,x)}{\partial t} + \frac{\partial q(t,x)}{\partial x} = 0 \tag{4}$$

and the flow relationship is

$$q(t,x) = \rho(t,x)v(t,x) \tag{5}$$

In the basic model we use the following for the velocity density relationship:

$$v = v_f(1 - \frac{\rho}{\rho_{\max}}) \tag{6}$$

For the diffusion model, we use

$$v_e = v_f[1 - \frac{\rho}{\rho_{\max}}] - D[\frac{\partial \rho}{\partial x}]/\rho \tag{7}$$

2.2 Feedback Control Design

In order to design a control law that attempts to achieve (2), we start by differentiating (1) by time to get the following:

$$\frac{d}{dt}e(t) = \dot{e}(t) = \frac{d}{dt}\int_0^L (\rho(t,x) - \rho_c)dx \tag{8}$$

Simplifying this expression stepwise, we obtain

$$\dot{e}(t) = \int_0^L \frac{d}{dt}\rho(t,x)dx \tag{9}$$

Using the conservation equation here after equating total to partial derivative, gives

$$\dot{e}(t) = -\int_0^L \frac{\partial}{\partial x}(q(t,x))dx \tag{10}$$

Equating the partial derivative to the total derivative, we get

$$\dot{e}(t) = -\int_0^L \frac{d}{dx}(q(t,x))dx \tag{11}$$

which gives

$$\dot{e}(t) = -\int_{q(t,0)}^{q(t,L)} dq(t,x) \tag{12}$$

Solving the first integral in (12) yields

$$\dot{e}(t) = q(t,0) - q(t,L) \tag{13}$$

The flow at the left most boundary is produced by the highway and ramp inflows. Therefore, we have, as before,

$$q(t,0) = u + f(t) \tag{14}$$

Utilizing (14) in (13) introduces the control variable in the differential equation for the error variable. This is shown as

$$\dot{e}(t) = u + f(t) - q(t, L) \tag{15}$$

Our aim is to make the control variable $u(.)$ a function of the traffic state variables in such a way that it can take the error variable to zero. We want to design the control law to make the error dynamics follow (2). In order to do that we present the feedback control law as

$$u = q(t, L) - f(t) - k_1 e(t) - k_2 \int_0^t e(s)ds \tag{16}$$

Using (16) in (15) gives (2), as desired. This control law works for models, basic and diffusion. When we use the basic model, the control law will expand as

$$u = v_f \rho(t, L)(1 - \frac{\rho(t, L)}{\rho_m}) - f(t) - k_1 e(t) - k_2 \int_0^t e(s)ds \tag{17}$$

When we use the diffusion model, the control law will expand as

$$\begin{aligned} u = {} & v_f \rho(t, L)(1 - \frac{\rho(t, L)}{\rho_m}) - D \left.\frac{\partial q}{\partial x}\right|_{x=L} \\ & - f(t) - k_1 e(t) - k_2 \int_0^t e(s)ds \end{aligned} \tag{18}$$

2.3 Simulation Program

The simulation program is presented below:

```
% Ramp Metering Code
clear;
clf;
clc;
```

```
global rhom rhoc vf lmax Dx k1 k2 n rmax Diff ie

% Input Parameters

Dx=1;
k1=2.25;
k2=0.01;

rhom = 60;                          % Jam density
rhoc = rhom/2;                      % Critical density
vf = 15;                            % freeflow velocity
lmax = 200;
Diff=10.0;

t0 = 0.0;
tf = 20;
h = 0.01;
m = (tf-t0)/h;
n = 10;                             % number of sections
rho=ones(m,n).*15;          % X array m rows, length state
columns
T=zeros(m,1);              % T array m rows (mx1)
L=[1:1:n]';
T(1)=t0;
l(1)=0;
ie=0;

rvar(1)=opder(1,l(1));
uvar(1)=opdeu3(1,rho(1,:),l(1),rvar(1));
fvar(1)=opdef(1);
evar(1)=0;
for j=1:n
   evar(1)=evar(1)+(rho(1,j)-rhoc);
end

%There are m-1 steps and m points maximum
for i=1:m-1;
   clc
   T(i)
   T(i+1)=t0 + h*i;


   flag=0;
   qin=vf*(rho(i,n-1)*(1-rho(i,n-1)/rhom))+Diff*(rho(i,n-1)-
rho(i,n));
```

```
      if flag==0
         qout=vf*(rho(i,n)*(1-rho(i,n)/rhom))+Diff*(rho(i,n-
1)-rho(i,n));
      else
         qout=0;
      end
         rhoinc=h*(qin-qout)/Dx;
      if rho(i,n)+rhoinc >=rhom
         rhoinc=rhom-rho(i,n);
         flag=1;
      else
         flag=0;
    end
    rho(i+1,n)=rho(i,n)+rhoinc;

   for j=n-1:-1:2
      qin=vf*(rho(i,j-1)*(1-rho(i,j-1)/rhom))+Diff*(rho(i,j-
1)-rho(i,j));
      if flag==0
         qout=vf*(rho(i,j)*(1-rho(i,j)/rhom))+Diff*(rho(i,j)-
rho(i,j+1));
      else
         qout=0;
      end
         rhoinc=h*(qin-qout)/Dx;
      if rho(i,j)+rhoinc >=rhom
         rhoinc=rhom-rho(i,j);
         flag=1;
      else
         flag=0;
    end
    rho(i+1,j)=rho(i,j)+rhoinc;
    end

   if flag==0
      qout=vf*(rho(i,1)*(1-rho(i,1)/rhom))+Diff*(rho(i,1)-
rho(i,2));
   else
      qout=0;
   end
   qin=opdef(i)+uvar(i);
   rhoinc=h*(qin-qout)/Dx;
   if rho(i,1)+rhoinc>=rhom
      rhoinc=rhom-rho(i,1);
```

```
      fvar(i)=qout+Dx*rhoinc/h;;
   end
   rho(i+1,1)=rho(i,1)+rhoinc;
   l(i+1)=l(i)+h*(opder(i,l(i))-uvar(i));
   rvar(i+1)=opder(i+1,l(i+1));
   uvar(i+1)=opdeu3(i+1,rho(i+1,:),l(i+1),rvar(i+1));
   fvar(i+1)=opdef(i+1);

   evar(i+1)=0;
   for j=1:n
      evar(i+1)=evar(i+1)+(rho(i+1,j)-rhoc);
   end
end
```

Figure 8-2: File opdemixedramp.m for New Isolated Control Law

```
function opder = opder(t,l)
global lmax
if l<lmax
   opder = 50*(1.0+0.2*sin(0.001*t));      % ramp inflow
else
   opder = 0;
end;
```

Figure 8-3: File opder.m for New Isolated Control Law

```
function opdef = opdef(t)
if t>75 & t<150
   opdef = 185*(1.0+0.2*sin(0.0025*t));
else
   opdef = 175*(1.0+0.2*sin(0.0025*t));
end
```

Figure 8-4: File opdef.m for New Isolated Control Law

```
function opdeu = opdeu(t,x,l,r)

global rhom rhoc vf lmax Dx k1 k2 n rmax Diff ie
e=0;
rdelqdx=0;
e=e+(x(1)-rhoc);
for j=2:n-1
   e=e+(x(j)-rhoc);
end
e=e+(x(n)-rhoc);
ie=ie+e;
q=vf*x(n-1)*(1-(x(n-1)/rhoc));
```

```
qd=vf*x(n)*(1-(x(n)/rhoc));
%qd=vf*x(n)*(1-(x(n)/rhoc))-Diff*(qd-q)/Dx;
F=qd-opdef(t);
opdeu=F-k1*e-k2*ie; % ramp outflow

if 1<=0
   if r<opdeu
      opdeu3 = r;
   end
end
if x(1)>=rhom
   opdeu = 0;
end
if opdeu<0
   opdeu=0;
end
```

Figure 8-5: File opdeu.m for New Isolated Control Law

2.4 Simulation Results

We will perform the following three simulations on this system.

1. Using control law (17) on the basic model with k_1=1.25, and k_2=0.00.
2. Using control law (17) on the diffusion model with k_1=7.25, and k_2=0.015, and Diff=10.0.
3. Using control law (18) on the diffusion model with k_1=7.25, and k_2=0.015, and Diff=10.0.

The results of these three types of experiments are presented next.

2.4.1 Basic Control Law on Basic Model

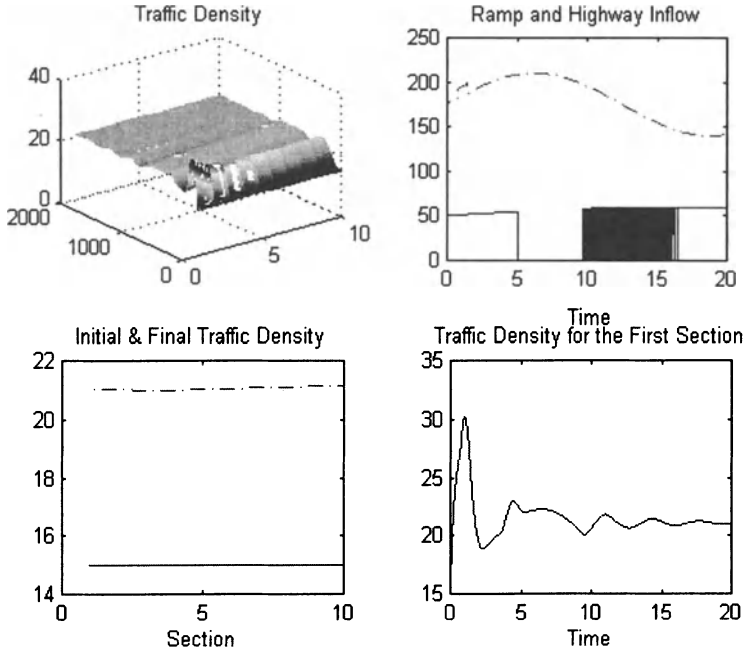

Figure 8-6: Plot-1 for Basic Control Law on Basic Model

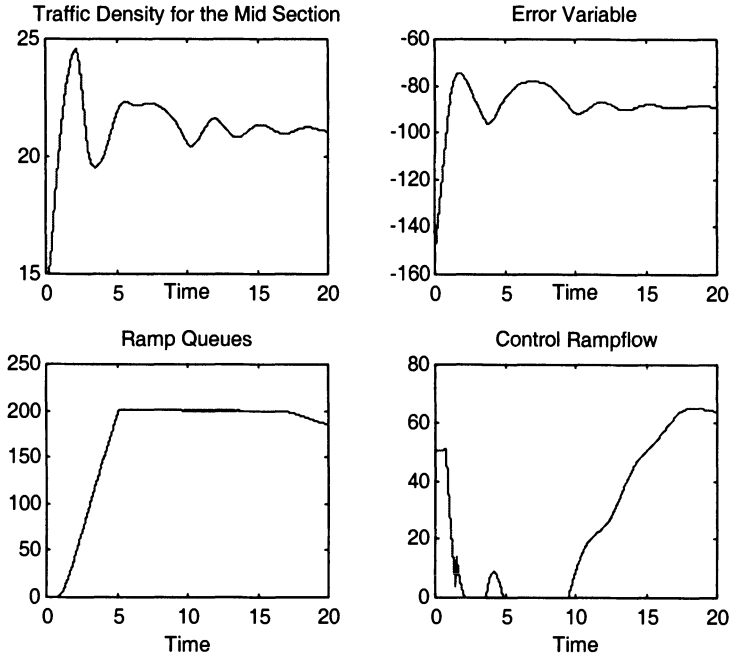

Figure 8-7: Plot-2 for Basic Control Law on Basic Model

2.4.2 Basic Control Law on Diffusion Model

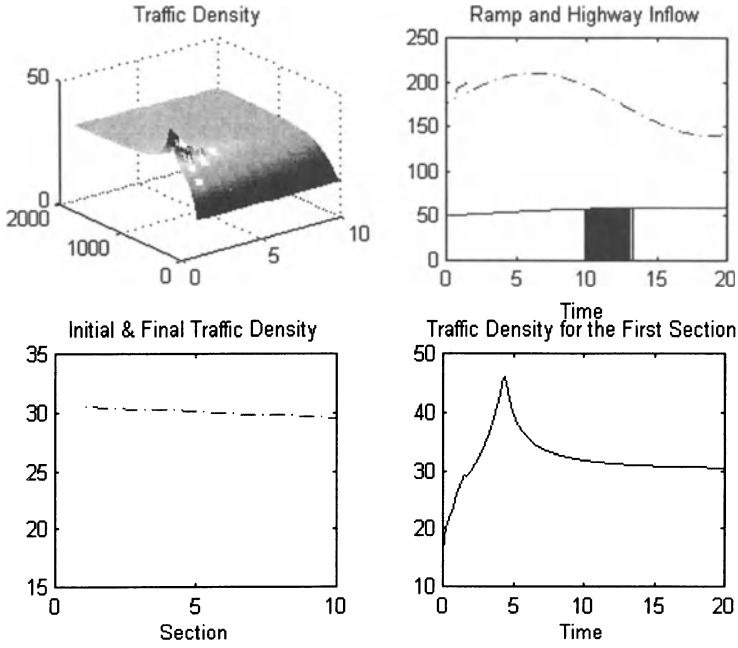

Figure 8-8: Plot-1 for Basic Control Law on Diffusion Model

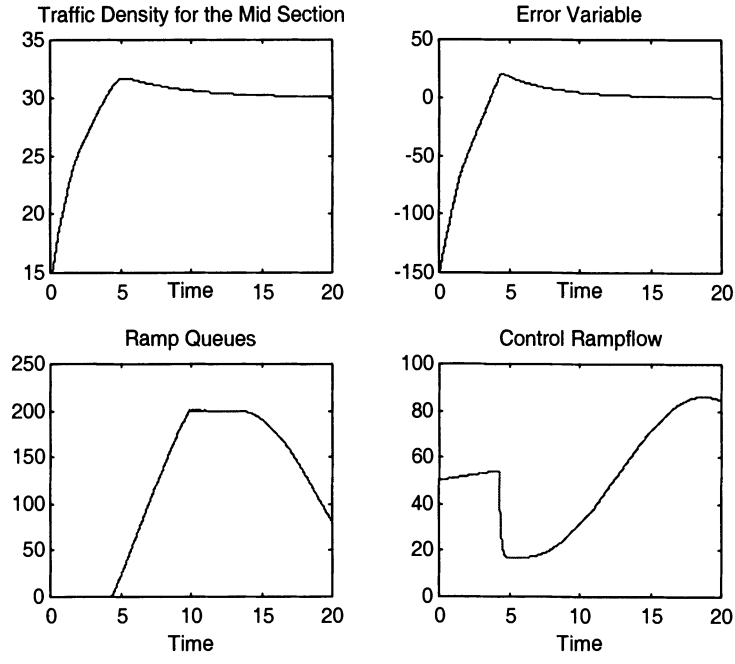

Figure 8-9: Plot-2 for Basic Control Law on Diffusion Model

2.4.3 Diffusion Control Law on Diffusion Model

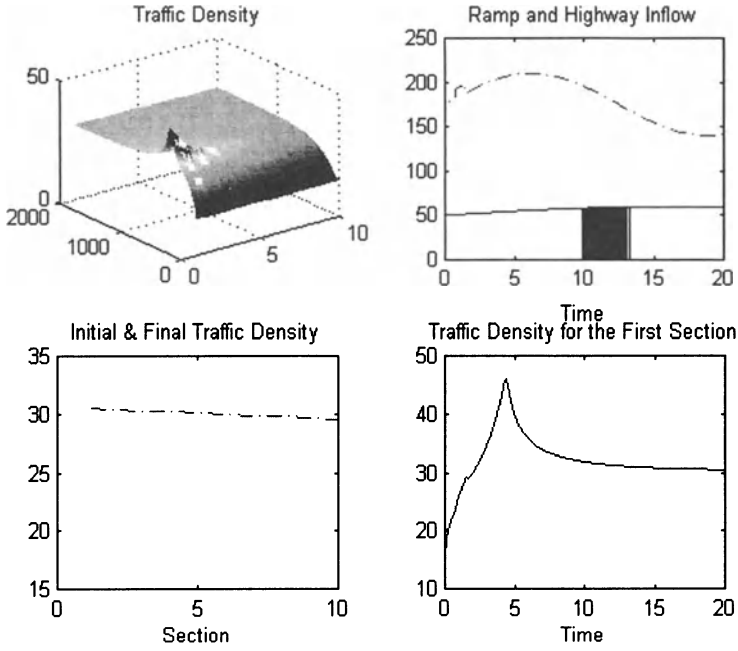

Figure 8-10: Plot-1 for Diffusion Control Law on Diffusion Model

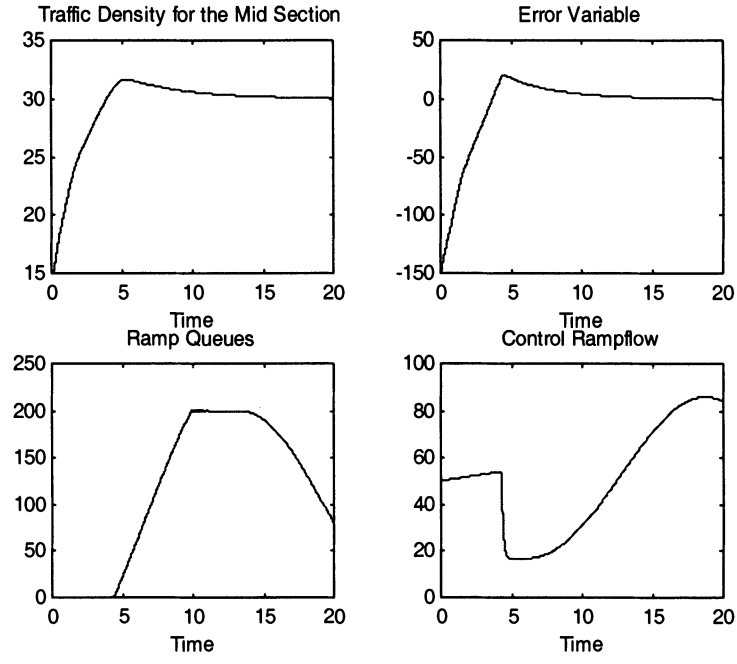

Figure 8-11: Plot-2 for Diffusion Control Law on Diffusion Model

These plots show that diffusion models give better results in systems. This is expected because they help to distribute the traffic in the mainline.

2.5 Analysis of the Control Objective and the Performance of the Controller

One very interesting thing to note about the control objective (1) is that the highway can give a zero value to error without having each point on the highway be at the critical density. We see that if two points on the highway have equal displacement of their traffic density values from the critical value but one has a positive variation and the other negative, then the overall integral in (1) is not affected by it. This seems to be a major limitation of this control design.

The most interesting thing about this controller, however, is that it gives excellent results. The reason for this is as follows. We will study the performance looking at two types of traffic distribution on the highway.

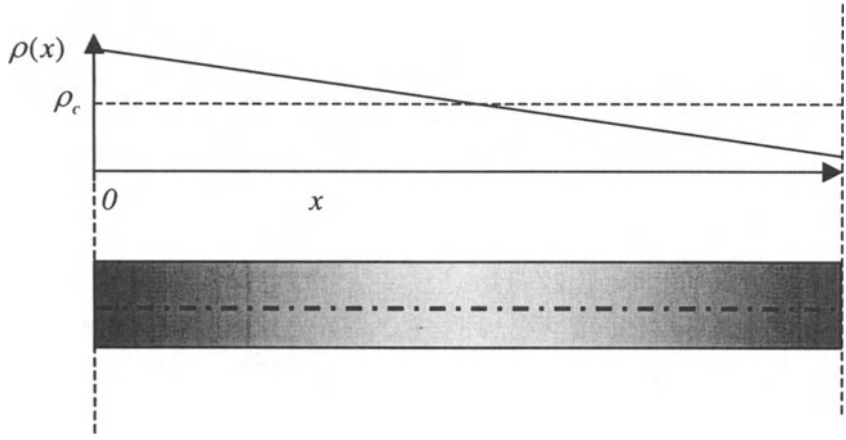

Figure 8-12: Decreasing Traffic Distribution

In the case of the decreasing traffic density shown in Figure 8-12, the controller will not add too much new traffic, and if it did, that could cause congestion.

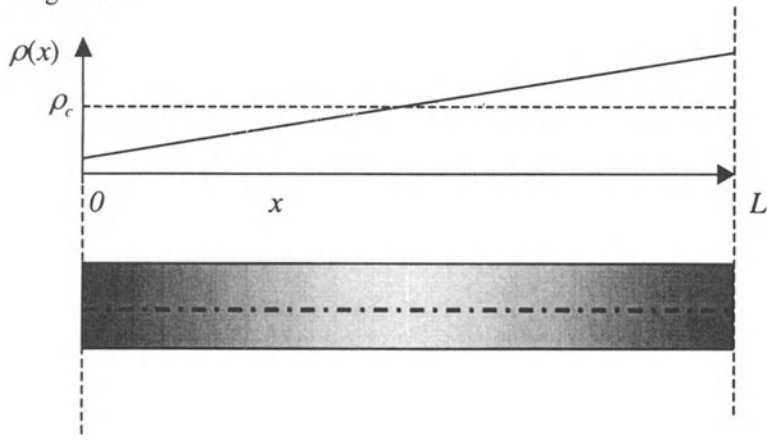

Figure 8-13: Increasing Traffic Distribution

Similarly, in the case of the increasing traffic density shown in Figure 8-13, the controller will not add too much new traffic, and if it did, that could cause congestion at the downstream. This analysis is good for traffic with

diffusion. In the case of traffic with high diffusion, the system has a tendency to even out the changing spatial densities, and therefore, with this control law, we can get good tracking of critical density.

3. COORDINATED RAMP CONTROL

Now, we will use the technique developed above and modify it for application to the coordinated problem. Refer to Figure 8-1 for this coordinated ramp problem.

3.1 Control Objective

The control objective for this new control law is to make the error term go to zero asymptotically. The limits of integral for this problem will be from the start to the end of the mainline that includes both ramps:

$$e(t) = \int_0^{L_2} (\rho(t,x) - \rho_c) dx \tag{19}$$

We will again strive to achieve the closed-loop dynamics represented by (2) to enable (3).

3.2 Feedback Control Design

In order to design a control law that attempts to achieve (2), we start by differentiating (19) by time to get

$$\frac{d}{dt} e(t) = \dot{e}(t) = \frac{d}{dt} \int_0^{L_2} (\rho(t,x) - \rho_c) dx \tag{20}$$

Since the mainline has two parts, we can write this as (refer to Figure 8-1):

$$\dot{e}(t) = \frac{d}{dt}\int_0^{L_1^-}(\rho(t,x)-\rho_c)dx = \frac{d}{dt}\int_0^{L_1^-}(\rho(t,x)-\rho_c)dx + \frac{d}{dt}\int_{L_1^+}^{L_2}(\rho(t,x)-\rho_c)dx \tag{21}$$

Simplifying this expression stepwise, we get

$$\dot{e}(t) = \int_0^{L_1^-}\frac{d}{dt}\rho(t,x)dx + \int_{L_1^+}^{L_2}\frac{d}{dt}\rho(t,x)dx \tag{22}$$

Using the conservation equation here after equating total to partial derivative, gives

$$\dot{e}(t) = -\int_0^{L_1^-}\frac{\partial}{\partial x}q(t,x)dx - \int_{L_1^+}^{L_2}\frac{\partial}{\partial x}q(t,x)dx \tag{23}$$

Equating the partial derivative to total derivative, we get

$$\dot{e}(t) = -\int_0^{L_1^-}\frac{d}{dx}q(t,x)dx - \int_{L_1^+}^{L_2}\frac{d}{dx}q(t,x)dx \tag{24}$$

which gives

$$\dot{e}(t) = -\int_0^{L_1^-}dq(t,x) - \int_{L_1^+}^{L_2}dq(t,x) \tag{25}$$

Solving the integrals in (25) yields

$$\dot{e}(t) = q(t,0) - q(t,L_1^-) + q(t,L_1^+) - q(t,L_2) \tag{26}$$

The flow at the left most boundary is produced by the highway and ramp inflows. Therefore, we have, as before,

$$q(t,0) = u_1 + f(t) \tag{27}$$

From the boundary condition at the second ramp, we also have

$$q(t, L_1^+) = q(t, L_1^-) + u_2 \tag{28}$$

Substituting (27) and (28) in (26) gives the error dynamics as

$$\dot{e}(t) = u_1 + u_2 + f(t) - q(t, L_2) \tag{29}$$

If we design the control variables with the following constraint

$$u_1 + u_2 = q(t, L_2) - f(t) - k_1 e(t) - k_2 \int_0^t e(s)ds \tag{30}$$

we will get the satisfaction of dynamics (2). This control law works for models, basic and diffusion. When we use the basic model, the control law will expand as

$$u_1 + u_2 = v_f \rho(t, L_2)(1 - \frac{\rho(t, L_2)}{\rho_m}) - f(t) - k_1 e(t) - k_2 \int_0^t e(s)ds \tag{31}$$

When we use the diffusion model, the control law will expand as

$$\begin{aligned} u_1 + u_2 &= v_f \rho(t, L_2)(1 - \frac{\rho(t, L_2)}{\rho_m}) - D \frac{\partial q}{\partial x}\Big|_{x=L_2} \\ &- f(t) - k_1 e(t) - k_2 \int_0^t e(s)ds \end{aligned} \tag{32}$$

Now the question becomes how to divide the right-hand sides of (30), (31), or (32) between the two ramp control flows. We will show this for (30). We can write (30) as

$$\begin{aligned} u_1 + u_2 &= q(t, L_2) - f(t) - k_1 e(t) - k_2 \int_0^t e(s)ds \\ &+ q(t, L_1^-) - q(t, L_1^-) \end{aligned} \tag{33}$$

We can break up the error term into two parts as

$$e(t) = \int_0^{L_1^-} (\rho(t,x) - \rho_c)dx + \int_{L_1^+}^{L_2} (\rho(t,x) - \rho_c)dx \tag{34}$$

we can name

$$e_1(t) = \int_0^{L_1^-} (\rho(t,x) - \rho_c)dx \tag{35}$$

and

$$e_2(t) = \int_{L_1^+}^{L_2} (\rho(t,x) - \rho_c)dx \tag{36}$$

so that

$$e(t) = e_1(t) + e_2(t) \tag{37}$$

Using (37) in (33) gives

$$\begin{aligned} u_1 + u_2 &= q(t,L_1^-) - f(t) - k_1 e_1(t) - k_2 \int_0^t e_1(s)ds \\ &+ q(t,L_2) - q(t,L_1^-) - k_1 e_2(t) - k_2 \int_0^t e_2(s)ds \end{aligned} \tag{38}$$

Now, we can divide the right-hand side of (38) as

$$u_1 = q(t,L_1^-) - f(t) - k_1 e_1(t) - k_2 \int_0^t e_1(s)ds \tag{39}$$

and

$$u_2 = q(t, L_2) - q(t, L_1^-) - k_1 e_2(t) - k_2 \int_0^t e_2(s) ds \tag{40}$$

Notice that (39) and (40) are the exact same control laws as (16). Therefore, this method produces decoupled control laws. However, we can also choose to divide the right-hand side in other ways so as to keep the ramp control inflows responsive to other sections.

The next section will show how to design coordinated ramp feedback control laws that take into account the ramp queues at all ramps in the system.

4. COORDINATED MIXED SENSITIVITY FEEDBACK RAMP CONTROL

The following is the development of the coordinated mixed sensitivity feedback control law. First, we present the control objective, followed by the control design.

4.1 Control Objective

The aim of the controller is to keep the traffic density at the critical value for the entire section that includes both ramps and at the same time keep the queue lengths at the two ramps small. Therefore, the error variable to accomplish both will be taken as

$$e(t) = \frac{w_1}{2} \int_0^{L_2} (\rho(t,x) - \rho_c)^2 dx + w_2 \ell_1 + w_3 \ell_2 \tag{41}$$

Since the first term in (41) is a squared term, and the second and third terms are queue lengths, which are nonnegative variables, the error term itself is always nonnegative. Our aim for the control law design is to satisfy the following objective:

$$\lim_{t \to \infty} e(t) = 0 \tag{42}$$

Note that if we take the weights for the two ramp queues to be zero, then this becomes a coordinated ramp control objective without mixed sensitivity.

This control objective does not suffer from the limitation of having non-critical density for zero error. The methodology for the feedback control design will be the same as that used in previous chapters, i.e., to use feedback linearization. With the integral term in the feedback linearization, the error dynamics in the closed loop will become

$$\dot{e}(t) + k_1 e(t) + k_2 \int_0^t e(s)ds = 0 \tag{43}$$

4.2 Feedback Control Design

In order to design a control law that attempts to achieve (42), we start by differentiating (41) by time to get

$$\frac{d}{dt}e(t) = \dot{e}(t) = \frac{d}{dt}[\frac{w_1}{2}\int_0^{L_2}(\rho(t,x)-\rho_c)^2 dx + w_2\ell_1 + w_3\ell_2] \tag{44}$$

Simplifying this expression stepwise, we get

$$\dot{e}(t) = w_1\int_0^{L_2}(\rho(t,x)-\rho_c)\frac{d}{dt}(\rho(t,x)-\rho_c)dx + w_2\dot{\ell}_1 + w_3\dot{\ell}_2 \tag{45}$$

Using the conservation equation and the ramp queue dynamics for both queues here gives

$$\begin{aligned}\dot{e}(t) &= -w_1\int_0^{L_2}(\rho_c-\rho(t,x))\frac{\partial}{\partial x}(q(t,x))dx \\ &+ w_2(r_1(t)-u_1) + w_3(r_2(t)-u_2)\end{aligned} \tag{46}$$

Simplifying this equation, we get

$$\begin{aligned}\dot{e}(t) &= -w_1[\int_0^{L_2}\rho_c\frac{\partial}{\partial x}(q(t,x))dx - \int_0^{L_2}\rho(t,x)\frac{\partial}{\partial x}(q(t,x))dx] \\ &+ w_2(r_1(t)-u_1) + w_3(r_2(t)-u_2)\end{aligned} \tag{47}$$

Since the critical density is constant, we get

$$\dot{e}(t) = -w_1[\rho_c \int_0^{L_2} \frac{\partial}{\partial x}(q(t,x))dx - \int_0^{L_2} \rho(t,x)\frac{\partial}{\partial x}(q(t,x))dx] + w_2(r_1(t)-u_1) + w_3(r_2(t)-u_2) \tag{48}$$

Equating the partial derivative to total derivative, we get

$$\dot{e}(t) = -w_1[\rho_c \int_0^{L_2} \frac{d}{dx}(q(t,x))dx - \int_0^{L_2} \rho(t,x)\frac{\partial}{\partial x}(q(t,x))dx] + w_2(r_1(t)-u_1) + w_3(r_2(t)-u_2) \tag{49a}$$

which gives

$$\dot{e}(t) = -w_1[\rho_c[\int_0^{L_1^-} dq + \int_{L_1^+}^{L_2} dq] - \int_0^{L_2} \rho(t,x)\frac{\partial}{\partial x}(q(t,x))dx] + w_2(r_1(t)-u_1) + w_3(r_2(t)-u_2) \tag{49b}$$

Solving the first integral in (49b) and using (27) and (28) here gives

$$\dot{e}(t) = -w_1[\rho_c[q(t,L_2)-u_1-u_2-f(t)] - \int_0^{L_2} \rho(t,x)\frac{\partial}{\partial x}(q(t,x))dx] + w_2(r_1(t)-u_1) + w_3(r_2(t)-u_2) \tag{50}$$

Combining the control terms together, we get

$$\dot{e}(t) = -w_1[\rho_c[q(t,L_2)-f(t)] - \int_0^{L_2} \rho(t,x)\frac{\partial}{\partial x}(q(t,x))dx] + w_2 r_1(t) + w_3 r_2(t) + (-w_1\rho_c - w_2)u_1 + (-w_1\rho_c - w_3)u_2 \tag{51}$$

This differential equation can be written cleanly in the following form:

$$\dot{e}(t) = F + u \tag{52}$$

where

$$F = -w_1[\rho_c[q(t,L_2) - f(t)] - \int_0^{L_2} \rho(t,x)\frac{\partial}{\partial x}(q(t,x))dx] + w_2 r_1(t) + w_3 r_2(t) \tag{53}$$

and

$$u = w_2(r_1(t) - u_1) + w_3(r_2(t) - u_2) \tag{54}$$

To get error dynamics (43), we use

$$u = -F - k_1 e(t) - k_2 \int_0^t e(s)ds \tag{55}$$

Using (55) in (52) gives (43), as desired. Now we have to divide the right-hand side of (55) into the two control ramp flows. We need to divide to satisfy

$$w_2(r_1(t) - u_1) + w_3(r_2(t) - u_2) = -F - k_1 e(t) - k_2 \int_0^t e(s)ds \tag{56}$$

We can use decoupled or coupled laws just as we did in (39) and (40) and using the arguments following that.

It can be seen easily that in the same way we designed feedback control laws in the coordinated ramp setup in which there were two ramps, we can also design similar feedback control laws when there are more than two entrance ramps.

5. SUMMARY

In this chapter, we studied:

- A new isolated ramp metering control law in distributed setting for basic and distributed models.

- We derived extension of this new law to design coordinated ramp control laws.

6. QUESTIONS

1. What is the difference between coordinated and isolated ramp metering control? What factors are considered in coordinated control?
2. What are the "coupled" and "decoupled" solutions to the ramp metering problem? Explain how these solutions approach the coordinated ramp metering problem.
3. How are the parameters k_1 and k_2 selected in the simulation?
4. In section 2.4, three different conditions are simulated. Compare the figures for case 2 and case 3.
5. What are the limitations of the controller given in Section 2.2?
6. What are the benefits of using the controller (Section 2.2)?
7. Is the coordinated ramp control given (Section 3) coupled or decoupled? Why? How can we convert the control from one type to the other?

7. PROBLEMS

1. Using (1), derive (12) in section 2.2.
2. Derive (38) in Section 3.2.
3. a. Refer to question 7; derive the other version of the control law (section 3.2).
   b. Write a simple MATLAB code for the control law derived in Section 3.2.
   c. Write a simple MATLAB code for the control law derived in (a).
   d. Compare the results. Which one gives better performance results? (Consider freeway density, error term, ramp queue)
4. Make the necessary changes in the MATLAB code given in Section 2.3 to simulate the coordinated mixed sensitivity feedback ramp control. Compare the results with the case of "diffusion control law on diffusion model."

8. REFERENCES

1. Papageorgiou, M., "Traffic Control," Handbook of Transportation Science, R.W. Hall, Editor, Kluwer Academic ,1999, 233-267.
2. Meldrum, D., and Taylor, C., Freeway traffic data prediction using artificial neural networks and development of a Fuzzy Logic Ramp Metering Algorithm Final Technical Report, Washington State Department of Transportation Report No. WA-RD 365.1, 1995.
3. Zhang, H.M., Ritchie S. G., and Recker, W. W., "Some general results on the optimal ramp , control problem," Transportation Research. -C, 4, 1996, 51-69.
4. Helleland, N., Joeppen, W., and Reichelt, P., "Die Rampendosierung an der A5 Bonn/Siegburg der BAB 3 in Richtung Koln," Strassenverkehrstechnik, 22, 1978 .44-51,
5. NN: Ramp Metering in Auckland, Traffic Engineering and Control, 24, 1983, 552-553.
6. Zachmanoglou, E. C., and Thoe, D. W., Introduction to Partial Differential Equations with Applications, Dover, 1986.
7. Logan, J. D., An Introduction to Nonlinear Partial Differential Equations, John Wiley, 1994.

Chapter 9

FEEDBACK CONTROL DESIGN USING THE ODE MODEL

This chapter uses the ordinary differential equation (ODE) model of the ramp system for designing feedback control laws. We will design feedback control laws for isolated ramp metering problems, isolated with mixed sensitivity, and coordinated with and without mixed sensitivity. Software and simulation results will also be presented.

1. MATHEMATICAL MODEL

The basic model used for the design of the feedback control law is presented below. In this model, we consider only one section of the mainline highway that is connected to the entrance ramp.

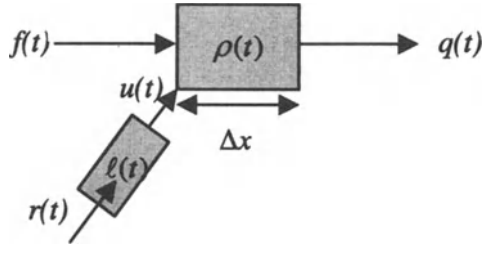

Figure 9-1: Ramp System

P. Kachroo et al., *Feedback Ramp Metering in Intelligent Transportation Systems*

In time Δt, the traffic density of the section of length Δx changes from $\rho(t)$ to $\rho(t+\Delta t)$. This change is caused by the effective inflow into the section. The effective inflow is given by the sum of the highway and ramp inflows after removing the outflow from the sum. This relationship in an equation form is given as

$$\rho(t+\Delta t)-\rho(t)=\Delta t\frac{(-q(t)+u+f(t))}{\Delta x} \tag{1}$$

Taking the infinitesimal time on the left-hand side and taking limits gives us

$$Lt_{\Delta t\to\infty}\frac{\rho(t+\Delta t)-\rho(t)}{\Delta t}=\frac{(-q(t)+u+f(t))}{\Delta x} \tag{2}$$

This can be expressed as the following ordinary differential equation:

$$\dot{\rho}=\frac{d\rho(t)}{dt}=\frac{1}{\Delta x}(-q(t)+u+f(t)) \tag{3}$$

The ramp dynamics are given as

$$\dot{\ell}=r(t)-u(t) \tag{4}$$

Combining (3) and (4), we can write the overall system dynamics as

$$\text{Dynamics: }\begin{cases}\dot{\rho}=\dfrac{d\rho(t)}{dt}=\dfrac{1}{\Delta x}(-q(t)+u+f(t))\\ \dot{\ell}=r(t)-u(t)\end{cases} \tag{5}$$

$$\text{Initial Conditions: }\begin{cases}\rho(0)=\rho_0\\ \ell(0)=\ell_0\end{cases} \tag{6}$$

The flow relationship is

$$q(t)=\rho(t)v(t) \tag{7}$$

We will take the velocity relationship as

$$v(t) = v_f(1 - \frac{\rho(t)}{\rho_{\max}}) \tag{8}$$

For simulation experiments, the model of the system will use the following diffusion relationship, for some examples:

$$v(t) = v_f[1 - \frac{\rho(t)}{\rho_{\max}}] - D[\frac{\partial \rho}{\partial x}]/\rho(t) \tag{9}$$

Of course, now since we have ODEs, we do not have any dependence of the density on the spatial coordinate. Therefore, (9) will be rewritten appropriately as

$$v = v_f[1 - \frac{\rho(t)}{\rho_{\max}}] - D[\frac{\rho_d(t) - \rho(t)}{\Delta x}]/\rho(t) \tag{10}$$

Here $\rho_d(t)$ refers to the traffic density of the section downstream to the main one.

2. CONTROL OBJECTIVE

The objective of a feedback control design is to make the error variable go to zero. That is,

$$\underset{t\to\infty}{Lt}\ e(t) = 0 \tag{11}$$

This can be achieved by designing control laws that make the system follow the closed-loop dynamics

$$\dot{e}(t) + k_1 e(t) + k_2 \int_0^t e(s)ds = 0 \tag{12}$$

We can come up with the appropriate form of the error $e(t)$ for different problems. The following are some of the ways we can design the error variable:

Control Objective 1 $e(t) = \rho(t) - \rho_c$ (13)

Control Objective 2 $e(t) = \mid \rho(t) - \rho_c \mid$ (14)

Control Objective 3 $e(t) = \frac{1}{2}(\rho(t) - \rho_c)^2$ (15)

Control Objective 4 $e(t) = \frac{w_1}{2}(\rho(t) - \rho_c)^2 + w_2 \ell$ (16)

Control Objective 5 $e(t) = w_1 \mid \rho(t) - \rho_c \mid + w_2 \ell$ (17)

We can also use optimal control-based principles to design a feedback law. We will show an example of this later. Now, we will design feedback control laws using control objectives 1, 4, and 5. Notice that control objectives 2 and 3 can be obtained by 4 and 5 by taking weight values to be 1 and 0 on the first and second terms, respectively.

3. CONTROL DESIGN

We will develop different control laws based on three control objectives from the previous section.

3.1 Control Objective 1

We start our feedback control design by differentiating the error equation (13):

$$\dot{e}(t) = \dot{\rho}(t) \tag{18}$$

Using the dynamics (5) here, we get

$$\dot{e}(t) = \frac{1}{\Delta x}(-q(t) + u + f(t)) \tag{19}$$

In order to obtain (12), we design the control law as

$$u = q(t) - f(t) - k_1 \Delta x e(t) - k_2 \Delta x \int_0^t e(s)ds \tag{20}$$

Substituting (20) in (19) satisfies the desired dynamics (12).

3.1.1 Comparison with Wattleworth Model

The control law that Wattleworth proposes [1] for ramp metering is given by

$$u = q(t) - f(t) \tag{21}$$

The dynamics of the traffic density as in (3) are

$$\dot{\rho} = \frac{1}{\Delta x}(-q(t) + u + f(t)) \tag{22}$$

If we substitute (21) in (22) we get

$$\dot{\rho} = 0 \tag{23}$$

which is a steady-state condition. Therefore, the Wattleworth control law is based on steady-state analysis of the system and is not designed for handling transients. If the system is operating at the critical density and we apply any of the two controllers, the result is the same. However, even a small change from that value can have a bad effect on the system controlled by the Wattleworth controller.

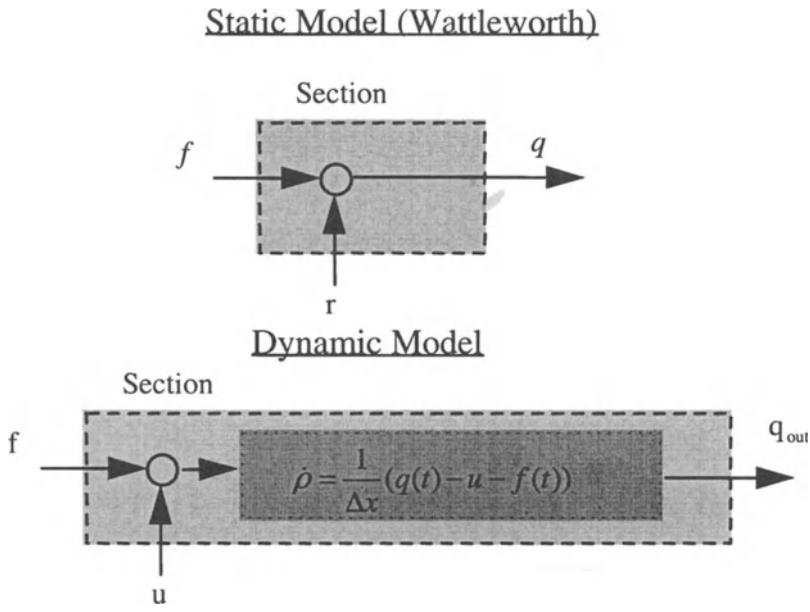

Figure 9-2: Comparison with Wattleworth Model

3.1.2 Comparison with ALINEA Model

The control law used in the ALINEA model is

$$u(k) = u(k-1) + ke(k) \tag{24}$$

where the error variable is given by (13). As we can see, this control law is based on a discrete time model of the system. It is also designed after linearization of the system dynamics, as compared to feedback linearization that we have used. Feedback linearization is a global technique and is valid for any region of operation, whereas linearization technique is guaranteed to work only near the equilibrium around which it has been linearized.

We can also come up with another interpretation of the ALINEA control law. It can be obtained as follows. We can rewrite (24) as

$$u(k) - u(k-1) = ke(k) \tag{25}$$

Dividing both sides by sampling time and taking limits as shown below

$$Lt_{\Delta t \to 0} \frac{u(k) - u(k-1)}{\Delta t} = Lt_{\Delta t \to 0} \frac{ke(k)}{\Delta t} \tag{26}$$

gives

$$\dot{u}(t) = Ke(t) \tag{27}$$

Here, the gain K satisfies

$$K = Lt_{\Delta t \to 0} \frac{k(\Delta t)}{\Delta t} \tag{28}$$

We can obtain the control law formula by integrating (27):

$$u = K \int_0^t e(s)ds \tag{29}$$

This shows that ALINEA actually uses only the integral term of the control law (20) we have designed, and essentially as an integral control law.

3.2 Control Objective 4

We start our feedback control design by differentiating the error equation (16):

$$\dot{e}(t) = w_1 \dot{\rho}(t)(\rho(t) - \rho_c) + w_2 \dot{\ell} \tag{30}$$

Using the dynamics (5) here, we get

$$\dot{e}(t) = w_1 \frac{1}{\Delta x}(-q(t) + u + f(t))(\rho(t) - \rho_c) + w_2(r(t) - u) \tag{31}$$

Collecting terms on the right-hand side gives

$$\dot{e}(t) = w_1 \frac{1}{\Delta x}(-q(t) + f(t))(\rho(t) - \rho_c) + w_2 r(t) + (w_1 \frac{1}{\Delta x}(\rho(t) - \rho_c) - w_2)u \tag{32}$$

This differential equation can be written cleanly in the following form:

$$\dot{e}(t) = F + Gu \tag{33}$$

where

$$F = w_1 \frac{1}{\Delta x}(-q(t) + f(t))(\rho(t) - \rho_c) + w_2 r(t) \tag{34}$$

and

$$G = (w_1 \frac{1}{\Delta x}(\rho(t) - \rho_c) - w_2) \tag{35}$$

In order to obtain (12), we design the control law as

$$u = G^{-1}[-F - k_1 e(t) - k_2 \int_0^t e(s)ds] \tag{36}$$

Substituting (36) in (33) satisfies the desired dynamics (12).

3.3 Control Objective 5

We start our feedback control design by differentiating the error equation (22). The system can be in two regions. One region is where the traffic density is greater than the critical density. The other region is where the traffic density is equal to or less than the critical density. We present these two regions in different sections below.

3.3.1 Region 1

In this region, the traffic density is greater than the critical density. The error in this region is equal to

$$e(t) = w_1(\rho(t) - \rho_c) + w_2\ell \tag{37}$$

Differentiating (37) we get

$$\dot{e}(t) = w_1\dot{\rho}(t) + w_2\dot{\ell} \tag{38}$$

Using the dynamics (5) here, we get

$$\dot{e}(t) = w_1\frac{1}{\Delta x}(-q(t) + u + f(t)) + w_2(r(t) - u) \tag{39}$$

Collecting terms on the right-hand side gives

$$\dot{e}(t) = w_1\frac{1}{\Delta x}(-q(t) + f(t)) + w_2 r(t) + (w_1\frac{1}{\Delta x} - w_2)u \tag{40}$$

This differential equation can be written cleanly in the following form:

$$\dot{e}(t) = F + Gu \tag{41}$$

where

$$F = w_1\frac{1}{\Delta x}(-q(t) + f(t)) + w_2 r(t) \tag{42}$$

and

$$G = (w_1\frac{1}{\Delta x} - w_2) \tag{43}$$

In order to obtain (12) in this region, we design the control law as

$$u = G^{-1}[-F - k_1 e(t) - k_2 \int_0^t e(s)ds] \tag{44}$$

Substituting (44) in (41) satisfies the desired dynamics (12) in this region.

3.3.2 Region 2

In this region, the traffic density is less than or equal to the critical density. The error in this region is equal to

$$e(t) = -w_1(\rho(t) - \rho_c) + w_2 \ell \tag{45}$$

Differentiating (45) we get

$$\dot{e}(t) = -w_1 \dot{\rho}(t) + w_2 \dot{\ell} \tag{46}$$

Using the dynamics (5) here, we get

$$\dot{e}(t) = -w_1 \frac{1}{\Delta x}(-q(t) + u + f(t)) + w_2(r(t) - u) \tag{47}$$

Collecting terms on the right-hand side gives

$$\dot{e}(t) = -w_1 \frac{1}{\Delta x}(-q(t) + f(t)) + w_2 r(t) + (-w_1 \frac{1}{\Delta x} - w_2)u \tag{48}$$

This differential equation can be written cleanly in the following form:

$$\dot{e}(t) = F + Gu \tag{49}$$

where

$$F = -w_1 \frac{1}{\Delta x}(-q(t) + f(t)) + w_2 r(t) \tag{50}$$

and

$$G = -w_1 \frac{1}{\Delta x} - w_2 \tag{51}$$

In order to obtain (12) in this region, we design the control law as

$$u = G^{-1}[-F - k_1 e(t) - k_2 \int_0^t e(s)ds] \tag{52}$$

Substituting (52) in (49) satisfies the desired dynamics (12) in this region.

3.3.3 Overall Control

We can combine the previous two subsections to come up with a control law that is applicable in both regions. The overall control law for control objective 5 is therefore given by

$$u = G^{-1}[-F - k_1 e(t) - k_2 \int_0^t e(s)ds] \tag{53}$$

where

$$F = sign(\rho(t) - \rho_c) w_1 \frac{1}{\Delta x}(-q(t) + f(t)) + w_2 r(t) \tag{54}$$

and

$$G = sign(\rho(t) - \rho_c) w_1 \frac{1}{\Delta x} - w_2 \tag{55}$$

4. SOFTWARE AND SIMULATION RESULTS

We will present the software and the simulation results for control-1 here. Simulation files for this control are presented below.

```
The simulation files for control-1 (20) are given below.
% Ramp Metering Code
clear;
```

```
clf;
clc;

global rhom rhoc vf lmax Dx k1 k2 n rmax Diff ie

% Input Parameters

Dx=1;
k1=15.25;
k2=0.15;

rhom = 60;                    % Jam density
rhoc = rhom/2;                % Critical density
vf = 15;                          % freeflow velocity
lmax = 200;
Diff=0.0;

t0 = 0.0;
tf = 20;
h = 0.01;
m = (tf-t0)/h;
n = 3;                        % number of sections
rho=ones(m,n).*15;            % X array m rows, length
state columns
T=zeros(m,1);              % T array m rows (mx1)
L=[1:1:n]';
T(1)=t0;
l(1)=0;
ie=0;

rvar(1)=oder(1,l(1));
uvar(1)=odeu(1,rho(1,:),l(1),rvar(1));
fvar(1)=odef(1);
evar(1)=rho(1,1)-rhoc;

%There are m-1 steps and m points maximum
for i=1:m-1;
   clc
   T(i)
   T(i+1)=t0 + h*i;
   flag=0;
   qin=vf*(rho(i,n-1)*(1-rho(i,n-
1)/rhom))+Diff*(rho(i,n-1)-rho(i,n));
      if flag==0
         qout=vf*(rho(i,n)*(1-
```

```
rho(i,n)/rhom))+Diff*(rho(i,n-1)-rho(i,n));
      else
         qout=0;
      end
        rhoinc=h*(qin-qout)/Dx;
      if rho(i,n)+rhoinc >=rhom
         rhoinc=rhom-rho(i,n);
         flag=1;
      else
         flag=0;
    end
    rho(i+1,n)=rho(i,n)+rhoinc;

   for j=n-1:-1:2
      qin=vf*(rho(i,j-1)*(1-rho(i,j-
1)/rhom))+Diff*(rho(i,j-1)-rho(i,j));
      if flag==0
         qout=vf*(rho(i,j)*(1-
rho(i,j)/rhom))+Diff*(rho(i,j)-rho(i,j+1));
      else
         qout=0;
      end
        rhoinc=h*(qin-qout)/Dx;
      if rho(i,j)+rhoinc >=rhom
         rhoinc=rhom-rho(i,j);
         flag=1;
      else
         flag=0;
    end
    rho(i+1,j)=rho(i,j)+rhoinc;
    end

   if flag==0
      qout=vf*(rho(i,1)*(1-
rho(i,1)/rhom))+Diff*(rho(i,1)-rho(i,2));
   else
      qout=0;
   end
   qin=odef(i)+uvar(i);
   rhoinc=h*(qin-qout)/Dx;
   if rho(i,1)+rhoinc>=rhom
      rhoinc=rhom-rho(i,1);
      fvar(i)=qout+Dx*rhoinc/h;;
   end
   rho(i+1,1)=rho(i,1)+rhoinc;
```

```
    l(i+1)=l(i)+h*(oder(i,l(i))-uvar(i));
    rvar(i+1)=oder(i+1,l(i+1));
    uvar(i+1)=odeu(i+1,rho(i+1,:),l(i+1),rvar(i+1));
    fvar(i+1)=odef(i+1);
    evar(i+1)=rho(i+1,1)-rhoc;
end
```

Figure 9-3: File odemixedramp.m

Notice that this file performs the simulation for three sections and includes the code for all the projection scenarios. We track only one section for the model we have chosen in this chapter.

```
function odeu = odeu(t,x,l,r)

global rhom rhoc vf lmax Dx k1 k2 n rmax Diff ie

e=x(1)-rhoc;
ie=ie+e;
q=vf*x(1)*(1-(x(1)/rhoc));
F=q-odef(t);
odeu=F-k1*e-k2*ie; % ramp outflow

if l<=0
   if r<odeu
      odeu = r;
   end
end
if x(1)>=rhom
   odeu = 0;
end
if odeu<0
   odeu=0;
end
```

Figure 9-4: File odeu.m

```
subplot(221);
plot(T,rho(:,1));
title('Mainline Traffic Density');
xlabel('Time');

subplot(222);
plot(T,rvar,'-',T,fvar,'-.');
title('Ramp and Highway Inflow');
xlabel('Time');
```

```
subplot(223);
plot(T,evar);
title('Error Variable');
xlabel('Time');

subplot(224);
plot(T,uvar);
title('Control Rampflow');
xlabel('Time');
```

Figure 9-5: File draw.m

```
function oder = oder(t,l)
global lmax
if l<lmax
   oder = 40*(1.0+0.2*sin(0.001*t));      % ramp inflow
else
   oder = 0;
end;
```

Figure 9-6: File oder.m

```
function odef = odef(t)
if t>75 & t<150
   odef = 185*(1.0+0.2*sin(0.0025*t));
else
   odef = 175*(1.0+0.2*sin(0.0025*t));
end
```

Figure 9-7: File odef.m

Simulation results using this control and the ODE model are excellent and are presented below.

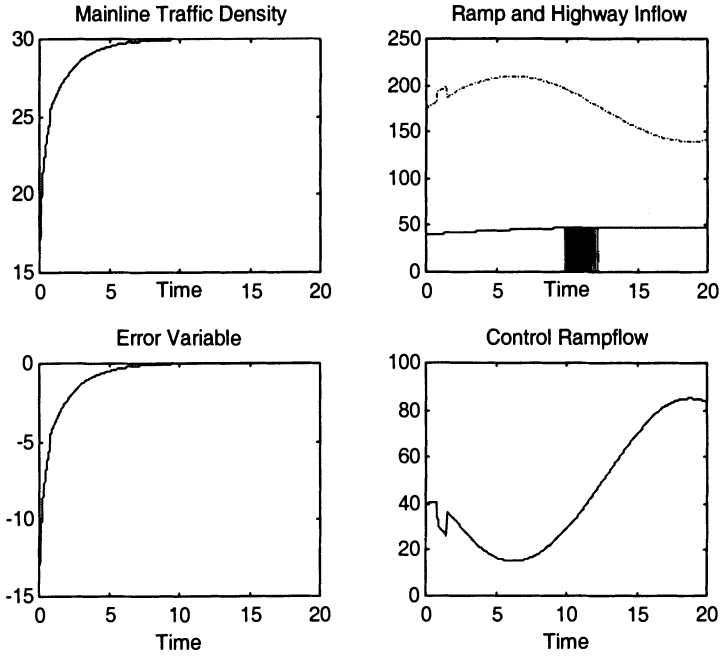

Figure 9-8: Simulation Results Using Control-1

5. COORDINATED RAMP CONTROL IN ODE SETTING

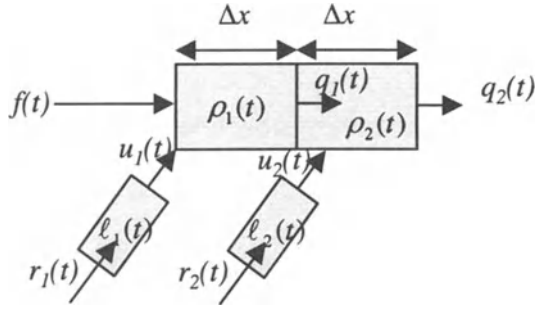

Consider the coordinated ramp metering problem as shown in Figure 9-9

Figure 9-9: Coordinated Ramp Metering in ODE Setting

5.1 Dynamics

The dynamics of this system are given by

$$\text{Dynamics: } \begin{cases} \dot{\rho}_1 = \dfrac{1}{\Delta x}(-q_1(t) + u_1 + f(t)) \\ \dot{\ell}_1 = r_1(t) - u_1(t) \\ \dot{\rho}_2 = \dfrac{1}{\Delta x}(-q_2(t) + u_2 + q_1(t)) \\ \dot{\ell}_2 = r_2(t) - u_2(t) \end{cases} \tag{56}$$

$$\text{Initial Conditions: } \begin{cases} \rho_1(0) = \rho_{10}, \rho_2(0) = \rho_{20} \\ \ell_1(0) = \ell_{10}, \ell_2(0) = \ell_{20} \end{cases} \tag{57}$$

The flow relationships are

$$q_i(t) = \rho_i(t) v_i(t), \quad i = 1,2 \tag{58}$$

We will take velocity relationships as

$$v_i(t) = v_f\left(1 - \frac{\rho_i(t)}{\rho_{\max}}\right) \tag{59}$$

5.2 Control Design

Let us take the control objective as (11), where the error variable is defined as

$$e(t) = w_1 \mid \rho_1(t) - \rho_c \mid + w_2 \ell_1 + w_3 \mid \rho_2(t) - \rho_c \mid + w_4 \ell_2 \tag{60}$$

We design for integral closed-loop dynamics (12) or the following:

$$\dot{e}(t) + k_1 e(t) = 0 \tag{61}$$

Equation (61) guarantees (11). We start our feedback control design by differentiating the error equation (60). The system can be in four regions. We present these four regions in different sections below.

5.2.1 Region 1

In this region, the traffic density of both sections is greater than the critical density. The error in this region is equal to

$$e(t) = w_1(\rho_1(t) - \rho_c) + w_2\ell_1 + w_3(\rho_2(t) - \rho_c) + w_4\ell_2 \tag{62}$$

Differentiating (62) we get

$$\dot{e}(t) = w_1\dot{\rho}_1(t) + w_2\dot{\ell}_1 + w_3\dot{\rho}_2(t) + w_4\dot{\ell}_2 \tag{63}$$

Using the dynamics (56) here, we get

$$\begin{aligned}\dot{e}(t) &= w_1\frac{1}{\Delta x}(-q_1(t) + u_1 + f(t)) + w_2(r_1(t) - u_1) \\ &+ w_3\frac{1}{\Delta x}(-q_2(t) + u_2 + q_1(t)) + w_4(r_2(t) - u_2)\end{aligned} \tag{64}$$

Collecting terms on the right-hand side gives

$$\begin{aligned}\dot{e}(t) &= w_1\frac{1}{\Delta x}(-q_1(t) + f(t)) + w_2r_1(t) + (w_1\frac{1}{\Delta x} - w_2)u_1 \\ &+ w_3\frac{1}{\Delta x}(-q_2(t) + q_1(t)) + w_4r_2(t) + (w_3\frac{1}{\Delta x} - w_4)u_2\end{aligned} \tag{65}$$

This differential equation can be written cleanly in the following form:

$$\dot{e}(t) = F + u \tag{66}$$

where

$$F = w_1 \frac{1}{\Delta x}(-q_1(t) + f(t)) + w_2 r_1(t) + w_3 \frac{1}{\Delta x}(-q_2(t) + q_1(t)) + w_4 r_2(t) \tag{67}$$

and

$$u = (w_1 \frac{1}{\Delta x} - \dot{w}_2)u_1 + (w_3 \frac{1}{\Delta x} - w_4)u_2 \tag{68}$$

In order to obtain (61) in this region, we design the control law as

$$u = -F - k_1 e(t) \tag{69}$$

Substituting (69) in (66) satisfies the desired dynamics (61) in this region.

5.2.2 Region 2

In this region, the traffic density in both sections is less than or equal to the critical density. The error in this region is equal to

$$e(t) = -w_1(\rho_1(t) - \rho_c) + w_2 \ell_1 - w_3(\rho_2(t) - \rho_c) + w_4 \ell_2 \tag{70}$$

Differentiating (70) we get

$$\dot{e}(t) = -w_1 \dot{\rho}_1(t) + w_2 \dot{\ell}_1 - w_3 \dot{\rho}_2(t) + w_4 \dot{\ell}_2 \tag{71}$$

Using the dynamics (56) here, we get

$$\dot{e}(t) = -w_1 \frac{1}{\Delta x}(-q_1(t) + u_1 + f(t)) + w_2(r_1(t) - u_1) - w_3 \frac{1}{\Delta x}(-q_2(t) + u_2 + q_1(t)) + w_4(r_2(t) - u_2) \tag{72}$$

Collecting terms on the right-hand side gives

$$\dot{e}(t) = -w_1 \frac{1}{\Delta x}(-q_1(t) + f(t)) + w_2 r_1(t) + (-w_1 \frac{1}{\Delta x} - w_2)u_1$$
$$- w_3 \frac{1}{\Delta x}(-q_2(t) + q_1(t)) + w_4 r_2(t) + (-w_3 \frac{1}{\Delta x} - w_4)u_2 \tag{73}$$

This differential equation can be written cleanly in the following form.

$$\dot{e}(t) = F + u \tag{74}$$

where

$$F = -w_1 \frac{1}{\Delta x}(-q_1(t) + f(t)) + w_2 r_1(t)$$
$$- w_3 \frac{1}{\Delta x}(-q_2(t) + q_1(t)) + w_4 r_2(t) \tag{75}$$

and

$$u = (-w_1 \frac{1}{\Delta x} - w_2)u_1 + (-w_3 \frac{1}{\Delta x} - w_4)u_2 \tag{76}$$

In order to obtain (61) in this region, we design the control law as

$$u = -F - k_1 e(t) \tag{77}$$

Substituting (77) in (74) satisfies the desired dynamics (12)in this region.

5.2.3 Region 3

In this region, the traffic density of the first section is greater than the critical density and it is less in the second section. The error in this region is equal to

$$e(t) = w_1(\rho_1(t) - \rho_c) + w_2 \ell_1 - w_3(\rho_2(t) - \rho_c) + w_4 \ell_2 \tag{78}$$

Differentiating (78) we get

$$\dot{e}(t) = w_1 \dot{\rho}_1(t) + w_2 \dot{\ell}_1 - w_3 \dot{\rho}_2(t) + w_4 \dot{\ell}_2 \tag{79}$$

Using the dynamics (56) here, we get

$$\begin{aligned}\dot{e}(t) &= w_1 \frac{1}{\Delta x}(-q_1(t) + u_1 + f(t)) + w_2(r_1(t) - u_1) \\ &- w_3 \frac{1}{\Delta x}(-q_2(t) + u_2 + q_1(t)) + w_4(r_2(t) - u_2)\end{aligned} \tag{80}$$

Collecting terms on the right-hand side gives

$$\begin{aligned}\dot{e}(t) &= w_1 \frac{1}{\Delta x}(-q_1(t) + f(t)) + w_2 r_1(t) + (w_1 \frac{1}{\Delta x} - w_2)u_1 \\ &- w_3 \frac{1}{\Delta x}(-q_2(t) + q_1(t)) + w_4 r_2(t) + (-w_3 \frac{1}{\Delta x} - w_4)u_2\end{aligned} \tag{81}$$

This differential equation can be written cleanly in the following form:

$$\dot{e}(t) = F + u \tag{82}$$

where

$$\begin{aligned}F &= w_1 \frac{1}{\Delta x}(-q_1(t) + f(t)) + w_2 r_1(t) \\ &- w_3 \frac{1}{\Delta x}(-q_2(t) + q_1(t)) + w_4 r_2(t)\end{aligned} \tag{83}$$

and

$$u = (w_1 \frac{1}{\Delta x} - w_2)u_1 + (-w_3 \frac{1}{\Delta x} - w_4)u_2 \tag{84}$$

In order to obtain (61) in this region, we design the control law as

$$u = -F - k_1 e(t) \tag{85}$$

Substituting (85) in (82) satisfies the desired dynamics (61) in this region.

5.2.4 Region 4

In this region, the traffic density in the first section is less than or equal to the critical density and greater in the second section. The error in this region is equal to

$$e(t) = -w_1(\rho_1(t) - \rho_c) + w_2\ell_1 + w_3(\rho_2(t) - \rho_c) + w_4\ell_2 \tag{86}$$

Differentiating (86) we get

$$\dot{e}(t) = -w_1\dot{\rho}_1(t) + w_2\dot{\ell}_1 + w_3\dot{\rho}_2(t) + w_4\dot{\ell}_2 \tag{87}$$

Using the dynamics (56) here, we get

$$\begin{aligned}\dot{e}(t) &= -w_1\frac{1}{\Delta x}(-q_1(t) + u_1 + f(t)) + w_2(r_1(t) - u_1) \\ &+ w_3\frac{1}{\Delta x}(-q_2(t) + u_2 + q_1(t)) + w_4(r_2(t) - u_2)\end{aligned} \tag{88}$$

Collecting terms on the right-hand side gives

$$\begin{aligned}\dot{e}(t) &= -w_1\frac{1}{\Delta x}(-q_1(t) + f(t)) + w_2r_1(t) + (-w_1\frac{1}{\Delta x} - w_2)u_1 \\ &+ w_3\frac{1}{\Delta x}(-q_2(t) + q_1(t)) + w_4r_2(t) + (w_3\frac{1}{\Delta x} - w_4)u_2\end{aligned} \tag{89}$$

This differential equation can be written cleanly in the following form:

$$\dot{e}(t) = F + u \tag{90}$$

where

$$\begin{aligned}F &= -w_1\frac{1}{\Delta x}(-q_1(t) + f(t)) + w_2r_1(t) \\ &+ w_3\frac{1}{\Delta x}(-q_2(t) + q_1(t)) + w_4r_2(t)\end{aligned} \tag{91}$$

and

$$u = (-w_1 \frac{1}{\Delta x} - w_2)u_1 + (w_3 \frac{1}{\Delta x} - w_4)u_2 \tag{92}$$

In order to obtain (61) in this region, we design the control law as

$$u = -F - k_1 e(t) \tag{93}$$

Substituting (93) in (90) satisfies the desired dynamics (61) in this region.

5.2.5 Overall Control

We can combine the previous four subsections to come up with a control law that is applicable in all four regions. The overall control law for the coordinated ramp problem is therefore given by

$$u = -F - k_1 e(t) \tag{94}$$

where

$$\begin{aligned} F = & sign(\rho_1(t) - \rho_c) w_1 \frac{1}{\Delta x}(-q_1(t) + f(t)) + w_2 r_1(t) \\ & + sign(\rho_2(t) - \rho_c) w_3 \frac{1}{\Delta x}(-q_2(t) + q_1(t)) + w_4 r_2(t) \end{aligned} \tag{95}$$

and

$$\begin{aligned} u = & (sign(\rho_1(t) - \rho_c) w_1 \frac{1}{\Delta x} - w_2)u_1 \\ & + (sign(\rho_1(t) - \rho_c) w_3 \frac{1}{\Delta x} - w_4)u_2 \end{aligned} \tag{96}$$

Actually (96) does not give the control laws but it gives the condition the control variables should satisfy. We can design the control laws in a decoupled way or coupled way.

5.2.5.1 Decoupled Control

Let us rewrite (95) as

$$F = F_1 + F_2 \tag{97}$$

where

$$F_1 = sign(\rho_1(t) - \rho_c) w_1 \frac{1}{\Delta x}(-q_1(t) + f(t)) + w_2 r_1(t) \tag{98}$$

and

$$F_2 = sign(\rho_2(t) - \rho_c) w_3 \frac{1}{\Delta x}(-q_2(t) + q_1(t)) + w_4 r_2(t) \tag{99}$$

Now, using (96), we can derive the decoupled control laws as

$$u_1 = G^{-1}(-F_1 - k_1 e_1(t)) \tag{100}$$

and

$$u_2 = G^{-1}(-F_2 - k_1 e_2(t)) \tag{101}$$

where

$$e(t) = e_1(t) + e_2(t) \tag{102}$$

The error terms are defined as

$$e_1(t) = w_1 \mid \rho_1(t) - \rho_c \mid + w_2 \ell_1 \tag{103}$$

and

$$e_2(t) = w_3 \mid \rho_2(t) - \rho_c \mid + w_4 \ell_2 \tag{104}$$

We get the following two decoupled closed loop dynamics by the application of (100) and (101):

$$\dot{e}_1(t) + k_1 e_1(t) = 0 \tag{105}$$

and

$$\dot{e}_2(t) + k_1 e_2(t) = 0 \tag{106}$$

5.2.5.2 Coupled Control Laws

Using (94) and (96) we can distribute the control effort between the two variables as

$$\begin{aligned} -F - k_1 e(t) &= (sign(\rho_1(t) - \rho_c) w_1 \frac{1}{\Delta x} - w_2) u_1 \\ &+ (sign(\rho_1(t) - \rho_c) w_3 \frac{1}{\Delta x} - w_4) u_2 \end{aligned} \tag{107}$$

The distribution we will use in our simulation will be

$$0.65(-F - k_1 e(t)) = (sign(\rho_1(t) - \rho_c) w_1 \frac{1}{\Delta x} - w_2) u_1 \tag{108}$$

and

$$0.35(-F - k_1 e(t)) = (sign(\rho_1(t) - \rho_c) w_3 \frac{1}{\Delta x} - w_4) u_2 \tag{109}$$

Therefore, the coupled control laws are

$$u_1 = (sign(\rho_1(t) - \rho_c) w_1 \frac{1}{\Delta x} - w_2)^{-1} 0.65(-F - k_1 e(t)) \tag{110}$$

and

$$u_2 = (sign(\rho_1(t) - \rho_c) w_3 \frac{1}{\Delta x} - w_4)^{-1} 0.35(-F - k_1 e(t)) \tag{111}$$

5.3 Simulation Files

In the simulations we will use software that allows us to simulate unmixed decoupled ramp feedback control systems, mixed decoupled ramp feedback control systems, and mixed coupled ramp feedback control

systems. The software also uses a different way to provide projections. The software is presented below.

```
% Ramp Metering Code
clear;
clf;
clc;
global rhom rhoc vf gain1 gain2 c w1 w2 w3 w4 l cgain1 cgain2
ccgain

% Input Parameters
c=input('unmixed(1) or mixed(2) or coupled(3)= ');

gain1=0.4;
gain2=0.4;
cgain1=0.1;
cgain2=0.1;
ccgain=0.25;

w1=0.75;
w2=0.25;
w3=0.75;
w4=0.25;
l=1;

rhom = 60;                      % Jam density
rhoc = rhom/2;                  % Critical density
vf = 15;                        % freeflow velocity
t0 = 0.0;
tf = 15;
h = 0.01;
m = (tf-t0)/h;
x0=[35 5 32 4];
T=zeros(m,1);            % T array m rows (mx1)
X=zeros(m,length(x0));  % X array m rows, length state columns
T(1)=t0;
f1(1)=f1coord(t0);
r1(1)=r1coord(t0);
r2(1)=r2coord(t0);
uvar1(1)=u1(t0,x0);
uvar2(1)=u2(t0,x0);
X(1,:)=x0;
%There are m-1 steps and m points maximum
for I=1:m-1;
   tI=T(I);
   clc;
```

```
  tI
  xI=X(I,:);
  k1=h*feval('rampcoorddynamics',tI,xI)';
  k2=h*feval('rampcoorddynamics',tI+h/2,xI+k1/2)';
  k3=h*feval('rampcoorddynamics',tI+h/2,xI+k2/2)';
  k4=h*feval('rampcoorddynamics',tI+h,xI+k3)';
  X(I+1,:)=xI+(k1+2*k2+2*k3+k4)/6;
  T(I+1)=t0 + h*I;
  f1(I+1)=f1coord(T(I+1));
  r1(I+1)=r1coord(T(I+1));
  r2(I+1)=r2coord(T(I+1));
  uvar1(I+1)=u1(I+1,X(I+1,:));
  uvar2(I+1)=u2(I+1,X(I+1,:));

    if (X(I+1,2)<0),
        X(I+1,2)=0;
    end
    if (X(I+1,1)<0),
       X(I+1,1)=0;
    end
      if (X(I+1,1)>rhom),
        X(I+1,1)=rhom;
    end
    if (X(I+1,4)<0),
        X(I+1,4)=0;
    end
    if (X(I+1,3)<0),
       X(I+1,3)=0;
    end
      if (X(I+1,3)>rhom),
        X(I+1,3)=rhom;
    end
end
subplot(221);
plot(T,X(:,1),'-',T,X(:,3),'-.');
title('Traffic Density1 & Traffic Density2');
xlabel('Time');
subplot(222);
plot(T,X(:,2),'-',T,X(:,4),'-.');
title('Queue Length1 & Queue Length2');
xlabel('Time');
subplot(223);
plot(T,f1,'-',T,r1,'-.',T,r2,':');
title('Mainline Inflow & Ramp Inflows');
xlabel('Time');
```

```
subplot(224);
plot(T,uvar1,'-',T,uvar2,'-.');
title('Control1 & Control2 Variables');
xlabel('Time');
```

Figure 9-10: File runcoordramp.m

```
function u1 = u1(t,x)

global rhom vf rhoc gain1 w1 w2 w3 w4 c 1 cgain1 ccgain
v1=vf*(1-(x(1)/rhom));
qout1=v1*x(1);
if c == 1
   e=x(1)-rhoc;
   u1=max(0,qout1-f1coord(t)-gain1*e);
elseif c == 2
   ff1=-w1*qout1/1;
    d1=w1*f1coord(t)/1+w2*r1coord(t);
    g1=w1/1-w2;
    ff2=w1*qout1/1;
    d2=-f1coord(t)*w1/1+w2*r1coord(t);
    g2=-w1/1-w2;
    e=w1*abs(x(1)-rhoc)+w2*abs(x(2));

   if x(1)>=rhoc
      u1=max(0,(-ff1-d1-(1-cgain1)*e)/g1);
   else
      u1=max(0,(-ff2-d2-(1-cgain1)*e)/g2);
   end
else
   e=w1*abs(x(1)-rhoc)+w2*abs(x(2))+w3*abs(x(3)-
rhoc)+w2*abs(x(4));
   ff1=f1coord(t)-qout1;
   ff2=qout1-x(3)*vf*(1-(x(3)/rhom));
   ff=w1*ff1*sign(x(1)-rhoc)+w2*r1coord(t)+w3*ff2*sign(x(3)-
rhoc)+w4*r2coord(t);
   g1=w1*sign(x(1)-rhoc)-w2;
   u1=max(0,-0.35*(ff+ccgain*e)/g1);
end
```

Figure 9-11: File u1.m

```
function u2 = u2(t,x)

global rhom vf rhoc gain2 w1 w2 w3 w4 c 1 cgain2 ccgain
```

```
v1=vf*(1-(x(1)/rhom));
qout1=v1*x(1);
v2=vf*(1-(x(3)/rhom));
qout2=v2*x(3);
f1=x(1)*vf*(1-(x(1)/rhom));

if c == 1
   e=x(3)-rhoc;
   u2=max(0,qout2-f1-gain2*e);
elseif c == 2
   ff1=-w1*qout2/l;
    d1=w1*f1/l+w2*r2coord(t);
    g1=w1/l-w2;
    ff2=w1*qout2/l;
    d2=-f1*w1/l+w2*r2coord(t);
    g2=-w1/l-w2;
    e=w1*abs(x(3)-rhoc)+w2*abs(x(4));
   if x(3)>=rhoc
      u2=max(0,(-ff1-d1-(1-cgain2)*e)/g1);
   else
      u2=max(0,(-ff2-d2-(1-cgain2)*e)/g2);
   end
else
    e=w1*abs(x(1)-rhoc)+w2*abs(x(2))+w3*abs(x(3)-
rhoc)+w2*abs(x(4));
   ff1=f1coord(t)-qout1;
   ff2=qout1-x(3)*vf*(1-(x(3)/rhom));
   ff=w1*ff1*sign(x(1)-rhoc)+w2*r1coord(t)+w3*ff2*sign(x(3)-
rhoc)+w4*r2coord(t);
   g2=w1*sign(x(3)-rhoc)-w2;
   u2=max(0,-0.65*(ff+ccgain*e)/g2);
end
```

Figure 9-12: File u2.m

```
function r1coord = r1coord(t)
r1coord = 10*(1.5+sin(0.5*t)); % ramp1 inflow
```

Figure 9-13: File r1coord.m

```
function r2coord = r2coord(t)
r2coord = 10*(1.5+sin(0.5*t)); % ramp2 inflow
```

Figure 9-14: File r2coord.m

```
function f1coord = f1coord(t)
```

```
f1coord = 30*(1.25+sin(1.0*t));% mainline inflow
```

Figure 9-15: File f1coord.m

```
function dy = rampdynamics(t,y)
dy = zeros(4,1);                                    % a column
vector
global rhom vf l
%closed loop dynamics

dy(1) = (-vf*y(1)*(1-(y(1)/rhom))+f1coord(t)+u1(t,y))/l;
dy(2) = r1coord(t)-u1(t,y);
dy(3) = (-vf*y(3)*(1-(y(3)/rhom))+vf*y(1)*(1-
(y(1)/rhom))+u2(t,y))/l;
dy(4) = r2coord(t)-u2(t,y);
```

Figure 9-16: File rampdynamics.m

We are using the Runga Kutta algorithm to solve the ODE numerically. Details of this algorithm can be obtained from any book on numerical methods [3-5].

5.4 Simulation Results

Simulation results for the three cases- unmixed decoupled ramp feedback control systems, mixed de-coupled ramp feedback control systems, and mixed coupled ramp feedback control systems are presented below.

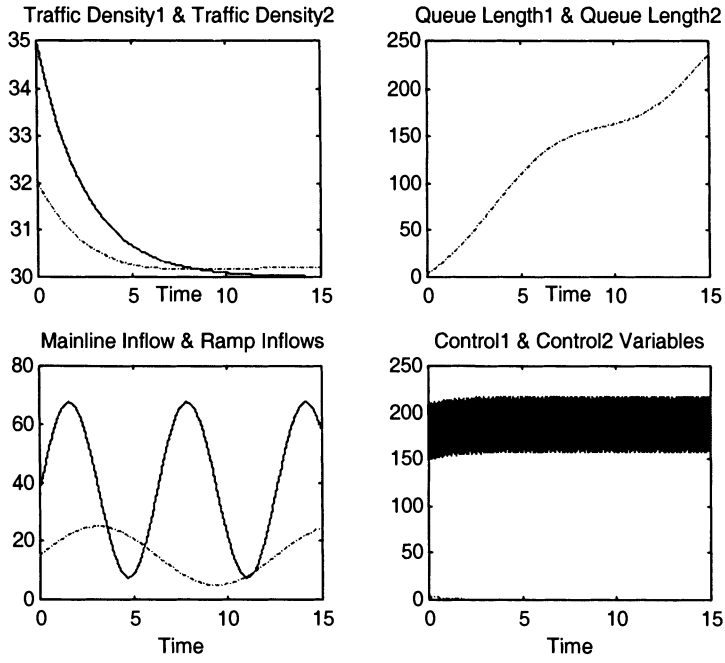

Figure 9-17: Simulation Results for Unmixed Decoupled Case

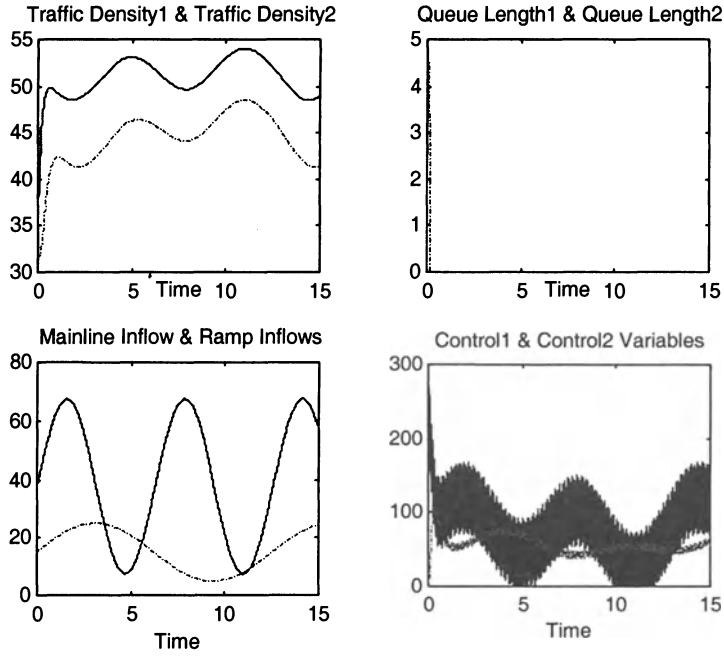

Figure 9-18: Simulation Results for Mixed Decoupled Case

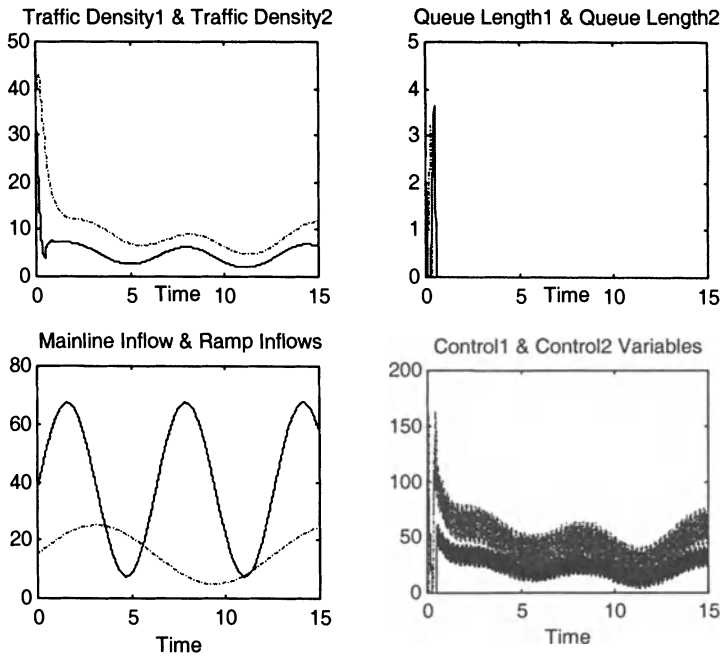

Figure 9-19: Simulation Results for Mixed Coupled Case

6. SUMMARY

In this chapter, we studied:

- The mathematical model for the ramp system in the ODE setting for various types of ramp metering control problems, such as isolated and coordinated problems, and with and without mixed sensitivity.
- Feedback control laws were designed for each type of problem.
- Simulations were performed to check the effectiveness of the feedback control laws.

7. QUESTIONS

1. State Wattleworth's control law for ramps. What are the limitations of the model? Compare it with the control derived in Section 3.1.

2. State the ALINEA model and its features.

8. PROBLEMS

1. Write your own simple MATLAB code for the Wattleworth model.
2. Write your own simple MATLAB code for the ALINEA model.
3. Write the MATLAB code for unmixed coupled ramp feedback control by making necessary changes in the code given in the chapter.

9. REFERENCES

1. Wattleworth, J. A, "System Demand Capacity Analysis on the Inbound Gulf Freeway," Texas Transportation Institute Reptort 24-8, 1964.
2. Papageorgiou, M., Habib, H. S., and Blosseville, J. M., "ALINEA: A Local Feedback Control Law for On-ramp Metering," Transportation Research Record, 1320, 1991,. 58-64.
3. Hilderbrand, F. B., *Introduction to Numerical Analysis*, Dover, 1987.
4. Hamming, R., *Numerical Methods for Scientists and Engineers*, Dover, 1987.
5. Isaacson, E., and Keller, H. B., *Analysis of Numerical Methods*, Dover, 1994.

Chapter 10

FEEDBACK CONTROL DESIGN USING THE FINITE DIFFERENCE MODEL

This chapter uses the finite difference equation model of the ramp system for designing feedback control laws. This model is obtained by time discretization of the ODE model. We will design feedback control laws for isolated ramp metering problems, isolated with mixed sensitivity, and coordinated with and without mixed sensitivity. Software and simulation results will also be presented.

1. FINITE DIFFERENCE MODEL

The finite difference model is obtained by time-discretizing the ODE model. The summary of the ODE model developed in the previous chapter is presented below:

$$\text{Dynamics: } \begin{cases} \dot{\rho} = \dfrac{1}{\Delta x}(-q(t) + u + f(t)) \\ \dot{\ell} = r(t) - u(t) \end{cases} \tag{1}$$

$$\text{Initial Conditions: } \begin{cases} \rho(0) = \rho_0 \\ \ell(0) = \ell_0 \end{cases} \tag{2}$$

The flow relationship is

P. Kachroo et al., *Feedback Ramp Metering in Intelligent Transportation Systems*

$$q(t) = \rho(t)v(t) \tag{3}$$

We will take the velocity relationship as

$$v(t) = v_f(1 - \frac{\rho(t)}{\rho_{\max}}) \tag{4}$$

By discretizing (1) in time we get the following difference equation dynamics with equations (2) to (4) still valid by replacing the time variable t by time instant k variable:

$$\text{Dynamics: } \begin{cases} \dfrac{\rho(k+1) - \rho(k)}{h} = \dfrac{1}{\Delta x}(-q(t) + u + f(t)) \\ \dfrac{\ell(k+1) - \ell(k)}{h} = r(t) - u(t) \end{cases} \tag{5}$$

In these equations, h is the sampling time. Now we can present the dynamics as

$$\text{Dynamics: } \begin{cases} \rho(k+1) = \rho(k) + \dfrac{h}{\Delta x}(-q(t) + u + f(t)) \\ \ell(k+1) = \ell(k) + h(r(t) - u(t)) \end{cases} \tag{6}$$

2. CONTROL OBJECTIVE

The objective of a feedback control design is to make the error variable go to zero. That is,

$$\lim_{k \to \infty} e(k) = 0 \tag{7}$$

This can be achieved by designing control laws that make the system follow the closed-loop dynamics

$$e(k+1) + Ke(k) = 0 \tag{8}$$

where

$$0 \leq K < 1 \tag{9}$$

We can see that (8) and (9) combined satisfy condition (7). We can come up with the appropriate form of the error $e(k)$ for different problems. The following are some of the ways we can design the error variable:

$$\text{Control Objective 1} \quad e(k) = \rho(k) - \rho_c \tag{10}$$

$$\text{Control Objective 2} \quad e(k) = | \rho(k) - \rho_c | \tag{11}$$

$$\text{Control Objective 3} \quad e(k) = w_1 | \rho(k) - \rho_c | + w_2 \ell \tag{12}$$

Now, we will design feedback control laws using control objectives 1 and 3. Control objective 2 can be obtained from 3 by using weights 1 and 0.

3. CONTROL DESIGN

We will develop different control laws based on two control objectives from the previous section.

3.1 Control Objective 1

We start our feedback control design by incrementing the error equation (10):

$$e(k+1) = \rho(k+1) - \rho_c \tag{13}$$

Using the dynamics (6) here, we get

$$e(k+1) = \rho(k) + \frac{h}{\Delta x}(-q(k) + u + f(k)) - \rho_c \tag{14}$$

In order to obtain (8), we design the control law as

$$u = q(k) - f(k) + \frac{\Delta x}{h}[\rho_c - \rho(k) - Ke(k)] \tag{15}$$

Substituting (15) in (14) satisfies the desired dynamics (8).

3.2 Control Objective 3

We start our feedback control design by incrementing the error equation (12). The system can be in two regions. One region is where the traffic density is greater than the critical density. The other region is where the traffic density is equal to or less than the critical density. We present these two regions in different sections below.

3.2.1 Region 1

In this region, the traffic density is greater than the critical density. The error in this region is equal to

$$e(k) = w_1(\rho(k) - \rho_c) + w_2\ell(k) \tag{16}$$

Incrementing (16) we get

$$e(k+1) = w_1(\rho(k+1) - \rho_c) + w_2\ell(k+1) \tag{17}$$

Using the dynamics (6) here, we get

$$\begin{aligned} e(k+1) &= w_1[\rho(k) - \rho_c + \frac{h}{\Delta x}(-q(k) + u + f(k))] \\ &+ w_2[\ell(k) + h(r(k) - u(t))] \end{aligned} \tag{18}$$

Collecting terms on the right-hand side gives

$$\begin{aligned} e(k+1) &= w_1[\rho(k) - \rho_c + \frac{h}{\Delta x}(-q(k) + f(k))] \\ &+ w_2[\ell(k) + hr(k)] + [w_1\frac{1}{\Delta x} - w_2]hu \end{aligned} \tag{19}$$

This difference equation can be written cleanly in the following form:

$$e(k+1) = F + Gu \tag{20}$$

where

$$F = w_1[\rho(k) - \rho_c + \frac{h}{\Delta x}(-q(k) + f(k))] + w_2[\ell(k) + hr(k)] \quad (21)$$

and

$$G = [w_1 \frac{1}{\Delta x} - w_2]h \quad (22)$$

In order to obtain (8) in this region, we design the control law as

$$u = G^{-1}[-F - Ke(k)] \quad (23)$$

Substituting (23) in (20) satisfies the desired dynamics (8) in this region.

3.2.2 Region 2

In this region, the traffic density is less than or equal to the critical density. The error in this region is equal to

$$e(k) = -w_1(\rho(k) - \rho_c) + w_2\ell(k) \quad (24)$$

Incrementing (24) we get

$$e(k+1) = -w_1(\rho(k+1) - \rho_c) + w_2\ell(k+1) \quad (25)$$

Using the dynamics (6) here, we get

$$\begin{aligned} e(k+1) &= -w_1[\rho(k) - \rho_c + \frac{h}{\Delta x}(-q(k) + u + f(k))] \\ &+ w_2[\ell(k) + h(r(k) - u(k))] \end{aligned} \quad (26)$$

Collecting terms on the right-hand side gives

$$e(k+1) = -w_1[\rho(k) - \rho_c + \frac{h}{\Delta x}(-q(k) + f(k))] + w_2[\ell(k) + hr(k)] + [-w_1 \frac{1}{\Delta x} - w_2]hu \quad (27)$$

This difference equation can be written cleanly in the following form:

$$e(k+1) = F + Gu \quad (28)$$

where

$$F = -w_1[\rho(k) - \rho_c + \frac{h}{\Delta x}(-q(k) + f(k))] + w_2[\ell(k) + hr(k)] \quad (29)$$

and

$$G = [-w_1 \frac{1}{\Delta x} - w_2]h \quad (30)$$

In order to obtain (8) in this region, we design the control law as

$$u = G^{-1}[-F - Ke(k)] \quad (31)$$

Substituting (31) in (28) satisfies the desired dynamics (8) in this region.

3.2.3 Overall Control

We can combine the previous two subsections to come up with a control law that is applicable in both regions. The overall control law therefore is given by

$$u = G^{-1}[-F - Ke(k)] \quad (32)$$

where

$$F = sign(\rho(k) - \rho_c)w_1[\rho(k) - \rho_c + \frac{h}{\Delta x}(-q(k) + f(k))] + w_2[\ell(k) + hr(k)] \quad (33)$$

and

$$G = [sign(\rho(k) - \rho_c)w_1 \frac{1}{\Delta x} - w_2]h \tag{34}$$

4. COORDINATED RAMP CONTROL IN ODE SETTING

The coordinated ramp metering control problem in the difference equation setting is obtained by discretizing the ODE dynamics of the same problem.

4.1 Dynamics

The ODE dynamics of this system are given by

$$\text{Dynamics: } \begin{cases} \dot{\rho}_1 = \dfrac{1}{\Delta x}(-q_1(t) + u_1 + f(t)) \\ \dot{\ell}_1 = r_1(t) - u_1(t) \\ \dot{\rho}_2 = \dfrac{1}{\Delta x}(-q_2(t) + u_2 + q_1(t)) \\ \dot{\ell}_2 = r_2(t) - u_2(t) \end{cases} \tag{35}$$

Discretizing (35) will give

$$\text{Dynamics: } \begin{cases} \rho_1(k+1) = \rho_1(k) + \dfrac{h}{\Delta x}(-q_1(t) + u_1 + f(t)) \\ \ell_1(k+1) = \ell_1(k) + h(r_1(t) - u_1(t)) \\ \rho_2(k+1) = \rho_2(k) + \dfrac{h}{\Delta x}(-q_2(t) + u_2 + q_1(t)) \\ \ell_1(k+1) = \ell_2(k) + h(r_2(t) - u_2(t)) \end{cases} \tag{36}$$

$$\text{Initial Conditions: } \begin{cases} \rho_1(0) = \rho_{10}, \rho_2(0) = \rho_{20} \\ \ell_1(0) = \ell_{10}, \ell_2(0) = \ell_{20} \end{cases} \tag{37}$$

The flow relationships are

$$q_i(k) = \rho_i(k) v_i(k), \quad i = 1,2 \tag{38}$$

We will take velocity relationships as

$$v_i(k) = v_f\left(1 - \frac{\rho_i(k)}{\rho_{\max}}\right) \tag{39}$$

4.2 Control Design

Let us take the control objective as (7), where the error variable is defined as

$$e(k) = w_1 \mid \rho_1(k) - \rho_c \mid + w_2 \ell_1 + w_3 \mid \rho_2(k) - \rho_c \mid + w_4 \ell_2 \tag{40}$$

We will design the control law to satisfy the closed-loop dynamics (8). We start our feedback control design by differencing the error equation (40). The system can be in four regions. We present these four regions in different sections below.

4.2.1 Region 1

In this region, the traffic density of both sections is greater than the critical density. The error in this region is equal to

$$e(k) = w_1(\rho_1(k) - \rho_c) + w_2 \ell_1 + w_3(\rho_2(k) - \rho_c) + w_4 \ell_2 \tag{41}$$

Incrementing (41) we get

$$\begin{aligned} e(k+1) &= w_1(\rho_1(k+1) - \rho_c) + w_2 \ell_1(k+1) \\ &+ w_3(\rho_2(k+1) - \rho_c) + w_4 \ell_2(k+1) \end{aligned} \tag{42}$$

Using the dynamics (6) here, we get

$$
\begin{aligned}
e(k+1) &= w_1[\rho_1(k) - \rho_c + \frac{h}{\Delta x}(-q_1(k) + u_1 + f(k))] \\
&+ w_2[\ell_1(k) + h(r_1(k) - u_1(k))] \\
&+ w_3[\rho_2(k) - \rho_c + \frac{h}{\Delta x}(-q_2(k) + u_2 + q_1(k))] \\
&+ w_4[\ell_2(k) + h(r_2(k) - u_2(k))]
\end{aligned}
\tag{43}
$$

Collecting terms on the right-hand side gives

$$
\begin{aligned}
e(k+1) &= w_1[\rho_1(k) - \rho_c + \frac{h}{\Delta x}(-q_1(k) + f(k))] \\
&+ w_2[\ell_1(k) + hr_1(k)] + [w_1 \frac{1}{\Delta x} - w_2]hu_1 \\
&+ w_3[\rho_2(k) - \rho_c + \frac{h}{\Delta x}(-q_2(k) + q_1(k))] \\
&+ w_4[\ell_2(k) + hr_2(k)] + [w_3 \frac{1}{\Delta x} - w_4]hu_2
\end{aligned}
\tag{44}
$$

This difference equation can be written cleanly in the following form.

$$e(k+1) = F + u \tag{45}$$

where

$$
\begin{aligned}
F &= w_1[\rho_1(k) - \rho_c + \frac{h}{\Delta x}(-q_1(k) + f(k))] \\
&+ w_2[\ell_1(k) + hr_1(k)] \\
&+ w_3[\rho_2(k) - \rho_c + \frac{h}{\Delta x}(-q_2(k) + q_1(k))] \\
&+ w_4[\ell_2(k) + hr_2(k)]
\end{aligned}
\tag{46}
$$

and

$$u = [w_1 \frac{1}{\Delta x} - w_2]hu_1 + [w_3 \frac{1}{\Delta x} - w_4]hu_2 \tag{47}$$

In order to obtain (8) in this region, we design the control law as

$$u = -F - Ke(k) \tag{48}$$

Substituting (48) in (45) satisfies the desired dynamics (8) in this region.

4.2.2 Region 2

In this region, the traffic density in both sections is less than or equal to the critical density. The error in this region is equal to

$$e(k) = -w_1(\rho_1(k) - \rho_c) + w_2\ell_1 - w_3(\rho_2(k) - \rho_c) + w_4\ell_2 \tag{49}$$

Incrementing (49) we get

$$\begin{aligned} e(k+1) &= -w_1(\rho_1(k+1) - \rho_c) + w_2\ell_1(k+1) \\ &- w_3(\rho_2(k+1) - \rho_c) + w_4\ell_2(k+1) \end{aligned} \tag{50}$$

Using the dynamics (6) here, we get

$$\begin{aligned} e(k+1) &= -w_1[\rho_1(k) - \rho_c + \frac{h}{\Delta x}(-q_1(k) + u_1 + f(k))] \\ &+ w_2[\ell_1(k) + h(r_1(k) - u_1(k))] \\ &- w_3[\rho_2(k) - \rho_c + \frac{h}{\Delta x}(-q_2(k) + u_2 + q_1(k))] \\ &+ w_4[\ell_2(k) + h(r_2(k) - u_2(k))] \end{aligned} \tag{51}$$

Collecting terms on the right-hand side gives

$$\begin{aligned} e(k+1) &= -w_1[\rho_1(k) - \rho_c + \frac{h}{\Delta x}(-q_1(k) + f(k))] \\ &+ w_2[\ell_1(k) + hr_1(k)] + [-w_1\frac{1}{\Delta x} - w_2]hu_1 \\ &- w_3[\rho_2(k) - \rho_c + \frac{h}{\Delta x}(-q_2(k) + q_1(k))] \\ &+ w_4[\ell_2(k) + hr_2(k)] + [-w_3\frac{1}{\Delta x} - w_4]hu_2 \end{aligned} \tag{52}$$

This difference equation can be written cleanly in the following form:

$$e(k+1) = F + u \tag{53}$$

where

$$\begin{aligned} F = & -w_1[\rho_1(k) - \rho_c + \frac{h}{\Delta x}(-q_1(k) + f(k))] \\ & + w_2[\ell_1(k) + hr_1(k)] \\ & - w_3[\rho_2(k) - \rho_c + \frac{h}{\Delta x}(-q_2(k) + q_1(k))] \\ & + w_4[\ell_2(k) + hr_2(k)] \end{aligned} \tag{54}$$

and

$$u = [-w_1 \frac{1}{\Delta x} - w_2]hu_1 + [-w_3 \frac{1}{\Delta x} - w_4]hu_2 \tag{55}$$

In order to obtain (8) in this region, we design the control law as

$$u = -F - Ke(k) \tag{56}$$

Substituting (56) in (53) satisfies the desired dynamics (8) in this region.

4.2.3 Region 3

In this region, the traffic density of the first section is greater than the critical density and it is less in the second section. The error in this region is equal to

$$e(k) = w_1(\rho_1(k) - \rho_c) + w_2\ell_1 - w_3(\rho_2(k) - \rho_c) + w_4\ell_2 \tag{57}$$

Incrementing (57) we get

$$\begin{aligned} e(k+1) = & w_1(\rho_1(k+1) - \rho_c) + w_2\ell_1(k+1) \\ & - w_3(\rho_2(k+1) - \rho_c) + w_4\ell_2(k+1) \end{aligned} \tag{58}$$

Using the dynamics (6) here, we get

$$
\begin{aligned}
e(k+1) &= w_1[\rho_1(k) - \rho_c + \frac{h}{\Delta x}(-q_1(k) + u_1 + f(k))] \\
&+ w_2[\ell_1(k) + h(r_1(k) - u_1(k))] \\
&- w_3[\rho_2(k) - \rho_c + \frac{h}{\Delta x}(-q_2(k) + u_2 + q_1(k))] \\
&+ w_4[\ell_2(k) + h(r_2(k) - u_2(k))]
\end{aligned} \tag{59}
$$

Collecting terms on the right-hand side gives

$$
\begin{aligned}
e(k+1) &= w_1[\rho_1(k) - \rho_c + \frac{h}{\Delta x}(-q_1(k) + f(k))] \\
&+ w_2[\ell_1(k) + hr_1(k)] + [w_1 \frac{1}{\Delta x} - w_2]hu_1 \\
&- w_3[\rho_2(k) - \rho_c + \frac{h}{\Delta x}(-q_2(k) + q_1(k))] \\
&+ w_4[\ell_2(k) + hr_2(k)] + [-w_3 \frac{1}{\Delta x} - w_4]hu_2
\end{aligned} \tag{60}
$$

This difference equation can be written cleanly in the following form:

$$e(k+1) = F + u \tag{61}$$

where

$$
\begin{aligned}
F &= w_1[\rho_1(k) - \rho_c + \frac{h}{\Delta x}(-q_1(k) + f(k))] \\
&+ w_2[\ell_1(k) + hr_1(k)] \\
&- w_3[\rho_2(k) - \rho_c + \frac{h}{\Delta x}(-q_2(k) + q_1(k))] \\
&+ w_4[\ell_2(k) + hr_2(k)]
\end{aligned} \tag{62}
$$

and

$$u = [w_1 \frac{1}{\Delta x} - w_2]hu_1 + [-w_3 \frac{1}{\Delta x} - w_4]hu_2 \tag{63}$$

In order to obtain (8) in this region, we design the control law as

$$u = -F - Ke(k) \tag{64}$$

Substituting (64) in (61) satisfies the desired dynamics (8) in this region.

4.2.4 Region 4

In this region, the traffic density in the first section is less than or equal to the critical density and greater in the second section. The error in this region is equal to

$$e(k) = -w_1(\rho_1(k) - \rho_c) + w_2\ell_1 + w_3(\rho_2(k) - \rho_c) + w_4\ell_2 \tag{65}$$

Incrementing (65) we get

$$\begin{aligned} e(k+1) &= -w_1(\rho_1(k+1) - \rho_c) + w_2\ell_1(k+1) \\ &+ w_3(\rho_2(k+1) - \rho_c) + w_4\ell_2(k+1) \end{aligned} \tag{66}$$

Using the dynamics (6) here, we get

$$\begin{aligned} e(k+1) &= -w_1[\rho_1(k) - \rho_c + \frac{h}{\Delta x}(-q_1(k) + u_1 + f(k))] \\ &+ w_2[\ell_1(k) + h(r_1(k) - u_1(k))] \\ &+ w_3[\rho_2(k) - \rho_c + \frac{h}{\Delta x}(-q_2(k) + u_2 + q_1(k))] \\ &+ w_4[\ell_2(k) + h(r_2(k) - u_2(k))] \end{aligned} \tag{67}$$

Collecting terms on the right-hand side gives

$$
\begin{aligned}
e(k+1) &= -w_1[\rho_1(k) - \rho_c + \frac{h}{\Delta x}(-q_1(k) + f(k))] \\
&+ w_2[\ell_1(k) + hr_1(k)] + [-w_1\frac{1}{\Delta x} - w_2]hu_1 \\
&+ w_3[\rho_2(k) - \rho_c + \frac{h}{\Delta x}(-q_2(k) + q_1(k))] \\
&+ w_4[\ell_2(k) + hr_2(k)] + [w_3\frac{1}{\Delta x} - w_4]hu_2
\end{aligned}
\tag{68}
$$

This difference equation can be written cleanly in the following form:

$$e(k+1) = F + u \tag{69}$$

where

$$
\begin{aligned}
F &= -w_1[\rho_1(k) - \rho_c + \frac{h}{\Delta x}(-q_1(k) + f(k))] \\
&+ w_2[\ell_1(k) + hr_1(k)] \\
&+ w_3[\rho_2(k) - \rho_c + \frac{h}{\Delta x}(-q_2(k) + q_1(k))] \\
&+ w_4[\ell_2(k) + hr_2(k)]
\end{aligned}
\tag{70}
$$

and

$$u = [-w_1\frac{1}{\Delta x} - w_2]hu_1 + [w_3\frac{1}{\Delta x} - w_4]hu_2 \tag{71}$$

In order to obtain (8) in this region, we design the control law as

$$u = -F - Ke(k) \tag{72}$$

Substituting (72) in (69) satisfies the desired dynamics (8) in this region.

4.2.5 Overall Control

We can combine the previous four sub-sections to come up with a control law that is applicable in all four regions. The overall control law for the coordinated ramp problem is therefore given by

$$u = -F - Ke(k) \tag{73}$$

where

$$\begin{aligned} F &= sign(\rho_1(k) - \rho_c) w_1 [\rho_1(k) - \rho_c + \frac{h}{\Delta x}(-q_1(k) + f(k))] \\ &+ w_2[\ell_1(k) + hr_1(k)] \\ &+ sign(\rho_2(k) - \rho_c) w_3 [\rho_2(k) - \rho_c + \frac{h}{\Delta x}(-q_2(k) + q_1(k))] \\ &+ w_4[\ell_2(k) + hr_2(k)] \end{aligned} \tag{74}$$

and

$$\begin{aligned} u &= [sign(\rho_1(k) - \rho_c) w_1 \frac{1}{\Delta x} - w_2] hu_1 \\ &+ [sign(\rho_2(k) - \rho_c) w_3 \frac{1}{\Delta x} - w_4] hu_2 \end{aligned} \tag{75}$$

Actually (75) does not give the control laws but it gives the condition the control variables should satisfy. We can design the control laws in a decoupled way or coupled way.

4.2.5.1 Decoupled Control

Let us rewrite (75) as

$$F = F_1 + F_2 \tag{76}$$

where

$$\begin{aligned} F_1 &= sign(\rho_1(k) - \rho_c) w_1 [\rho_1(k) - \rho_c + \frac{h}{\Delta x}(-q_1(k) + f(k))] \\ &+ w_2[\ell_1(k) + hr_1(k)] \end{aligned} \tag{77}$$

and

$$F_2 = sign(\rho_2(k) - \rho_c)w_3[\rho_2(k) - \rho_c + \frac{h}{\Delta x}(-q_2(k) + q_1(k))] + w_4[\ell_2(k) + hr_2(k)] \quad (78)$$

Now, using (75), we can derive the decoupled control laws as

$$u_1 = G^{-1}(-F_1 - Ke_1(k)) \quad (79)$$

and

$$u_2 = G^{-1}(-F_2 - Ke_2(k)) \quad (80)$$

where

$$e(k) = e_1(k) + e_2(k) \quad (81)$$

The error terms are defined as

$$e_1(k) = w_1 \mid \rho_1(k) - \rho_c \mid + w_2\ell_1 \quad (82)$$

and

$$e_2(k) = w_3 \mid \rho_2(k) - \rho_c \mid + w_4\ell_2 \quad (83)$$

We get the following two decoupled closed loop dynamics by the application of (79) and (80).

$$e_1(k+1) + Ke_1(k) = 0 \quad (84)$$

and

$$e_2(k+1) + Ke_2(k) = 0 \quad (85)$$

4.2.5.2 Coupled Control Laws

Using (75) and (73) we can distribute the control effort between the two variables as

$$-F - Ke(k) = [sign(\rho_1(k) - \rho_c)w_1 \frac{1}{\Delta x} - w_2]hu_1 + [sign(\rho_2(k) - \rho_c)w_3 \frac{1}{\Delta x} - w_4]hu_2 \quad (75)$$

The distribution we will use in our simulation will be

$$0.65(-F - Ke(k)) = [sign(\rho_1(k) - \rho_c)w_1 \frac{1}{\Delta x} - w_2]hu_1 \quad (76)$$

and

$$0.35(-F - Ke(k)) = [sign(\rho_2(k) - \rho_c)w_3 \frac{1}{\Delta x} - w_4]hu_2 \quad (77)$$

Therefore, the coupled control laws are

$$u_1 = h^{-1}[sign(\rho_1(k) - \rho_c)w_1 \frac{1}{\Delta x} - w_2]^{-1} 0.65(-F - Ke(k)) \quad (78)$$

and

$$u_2 = h^{-1}[sign(\rho_2(k) - \rho_c)w_3 \frac{1}{\Delta x} - w_4]^{-1} 0.35(-F - Ke(k)) \quad (79)$$

4.3 Simulation Files

In the simulations we will use software that allows us to simulate unmixed decoupled ramp feedback control systems, mixed de-coupled ramp feedback control systems, and mixed coupled ramp feedback control systems. The software also uses a different way to provide projections. The software is presented below.

```
% Ramp Metering Code
clear;
clf;
clc;
global rhom rhoc vf gain1 gain2 c w1 w2 w3 w4 l cgain1 cgain2
```

```
ccgain

% Input Parameters
c=input('unmixed(1) or mixed(2) or coupled(3)= ');

gain1=0.4;
gain2=0.4;
cgain1=0.1;
cgain2=0.1;
ccgain=0.25;

w1=0.75;
w2=0.25;
w3=0.75;
w4=0.25;
l=1;

rhom = 60;                          % Jam density
rhoc = rhom/2;                      % Critical density
vf = 15;                            % freeflow velocity
t0 = 0.0;
tf = 15;
h = 0.01;
m = (tf-t0)/h;
x0=[35 5 32 4];
T=zeros(m,1);              % T array m rows (mx1)
X=zeros(m,length(x0));  % X array m rows, length state columns
T(1)=t0;
f1(1)=f1coord(t0);
r1(1)=r1coord(t0);
r2(1)=r2coord(t0);
uvar1(1)=u1(t0,x0);
uvar2(1)=u2(t0,x0);
X(1,:)=x0;
%There are m-1 steps and m points maximum
for I=1:m-1;
   tI=T(I);
   clc;
   tI
  xI=X(I,:);
  k=h*feval('rampcoorddynamics',tI,xI)';

  X(I+1,:)=xI+k;
  T(I+1)=t0 + h*I;
  f1(I+1)=f1coord(T(I+1));
```

```
  r1(I+1)=r1coord(T(I+1));
  r2(I+1)=r2coord(T(I+1));
  uvar1(I+1)=u1(I+1,X(I+1,:));
  uvar2(I+1)=u2(I+1,X(I+1,:));

    if (X(I+1,2)<0),
        X(I+1,2)=0;
    end
    if (X(I+1,1)<0),
       X(I+1,1)=0;
    end
     if (X(I+1,1)>rhom),
       X(I+1,1)=rhom;
    end
    if (X(I+1,4)<0),
        X(I+1,4)=0;
    end
    if (X(I+1,3)<0),
       X(I+1,3)=0;
    end
     if (X(I+1,3)>rhom),
       X(I+1,3)=rhom;
    end



end
subplot(221);
plot(T,X(:,1),'-',T,X(:,3),'-.');
title('Traffic Density1 & Traffic Density2');
xlabel('Time');
subplot(222);
plot(T,X(:,2),'-',T,X(:,4),'-.');
title('Queue Length1 & Queue Length2');
xlabel('Time');
subplot(223);
plot(T,f1,'-',T,r1,'-.',T,r2,':');
title('Mainline Inflow & Ramp Inflows');
xlabel('Time');
subplot(224);
plot(T,uvar1,'-',T,uvar2,'-.');
title('Control1 & Control2 Variables');
xlabel('Time');
```

Figure 10-1: File druncoordramp.m

```
function u1 = u1(t,x)

global rhom vf rhoc gain1 w1 w2 w3 w4 c 1 cgain1 ccgain
v1=vf*(1-(x(1)/rhom));
qout1=v1*x(1);
if c == 1
   e=x(1)-rhoc;
   u1=max(0,qout1-f1coord(t)-gain1*e);
elseif c == 2
   ff1=-w1*qout1/1;
    d1=w1*f1coord(t)/1+w2*r1coord(t);
    g1=w1/1-w2;
    ff2=w1*qout1/1;
    d2=-f1coord(t)*w1/1+w2*r1coord(t);
    g2=-w1/1-w2;
    e=w1*abs(x(1)-rhoc)+w2*abs(x(2));

   if x(1)>=rhoc
      u1=max(0,(-ff1-d1-(1-cgain1)*e)/g1);
   else
      u1=max(0,(-ff2-d2-(1-cgain1)*e)/g2);
   end
else
   e=w1*abs(x(1)-rhoc)+w2*abs(x(2))+w3*abs(x(3)-
rhoc)+w2*abs(x(4));
   ff1=f1coord(t)-qout1;
   ff2=qout1-x(3)*vf*(1-(x(3)/rhom));
   ff=w1*ff1*sign(x(1)-rhoc)+w2*r1coord(t)+w3*ff2*sign(x(3)-
rhoc)+w4*r2coord(t);
   g1=w1*sign(x(1)-rhoc)-w2;
   u1=max(0,-0.35*(ff+ccgain*e)/g1);
end
```

Figure 10-2: File du1.m

```
function u2 = u2(t,x)

global rhom vf rhoc gain2 w1 w2 w3 w4 c 1 cgain2 ccgain

v1=vf*(1-(x(1)/rhom));
qout1=v1*x(1);
v2=vf*(1-(x(3)/rhom));
qout2=v2*x(3);
f1=x(1)*vf*(1-(x(1)/rhom));

if c == 1
```

```
   e=x(3)-rhoc;
   u2=max(0,qout2-f1-gain2*e);
elseif c == 2
   ff1=-w1*qout2/l;
    d1=w1*f1/l+w2*r2coord(t);
    g1=w1/l-w2;
    ff2=w1*qout2/l;
    d2=-f1*w1/l+w2*r2coord(t);
    g2=-w1/l-w2;
    e=w1*abs(x(3)-rhoc)+w2*abs(x(4));
   if x(3)>=rhoc
      u2=max(0,(-ff1-d1-(1-cgain2)*e)/g1);
   else
      u2=max(0,(-ff2-d2-(1-cgain2)*e)/g2);
   end
else
    e=w1*abs(x(1)-rhoc)+w2*abs(x(2))+w3*abs(x(3)-
rhoc)+w2*abs(x(4));
   ff1=f1coord(t)-qout1;
   ff2=qout1-x(3)*vf*(1-(x(3)/rhom));
   ff=w1*ff1*sign(x(1)-rhoc)+w2*r1coord(t)+w3*ff2*sign(x(3)-
rhoc)+w4*r2coord(t);
   g2=w1*sign(x(3)-rhoc)-w2;
   u2=max(0,-0.65*(ff+ccgain*e)/g2);
end
```

Figure 10-3: File u2.m

```
function r1coord = r1coord(t)
r1coord = 10*(1.5+sin(0.5*t)); % ramp1 inflow
```

Figure 10-4: File dr1coord.m

```
function r2coord = r2coord(t)
r2coord = 10*(1.5+sin(0.5*t)); % ramp2 inflow
```

Figure 10-5: File dr2coord.m

```
function f1coord = f1coord(t)
f1coord = 30*(1.25+sin(1.0*t));% mainline inflow
```

Figure 10-6: File df1coord.m

4.4 Simulation Results

Simulation results for the three cases unmixed decoupled ramp feedback control systems, mixed decoupled ramp feedback control systems, and mixed coupled ramp feedback control systems are presented below.

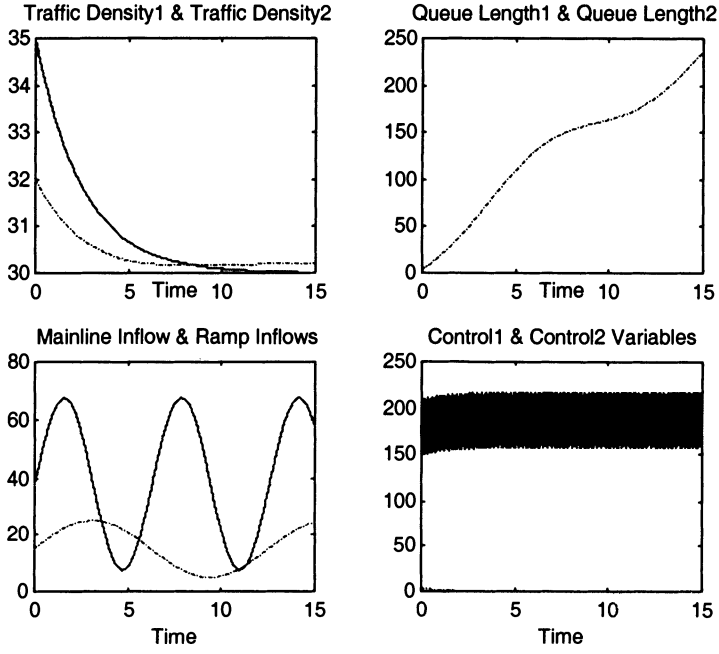

Figure 10-7: Simulation Results for Unmixed Decoupled Case

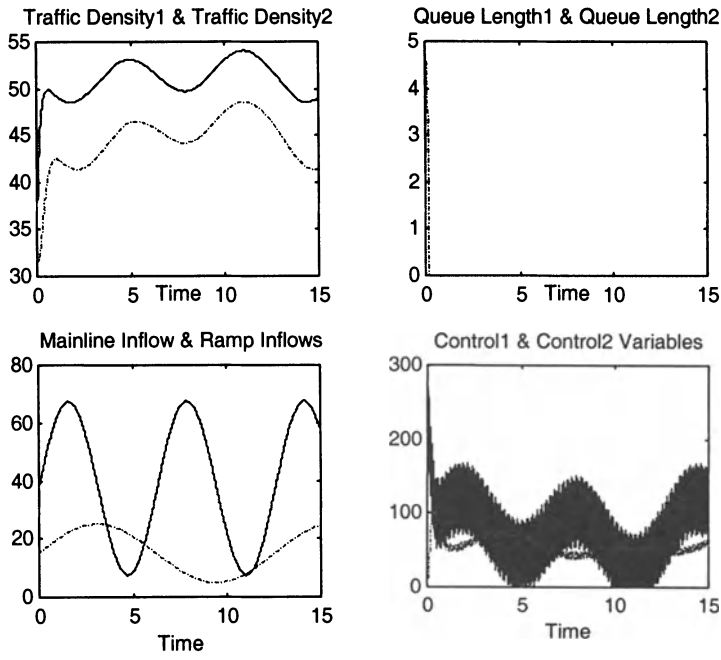

Figure 10-8: Simulation Results for Mixed Decoupled Case

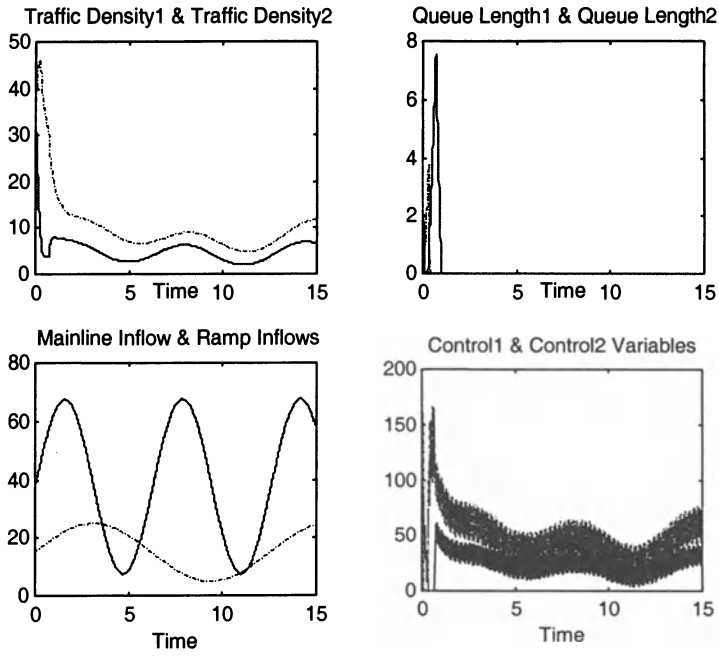

Figure 10-9: Simulation Results for Mixed Coupled Case

5. SUMMARY

In this chapter, we studied:

- The mathematical model for the ramp system in the difference equation setting for various types of ramp metering control problems, such as isolated and coordinated problems, and with and without mixed sensitivity.
- Feedback control laws were designed for each type of problem.
- Simulations were performed to check the effectiveness of the feedback control laws.

6. QUESTIONS

1. Explain the finite difference model. What is the use of the finite difference model in ramp metering control?

2. Why does the parameter k in (8) have values between zero and one?
3. What is the difference between using control objective 1 and control objective 2? Which one would provide better results?

7. PROBLEMS

1. Consider a one-mile freeway section with two lanes in each direction with a maximum capacity of 2000 vehicles per hour per lane and free flow speed of 65 miles per hour. Assume that the traffic is consistent with Greenshield's traffic flow model. For a freeway demand of 1200 vehicles per hour per lane, a ramp demand of 900 vehicles per hour, write a MATLAB code to test the control laws derived in the chapter. Assess the impact of different weight factors or k values. Determine optimal values for the given conditions.

8. REFERENCES

1. Wattleworth, J. A., "System Demand Capacity Analysis on the Inbound Gulf Freeway," Texas Transportation Institute Report. 24-8, 1964.
2. Papageorgiou, M., Habib, H. S., and Blosseville, J. M., "ALINEA: A Local Feedback Control Law for On-ramp Metering," Transportation Research Record, 1320, 1991, 58-64.

Chapter 11

NONLINEAR H_∞ FEEDBACK CONTROL DESIGN USING THE ODE MODEL

This chapter will solve the mixed sensitivity isolated ramp metering problem using nonlinear H_∞ control theory. We will design the control law so that we achieve some optimization of an appropriately chosen criterion that is based on the traffic density on the highway and the queue lengths. We will also present simulation software and results.

1. INTRODUCTION

In this chapter, we will use the theory of nonlinear H_∞ control to design a ramp control law, which minimizes a weighted function of the ramp queues and the difference of the mainline density to the desired mainline density. In order to design the controller, we need the system dynamics equations. We present the system dynamics next followed by the theory of nonlinear H_∞ control, which is then applied to the ramp control problem.

2. SYSTEM MODELING [1]

The first step in the design of feedback controllers for ramp metering is to model the system dynamics appropriately. A macroscopic model of the traffic can effectively be used in this context. From the macroscopic perspective, the traffic flow is considered analogous to a fluid flow, which is a distributed parameter system represented by partial differential equations.

P. Kachroo et al., *Feedback Ramp Metering in Intelligent Transportation Systems*

Mass conservation model of a highway, characterized by $x \in [0, L]$, which is the position on the highway, is given by

$$\frac{\partial}{\partial t}\rho(x,t) = -\frac{\partial}{\partial x}q(x,t) \quad x \in [0,L] \tag{1}$$

where $\rho(x,t)$ is the density of the traffic as a function of x and time t, and $q(x,t)$ is the flow at given x and t. The flow $q(x,t)$ is a function of $\rho(x,t)$, and the velocity $v(x,t)$, as shown below:

$$q(x,t) = \rho(x,t)v(x,t) \tag{2}$$

This model of a highway section is shown in Figure 11-1.

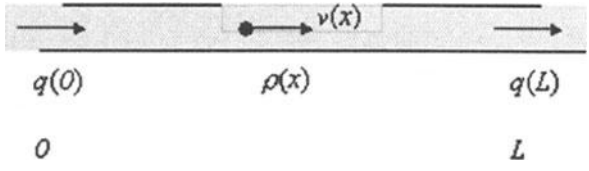

Figure 11-1: Segment of Highway Model

There are various static and dynamic models which have been used to represent the relationship between $v(x,t)$ and $q(x,t)$. One of the simplest models has been proposed by Greenshield [2], which hypothesizes a linear relationship between the two variables.

$$v = v_f\left(1 - \frac{\rho}{\rho_{\max}}\right) \tag{3}$$

where v_f is the free flow speed and $\rho_{\max}$ is the jam density.

2.1 Discretized System Dynamics

Many researchers have studied and designed optimal open-loop controllers utilizing space and time discretized models of traffic flow. Some researchers have also designed feedback control laws using similar models. The reason for the popularity of these models is that there are many techniques available to deal with discretized systems. The same is also true for feedback control, and hence, in order to utilize the various linear and nonlinear control techniques available for lumped parameter systems, the

distributed parameter model is space discretized. For this the highway is subdivided into several sections as shown in Figure 11-2.

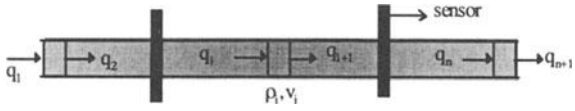

Figure 11-2: Highway Divided into Sections

Space discretization is performed by dividing the considered highway links into segments. In general the length of each segment is taken to be between 0.5 and 1 mile. This approximation is quite realistic since the traditional sensors like loop detectors along a freeway are generally installed at least 1 mile apart. Although a smaller step size for space discretization will undoubtedly improve the accuracy of the simulation, in reality it is not possible to measure speed and flow variables at smaller intervals due to limited availability of sensors along freeways. Thus, 1-mile segment length for space discretization appears to be a realistic assumption. On the other hand, the time discretization can be done using very small time steps since traffic data can be downloaded from sensors practically every second. The space discretized form of (1) produces the following n continuous ODEs for the n sections of the highway:

$$\frac{d}{dt}\rho_i = \frac{1}{\delta_i}[q_i(t) - q_{i+1}(t) + r_i(t) - s_i(t)], \quad i = 1,2,...n \tag{4}$$

Here, $r_i(t)$ and $s_i(t)$ indicate the on-ramp and off-ramp flows. The mathematical model for the highway can be represented in a standard nonlinear state space form for control design purposes:

$$y_j = g_j(\rho_1, \rho_2, ..., \rho_n), \quad j = 1,2,..., p \tag{5}$$

The standard state space form is

$$\frac{d}{dt}x(t) = f[x(t), u(t)],$$

$$y(t) = g[x(t), u(t)], \tag{6}$$

$$x(0) = x_0,$$

where $x = [\rho_1, \rho_2, ..., \rho_n]^T$ and $u(t) = r(t)$.

There are various other proposed models, which are more detailed in the description of the system dynamics. The phenomenon of shock waves, which is very well represented in the PDE representation of the system, is modeled by expressing the traffic flow between two contiguous sections of the highway, as the weighted sum of the traffic flows in those two sections, which correspond to the densities in those two sections [3, 4]. A dynamic relationship instead of a static one like (3) has also been proposed [5] and used successfully.

The model thus obtained can also be time discretized to transform the continuous time model into a discrete time mode. A comprehensive model, which incorporates shock waves, as well as represents the dynamic nature of mean speed propagation, is shown in [6] and is reproduced here for completion. The difference equations

$$\rho_j(k+1) = \rho_j(k) + \frac{T}{\delta_j}[q_{j-1}(k) - q_j(k) + r_j(k) - s_j(k)],$$

$$v_j(k+1) = v_j(k) + \frac{T}{\tau}[v_e(\rho_j(k)) - v_j(k)] + \frac{T}{\delta_j} v_j(k)[v_{j-1}(k) - v_j(k)]$$
$$- \frac{vT}{\tau\delta_j}\left[\frac{\rho_j(k+1) - \rho_j(k)}{\rho_j(k) + \vartheta}\right] \tag{7}$$

with the relationships

$$q_j(k) = \alpha\rho_j(k)v_j(k) + (1-\alpha)\rho_{j+1}(k)v_{j+1}(k), 0 \le \alpha \le 1,$$

$$v_e(\rho) = v_f\left[1 - \left(\frac{\rho}{\rho_{\max}}\right)^l\right]^m, \tag{8}$$

output measurements of traffic flows q and time mean speeds y, shown as

$$y_j(k) = \gamma v_j(k) + (1-\gamma) v_{j+1}(k), \quad 0 \le \gamma \le 1 \tag{9}$$

and the boundary conditions

$$\begin{aligned} v_0(k) &= y_0(k) \\ \rho_{n+1}(k) &= q_n(k) / y_n(k) \end{aligned} \tag{10}$$

give the discrete system dynamics, which can be represented in the standard nonlinear discrete time form

$$\begin{aligned} x(k+1) &= f(x(k), u(k)) \\ y(k) &= g(x(k), u(k)) \\ x(0) &= x_0, \end{aligned} \tag{11}$$

where control $u(k)$ is the vector of ramp input flows.

If the control actuation is discrete, such as the ones implemented by microprocessors and computers, feedback control laws can be designed based on the discrete model (11), or can be designed using (6) after which the controller can be discretized.

The dynamics of the ramp queue are represented by the conservation equation where the rate of change of the number of vehicles in the queue is equal to the input flow to the queue subtracted from the outflow as seen in (12).

3. BACKGROUND (NONLINEAR H_∞ CONTROL)

Consider the system

$$\dot{x} = a(x) + b(x)u + g(x)d_1, \quad a(0) = 0 \tag{12}$$

$$y = c(x) + d_2, \quad c(0) = 0$$

$$z = \begin{bmatrix} h(x) \\ u \end{bmatrix}, \quad h(0) = 0$$

where $x = (x_1, ..., x_n)$ are local coordinates for a C^∞ state space manifold M, $u \in R^m$ the control inputs, $d_1 \in R^r$ and $d_2 \in R^\rho$ the exogenous inputs consisting of reference and/or disturbance signals, $y \in R^\rho$ the measured outputs, and $z \in R^s$ the outputs to be controlled. The system (12) is identified by G. For a full-state measurement case $y = x$. The controller is identified by K. The closed-loop system in Figure 11-3 will be denoted by $\Omega(G/K)$.

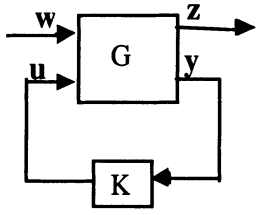

Figure 11-3: Block Diagram for Nonlinear H_∞ Formulation

Definition 1: The closed loop system $\Omega(G/K)$ is said to have L_2 gain less than or equal to γ for some $\gamma > 0$ if

$$\int_0^T \|z(t)\|^2 dt \le \gamma^2 \int_0^T \|w(t)\|^2 dt + b(x_0) \tag{13}$$

$\forall\ T > 0$ and $w(t) \in L_2[0,T]$, where $b(x_0)$ is a positive constant depending on initial condition x_0.

State Feedback H_∞ Control Problem: Find a state feedback controller $K : u = u(x)$ if any, such that the closed-loop system $\Omega(G/K)$ is asymptotically stable and has $L_2 - gain \le \tilde{\gamma}$.

Solution [7-11]: If there exists a smooth function $V(x) \ge 0$ which satisfies the Hamilton-Jacobi (HJ) inequalities

$$V_x(x)a(x) + \frac{1}{2}V_x(x)\left[\frac{1}{\gamma^2}g(x)g^T(x) - b(x)b^T(x)\right]V_x^T(x) \tag{14}$$
$$+\frac{1}{2}h^T(x)h(x) \le 0, V(0) = 0$$

and we set

$$u_* = -b^T(x)V_x(x) \tag{15}$$

then the closed loop system $\Omega(G/u_*)$ has gain at most γ. Moreover if $V(x)$ has a strict local minimum at $x=0$ and the system

$$\dot{x} = a(x) \tag{16}$$
$$z = \begin{bmatrix} h(x) \\ -b^T(x)V_x^T(x) \end{bmatrix}$$

is zero-state detectable (i.e. $\dot{x} = a(x)$ and $z(x(t)) \equiv 0$ for $t \geq 0 \Rightarrow Lim x(t) = 0$), then $x=0$ is a locally asymptotically stable equilibrium of

$$\dot{x} = a(x) - b(x)b^T(x)V_x^T(x) \tag{17}$$

If additionally, V has a global strict minimum at $x=0$ and V is proper (so the inverse image of a compact set under V is again compact), then $x=0$ is a globally asymptotically stable equilibrium of (17).

For the finite-time horizon problem, where final time T is finite, the solution is given by $u = -b^T(x)V_x(t,x)$, where $V(t,x) \geq 0$ satisfies the following HJ equation:

$$V_t(t,x) + V_x(x)a(x) + \frac{1}{2}V_x(x)\left[\frac{1}{\gamma^2}g(x)g^T(x) - b(x)b^T(x)\right]V_x^T(x) \tag{18}$$
$$+\frac{1}{2}h^T(x)h(x) = 0, V(T,x) = V_f(x)$$

The solution for the finite-time case can be derived from a min-max differential game perspective [12].

Measurement Feedback H_∞ Control Problem: Find a dynamic feedback controller

$$K\begin{cases} \dot{\eta} = \kappa(\eta) + \ell(\eta)y \\ u = m(\eta) \end{cases} \tag{19}$$

so that the closed-loop system $\Omega(G/K)$ is asymptotically stable and has $L_2 - gain \leq \gamma$.

Solution [28,29,30, 32,34]: A necessary condition for the existence of solutions for which the closed-loop system has a smooth storage function is that there exists a solution $V(X) \geq 0$ of (14) as well as a solution $R(X) \geq 0$ of

$$R_x(x)a(x) + \frac{1}{2\gamma^2} R_x(x)g(x)g^T(x)R_x^T(x) + \frac{1}{2}h^T(x)h(x) - \frac{1}{2}\gamma^2 c^T(x)c(x) \leq 0, R(0) = 0 \tag{20}$$

such that $V(X) \leq R(X)$ for all x.

Conversely, conditions (14) and (20) are sufficient to solve, at least locally, the measurement feedback-problem. A more complicated version of (20), involving an "information state" in combination with (14), leads to compensators that solve the problem. However, these compensators are in general infinite-dimensional. This is an ongoing area of research, which is beyond the scope of this book.

4. RAMP CONTROL DESIGN

We present two control laws for isolated ramp metering control: one using space discretized dynamics and the other one using space and time discretized dynamics.

4.1 Continuous-Time Case

In order to illustrate the ideas discussed above, we have designed a feedback control law for a space discretized system. The isolated ramp metering problem area is shown in Figure 11-4

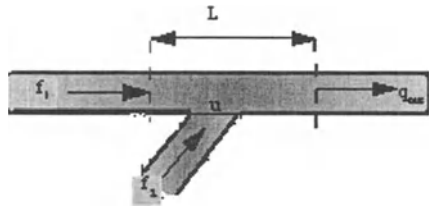

Figure 11-4: Traffic Flow for an Isolated Ramp Metering

The dynamic equation for this problem is given by

$$\frac{d}{dt}\rho=\frac{1}{L}[q_1(t)-q_{out}(t)+r(t)] \tag{21}$$
$$\frac{d}{dt}l=q_2(t)-r(t)$$
$$\frac{d}{dt}r=u(t)$$

where,

ρ = Traffic density on the mainline (veh/mile)
l = Number of vehicles (queue length) on the ramp
L = Length of the mainline section (mile)
r = Rate of flow of traffic into the mainline from the ramp (veh/hour)
q_1 = Traffic flow entering the mainline section from the highway (veh/hour)
q_2 = Traffic flow entering the ramp (veh/hour)
q_{out} = Traffic flow leaving the mainline section (veh/hour)
According to Greenshield formula we have

$$q_{out}(t)=v_f\rho(1-\frac{\rho}{\rho_m}) \tag{22}$$

where,

v_f = Freeflow speed on mainline (miles/hour)
ρ_m = Jam density on the mainline (veh/mile)

Therefore, we can replace (21) by

$$\begin{aligned}
&\frac{d}{dt}\rho=\frac{1}{L}[q_1-v_f\rho(1-\frac{\rho}{\rho_m})+r] \\
&\frac{d}{dt}l=q_2-r \\
&\frac{d}{dt}r=u
\end{aligned} \tag{23}$$

Then defining the error e as $\rho-\rho_c$, making the substitution of $\rho=e+\rho_c$ into (23a), and assuming $L=1$ the following equations are obtained:

$$\begin{aligned}
&\frac{d}{dt}\rho=q_1-v_f(e+\rho_c)\left(1-\frac{e+\rho_c}{\rho_m}\right)+r \\
&\frac{d}{dt}l=q_2-r \\
&\frac{d}{dt}r=u
\end{aligned} \tag{23b}$$

We can now define the state vector x as $x=[e,l,r]'$. We can now present the ramp metering system in the form given by (12):

$$f=\frac{d}{dt}\begin{bmatrix}e\\l\\r\end{bmatrix}=\begin{bmatrix}-v_f(e+\rho_c)\left(1-\dfrac{e+\rho_c}{\rho_m}\right)+r\\-r\\0\end{bmatrix}+\begin{bmatrix}q_1\\q_2\\0\end{bmatrix}+\begin{bmatrix}0\\0\\1\end{bmatrix}u \tag{24}$$

The objective of the control can be taken as

$$z=\begin{bmatrix}e\\l\end{bmatrix} \tag{25}$$

Using this formulation, we can obtain the controller by solving the Hamilton-Jacobi equation like (18) associated with this system.

4.1.1 Nonlinear H_∞ Solution for Two Cost Functions

The two cost functions to be extremized are (26) and (27). These equations are posed such that the disturbance q will be maximized and the arguments of z and the control u will be minimized.

$$J_a = \int_0^\infty \tfrac{1}{2}\left(z^T z + u^2 - \gamma^2 q^T q\right)dt \tag{26}$$

$$J_b = \int_0^\infty \tfrac{1}{2}\left(z^T z + u^2 - \gamma^2 q^T q - k^2 r^2\right)dt \tag{27}$$

The pre-Hamiltonian of (26) and (27) are (28) and (29), respectively

$$H_{pa} = \tfrac{1}{2}\left(z^T z + u^2 - \gamma^2 q^T q\right) + \lambda^T f \tag{28}$$

$$H_{pb} = \tfrac{1}{2}\left(z^T z + u^2 - \gamma^2 q^T q - k^2 r^2\right) + \lambda^T f \tag{29}$$

where

$$\lambda = \begin{bmatrix} \lambda_1 \\ \lambda_2 \\ \lambda_3 \end{bmatrix}$$

and are the Lagrange multipliers that provide the constraints along with (24).

The stationarity conditions for the problem are

$$\frac{\partial H_p}{\partial u} = 0 \tag{30}$$

and

$$\frac{\partial H_p}{\partial \mathrm{q}} = 0 \tag{31}$$

These conditions ensure that the control is minimized and the disturbance is maximized.

4.1.1.1 Derivation of the Optimal Control for J_a

For the cost function defined in (26) the following demonstrates the method used to find the optimal control:

$$\frac{\partial H_p}{\partial u} = 0 = u + \lambda_3 \Rightarrow u = -\lambda_3 \tag{32}$$

$$\frac{\partial H_p}{\partial q} = 0 = \gamma^2 q + \begin{bmatrix} \lambda_1 \\ \lambda_2 \end{bmatrix} \Rightarrow q_1 = \frac{\lambda_1}{\gamma^2}, q_2 = \frac{\lambda_2}{\gamma^2} \tag{33}$$

Substituting (32) and (33) into (28) the following results

$$\begin{aligned} H_a &= \tfrac{1}{2}(e^2 + l^2 + \lambda_3^2 - \frac{\lambda_1^2}{\gamma^2} - \frac{\lambda_2^2}{\gamma^2}) \\ &+ \lambda_1\left(-v_f(e+\rho_c)\left(1 - \frac{e+\rho_c}{\rho_m}\right) + \frac{\lambda_1}{\gamma^2} + r\right) \\ &+ \lambda_2\left(\frac{\lambda_2}{\gamma} - r\right) - \lambda_3^2 \end{aligned} \tag{34}$$

Another necessary condition that needs to be satisfied is the costate equations

$$\frac{\partial H_a}{\partial \mathrm{x}} = -\begin{bmatrix} \dot{\lambda}_1 \\ \dot{\lambda}_2 \\ \dot{\lambda}_3 \end{bmatrix} = \begin{bmatrix} e + v_f\left(2\dfrac{\rho_c + e}{\rho_m} - 1\right)\lambda_1 \\ l \\ \lambda_1 - \lambda_2 \end{bmatrix} \tag{35}$$

From the above costate equations it can be seen that

$$\lambda_2 = -\int_0^t l ds \tag{36}$$

This result can then be substituted into the $\dot{\lambda}_3$ equation that results in

$$-\dot{\lambda}_3 = \lambda_1 + \int_0^t l ds \tag{37}$$

Now recognizing the relationship between u and λ_3, the following can be stated.

$$u = -\lambda_3 \Rightarrow \dot{u} = -\dot{\lambda}_3 = \ddot{r} \tag{38}$$

And λ_1 can be solved for and $\dot{\lambda}_1$ can be found.

$$\lambda_1 = \dot{u} - \int_0^t l ds \Rightarrow \dot{\lambda}_1 = \ddot{u} - l \tag{39}$$

Then substituting these results into the $\dot{\lambda}_1$ equation, we obtain the following equation, independent of λ_i:

$$\ddot{u} = l - e - v_f \left(\frac{\rho_c + e}{\rho_m} - \left(1 - \frac{\rho_c + e}{\rho_m} \right) \right) \left(\dot{u} - \int_0^t l ds \right) \tag{40}$$

From this a state equation for the feedback system can be written; the states for the system are as follows:

$$\begin{aligned} I &= \int l \Rightarrow \dot{I} = l \\ u_1 &= u \\ u_2 &= \dot{u}_1 \\ \dot{u}_2 &= \ddot{u} \end{aligned} \tag{41}$$

Adding these states to the states already defined creates the following state equations

$$\begin{bmatrix} \dot{e} \\ \dot{l} \\ \dot{r} \\ \dot{I} \\ \dot{u}_1 \\ \dot{u}_2 \end{bmatrix} = \begin{bmatrix} -v_f(e+\rho_c)\left(1-\frac{(e+\rho_c)}{\rho_m}\right)+q_1+r \\ q_2-r \\ u_1 \\ l \\ u_2 \\ l-e-v_f\left(2\frac{(\rho_c+e)}{\rho_m}-1\right)(u_2-I) \end{bmatrix} \tag{42}$$

4.1.1.2 Derivation of the Optimal Control for J_b

Following is the analysis used to find the optimal control for (27):
The stationarity conditions for the problem are the same as before:

$$\frac{\partial H_p}{\partial u}=0 \text{ and } \frac{\partial H_p}{\partial \mathbf{q}}=0$$

For (27) this turns out to be the same also

$$\frac{\partial H_p}{\partial u}=0=u+\lambda_3 \Rightarrow u=-\lambda_3$$

$$\frac{\partial H_p}{\partial q}=0=\gamma^2 q+\begin{bmatrix}\lambda_1 \\ \lambda_2\end{bmatrix} \Rightarrow q_1=\frac{\lambda_1}{\gamma^2},\quad q_2=\frac{\lambda_2}{\gamma^2}$$

Substituting (32) and (33) into (29) yields

$$\begin{aligned} H_a &= \tfrac{1}{2}(e^2+l^2+\lambda_3^2-\frac{\lambda_1^2}{\gamma^2}-\frac{\lambda_2^2}{\gamma^2}-k^2 r) \\ &+\lambda_1\left(-v_f(\rho_c+e)\left(1-\frac{\rho_c+e}{\rho_m}\right)+\frac{\lambda_1}{\gamma^2}+r\right)+\lambda_2\left(\frac{\lambda_2}{\gamma}-r\right)-\lambda_3^2 \end{aligned} \tag{43}$$

Another necessary condition that needs to be satisfied is the resulting costate equations:

$$\frac{\partial H_a}{\partial \mathbf{x}} = -\begin{bmatrix} \dot{\lambda}_1 \\ \dot{\lambda}_2 \\ \dot{\lambda}_3 \end{bmatrix} = \begin{bmatrix} e + v_f\left(2\dfrac{\rho_c + e}{\rho_m} - 1\right)\lambda_1 \\ l \\ \lambda_1 - \lambda_2 - k^2 r \end{bmatrix} \tag{44}$$

From the above costate equations it can be seen that

$$\lambda_2 = -\int_0^t l ds$$

This result is the same as above also, and is substituted into the $\dot{\lambda}_3$ equation yields a different result than above

$$-\dot{\lambda}_3 = \lambda_1 + \int_0^t l ds - k^2 r \tag{45}$$

Then, as above we use the relationship of (38) to solve for λ_1 which in this case is

$$\lambda_1 = \dot{u} - \int_0^t l ds + k^2 r \tag{46}$$

Using the same argument as in (39)

$$\dot{\lambda}_1 = \ddot{u} - l + k^2 \dot{r} = \ddot{u} - l + k^2 u \tag{47}$$

Now substituting (46) and (47) into the $\dot{\lambda}_1$ equation of (44) the following results

$$\ddot{u} = l - k^2 u - e\left(\frac{2(e + \rho_c)}{\rho_m} - 1\right)\left(\dot{u} - I + k^2 r\right) \tag{48}$$

Using the definitions in (41) the state equations utilizing the control can be written as follows:

$$\begin{bmatrix} \dot{e} \\ \dot{l} \\ \dot{r} \\ \dot{I} \\ \dot{u}_1 \\ \dot{u}_2 \end{bmatrix} = \begin{bmatrix} -v_f(e+\rho_c)\left(1-\dfrac{(e+\rho_c)}{\rho_m}\right)+q_1+r \\ q_2-r \\ u_1 \\ l \\ u_2 \\ l-k^2u_1-e-\left(2\dfrac{e+\rho_c}{\rho_m}-1\right)(u_2-I+k^2r) \end{bmatrix} \tag{49}$$

where $q_1 = (u - I + k^2 r)/\gamma^2$ and $q_2 = -I/\gamma^2$.

4.1.2 Discretization of the Resulting System

In discretizing the above equations it is important to realize there are certain limits physically placed on the system. The limits on this system are as follows:

$$\begin{aligned} 0 \le \rho \le \rho_m \Rightarrow -\rho_c \le e \le \rho_m - \rho_c \\ 0 \le q_1 \le \rho_m \\ 0 \le q_2 \\ 0 \le l \\ 0 \le r \\ u_{1,\min} \le u_1 \le u_{1,\max} \end{aligned} \tag{50}$$

Since there are constraints on the controls and the states, the method chosen for discretization of the system is the Euler method which is demonstrated by the following:

$$\begin{aligned} &\frac{dx}{dt} = f(x) \approx \frac{x(t+h)-x(t)}{(t+h)-t} = \frac{x(t+h)-x(t)}{h} \\ &\Rightarrow \frac{dx(i)}{dt} = f(x,i) \approx \frac{x(i+1)-x(i)}{h} \\ &x(i+1) = x(i) + h \cdot f(x,i) \end{aligned} \tag{51}$$

For (42) the discrete time system is as follows:

$$
\begin{aligned}
e(i+1) &= e(i) + h\cdot\left(v_f\left(e(i)+\rho_c\right)\left(1-\frac{e(i)+\rho_c}{\rho_m}\right) + q_1(i) + r(i)\right)\\
l(i+1) &= l(i) + h\cdot\left(q_2(i) - r(i)\right)\\
r(i+1) &= r(i) + h\cdot u_1(i)\\
I(i+1) &= I(i) + h\cdot l(i)\\
u_1(i+1) &= u_1(i) + h\cdot u_2(i)\\
u_2(i+1) &= u_2(i) + h\cdot\left(l(i) - e(i) - v_f\left(2\frac{e(i)+\rho_c}{\rho_m} - 1\right)\left(u_2(i) - I(i)\right)\right)
\end{aligned}
\tag{52}
$$

where h is the size of the time step.

The discrete time system for (49) is very similar to (52) and will not be shown here.

4.2 Discrete-Time Case

The dynamic equation for the space and time discretized form is

$$
\begin{aligned}
\rho(k+1) &= \rho(k) + \frac{T}{L}\left[f_1 - v_f\rho\left(1-\frac{\rho}{\rho_m}\right) + u\right]\\
q(k+1) &= q(k) + T(f_2 - u)
\end{aligned}
\tag{53}
$$

We can transform these equations also into a state space form like (24) and use a similar technique for the discrete time case as we used in the continuous time case. However, this will not be shown in this chapter mainly due to space limitations.

5. SOFTWARE AND SIMULATION RESULTS

We will present the software and the simulation results for the optimal control here. The simulation file for this control is presented below.

```
% Ramp Metering Code
clear;
```

```
clf;
clc;
global rhom k
% Input Parameters
k=input('k= ');
rhom = 60;
t0 = 0.0;
tf = 15;
h = 0.01;
m = (tf-t0)/h;
x0=[35 5 4 0.0 0.0 0.0];
T=zeros(m,1);            % T array m rows (mx1)
X=zeros(m,length(x0));  % X array m rows, length state columns
T(1)=t0;
f1(1)=q1(t0);
f2(1)=q2(t0);
X(1,:)=x0;
%There are m-1 steps and m points maximum
for I=1:m-1;
   tI=T(I);
   clc;
   tI
  xI=X(I,:);
k1=h*feval('rampdynamics',tI,xI)';
k2=h*feval('rampdynamics',tI+h/2,xI+k1/2)';
k3=h*feval('rampdynamics',tI+h/2,xI+k2/2)';
k4=h*feval('rampdynamics',tI+h,xI+k3)';
  X(I+1,:)=xI+(k1+2*k2+2*k3+k4)/6;
  T(I+1)=t0 + h*I;
  f1(I+1)=q1(T(I+1));
  f2(I+1)=q2(T(I+1));
   if (X(I+1,2)<0),
        X(I+1,2)=0;
        X(I+1,3)=q2(T(I+1));
        X(I+1,4)=0;
        X(I+1,5)=0;
           X(I+1,6)=0;
     end
    if (X(I+1,3)<0),
        X(I+1,3)=0;
        X(I+1,4)=0;
        X(I+1,5)=0;
           X(I+1,6)=0;
    end
    if (X(I+1,1)<0),
       X(I+1,1)=0;
    end
```

```
      if (X(I+1,1)>rhom),
        X(I+1,1)=rhom;
     end
end

subplot(221);
plot(T,X(:,1),'-',T,X(:,2),'-.');
title('Traffic Density & Queue Lengths');
xlabel('Time');
subplot(222);
plot(T,X(:,3),'-',T,X(:,4),'-.');
title('Ramp Rate & Integral Queue Length');
xlabel('Time');
subplot(223);
plot(T,X(:,5),'-',T,X(:,6),'-.');
title('Ramp Rate Velocity & Ramp rate Acceleration');
xlabel('Time');
subplot(224);
plot(T,f1,'-',T,f2,'-.');
title('Mainline Inflow & Ramp Inflow');
xlabel('Time');
```

Figure 11-5: File runramp.m

Simulation results using this control are presented below.

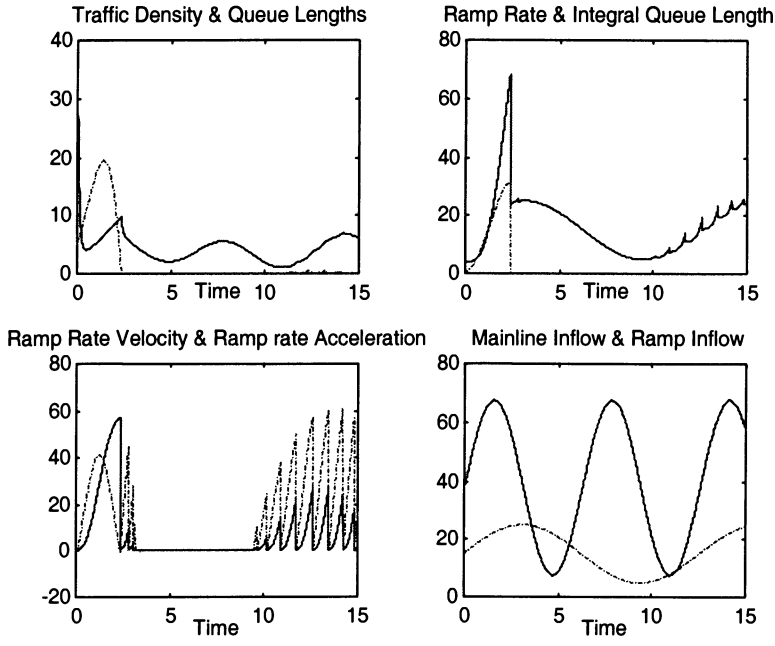

Figure 11-6: Simulation Results Using Control-1

6. SUMMARY

In this chapter, we did the following

- A nonlinear H_∞ control formulation for an isolated mixed sensitivity ramp control problem was presented.
- A feedback control law was designed for this problem.
- Simulations were performed to check the effectiveness of the feedback control law.

7. QUESTIONS

1. For space discretization, what is the realistic approximate of the highway segments? Why?
2. Express the ramp metering problem in the state space form.
3. Explain why (26) and (27) are chosen as the cost functions to be maximized and minimized, respectively.

8. PROBLEMS

1. Write down the state space form of the (53).

9. REFERENCES

1. Kachroo, P., Ozbay, K., Kang, S., and Burns, J. A., "System Dynamics and Feedback Control Problem Formulations for Real Time Dynamic Traffic Routing," Mathl. Comput. Modelling, 27, 9-11,1998, 27-49.
2. Gazis, Denos, C., "Traffic Science", "Edie, L. C., 'Flow Theories'", John Wiley, 1974.
3. Richards, P. I., "Shock Waves on the Highway", Operations Research, 1956, 42-51.
4. Berger, C.R., and Shaw, L., "Discrete Event Simulation of Freeway Traffic," Simulation council Proc. Ser. 7, 1977, 85-93.
5. Payne, H. J., "Models of Freeway Traffic and Control," Simulation Council Proc., 1971, 51-61.
6. Papageorgiou, M., "Applications of Automatic Control Concepts to Traffic Flow Modelling and Control," Springer-Verlag, 1983.
7. Ball, J. A., Helton, J. W., and Walker, M. L., H_∞ Control for Nonlinear Systems with Output Feedback, IEEE Transactions on Automatic Control, April 1993.
8. Lu, W. M., and Doyle, J. C., "H∞ Control of Nonlinear Systems via Output Feedback: Controller Parametrization," IEEE Transactions on Automatic Control, 39, 1994.
9. Isidori, A., and Kang, W., "H_∞ Control via Measurement Feedback for General Nonlinear Systems", IEEE Transactions on Automatic Control, 40, 1995.
10. van der Schaft, A. J., "Nonlinear State Space H_∞ Control Theory", Perspectives in Control, Feb. 1993.
11. van der Schaft, A. J., L2-gain and Passivity Techniques in Nonlinear Control, Springer LNCIS #218, 1996.
12. Basar, T., and Berhard, P., H_∞ -Optimal Control and Related Minimax Design Problems: A Dynamic Game Approach, Birkhouser, 1991.
13. Krener, A. J., "Necessary and Sufficient Conditions for Nonlinear Worst Case (H_∞) Control and Estimation," Journal of Mathematical Systems, Estimation and Control, 4, 1994, 1-25.

Chapter 12

PARAMICS

This chapter introduces PARAMICS (PARAllel MICroscopic Simulation) software, a microscopic traffic simulation program, and discusses its use for testing and validating ramp metering algorithms discussed in the previous chapters of this book Chapters 9 (ALINEA), 10 (Mixed Control), 11 (New Control). The Quadstone website at *www.paramics-online.com* provides an overview of each module.

1. INTRODUCTION TO PARAMICS

PARAMICS is a software tool for the simulation of traffic, and allows the modeling of the movement and behavior of individual vehicles on roadways. The software is comprised of five modules:

1. Modeller – The simulation and visualization tool.
2. Processor – The simulation configuration tool.
3. Analyzer – Postsimulation statistics viewing tool.
4. Programmer – API interface of Paramics.
5. Monitor – The interface to pollution emissions model.

'Paramics Modeller' allows three different operations, which include building the traffic model, running the simulation for the model and finally obtaining results of the simulation through a graphical user interface. Paramics has a very neat graphic-based simulation environment and therefore allows the user to view their model in real time as the simulation is running. This makes for a good presentation when meeting with a nontechnical audience and thus is a lot more convincing then simple

P. Kachroo et al., *Feedback Ramp Metering in Intelligent Transportation Systems*

numbers. Advanced Signal Control, High-Occupancy Vehicle lanes and Incident Management are among some of the features of transportation networks that can be modeled using Paramics.

'Paramics Processor' is used for running the simulation in batch mode i.e., running the simulation without any visualization. This feature speeds up the simulation process and thus leads to the collection of data in a shorter amount of time.

'Paramics Analyzer' is primarily used to display and report the statistical results obtained from the simulation runs obtained from Processor and Modeller.

'Programmer' is a tool that comes in handy for researchers who need to work with customized models of traffic, whereby they can specify their parameters for driver behavior and vehicle models etc.

'Monitor' is a tool that helps to calculate the pollution due to traffic emissions and this is computed for the entire system by breaking the system down into the various links that the system is comprised of.

2. ADVANTAGES OF PARAMICS SIMULATION

Paramics provides a very comprehensive 3D visualization system. The high-fidelity graphic representation and an extensive set of controls provides a very user-friendly system, making modification of the network model, and its associated parameters, a very simple task. Important characteristics of traffic flow such as lane usage, shockwaves (front, back and stationary) are easily dealt with by simulating the movement of individual vehicles.

The Origin-Destination matrix is treated as an input for Paramics. This allows trips to be generated from zone to zone, in the form of unique vehicles being created for each trip. During their flow from the origin to the destination, the vehicles follow Paramics' sophisticated car following and lane changing algorithms.

Data about vehicles can be collected from the simulation by placing a number of detectors, called 'LOOPS', one for each link. The detectors collect data for each lane of a particular link and therefore can also be looked at as effectively being individual lane monitors. The detector can be placed anywhere on the link between the entry and exit points of the link in question. The following types of data can be collected using these detectors:

- Gap – Time between vehicles
- Occupancy – Total time lane is occupied
- Instantaneous Flow – Inverse of Gap and Occupancy
- Count – Count of vehicles

- Type-Count – Count of different types of vehicles

Information collected from these detectors is stored in the form of database. Real-time access may be needed as in the case of feedback systems such as 'Actuated Signal' control or 'Ramp-Metering' systems. In Paramics, actuated signal control is implemented by giving the user the option of making temporary and permanent changes to signal timing. This is done in a language, which is similar to the 'C programming language'. The program normally consists of two parts:

1. The definition of Plans (Plan File)
2. The assignment of the plans to different phases in the network (Phases File)

The Plans file contains a plan of the signal plans that would be implemented in a network. Each plan is associated with a set of loops and a set of parameters associated with one phase of a node. The file also defines the modifications that need to be made to the signal plan when anyone of a set of events is triggered.

The inputs to the signal plan file are comparison of various parameters such as variable parameters or predefined threshold values. These inputs include values such as critical density in a particular time step, and depending on the outcome of the comparison can lead to any one of a number of actions being taken.

3. PARAMICS APPLICATIONS AND VALIDATION STUDIES

Paramics has become on of the most widely used traffic modeling and simulation software all around the world, including Argentina, Hong Kong, Spain, France, UK, Malaysia, Singapore and the US. PARAMICS is also being used at various universities around the such as Rutgers-NJ, University of Utah, University of California, University of Toronto-Canada and University of Aachen-Germany, among others. Some of the modeling applications of Paramics being used in research include:

- New Intersection Design
- High Occupancy Vehicle Lanes
- Ramp Metering
- Toll Plazas
- Vehicle Loop Detection

- Incidents
- Automated Highway Systems
- Pollution Emissions

PARAMICS has been validated against software such as ARCADY, PICADY and TRANSYT, which are used for roundabouts, priority junctions and signalized junctions respectively. Usually major adjustments are made to the model so that it represents the real world environment as accurately as possible. Additionally various parameters can be modified, such as 'mean headway', 'mean reaction time' and 'driver aggression', to control the overall behavior of the model.

Calibration and Validation is done by comparing the results of the simulations with actual data obtained from obtained from roadways. Visualization comparisons are also made between videos of roadways and the simulation while it is running. This provides a quantitative and qualitative analysis in order to better calibrate as well as validate the model.

One of the recent PARAMICS validation studies performed by California PATH is the "Bay Area Simulation and Ramp Metering Study" [2]. In this study, several simple networks were created and the PARAMICS models were tested in very simple situations in which the predicted model results could be compared with known accepted results. Three freeway test networks were simulated, a straight-pipe freeway section, a lane-drop freeway section, and a single on-ramp freeway section, under a range of traffic demand situations, and the model results were compared based on the Highway Capacity Manual. With few exceptions, it was found that predicted hourly flow rates fell outside the expected range both in terms of the central tendency and the temporal and spatial variations for all three simple networks. The variations of flows were generally higher than expected. This was explained by the nature of the microscopic simulation: by modeling individual vehicles instead of using an aggregated macroscopic approach, the range of predicted values over the time-space domain is likely to be wider when the vehicles are re-aggregated into flows. In terms of speeds, they found that the average speeds predicted by the model generally matched the expected values in the lane-drop and ramp-merge examples. However, the speeds were slightly lower than expected at the vicinity of lane-drops and ramp-merges.

A fourth experiment, a traffic responsive ramp metering modeling with PARAMICS, was performed as well. The main purpose of the ramp metering experiment was to investigate the capability of PARAMICS to simulate a specific local traffic-responsive control strategy. The PARAMICS

plan language proved an efficient and powerful tool in developing and testing ramp metering strategies.

4. PARAMICS RAMP METERING APPLICATIONS

A number of PARAMICS Project Examples of ramp metering are available, some of which are viewable online, *www.paramics-online.com.*

In USA, the Institute of Transportation Studies at the University of California in Irvine is using the system for research and development in collaboration with Caltrans [9]. The aims include constructing an instrumented test-bed network for the city of Irvine and assessing new strategies for adaptive ramp metering, intersection control, and real-time OD estimation techniques. Oak Ridge National Laboratory (ORNL) is also conducting research using Paramics (www.ornl.gov), together with the US Federal Highway Agency, are assessing the benefits of using PARAMICS in comparison to their existing software.

Some examples of ramp metering projects carried out by PARAMICS are given in the following. Project details and more examples can be found on the web.

Evaluating Adaptive Ramp Metering Control project [11] proposes to evaluate a number of off-the-shelf as well as new ramp metering algorithms using PARAMICS, identify the most promising ramp metering algorithm and implement it in District 12 and possibly in District 4.

Development and Evaluation of Adaptive Ramp Metering project [10] proposes to evaluate a number of off-the-shelf as well as new ramp metering algorithms using PARAMICS, identify the most promising ramp metering algorithm and implement it in District 12 and possibly in District 4.

In Bay Area Simulation and Ramp Metering Study [2], PARAMICS' simulation capacity was used in (1) analyzing the effects of new traffic management strategies, (2) analyzing the effects of applying existing strategies in specific situations, and (3) developing and testing traffic theory.

In Evaluation of On-ramp Control Algorithms [6], it was aimed to (1) review existing ramp metering algorithms and choose a few attractive ones for further evaluation, (2) develop a ramp metering evaluation framework using microscopic simulation, and (3) compare the performances of the selected algorithms and make recommendations about future developments and field tests of ramp metering systems. About 17 ramp metering algorithms, ranging from simple local algorithms to complex integrated algorithms, are first categorized and assessed qualitatively. Based on the qualitative assessment, ALINEA, Bottleneck, SWARM, and Zone algorithms were selected for further evaluation. PARAMICS was adopted as

the simulation platform for further evaluation of the selected metering algorithms. Several API (Application Programming Interface) modules, including Loop Aggregation API (on-line data collection), Ramp API (mimics ramp signal operations), and Ramp Algorithm APIs (metering logic implementations), are developed to build a simulation-based ramp metering evaluation framework. The four selected algorithms were coded into this framework for a stretch of southbound Interstate 405 located in Orange County, California. To compare the performance of these algorithms, multiple simulation runs were made under different demand patterns.

5. SIMULATION OF THE STUDY NETWORK

In this section, "feedback"-based ramp metering strategies are tested using PARAMICS on a test network located in Hayward, California. "Mixed ramp control strategy," ALINEA (Papageorgiou, 1991), and New Control (Kachroo and Ozbay, 2003) are implemented using the same test network. The results of all three ramp metering strategies are then compared using various measures of effectiveness, to evaluate the effectiveness of each control strategy with respect to the others as well as with respect to "no control" case where ramp metering is not used.

Thirty-eight nodes, four of which provide the connection of ramp links to the freeway, were used to form the study network using the sketch network shown in Figure 12-1. Only northbound section of the network was used for the simulation.

As the next step, these nodes were connected by links, and the link attributes (e.g., number of lanes, link free flow speed) were edited using network editor window. The number of lanes on the 9.2-mile long study section varies between 3 and 5 lanes. Free flow speed of the links was taken as 60 mph. Figure 12-2 shows a screen capture of the PARAMICS model of the freeway and ramps created using the available geometric and traffic demand data. In this section, "isolated ramp metering" strategies are to be tested; therefore, ramp metering was applied only to the ramp shown in zone 5 of Figure 12-2. The freeway section upstream and downstream of the ramp consists of 5 lanes, with 1-lane on-ramp. Then, six zones were created for traffic generation, two of which was located on both ends of the mainline, and the remaining were located on the ends of the on-ramp links. Seventeen detectors, named using the node numbers that are given in the sketch (Figure 12-1), were located on the network to collect statistical information about the vehicles on the link.

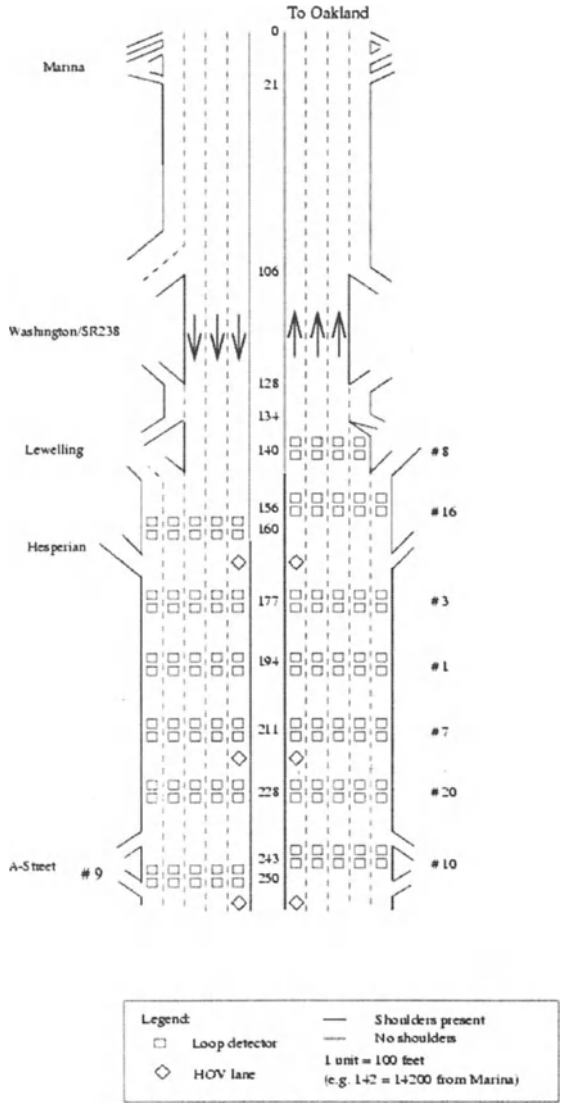

Figure 12-1: The FSP Study Section [10]

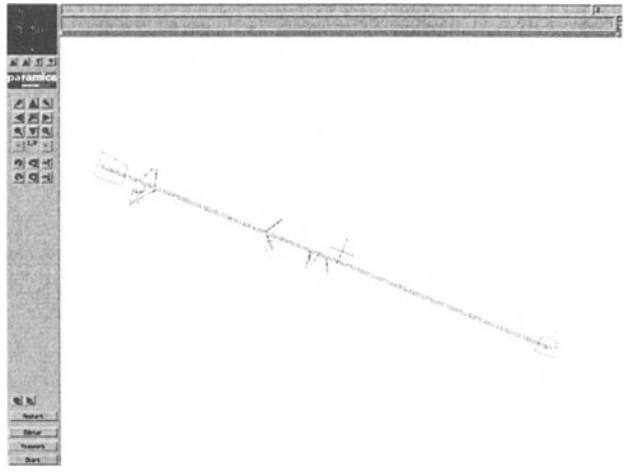

Figure 12-2: PARAMICS Model of the Study Network

Then, an API was written to assign demand in PARAMICS every minute in such a way that the number of vehicles generated in PARAMICS every minute closely matches the observed vehicle counts obtained from the loop detectors. The calibration and validation of the demand assignment and other attributes of the network, such as mean target headway and mean reaction time, were performed based on real-world data from the Freeway Patrol Evaluation Project Database, conducted as part of the PATH program at the University of California, Berkeley (Petty et al., 1995). However, the observed demand data for specific zones were increased so that the ramp metering strategies could be tested under fairly congested traffic conditions. The hourly demand from zone 2 to zone 1 was taken to be 35% more than the observed hourly demand from zone 2 to zone 1, which was given as 5050 veh/hr, and the hourly demand from zone 5 (ramp demand) to zone 1 was taken to be by 3% less than the observed hourly demand of 580 veh/hr.

A vehicles file, which was generated automatically, was edited to represent the traffic on the study network. Thus, characteristics of each vehicle, and assignment information for each vehicle type were specified in this file. The percentages and attributes of the vehicles selected to represent the typical combination of vehicle types in the network are given in Table 12-1.

Table 12-1: Types and Percentages of the Vehicles Used in the Simulation

Type	%	Length (m)	Height (m)	Width (m)	Weight (Tone)	Top Speed (km/h)	Acceleration (m/s2)	Deceleration (m/s2)
Car	85	4.0	1.5	1.6	0.8	158.4	2.5	4.5
Lgv	7.8	6.0	2.6	2.3	2.5	126.0	1.8	3.9
Ogv1	3.2	8.0	3.6	2.4	15.0	104.4	1.1	3.2
Ogv2	2.8	11.0	4.0	2.5	38.0	118.8	1.4	3.7
Coach	1.2	10.0	3.0	2.5	12.0	126.0	1.2	3.7

Two files, namely, the configuration file and the measurements file to extract PARAMICS model statistics were edited. The configuration file is generated automatically, whereas the measurements file has to be created in order to specify the data requirements to be gathered. In the measurements file, "gather link data" was written to be able to collect link flow, link speed, and link density, while "gather trip info" was coded to obtain the travel times for the links of the specified trips from zone to zone. Trip info requires a separate file, called trips file, which is used to specify the trips (from zones 2 and 5 to 1) for travel time data collection.

The simulation was run for 3 hours and 15 minutes, allowing the initial 1 hour 15 minutes for loading the facility and 1 hour at the end to eliminate any effects from the simulation ending. Using configuration and measurements files, statistics were collected for the one hour portion of the simulation from the detectors located 721.6 ft downstream and 468.3 ft upstream of the ramp and two additional detectors, one at the exit and one at the entrance of the ramp.

```
start time  07:45:00
simulation time  03:15:00
demand weight  100.0
seed  120
demand matrix tuning level  0
turning penalties visible to all
generator  0
loop length  6.56 ft
speed memory  3
closest origin carpark  disabled
closest destination carpark  enabled
file time  "-"
curve speed factor  1.00
amber time  3.0
```

```
right hand drive
units us
timestep detail  2
mean headway  1.60
mean reaction time  0.40
cost coefficients  1.000, 0.000 mins per mile, 0.000
queue speed  4.5 mph
queue distance  32.8 ft
weight heavy  2.9 ton
feedback 00:00:00
feedback smoothing factor 0.500
feedback decay factor 0.995
perturbation disabled
read parameters file "API_Example4"
```

Figure 12-3: PARAMICS Configuration File for all the Control Strategy Implementations

There is a large amount of options in the configuration file that can be used to calibrate the model to represent the real network conditions. However, for this study network, except the simulation start and run time, seed, mean headway, and mean reaction time, all configuration input values are kept as default values (Figure 12-3). For example, time step was taken as 2, the default time step, which provides that calculations are done every 0.5 second of simulation.

The overall behavior of the model was calibrated by adjusting the "mean headway" and the "mean reaction time" to obtain results close to real-world data. The values of the mean target headway and the mean reaction time are calibrated as 1.6 seconds and 0.4 second, respectively. The aggression and awareness factors for each vehicle are determined when the vehicle is released onto the network with the levels of these falling within a normal distribution (default value). After this model calibration, the output is observed to represent field data within an acceptable level of accuracy. Therefore, the calibrated and validated model was used to simulate the traffic operations of the study site.

A plan file or an API can be used to simulate actuated signals. In this study, however, we used a plan file, which consists of a description of any signal plan that should be used within the network.

A plan file has an associated number of loops (detectors), and a set of parameters. Loops are defined and the parameters are initialized in the phases file. The format of the language for the plans file has syntax similar to C programming language. The definition of the language consists of actions and clauses. In the following, descriptions of the plans and phases files for each control strategie are illustrated.

```
plan count 1
plan 1 definition
loops 12
parameters 48

if (init)  { fixed; }
if (parameter [1] < 40)
{
parameter [1] = parameter [1] + 1;

##occupancy calculation for the first lane (downstream)
if (occupancy [5] running <= 0.5)
{
parameter [2] = occupancy [5] running;
}
if (occupancy [5] running > 0.5)
{
parameter [2] = 0.5;
}
##parameter [2] is downstream occupancy on the first lane
##Then, the same procedure is applied to the remaining 4 lanes
##on the downstream and to the 5 lanes on the upstream of
##the ramp on the freeway section, which is given in Appendix
##A.

##parameter [2] is downstream occupancy on the first lane
##parameter [3] is downstream occupancy on the second lane
##parameter [31] is downstream occupancy on the third lane
##parameter [37] is downstream occupancy on the fourth lane
##parameter [38] is downstream occupancy on the fifth lane
##parameter [4] is upstream   occupancy on the first lane
##parameter [5] is upstream   occupancy on the second lane
##parameter [32] is upstream   occupancy on the third lane
##parameter [39] is upstream   occupancy on the fourth lane
##parameter [40] is upstream   occupancy on the fifth lane

##lane usage calculation:
parameter [6] =  count [5] / (count [5] + count [6] + count
[10] + count [11] + count [12]); ## %nv on lane 1 downstream
##Similarly, the rest of the lane usage calculations are
##illustrated in Appendix A.
##parameter [7]  is %nv on lane 2 downstream
##parameter [33] is %nv on lane 3 downstream
##parameter [41] is %nv on lane 4 downstream
##parameter [42] is %nv on lane 5 downstream
```

```
##parameter [8]  is %nv on lane 1 upstream
##parameter [9]  is %nv on lane 2 upstream
##parameter [34] is %nv on lane 3 upstream
##parameter [43] is %nv on lane 4 upstream
##parameter [44]  is %nv on lane 5 upstream

##downstream occupancy calculation using lane usage:
parameter [10] = parameter [10] + (parameter [2] * parameter
[6] + parameter [3] * parameter [7] + parameter [31]
*parameter [33] + parameter [37] * parameter [41] + parameter
[38] * parameter [42]);
##upstream occupancy calculation using lane usage:
parameter [11] = parameter [11] + (parameter [4] * parameter
[8] + parameter [5] * parameter [9] + parameter [32] *
parameter [34] + parameter [39] * parameter [43] + parameter
[40] * parameter [44] );
green2 = parameter [14];
green3 = parameter [14];
}
else
{
parameter [27]=flow [5]; ##downstream lane 1
parameter [28]=flow [6]; ##downstream lane 2
parameter [29]=flow [3]; ##upstream   lane 1
parameter [30]=flow [4]; ##upstream   lane 2
parameter [35]=flow [7]; ##upstream   lane 3
parameter [36]=flow [10];##downstream lane 3
parameter [45]=flow [11];##downstream lane 4
parameter [46]=flow [12];##downstream lane 5
parameter [47]=flow [8]; ##upstream   lane 4
parameter [48]=flow [9]; ##upstream   lane 5

parameter [12] = parameter [10] / 20;  ## % downstream
occupancy= sum/ (40*0.5) =sum/20, to find the occ percentage
it is divided by 0.5
parameter [13] = parameter [11] / 20;  ## % upstream occupancy

##ALINEA Implementation:
parameter [14]= parameter[14] + (0 - 20 * (180 / 730 ) ) *
parameter [20] * (  parameter [12] - parameter [15] );

        if ( parameter [14] < parameter [25] )
##parameter[25]is minimum green time
            {
        parameter [14] = parameter [25];
```

```
            }
    if ( parameter [14] > parameter [26] )
##parameter[26]is maximum green time
            {
        parameter [14] = parameter [26] ;
            }

if (count [1] - count [2] > 45)
{
```

```
parameter [14] = parameter [26] ;
}
green2=parameter [14];
green3=parameter [14];

parameter [1] = 1;
parameter [10] = 0;
parameter [11] = 0;
}
```

Figure12-4: ALINEA Plans File

Single plans file is used for the actuated signal implementation in PARAMICS. PARAMICS' internal output is collected from twelve loops that are named and numbered in the phases file. In the plans file, by using these internal output values, parameters are defined in order to calculate desired variables. The number of parameters that are used in this plans file is equal to forty-eight. The cycle length is defined as a fixed quantity.

In this study, it was decided that the percent lane occupancy be used in the local traffic responsive ramp metering control investigations. As the downstream traffic conditions get heavier, the percent lane occupancy increases, and the need for restricting the entering flow from the on-ramp increases.

The ramp signal has two phases, namely red and green. The total cycle time of the signal is fixed to 20 seconds, this means the sum of the red time and green time is fixed to 20 seconds. The ramp metering control calculates the green time for every cycle using the traffic conditions information collected by the detectors and the control law. The red time is automatically determined by subtracting the green time from the 20 seconds cycle time.

Since the ramp metering rate is to be updated every 20 seconds, a counter was placed in the first part of the plan file, where upstream and downstream occupancies are summed for that interval. The upper limit for the counter is equal to the number 40 due to the fact that the time step is 2, which means

that calculations are done every 0.5 second of the simulation. The occupancy values, which are summed in the counter section of the code, are initialized as zero, after each complete cycle of 20 seconds. Similarly, the counter is also initialized as one after the calculations are completed for the 20-second time interval.

Once the upstream and downstream accumulated occupancy values are obtained, then for all the lanes (5 lanes), downstream of the ramp on the freeway section, the averages are calculated for a 20-second time interval. However, the occupancy, which is used in the control law equation, was defined as the weighted average occupancy of lanes 1 through 5. Therefore, the lane occupancies are multiplied by the corresponding lane usage and then they are summed together. An "if loop" is used to make sure that the calculated occupancy values are less than the maximum occupancy values. That is, each time step is 0.5 seconds, and the maximum occupancy value for each time step is, therefore, 0.5 seconds. As a part of the calibration of the PARAMICS model of the network, critical occupancy of the freeway section used for control strategies implementations is found as 26%. Thus, set occupancy for all control strategies was chosen as 25%.

The ALINEA control law, proposed by Papageorgiou et al. (1991), is a local feedback ramp metering strategy that attempts to maximize the mainline throughput through maintaining a desired (or optimal) occupancy on the downstream mainline freeway.

ALINEA uses the previous time step's metering rate, regulator constant, critical (or set) occupancy, and the present downstream occupancy values to determine the next time step's ramp metering rate. However, in order to implement this metering rate, it needs to be converted to the corresponding green phase time in the plans file. Therefore, the following equation is used to convert the metering rate to the green phase:

$$g = (u / u_{sat}) \cdot c \tag{1}$$

where C is the cycle length (sec), u is the ramp metering rate (veh/cycle), u_{sat} (veh/cycle) is the saturated ramp flow. The ALINEA control law is given as:

$$u(k) = u(k-1) + ke(k) \tag{2}$$

where $u(k)$ is the next time step's metering rate, $u(k-1)$ is the previous time step's metering rate, k is the regulator constant, $e(k)$ is the error term, which is defined as $e(k) = (o(k) - o_c)$.

The implementation of the control law in the plans file code is given as:

```
parameter [14] = parameter [14] - 20 * (180 / 730 ) *
parameter [20] * ( parameter [12] - parameter [15] )
```

where;

parameter [14] is the calculated green phase time for the next time step in seconds

20 * (180 / 730) is the conversion constant that converts metering rate to green phase time in seconds,

parameter [20] is the regulator constant

parameter [12] is the downstream occupancy at current time interval

parameter [15] is the set occupancy, which is equal to 25%.

The minimum and maximum green phase times are chosen as 2 and 15 seconds, respectively. In ALINEA implementation, a queue override strategy that sets the green time to its maximum allowed value when the occupancy of the ramp detector exceeds a certain threshold (>45 vehicles on the ramp) is integrated into the ALINEA control to avoid interference with surface street traffic. The time interval to update the metering for controls is equal to 20 seconds.

This plans file depicts the implementation of ALINEA and it also contains the command lines needed for PARAMICS to produce the output, used for evaluation and comparison of the performance of this control strategy.

```
use plan 1
     on node 43 phase 1
     with loops
          10RUP lane 1  ##1
          10RON lane 1  ##2
          10U lane 1    ##3
          10U lane 2    ##4
          20D lane 1    ##5
          20D lane 2    ##6
                 10U lane 3    ##7
                 10U lane 4    ##8
                 10U lane 5    ##9
                 20D lane 3    ##10
                 20D lane 4    ##11
                 20D lane 5    ##12

     with parameters
1         ##1
0         ##2
```

```
0         ##3
0         ##4
0         ##5
0         ##6
0         ##7
0         ##8
0         ##9
0         ##10
0         ##11
0         ##12 downstream occupancy
0         ##13 upstream occupancy
0         ##14 green time
0.25      ##15 critical occupancy, critical =0.26
0         ##19 the no of vehicles on the ramp per 20 seconds
208.57    ##20 is the k value
2         ##25 minimum green phase time
15        ##26 maximum green phase time
0         ##27
0         ##28
0         ##29
0         ##30
0         ##31
0         ##32
0         ##33
0         ##34
0         ##35
0         ##36
0         ##37
0         ##38
0         ##39
0         ##40
0         ##41
0         ##42
0         ##43
0         ##44
0         ##45
0         ##46
0         ##47
0         ##48
```

Figure 12-5: ALINEA Phases File

In the phases file, the loops and the parameters used in the plans file are defined. Furthermore, a description of these parameters is given in the plans and phases files.

New Control implementation in PARAMICS is performed in the same manner as ALINEA (Appendix A).

The simulation output is collected from twelve loop detectors that are defined in the phases file, just as before. The number of parameters, which help to obtain the customized results from PARAMICS' internal output, is equal to fifty.

With the help of a counter, which has an upper limit of 20-second simulation period, the summation of upstream and downstream occupancies on the mainline for all 5 lanes are determined. Then, the weighted average of the collected upstream and downstream occupancies are calculated. These calculated values are then compared with the maximum occupancy values to check if they are greater than the maximum values, and if they are, the calculated values are taken as maximum occupancy.

After determining occupancy, next step is to implement the New Control (Kachroo, Ozbay, 2003). New Control is given as:

$$u(k) = -K[o(k) - o_{cr}] + [q_{out}(k) - q_{in}(k)] \tag{3}$$

Where,

$u(k)$ is the calculated metering rate at time step k

K is the regulator constant

$o(k)$ is the downstream occupancy at time step k

o_{cr} is the set occupancy value

$q_{in}(k)$ is the mainline inflow at time step k

$q_{out}(k)$ is the mainline outflow at time step k

The ramp control strategy is implemented in the plans file as follows:

```
parameter [14] = 20 * (180 / 730) * ((0 - parameter
[20])* (parameter [12] - parameter [15]) + (parameter
[27] +parameter [28] + parameter [36] +parameter [45] +
parameter [46] - parameter [29] - parameter [30] -
parameter [35] - parameter [47] - parameter [48]))/180;
```

Where,

`parameter [14]` is the calculated green phase time for the next time step in seconds,

`20*(180/730)` is the conversion constant (2) that converts metering rate to green phase time,

`parameter [20]` is the regulator constant,

`parameter [12]` is the downstream occupancy at current time interval,

`parameter [15]` is the set occupancy, which is equal to 25%.

`parameters [27],[28],[36],[45],[46]` are the mainline outflow at time step k for each 5- lanes,

`parameters [29],[30],[35],[47],[48]` are the mainline inflow at time step k for each 5lanes

The numbers in the control implementation code come from the conversion of the metering rate to green phase time and some constants, which are a part of the derived control law.

The minimum value of green time is 2 second, and the maximum value of green time is 15 seconds. If the initial calculated value of green time is less then 2 or greater than 15, the algorithm forces the value to be within this range. Time step was taken as 2, the default time step, which provides that calculation are done every 0.5 seconds of simulation.

Since the queue on the ramp is not taken into consideration in the control law, it is made sure that the number of total vehicles on the ramp never exceeds storage capacity by hard coding it into the plans file. A queue detector is located at the entrance of the ramp, and the number of vehicles in the ramp is counted by finding the difference between the number of vehicles crossing the upstream and downstream detectors. Whenever the number of vehicles in the ramp exceeds a threshold value, indicating a queue is forming at the ramp, the metering rate is increased to the maximum metering rate to release the vehicles in the queue. A similar threshold, as in ALINEA, strategy (>35 vehicles) was used for the on-ramp queue. The control gain, K, for the study network, was found as 15996.

After calculation of the parameters for one 20-second time interval, the plans file is completed with the initialization of the counter for the next time interval.

```
use plan 1
    on node 43 phase 1
    with loops
        10RUP lane 1  ##1
        10RON lane 1  ##2
        10U lane 1    ##3
        10U lane 2    ##4
        20D lane 1    ##5
        20D lane 2    ##6
               10U lane 3    ##7
               10U lane 4    ##8
               10U lane 5    ##9
               20D lane 3    ##10
               20D lane 4    ##11
               20D lane 5    ##12
```

```
    with parameters
1         ##1
0         ##2
0         ##3
0         ##4
0         ##5
0         ##6
0         ##7
0         ##8
0         ##9
0         ##10
0         ##11
0         ##12 downstream occupancy
0         ##13 upstream occupancy
0         ##14 green time
0.25      ##15 critical occupancy, critical =0.26
0         ##19 the number of vehicles on the ramp per 20
seconds
15996     ##20 is the k value
2         ##25 minimum green phase time
15        ##26 maximum green phase time
0         ##27
0         ##28
0         ##29
0         ##30
0         ##31
0         ##32
0         ##33
0         ##34
0         ##35
0         ##36
0         ##37
0         ##38
0         ##39
0         ##40
0         ##41
0         ##42
0         ##43
0         ##44
0         ##45
0         ##46
0         ##47
0         ##48
0         ##49
0         ##50
```

Figure 12-6: New Control Phases File

The loop detectors that are used in the plans file are named and numbered in the phases file. The locations of the loops can be found in the detectors file, where the name, the location of the loops in the specific link, and the length of the loop are specified in detail. Additionally, initialization of all parameters used in the plans file is done in this file. A description of some of the parameters is also given, a few of which were explained in the plans file with the help of comments.

Mixed control plans file starts with the specification of the number of loops and parameters used in the file, which are 12 and 48, respectively (Appendix A).

The cycle length of the signal for the ramp was taken as a fixed quantity, as in the implementation of other control strategies. As the time step duration is 20 seconds, the occupancies, which are used in the control law equation, are summed over that interval by means of a counter. Then, the weighted averages of the five lanes' (on the mainline) occupancies are obtained for that interval. It is also ensured that the calculated occupancies do not exceed the maximum value of the occupancy.

The next step is to implement Mixed Control on the study network by coding the plans file using the control law equations. Mixed Control law (Kachroo, Ozbay, 2003) is given as:

$$u = G^{-1}[-F - Ke(k)] \tag{4}$$

where,

$$F = sign(\rho(k) - \rho_c) w_1 [\rho(k) - \rho_c + \frac{h}{\Delta x}(-q(k) + f(k))]$$
$$+ w_2 [\ell(k) + hr(k)]$$

and

$$G = [sign(\rho(k) - \rho_c) w_1 \frac{1}{\Delta x} - w_2] h$$

where

$\rho(k)$ is the density of the freeway segment at time step k

ρ_c is the set density of the freeway segment

w_1 is the weight factor for the freeway segment
w_2 is the weight factor for the on-ramp queue length
$q(k)$ is the downstream flow (outflow) on the mainline
$f(k)$ is the upstream flow (inflow) on the mainline
$\ell(k)$ is the length of the queue at time step k
$r(k)$ is the ramp inflow at time step k
h is the time step duration
Δx is the length of the freeway segment
K is the gain parameter
$e(k) = w_1 \mid \rho(k) - \rho_c \mid + w_2 \ell$

As is seen from the equations above, Mixed Control is composed of two regions. The first region is where the traffic density is greater than or equal to the critical density, and the second region is where the traffic density is less than the critical density. These two regions are represented in the plans file with an "if loop" in which the current step's density is located in either of these regions and then, the next time step's green phase time is calculated.

```
if (parameter[16] >= parameter [18])
{
parameter [14] = 20 * (180 / 730 )* ( (0 -
parameter[21]) * parameter[17] + (parameter [21] *
parameter [24] / parameter [23] ) * (parameter
[27]+parameter [28]+parameter [36]+parameter
[45]+parameter [46]) - (parameter [21] * parameter [24]
/ parameter [23] ) * (parameter [29] + parameter [30] +
parameter [35]+parameter [47]+parameter [48]) -
(parameter [22] * parameter [24]) * (flow [1]/180) -
parameter[22] * parameter [19] - parameter [20] *
parameter [21] * parameter [17] - parameter [20] *
parameter [22] * parameter [19]) / (( parameter [21] *
parameter [24] )/ parameter [23] - parameter [22] *
parameter [24] );
}
else
{
parameter [14] = 20 * (180 / 730 ) * ( parameter[21] *
parameter[17] - (parameter [21] * parameter [24] /
parameter [23] ) * (parameter [27]+parameter
[28]+parameter [36]+parameter [45]+parameter [46]) +
(parameter [21] * parameter [24] / parameter [23] ) *
(parameter [29] + parameter [30] + parameter
[35]+parameter [47]+parameter [48]) - (parameter [22] *
parameter [24]) * (flow [1]/180) - parameter[22] *
parameter [19] + parameter [20] * parameter [21] *
```

```
parameter [17] - parameter [20] *  parameter [22] *
parameter [19] ) / ((0 - parameter [21] * parameter [24]
)/ parameter [23] - parameter [22] * parameter [24] ) ;
}
```

In order to compute the green phase time, a number of parameters are defined and used in the control equation implementation in the plans file, (given in the part of the plans code above) where:

`parameter [14]` is the green phase time calculated through control law equation and converted from the ramp metering rate (sec),

`parameter [21]` is the weight factor for the mainline segment,

`parameter [17]` is the difference between density and the set density (veh/mile),

`parameter [24]` is the duration of each time step (20 seconds)

`parameter [23]` is the length of the freeway segment, L= 0.089 mile,

`parameters [27],[28],[36],[45],[46]` are the mainline outflow at time step k for each 5- lanes,

`parameters [29],[30],[35],[47],[48]` are the mainline inflow at time step k for each 5lanes,

`parameter [22]` is the weight factor for the ramp,

`parameter [19]` is the number of vehicles on the ramp per time step (=20 seconds),

`parameter [20]` is the regulator constant,

`flow [1]` is the ramp demand (veh/hr).

In Mixed Control implementation, control gain, K, w_1 and w_2 were calibrated as 0.95, 0.15 and 0.85, respectively. Unlike ALINEA and New Control, Mixed Control performs satisfactorily without a queue override strategy that shuts off the ramp metering and creates unwanted fluctuations. This way of regulating smoothly the freeway and queue build-ups gives it superiority over other controls that do not explicitly consider the queues specifically created as a result of ramp metering.

One distinct feature of this control law is that it makes use of density of the freeway segment, instead of using the downstream occupancy, as in the case of ALINEA and New control. Therefore, a constant quantity is used to convert the occupancy into density so that it can be used in the Mixed Control law equation.

$$Density = \frac{(Occupancy * 5280)}{(Avg.Vehicle\ Length + Avg.Detector\ Length)} \tag{5}$$

After making sure that the calculated green phase time is within the specified limits, the counter and the parameters summed in the counter are initialized as one and zero, respectively.

The most significant feature, which distinguishes this control strategy from ALINEA and New Control, is the queue length consideration. As the queue on the ramp is taken into consideration in this control strategy, no limit has been set on the number of vehicles that are allowed on the ramp.

```
use plan 1
     on node 43 phase 1
     with loops
          10RUP lane 1  ##1
          10RON lane 1  ##2
          10U lane 1    ##3
          10U lane 2    ##4
          20D lane 1    ##5
          20D lane 2    ##6
                 10U lane 3    ##7
                 10U lane 4    ##8
                 10U lane 5    ##9
                 20D lane 3    ##10
                 20D lane 4    ##11
                 20D lane 5    ##12

     with parameters
1         ##1
0         ##2
0         ##3
0         ##4
0         ##5
0         ##6
0         ##7
0         ##8
0         ##9
0         ##10
0         ##11
0         ##12 downstream occupancy
0         ##13 upstream occupancy
0         ##14 green time
0.25      ##15 critical occupancy, critical =0.26
0         ##16 density
0         ##17 (occupancy - critical occupancy) *
##(5280/13.6596)
97        ##18 critical density
0         ##19 the number of vehicles on the ramp per 20
```

```
seconds
0.95      ##20 is the k value
0.15      ##21 weight factor for the mainline, w1
0.85      ##22 weight factor for the ramp, w2
0.261591 ##23 length of the freeway segment (mile)
20        ##24 time step duration in seconds
2         ##25 minimum green phase time
15        ##26 maximum green phase time
0         ##27
0         ##28
0         ##29
0         ##30
0         ##31
0         ##32
0         ##33
0         ##34
0         ##35
0         ##36
0         ##37
0         ##38
0         ##39
0         ##40
0         ##41
0         ##42
0         ##43
0         ##44
0         ##45
0         ##46
0         ##47
0         ##48
```

Figure 12-7: Mixed Control Phases File

The phases file defines and initializes a number of parameters. First, the node at which the ramp-metering signal is placed is specified in the phases file. Second, the loop detectors and the parameters used in the plans file are defined. Finally, initialization of all the parameters used in this control strategy takes place in this file.

In PARAMICS plans file, the control law equation for each ramp metering control was converted into green phase time (Equation 1), so the unit of each gain parameter is different from the unit definition in the original control laws of ALINEA, New Control and Mixed Control shown in equations. After implementing ALINEA, New Control and Mixed Control using plans and phases files within PARAMICS Modeller, a series of simulation runs were carried out to determine the gain parameter, K, as it is

complicated to analytically determine K value that produces desirable performance for each ramp metering control law. This approach is similar to the one adopted by Zhang et al. (2001).

6. SIMULATION RESULTS

All the simulations were run for three seed values (117, 120, 125) for each scenario and the average of the results are presented in this section.

For this isolated ramp metering evaluation study, we defined the system as the "upstream and downstream and ramp" links around the ramp where ramp metering is implemented, therefore, the average values of measures of effectiveness are obtained over the simulation time for one link for each section of the system (downstream (one link), upstream (one link) and ramp (one link).

One of the measures of effectiveness is the mean congestion duration (sec) on the downstream freeway link. Mean congestion duration is the accumulated period of time during the simulation where the measured occupancy per time interval (20 sec) is larger than the critical occupancy, $o_{cr} = 26\%$.

$$Mean\ CongestionDuration\ (\text{sec}) = n.T \tag{6}$$

Where n is the number of times the measured occupancy on the downstream link is larger than critical occupancy, T is the time step interval (20 sec).

Simulation results (Table 12-2) show that both Mixed Control strategy and ALINEA reduce mean congestion duration significantly on the mainline by 47 %, 36%, respectively, compared to No Control scenario.

New Control (-50%) performed slightly better in reducing the mean congestion duration compared to Mixed Control (-47%) in the expense of large waiting times for the vehicles on the ramp.

Table 12-2: Mean Congestion Duration on the Downstream Freeway Link

	No of time step	Mean congestion duration (min)	%Change
No Control	125	41.67	-
ALINEA	80	26.67	-36.00%
New Control	62	20.67	-50.40%

Mixed Control	66	22.00	-47.20%

Occupancy of the freeway section (both upstream and downstream of the ramp) is gathered by means of plans file report for each time step (20 sec). The following formula gives one-link's (upstream or downstream) mean occupancy based on the occupancy measurements in n time steps:

$$Mean\ Occupancy(\%) = \frac{\sum_{i=1}^{m} o_i}{m} \tag{7}$$

Where o_i is the occupancy on the downstream freeway link at time step i, m is the number of time step during the simulation

All the ramp control strategies were able to reduce the average downstream occupancy compared to No Control scenario. The downstream occupancy was reduced below critical occupancy, 26%, by all three control strategies. ALINEA reduced the downstream occupancy by 9%, whereas New Control and Mixed Control reduced the same measure by 14% and 10%, respectively (Table 12-3).

Table 12-3: Mean and Maximum Downstream Occupancy on the Freeway

	Mean Occupancy (%)	% of change	Max Occupancy (%)	% of change
No Control	28.0	-	40.0	-
ALINEA	25.5	-8.93%	44.3	10.75%
New Control	24.1	-13.93%	41.7	4.25%
Mixed Control	25.1	-10.36%	43.1	7.75%

Another measures of effectiveness for the evaluation of the ramp controls is average speed, density and flow on the freeway and ramp links. Speed (mph), flow (veh/hour) and density (veh/mile) measurements for each time step on each link in the study section were gathered from the PARAMICS output statistics every minute during the simulation. Then, using following formula, the averages for each measures are obtained for each link in the system (one upstream link, one downstream link and one ramp link).

$$Mean\ Speed\ (mph) = \frac{\sum_{i=1}^{m} S_i}{m}, Mean\ Density\ (veh/mile) = \frac{\sum_{i=1}^{m}}{n} \quad (8)$$

$$Mean\ Flow\ (veh/hour) = \frac{\sum_{i=1}^{m} F_i}{m}$$

Where S_i is the speed on one link at time step i, D_i is the density on the link at time step i, F_i is the instantaneous flow at time step i, m is the number of time step during the simulation.

The improvement in mainline upstream link flow as a result of the implementation of the control strategies was insignificant as it can be seen in Table 12-4. Similarly, the effect of the controls on the speed of the upstream mainline link was quite small. Except ALINEA, all the controls achieved producing lesser density values on the upstream link of the freeway (Table 5.4), which might be due to the fact that ALINEA does not consider the upstream in its control law.

Table 12-4: Average Upstream Speed, Density, and Flow Values on the Freeway

	Speed (mph)	% change	Density (veh/mile)	% f change	Total Flow (veh/hr)	% of change
No Control	55.13	-	23.90	-	6390.65	-
ALINEA	56.53	2.55%	23.94	0.19%	6369.88	-0.33%
New Control	58.55	6.22%	22.33	-6.54%	6410.84	0.32%
Mixed Control	56.22	1.99%	23.56	-1.42%	6318.67	-1.13%

Table 12-5 demonstrates the average value of the speeds, densities and flows collected from downstream detectors on the freeway. It is clear that all the controls performed well on the downstream link. The average downstream freeway speed, measured for the simulation period, has increased with the implementation of all the controls (Table 5.5). Mixed Control and ALINEA increased the average downstream link speed by 16% and 15%, respectively. New Control, however, increase the same measure by 21%.

Table 12-5: Average Downstream Speed, Density, and Flow Values on the Freeway

	Speed (mph)	% change	Density (veh/mile)	% change	Total Flow (veh/hr)	% change
No Control	32.22	-	48.58	-	7280.07	-
ALINEA	37.23	15.57%	42.23	-13.07%	7235.46	-0.61%
New Control	39.01	21.08%	41.44	-14.69%	7199.33	-1.11%
Mixed Control	37.49	16.36%	42.97	-11.56%	7194.03	-1.18%

All controls performed similarly on the downstream link. New Control, however, performed slightly better than Mixed Control in reducing the average density and increasing the average speed on the freeway.

Figures 12-8 and 12-9 show the time-dependent speed and density values on the downstream of the freeway. These figures demonstrate that all the controls can make improvements to the freeway conditions. It can be seen that all the controls kept the speed higher than No Control case, and they also kept density at lower level.

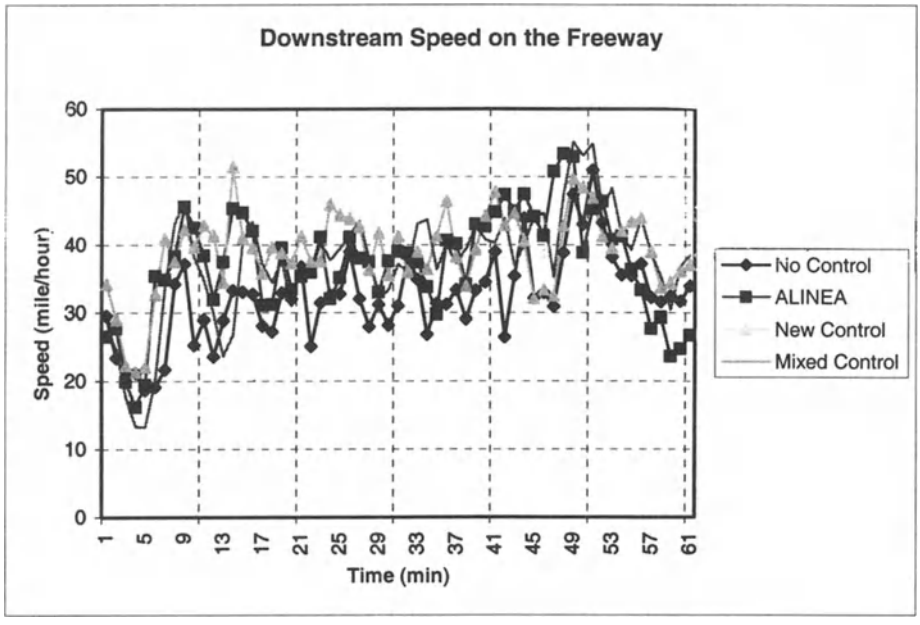

Figure 12-8: Average Time-dependent Speed for all 5 Lanes on Downstream Section

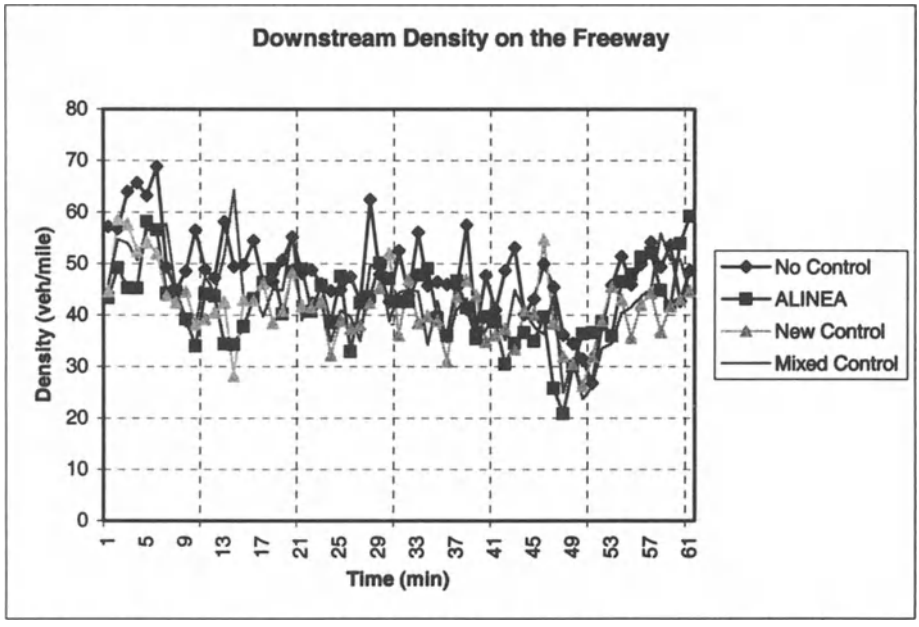

Figure 12-9: Average Time-dependent Density for all 5 Lanes on Downstream Section

Another performance measure used to analyze the impact of ramp metering is to compare the travel times for the upstream, downstream sections and ramp links, which are calculated using the following equation:

$$Average\ Link\ Delay\ (veh.hour) = (ATT \times p)/3600 \qquad (9)$$

Where ATT (sec) is the average travel time spent on the link (downstream, upstream, or ramp link) per vehicle , which is obtained in the specific PARAMICS output file named "trips link delay", p (veh) is the total number of vehicles on the link during the simulation period.

Table 12-6: Average Upstream and Downstream Link Delays on the Freeway (vehicle-hour)

	Mainline Delay			
	Upstream Link	% change	Downstream link	% change
No Control	110.40	-	343.21	-
ALINEA	110.56	0.15%	325.69	-5.11%

New Control	100.90	-8.60%	308.36	-10.15%
Mixed Control	105.23	-4.68%	310.96	-9.40%

For upstream (8.60 %) and downstream (10.15 %) freeway links, New Control provided the best results in terms of achieving largest reduction in the travel time. Mixed Control was also able to reduce travel times by 4.69 % and 9.39 % in the upstream and downstream links, respectively. ALINEA, however, was unable to improve the upstream link conditions; it resulted in slight (0.15%) increase in upstream freeway link. On the other hand, it was able to reduce the downstream link travel time by 5.11%.

It is clear that due to control application on the ramp, increase in ramp travel times can be expected. However, for the ramp link, Mixed Control produced the best results among all the control strategies. Mixed Control kept the travel times almost close to the No Control case, whereas ALINEA and New Control resulted in increased ramp travel times by 478% and 202%, respectively (Table 12-7). Even though freeway travel time reductions were the best for New Control, Mixed Control proved to perform better by preventing larger waiting times on the ramp; and therefore resulting in better system performance (upstream+downstream+ramp links) level. Thus, total system travel time, consisting of one upstream link, one downstream link and one ramp link, travel time was reduced with Mixed Control by 7.89 %; on the other hand, the corresponding travel time amelioration of New Control was only 4.56% compared to No Control scenario. ALINEA, on the other hand, resulted in increase in the link based system level by 8% due to large travel delays on the ramp. Therefore, the downstream amelioration of ALINEA couldn't compensate the delays experienced on the ramp links.

Table 12-7: Average freeway, ramp and total system link delays (veh.hour)

	Freeway Delay		Ramp Delay		Total Delay	
	Freeway	% change	Ramp	% change	Mainline & ramp	% change
No Control	452.36	-	11.43	-	463.79	-
ALINEA	434.89	-3.86%	66.37	480.39%	501.25	8.08%
New Control	408.16	-9.77%	34.49	201.60%	442.65	-4.56%
Mixed Control	415.14	-8.23%	12.06	5.51%	427.21	-7.89%

However, it is also important to carefully analyze the system-wide impact of these improvements on the freeway. Table 5.8 shows system-wide

performance of each ramp control strategy and compares them to the "no control" scenario.

ALINEA results obtained from our simulation study for the overall system showed resemblance to another study by Gardes et al. (2003). In this recent study, ALINEA was tested on a section of I-680 freeway. They also found that the improvements of traffic conditions on the mainline freeway due to ramp control did not overweigh the deterioration of the traffic performances on the on-ramps with the implementation of ALINEA control strategy. Therefore, it was concluded that the system did not perform better after the implementation of ALINEA ramp control for the particular conditions that were simulated.

Looking at the system-wide statistics, in terms of travel time spent in the system, it was found that the system did perform better after the implementation of Mixed Control compared to other controls. As expected, the mainline freeway did experience better traffic conditions when the metering system was implemented; in addition, the level of benefits obtained on the freeway exceeded the additional delay experienced on the ramps.

In order to analyze the on-ramp traffic more elaborately, on-ramp mean speed, density and flow values were also compared for all the scenarios (Table 12-8).

Table 12-8: Average downstream speed-density-flow values on the ramp

	Speed (mph)	% change	Density (veh/mile)	% change	Total Flow (veh/hr)	% change
No Control	15.66	-	21.87	-	661.05	-
ALINEA	13.19	-15.77%	33.43	52.82%	752.85	13.89%
New Control	12.63	-19.33%	28.77	31.54%	644.49	-2.51%
Mixed Control	16.70	6.67%	28.08	28.37%	770.63	16.58%

Mixed Control maintained optimal flow on the mainline while moderating on-ramp queues with the help of weight factors for each. Therefore, mean density on the ramp was increased by certain amount compared to No Control scenario. On the other hand, this increase was high for ALINEA and New Control due to the lack of on-ramp queue consideration. Except Mixed Control, all the control strategies have led to reduction in the on-ramp speed.

On-ramp queue length is the number of vehicles on the ramp per time step (20 sec). This measure is gathered through PARAMICS plans report data for each time step. Then, the average length of the on-ramp queue (on one-ramp-link) per time interval (20 sec) was found using following equation:

$$On-ramp\ queue\ (mph) = \frac{\sum_{i=1}^{m} queue_{ramp_i}}{m}, \tag{10}$$

Where $queue_{ramp_i}$ is the on-ramp queue at time step i, m is the number of time step during the simulation.

The average length and maximum length of ramp queues are given in Table 12-9. The queue thresholds are used in ALINEA and New Control strategy to try to prevent the ramps from being overloaded. When queue thresholds are activated, the metering rate switches to the maximum metering rate so that more vehicles can enter the freeway. Queue control is critical to ensure that the ramp delays do not reach unacceptable levels. However, it reduces the potential of the freeway control strategy to adjust the metering rates so as to obtain optimized traffic conditions on the freeway. As it is seen from the Table 12-9 and the Figure 12-10, unlike other controls, Mixed Control provided better management of the on-ramp queues, by acting smoothly before the number of vehicles reaches large values, which might block the arterial network traffic. Due to controls that only considers freeway traffic, some amount of increase in the ramp traffic and therefore, increase in the ramp delays is expected. On the other hand, Mixed Control achieved optimal flow on the ramp, while keeping the on-ramp queues almost the same size as no control scenario.

The results indicated that the Mixed Control could shorten the queue length on the ramp yet without significant reduction of the freeway throughout. ALINEA and New Control, however, do not consider queue spill-back directly, which was handled through overriding restrictive metering rates, and therefore, those controls had difficulty to balance freeway congestion and ramp queues when traffic becomes heavily congested.

Table 12-9: Average and maximum length of ramp queue

	Mean ramp queue	Max ramp queue
No Control	3.72	10
ALINEA	33.00	41
New Control	14.02	40
Mixed Control	3.34	9

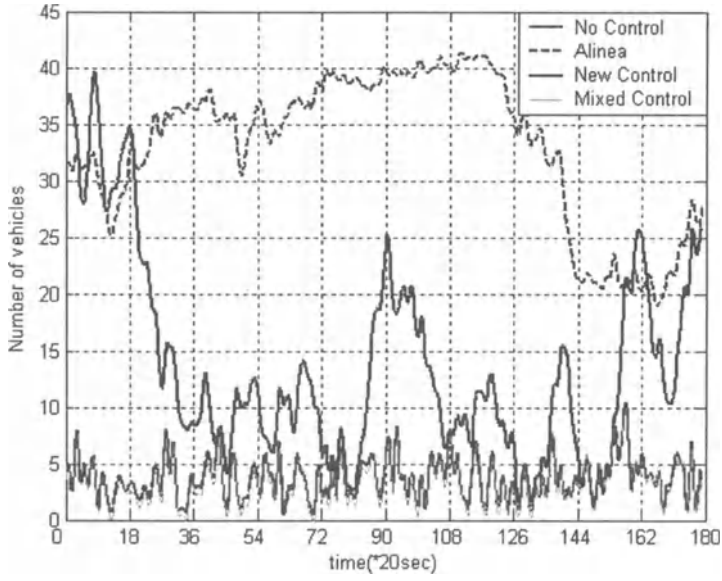

Figure 12-10: Time-dependent ramp queue plot

7. CONCLUSIONS

Since the focus of this chapter is on the evaluation of the isolated ramp control strategies, change in demand due to ramp metering is not considered and the microscopic simulation study was conducted with the assumption that both freeway and ramp demands will remain the same after the implementation of ramp control strategies. For this isolated ramp metering evaluation study, we define the system as the "upstream and downstream and ramp" links around the ramp where ramp metering is implemented. As a result of multiple simulation runs using calibrated PARAMICS model, it was found that the system did perform better after the implementation of Mixed Control compared to other ramp control strategies. As expected, the mainline freeway did experience better traffic conditions when any of the three tested ramp metering strategies was implemented. However, when the queue thresholds are used in ALINEA and New Control trying to prevent the ramps from being overloaded, the system benefits of these strategies were reduced. Mixed Control that significantly improved system performance compared to other two control strategies under these congested conditions was proven to be quite effective.

In fact, New Control has provided slightly better amount of reduction than Mixed Control in terms of mean congestion duration on the freeway but the major strength of Mixed Control comes from the fact that it maintains the occupancy below the set value (Table 12-3) while preventing the number of vehicles in the queue from exceeding the ramp storage capacity (Figure 12-10). This feature makes Mixed Control a better option for real-world implementation.

More research is needed for the real-world implementation of this kind of ramp control strategies that can explicitly model ramp queues.

8. SUMMARY

In this chapter, we studied:

- PARAMICS, microscopic simulation software and some examples of ramp metering applications of this software.
- Using PARAMICS, ALINEA (Chapter 9), Mixed Control (Chapter 10), and New Control (Chapter 11) are implemented on a real-world network.

9. QUESTIONS

1. Discuss the differences between New Control and Mixed Control.
2. Suggest a methodology for estimating gain values for different types of ramp control strategies tested in this chapter.

10. PROBLEMS

1. (For students who have access to PARAMICS). Download PARAMICS files for the test network from the following web site and run the plans files discussed in this chapter.
2. Increase the demand by another 15% and compare the benefits obtained from ramp metering.

11. REREERENCES

1. PARAMICS Modeller User Guide
2. Bay Area Simulation and Ramp Metering Study, Yonnel Gardes, Adolf D. May, Joy Dahlgren, and Alex Skarbardonis, California PATH Research Report, UCB-ITS-PRR-2002-6
3. http://www.paramics-online.com/projects/index.htm
4. http://www.paramics-online.com/tech_support/customer/cust_doc.htm
5. Evaluation of On-ramp Control Algorithms, Michael Zhang, Taewan Kim, Xiaojian Nie, Wenlong Jin, Lianyu Chu, and Will Recker, California PATH Research Report, UCB-ITS-PRR-2001-36
6. http://database.path.berkeley.edu/quarterly/index.cgi?reqtype=publiclistmous&section=Public
7. University of California Irvine ITS Center for Traffic Simulation Studies http://repositories.cdlib.org/itsirvine/ctss/
8. Zhang et al. (2001). Development and Evaluation of Adaptive Ramp Metering, PATH Program Wide Research Meeting, October 17-18, 2001
9. UCI Testbed Micro-simulation Lab, http://www.its.uci.edu/pctss/ramp/ramp.html
10. Petty, K., FSP 1.1 The Analysis Software for the FSP Project, Department of Electrical Engineering and Computer Science, University of California, 1994

Index